STUDIES IN ABSORPTION PHENOMENA AT AN ELECTRODE SURFACE

A Thesis Submitted for the Degree of
Diploma of Imperial College

Julian Fell Tyson B.Sc.

Department of Chemistry,
Imperial College of Science and Technology,
London, S.W.7.

June 1975

ABSTRACT

The possibility of devising a new analytical technique based on the generation and measurement of optically absorbing species at an inert electrode surface is studied.

The analytical technique of atomic absorption spectroscopy is briefly discussed to outline the aim of the study, and the applications of optical methods in electrochemistry are reviewed. Preliminary experiments are described in which absorption signals are detected for dilute aqueous solutions of Cu^{2+} in an excess concentration of inert background electrolyte at a polished cathode surface during reduction. Suitable instrumentation is devised and used to study the phenomenon for a number of other metal ions.

The absorption signals are found to be dependent on wavelength, potential, concentration of metal ion and electrode pretreatment. Brief reviews of the mechanism of metal deposition, charge transfer and the status of hydrated electrons in aqueous electrochemical reactions are given. A systematic study of the phenomenon for Cd^{2+} by both electrochemical and spectroscopic methods is described.

An equation relating the absorbance to a number of experimental parameters and physical constants is derived and its applicability discussed. Reviews of the theories of the nature of the anodically treated platinum surface, of the mechanism of the reduction of oxygen and of the

reduction of the anodic film are given.

A mechanism for the process occurring at the electrode and the production of the absorption signals is proposed in terms of alkalization of the catholyte.

Preliminary experiments with organic dyestuffs are reported and the use of these compounds to determine the electrode pathlength and the beam thickness is demonstrated. The determination of the molar absorptivities of electrogenerated species is discussed.

Finally, the analytical possibilities are critically assessed in the light of existing techniques.

ACKNOWLEDGEMENTS

I would like to thank my supervisor, Professor T.S. West, for giving me the opportunities and encouragement to carry out these studies and for his continued enthusiasm and support during the past three years. I am also grateful to the other members of the analytical research group at Imperial College for helpful discussion and to the Science Research Council for financial support.

CONTENTS

1. INTRODUCTION

1.1 Aim of the Studies

When a metal ion solution is sprayed into a flame the solvent is evaporated or burned and the compounds formed are thermally decomposed and converted into a gas of the individual atoms that are present. The large majority of these atoms are in the ground state, and if light of the appropriate wavelength is shone through the flame the metal atoms absorb the radiation. The resulting decrease in the intensity of the light is proportional to the concentration of the metal ions in the original solution. This is the basis of the analytical technique commonly known as atomic absorption spectroscopy (AAS). In the practical application of the technique there are, of course, a number of problems to be overcome. The most important of these is probably the requirement of a light source with a narrow line emission profile so that the narrow absorption profile of the ground state metal atoms can absorb all the energy in the source line width (if the emission profile from the lamp were broad, then the narrow absorption in the flame would not be detected). Emission from the flame at the analysing wavelength must be compensated for and sample introduction must be uniform so that a steady signal may be measured. These requirements are met by the use of hollow cathode lamps or electrodeless discharge lamps as light sources, modulating the light source either

electronically or mechanically and tuning the detector system to the modulation frequency, and by suitable design of burner aspirators or nebulizers. In addition, a monochromator will be required to separate the line of interest from neighbouring spectral lines. Using a pre-mixed air/acetylene or nitrous oxide/acetylene flame, a large number of metals and semi-metals may be determined with sensitivities (concentration for 1% absorption) of 0·1 ppm (1).

Flames, however, suffer from a number of disadvantages as atom sources. The atom concentration attainable is limited by the dilution effects of the relatively high flow rate of the flame support gas used to transport the sample to the flame and the expansion of the flame gas on combustion. Secondly, precise control over the chemical environment in the flame is not possible and despite variation in the fuel to oxidant ratio (which simultaneously changes the flame temperature and spectral characteristics) certain thermally stable oxides may not be broken down and atom production for these elements will be low. Inefficiencies in nebulization will also limit the atom concentration. And thirdly, a relatively large volume of sample solution is needed. In addition flame background absorption or emission at the wavelength of the resonance line of the analyte element may give rise to unacceptable noise levels with a resultant loss in precision.

As a result, there has been an increase in interest in

the use of non-flame methods to produce atomic populations. Resistively heated graphite furnaces, rods and tubes have been used as well as metallic strips and filaments. The situation up to 1971 has been reviewed by Kirkbright (2) and there has been little significant development since then. Non-flame cells have advantages in that small sample volumes may be used (1-25μl) or solids may be nebulized directly, and the sensitivities for many elements may be increased by two orders of magnitude as a result of concentrating atoms in a smaller cell volume. However, the detection system must be capable of monitoring a transient signal and a storage oscilloscope may be necessary. The precision of the method is poor (coefficient of variation 5-10%) due to the difficulty of reproducibly transferring small sample volumes to the cell. Also, there are similar matrix effects to those observed with flames such as compound formation. There may also be scattering of the analysing light beam by solid particles in the light path as well as undesirable memory effects or emission from the atom cell.

It is apparent that both flame and non-flame cells suffer from some disadvantages, and in the case of AAS using flames they represent the limiting factor in sensitivity. Non-flame cells increase the sensitivity but are accompanied by a loss of precision.

In the case of metal ions, the overall function of the atom cell is to supply electrons to reduce the ions to atoms, desolvate and separate the atoms. Leaving aside

the consideration of providing a gaseous population, the basic requirement is a source of electrons. For a metal ion solution these electrons could come either from another chemical entity in solution (a reducing agent) or from a negatively charged electrode immersed in the solution (together with a suitable counter electrode to complete the circuit). In a dilute solution the ions would be separated and the resulting atoms might well exist in this heavily condensed 'gaseous' phase for sufficiently long periods of time before aggregation and precipitation to interact with an analysing light beam.

The aim of the experiments reported here was to investigate the possibility of devising a new technique of AAS by producing and measuring atomic species at an inert electrode surface.

1.2 Optical Methods in Electrochemistry

As most of the experiments described later are a novel combination of spectroscopic and electrochemical methods, it is of interest to consider briefly the existing applications of optical methods in electrochemistry.

Recently, a review of this title has been published in Advances in Electrochemistry and Electrochemical Engineering (3). The emphasis is placed decidedly on the theoretical side of the methods and little space is devoted to the applications of the techniques. A review by Kuwana and Winograd (4) is more readily understandable from the theoretical viewpoint and also discusses in much greater detail the applications of the methods, though only methods using optically transparent electrodes are reviewed. A series of papers in a recent volume of Ber. Bunsenges. phys. Chem. (5) also gives a good insight into the applications of a number of optical methods. The scope is also demonstrated in the papers presented at the Fourth Symposium of the Faraday Society (6) and to a lesser extent in a recent edition of the Faraday Discussions (7).

1.2.1 Optically Transparent Electrodes

Two types of electrode are in common use; thin film electrodes made by coating a transparent substrate with metals (Pt, Au, Ag) or doped oxides (tin oxide or indium oxide), and minigrid electrodes using a fine wire mesh, but which are usually made by etching rectangular holes on fine metal foils, usually gold. The properties of tin

oxide surfaces have been studied extensively (8,9,10). The first use of this type of electrode with transmission spectroscopy was reported by Kuwana et al (11). The scope of this type of system is well demonstrated by Kuwana and Strojek (12) who derive an equation relating absorbance with time under semi-infinite linear diffusion conditions for a chronoamperometric experiment and show that the oxidation of ferrocyanide gives results in accordance with this equation. They also show how the technique can be used to evaluate rate constants for the two stage oxidation of o-tolidine. Use of the technique in the uv spectral region by changing to an electrode made by coating quartz with antimony doped tin oxide is applied to the oxidation of p-aminophenol to study the rate of reaction and also to determine the products. Further applications of the use of transmission spectroscopy at thin film electrodes are given in recent reviews by Kuwana (13) and Kuwana and Winograd (4). It has been shown that platinum acts as a neutral density filter (14) and the uv part of the spectrum can be monitored using a film of platinum on quartz. A film of mercury on platinum has been used to follow metal deposition and dissolution (15). The molar absorptivities of metals dissolved in the mercury have been measured (16) and for lead, cadmium, thallium and zinc appear to be in the range 3 to 8×10^3 l $mole^{-1}$ cm^{-1}. The absorbances showed little variation with wavelength and the results were obtained at 589 nm.

The use of minigrid electrodes and transmission spectroscopy has been applied by Murray et al (17). They point out that, as the transmission arises from the perforated character of the electrode, the minigrid should be less susceptible to artifacts caused by film deposition during electrolysis and, furthermore, as the surface properties are essentially those of the bulk metal (gold in this case), the electrode does not show any of the eccentricities exhibited by doped tin oxide films. They derive equations relating absorbance to time and current for a number of electrochemical experiments (potential step, double potential step, current step etc), pointing out that the light beam will traverse two diffusion profiles. The application of the equations is demonstrated for the oxidation of o-tolidine and the reduction of Ti(IV).

1.2.2 Internal Reflection Spectroscopy

The use of this technique with optically transparent electrodes provides a method for monitoring what is essentially the surface concentrations of the electroactive species. The basis of this technique is the fact that when a light beam undergoes total internal reflection at a phase boundary, the light beam actually penetrates the rarer medium, where the electric field intensity falls off exponentially (18). The complete, though somewhat complex, mathematical theory for the three phase problem (glass,

film, solution) is given by Hansen (19,20). The use of the technique in electrochemistry stems from the work of Hansen, Kuwana and Osteryoung (21). In a slightly later publication (22) which has proved to be a definitive study of the technique, a clear exposition of the theory is given. The results of experiments with o-tolidine very neatly show the ability of the technique to monitor the surface concentration of electroactive species, and how, when coupled with potential sweep, chronoamperometric, or chronopotentiometric experiments, electrochemical parameters may be determined. The technique has been extensively applied in the determination of reaction mechanisms (23,24,25,26,27) and has also been used to monitor species adsorbed onto the electrode surface (6,28). The use of a germanium electrode extends the application of the technique to the ir region of the spectrum (29,30,31).

1.2.3 Specular Reflection Spectroscopy

This is an external reflection technique where the light beam impinges on the electrode surface from the solution side, usually at oblique incidence. The optical parameters to be considered are identical with those of the internal reflection spectroscopy case. The development of the method for *in situ* electrochemical investigations stems from the work of Koch and co-workers (32,33). The theory and application of the method has been comprehensively

reviewed by McIntyre (3) and a simplified treatment of the theory has been given by Kuwana (13). The technique has been used for the study of the formation and optical behaviour of monolayer films on electrodes (6), adsorbed layers on electrodes (34,35) and for detecting intermediates and products in heterogeneous electrochemical reactions (7). There is often considerable difficulty in interpreting the results of experiments and ambiguities do occur (36). The divergence of opinion that can arise has been shown by the discussions in the literature on Walker's results (37) for multiple reflection of laser light at an elliptical silver electrode. This will be discussed in more detail later (see Section 5.3).

1.2.4 Ellipsometry

Ellipsometry is similar to specular reflection spectroscopy in that the technique is used for probing the nature of the electrode surface. Two parameters are measured, the change in relative amplitude and relative phase of two orthogonal components of light due to reflection. In other words, the change in the state of polarization due to reflection is measured and from this two parameters of the reflecting surface can be derived. For a bare surface these can be the real and imaginary parts of the refractive index and for a surface covered with a transparent film, the thickness and refractive index of the film can be determined. The theory of the method

has been given by Muller (38) and the applications have been comprehensively reviewed by Kruger (39). Ellipsometry has been applied to the study of adsorption onto the electrode surface of gases, ions and organic compounds as well as the study of passive films and corrosion effects. Bockris et al (40) have applied the technique to the study of anodic dissolution and precipitation processes.

1.2.5 Thin Layer Cells

The essential feature of these cells is that the electrolyte volume is small (a few μl) and the thickness of the cell is small (of the order of 10^{-3} cm) so that exhaustive electrolysis occurs after a few hundred milleseconds because the reactant is confined within a layer considerably smaller than the diffusion layer which would exist under conditions of semi-infinite diffusion. As a result, the observed current-potential behaviour is simple to understand. The use of these types of cells stems from the work of Schmidt and Gygax (41) on metal deposition reactions. The theory and applications of the thin layer cell have been comprehensively reviewed by Hubbard and Anson (42) and a particularly well presented review is given by Reilley (43). Thin layer cells have been used in conjunction with optically transparent electrodes (both films and minigrids) and also specular reflection spectroscopy (44). The use of gold minigrid electrodes was proposed by Murray et al (45) who showed

the application of the method by studying the model system of o-tolidine oxidation. A particularly interesting use of the technique is with twin working electrodes, one on either side of the thin layer, where the potential of each electrode is controlled independently. Steady state conditions can be obtained by oxidizing at one electrode and reducing at the other (42). The use of this type of cell with platinum film electrodes is described by Reilley et al (14) who investigated the application of electrochemical as well as optical methods. They applied transmission spectroscopy to the identification of products in the oxidation of rubrene. They also reported preliminary fluorescence studies with the same compound which considerably increased the sensitivity of the technique (by several orders of magnitude). In addition, they suggested a number of applications of thin layer cells in analytical chemistry such as use as a detector for liquid chromatography and determination of dissolved oxygen.

1.2.6 Other Methods

A number of other methods are being applied to the study of electrode processes by probing the nature of the surface or of the solution near to the electrode. These include interferometry, holography and optical microscopy. The applications of these techniques have been recently reviewed (3). Optical microscopy has been used to study transient processes preceding electrodeposition (46).

Perone et al (47,48) have used the combination of optical and electrochemical methods the other way round, ie they used electrochemical techniques to investigate intermediates formed by flash photolysis. The analytical applications are not stressed, however, in the reports of the technique.

In the mid-fifties there was a sudden interest in the use of spectrophotometric techniques for end point detection in coulometric titrations (49,50,51). The method involved monitoring the absorbance of the bulk solution (by conventional transmission spectroscopy) so that the appearance of an absorbing product (or disappearance of an absorbing reactant) could be observed during a coulometric titration. Usually the analyte solution was overtitrated and the absorbance values extrapolated back to find the end point. This method is, of course, identical to the familiar technique of spectrophotometric titration, though in this case the titrant is generated electrochemically instead of being added from a burette.

Apart from this technique, there have been no applications of the combination of spectroscopic and electrochemical methods in quantitative analysis, though the possibility with internal reflection spectroscopy was mentioned by Kuwana (22). The main drawback with all of the methods is that they are insensitive due to the very short path length that the analysing light beam travels in the absorbing medium. Obviously, specular

reflection spectroscopy and ellipsometry are less suited to application in quantitative analysis as these techniques are designed specifically to probe the nature of the surface of the electrode rather than the species in the solution. Possibly the most promising line of development is that of fluorescence measurements in thin layer cells (14).

2. PRELIMINARY EXPERIMENTS

2.1 Chemical Reduction

In this preliminary work a commercial instrument was used. A Varian Techtron model 1000 atomic absorption spectrophotometer was modified by the removal of the burner and nebulizer assembly. The power supply to the hollow cathode lamps which was modulated at 285 Hz was modified so that the lamps could be run demodulated if required. A schematic diagram of the instrument is shown in Figure 2.1

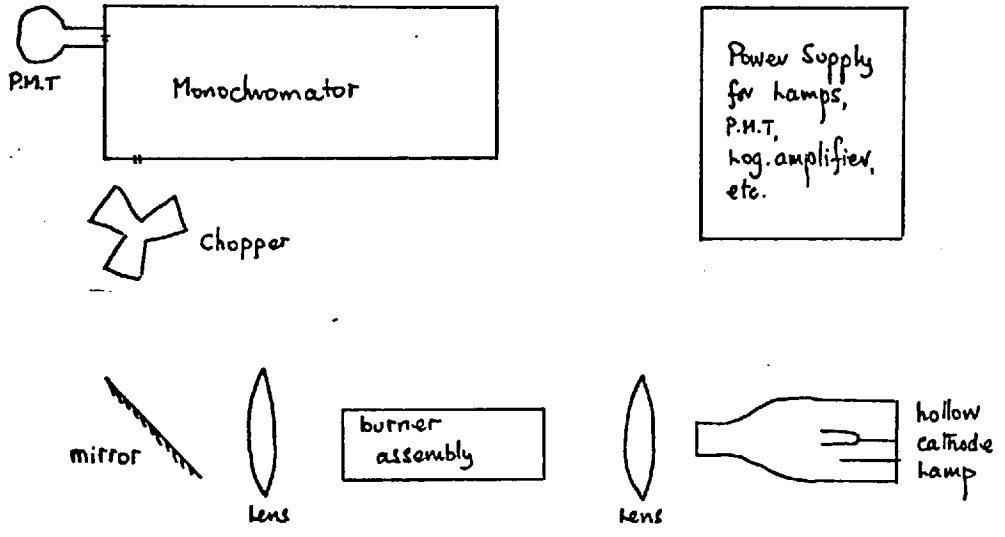

Figure 2.1 Schematic Diagram of the Varian Techtron 1000

In the experiments with the mercury solution an electrode-less discharge lamp was used, powered by a micro-wave generator. The first experiments were to investigate the possibility of detecting absorption by atoms produced in the solution

by chemical reduction. Two methods were used, 1. the reducing agent was added dropwise to a solution of the reducible metal ion 2. a solution of the reducing agent was allowed to diffuse into a solution of the reducible metal ion, a layer of reducing agent being placed in the bottom of the cell by lowering the tip of a pipette into the solution. The change in intensity of the light from a hollow cathode lamp with time was monitored using a chart recorder (Smiths 'Servoscribe' type Re 511.20). The results obtained are summarized below.

1. Reduction of cupric ions with dithionite.

Both methods were tried (i.e. dropwise addition and diffusion) using 10 ppm Cu^{2+} and 0·1 M dithionite. In both cases no difference between the results obtained using a copper hollow cathode lamp at 324·8 nm and an indium lamp at 451·1 nm was observed.

2. Reduction of silver ions by mercury.

A mercury pool was used as the reducing agent and the light beam was passed across the surface of the pool. Solutions containing 1 ppm, 10 ppm and 100 ppm Ag^{+} were used. A decrease in transmission was only observed for the 100 ppm solution and because of the similarity between the results for Ag^{+} and Cu^{2+} the change in transmission was attributed to scatter.

3. Reduction of mercuric ions with stannous chloride.

Again

both methods were tried using 10 and 100 ppm Hg^{2+} and 0·1 M stannous chloride. A mercury electrodeless discharge lamp was used at 253·7 and 265·5 nm. In this case, after the addition of a drop of reducing agent a decrease in transmission was observed at 253·7 nm which was not observed in the absence of the mercuric ions or for the mercuric solution at 265·5 nm.

Only with the mercury solutions was any evidence found for absorption by a reduced species in the solution. The copper and silver solutions gave rise only to scatter signals. It would, therefore, not seem possible by the methods used here to produce a population of free absorbing atoms in the solution as before a sufficiently high population to give an absorption signal can be built up the atoms aggregate to form colloidal particles which scatter the light. It was felt that this line of experimentation would prove unfruitful and so attention was turned to the study of electro-reduction.

2.2 Electrochemical Reduction

The aim of the experiments was to monitor the intensity of a narrow light beam passing over an electrode surface as a potential difference was applied between the electrodes. The Varian Tectron model 1000 was used as described for the previous experiments. In addition, a function generator

(Hewlett Packard type 3310A) was used to provide a potential difference between the electrodes. The various types of electrode used are shown in Figure 2.2.

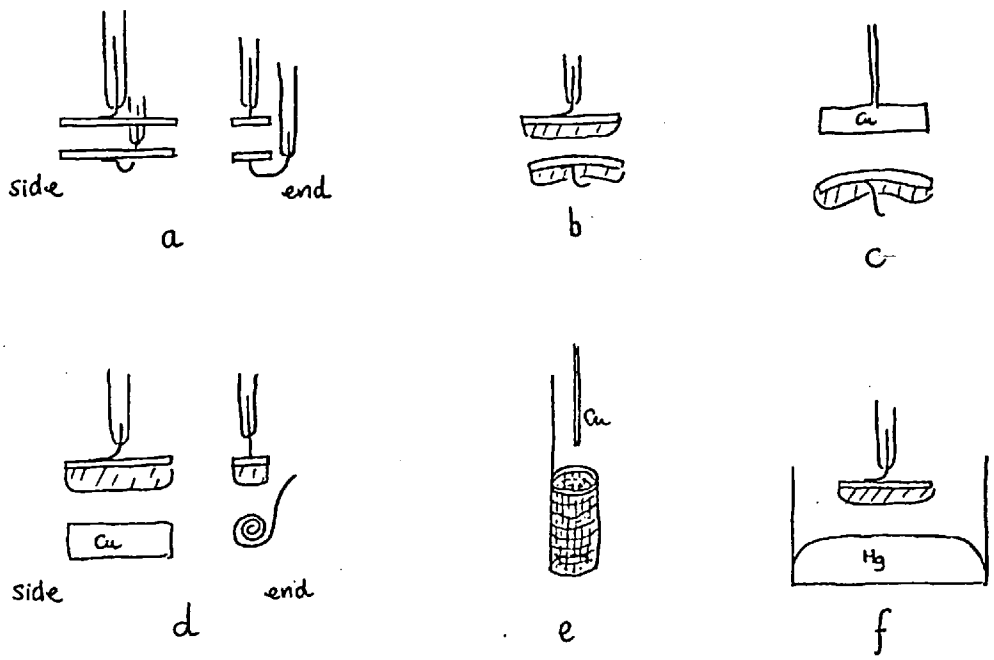

Figure 2.2 Types of Electrode Used

a, Pt plates. b, wax coated Pt plates. c, Cu sheet anode, Pt cathode. d, Pt anode, Cu coil cathode. e, Cu wire anode, Pt gauze cathode. f, Pt anode, Hg pool cathode.

For most of the experiments a 1% solution of copper sulphate was used. Such a high concentration of copper ions was used because it was possible to observe visually when material was being deposited on or removed from the electrode. An aliquot of the solution was placed in the

cell and the gain adjusted to give 100% transmission. The function generator was switched to give a potential difference of about 2 volts between the electrodes with the electrode in the light path as the cathode. Any resulting change in light intensity was monitored with a chart recorder or, on occasions, with a cathode ray oscilloscope. The results are summarized in Table 2.1

Table 2.1 Results With Various Electrode Types

Electrodes		Results
Anode	Cathode	
Cu plate	Pt plate	no change in absorbance until hydrogen evolved
Cu wire	Pt gauze	no change in absorbance
Pt plate	Hg pool	transient increase in absorbance observed, also seen with 100 ppm Cu and with an Ag hollow cathode lamp. Observation of surface with magnifying glass showed distortion on applying potential.
Pt plate	Pt plate	electrodes well separated to avoid obstruction by oxygen evolved from anode. Complex variation of absorption with time observed.

From the Table it can be seen that it was necessary to avoid obstructing the light path by the evolution of oxygen from the anode. If the potential difference was too large hydrogen was evolved from the cathode and this,

of course, also obstructed the light path. The most promising results seem to have been obtained with the platinum plate electrodes, where a fairly complex variation of absorption with time was recorded. This is shown in Figure 2.3.

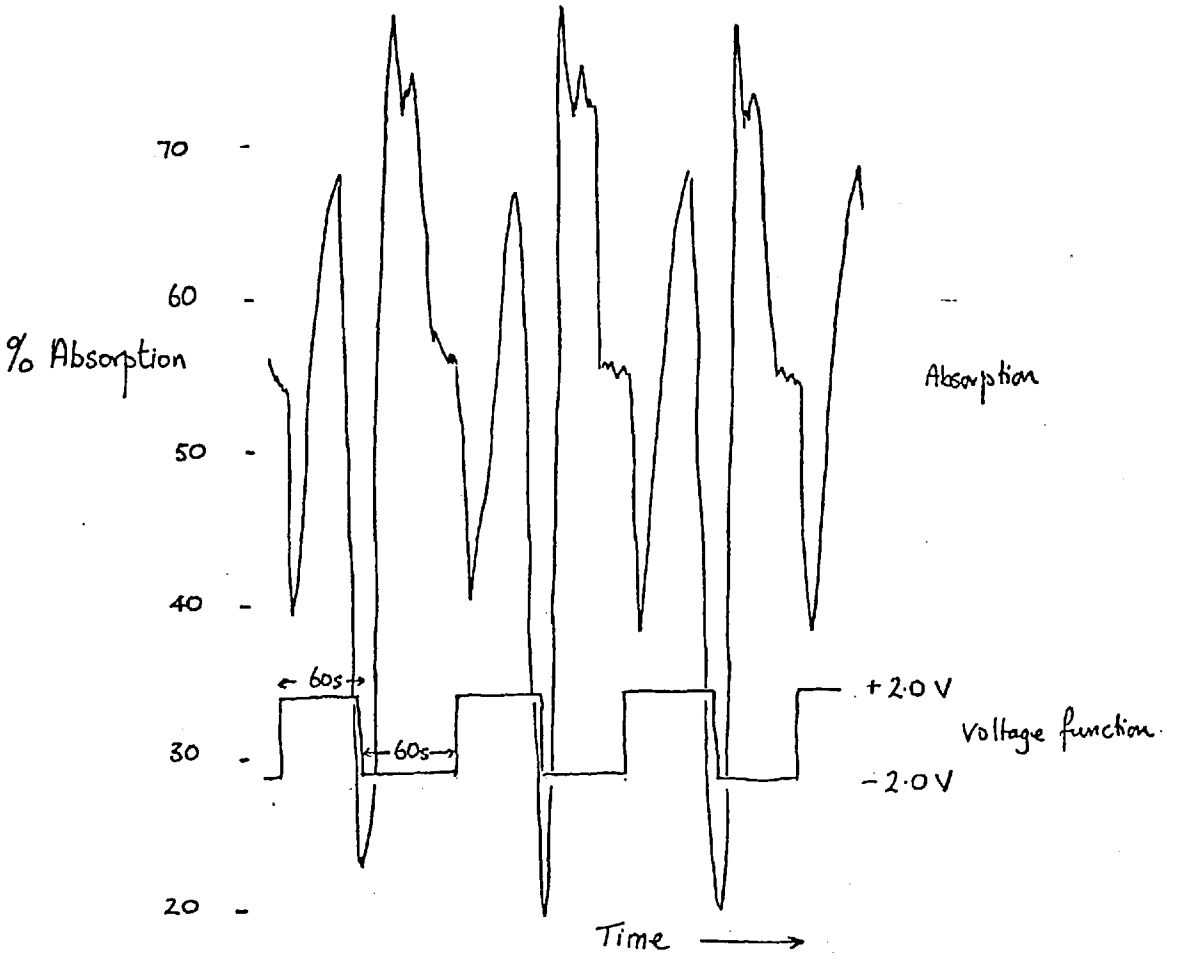

Figure 2.3 Variation of Absorption with Time

2.3 Variation of Signal Intensity with Experimental Parameters

To investigate the nature of the increase in absorption a number of experimental parameters were varied in turn keeping the others fixed. These parameters included concentration of reducible species, potential difference applied, background electrolyte, dissolved oxygen, light source intensity and wavelength.

The apparatus used was the same as for the previous experiments. The two platinum plate electrodes were used and a voltmeter was introduced into the electrical circuit to measure the amplitude of both the positive and negative regions of the voltage pulse. In most cases, though, the potential was stepped from zero to the preset required value. A modulated copper hollow cathode lamp was used and the absorption at 324·8 nm was monitored.

The procedure used in these experiments was as follows. A 5 ml aliquot of the required solution was placed in the cell and the gain of the system adjusted to zero the chart recorder. With the light beam obstructed by a piece of opaque material, 100% absorption was set on the chart recorder. The function generator was then switched on to the required preset voltage function and the change in absorption recorded. The solution was removed from the cell by suction, a glass capillary was lowered into the cell and connected via a stop-cock to a filter pump,, solutions could thus be removed from the cell by suction

when required without disturbing the position of the electrodes. The electrodes were cleaned by washing with concentrated nitric acid, followed by rinsing three times with distilled water. The next aliquot was then placed in the cell.

2.3.1 Concentration of Copper

With the 1% copper sulphate solution the variation of absorption obtained was quite complex (see Figure 2.3). However, considerable simplification of the peak shape occurred when the concentration was 50 ppm or less in an inert supporting electrolye of 0·1 M potassium nitrate. When the potential was switched on the signal increased to a maximum and maintained this value while the potential was held. When the potential difference reverted to zero the absorption decreased rapidly. A linear relation between absorbance and concentration was obtained between 0 and 40 ppm. This is shown in Figure 2.4.

2.3.2 Variation of Absorbance with Voltage

Using a 40 ppm solution in a background electrolyte of 0·1 M KNO_3 it was found that a potential difference of 1·8 V was required to produce a signal. The evolution of hydrogen was found not to obstruct the light path until 2·2 V was applied. In most of these initial experiments a potential difference of 2·0 V was used.

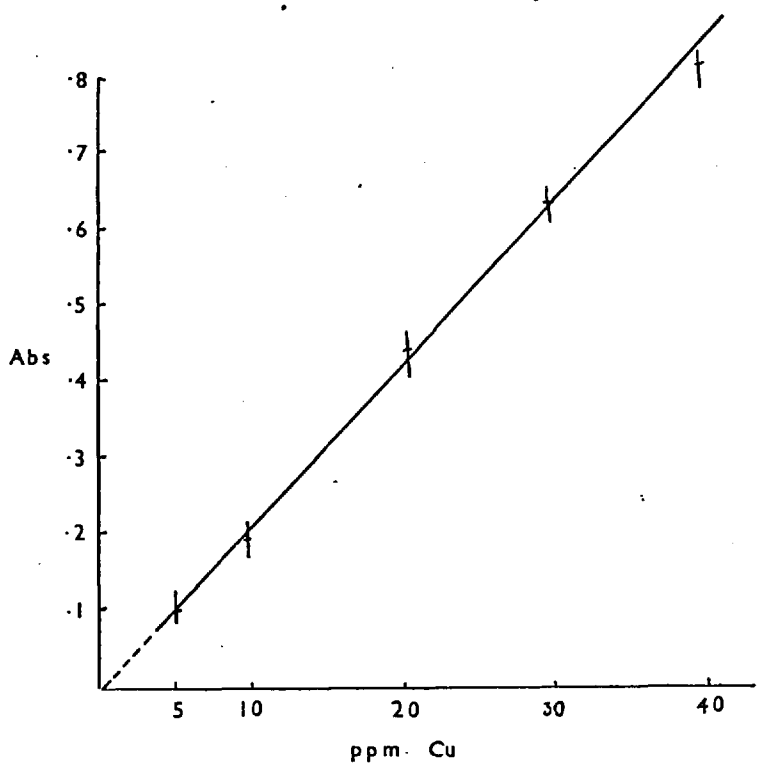

Figure 2.4 Analytical Growth Curve for Copper

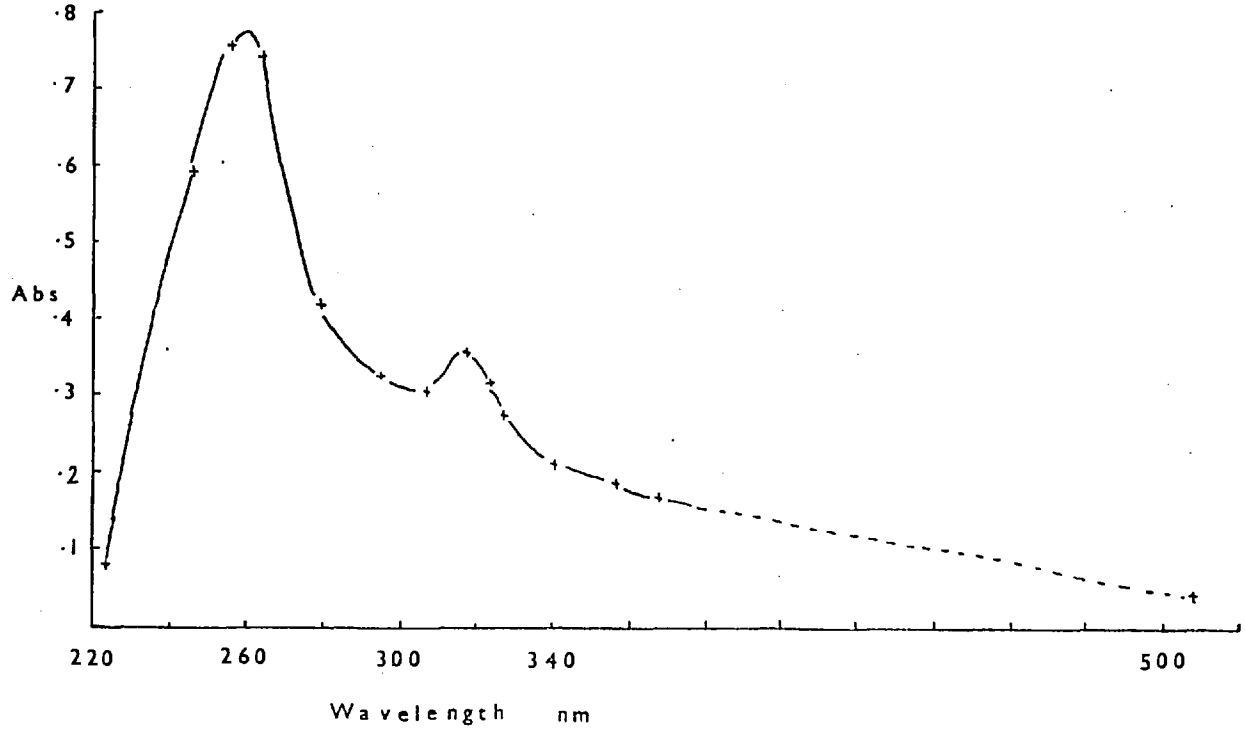

Figure 2.5 Absorption Spectrum for Copper

2.3.3 Variation of Absorbance with Background Electrolyte

It was found that in the absence of a background electrolyte, erratic and poorly reproducible absorption signals were obtained. For a given concentration of copper ions, a similar change in absorption was obtained in 0·1 M potassium chloride and 0·1 M potassium nitrate.

2.3.4 Variation of Absorption with Dissolved Oxygen Content

De-aeration of the solutions with oxygen free (white spot) nitrogen produced no appreciable difference in the changes in absorption measured.

2.3.5 Variation of Absorbance with Light Intensity

The light intensity was varied by altering the lamp current. The variation in absorbance at 324·8 nm for a 30 ppm Cu^{2+} solution in 0·1 M KCl with lamp current is shown in Table 2.2.

Table 2.2 Variation of Absorbance with Lamp Current

Current mA	Absorbance
1·1	0·30
1,2	0·29
1·5	0·29
2·9	0·27
4·3	0·27
5·9	0·28
8·5	0·28
10·0	0·28

It can be seen from the Table that the absorbance was not dependent on the light intensity.

2.3.6 Variation of Absorbance with Wavelength

As a hollow cathode lamp was used as a light source, the change in absorbance could only be monitored at a limited number of wavelengths. The results for a 30 ppm Cu^{2+} solution in 0·1 M KCl are shown in Figure 2.5.

2.3.7 Variation of Current with Voltage

With a 1% copper solution, a sharp increase in current was observed at a potential difference of 1·2 V and metallic copper could be seen on the electrode at 1·4 V. The results are shown in Figure 2.6 from which it can be seen that the cell decomposition potential was approximately 1·2 V.

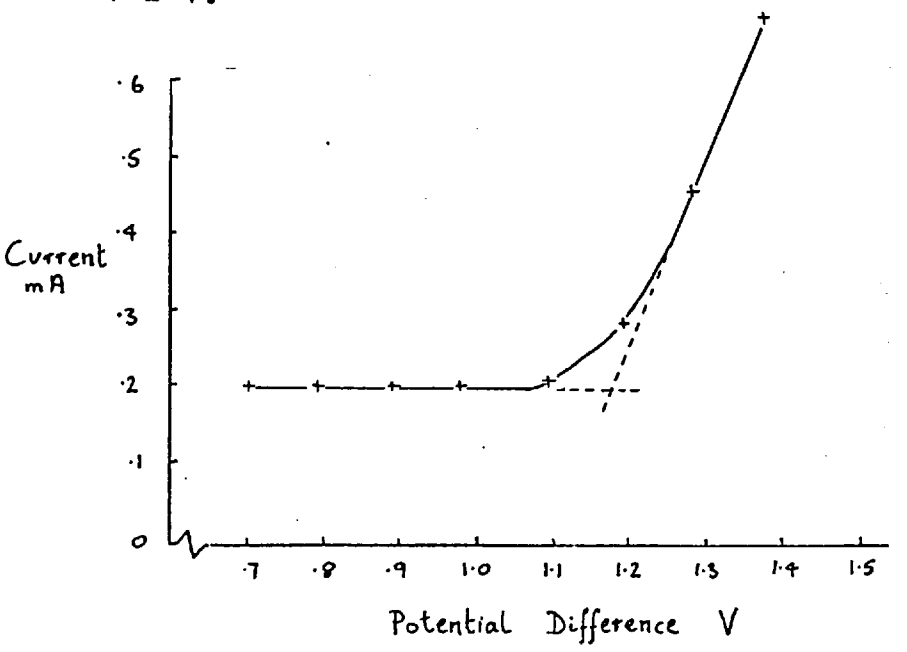

Figure 2.6 Variation of Current with Voltage

2.3.8 Summary of Results

From the results of the preceeding experiments, it is seen that the absorbance obtained on electrolysing a dilute solution of copper ions in an inert background electrolyte at platinum electrodes is:-

1. Dependent on the concentration of reducible metal ion.
2. Dependent on the potential difference between the electrodes.
3. Is erratic or non-existant in the absence of inert background electrolyte.
4. Independent of the amount of dissolved oxygen present.
5. Independent of the light source intensity.
6. Dependent on the wavelength at which the absorbance is measured.

2.4 Discussion

From the variation of current with voltage, it is deduced that at a potential difference greater than 1·2 V, electrolysis is occurring in 1% copper solutions. A theoretical decomposition potential may be calculated as follows on the basis of the Nernst equation (52).

The anode reaction is $2H_2O \longrightarrow O_2 + 4H^+ + 4e^-$ $E^o = 1{\cdot}229$ V

now

$$E = E^o + \frac{0{\cdot}059}{4} \log \frac{P_{O_2}[H^+]^4}{[H_2O]^2}$$

If the partial pressure of O_2 is taken as that in the atmosphere, i.e. 0·21 then

$$E = 1{\cdot}229 - 0{\cdot}425$$
$$= 0{\cdot}804 \text{ V}$$

The overvoltage for the discharge of O_2 at a smooth platinum surface is about 0·8 V (53).

The cathode reaction is

$$Cu^{2+} + 2e^- \longrightarrow Cu \qquad E^o = 0{\cdot}337 \text{ V}$$

and

$$E = E^o + \frac{0{\cdot}059}{2} \log Cu^{2+}$$

$$= 0{\cdot}337 - 0{\cdot}023$$

$$= 0{\cdot}314 \text{ V}$$

Therefore

$$E_{cell} = 0{\cdot}804 + 0{\cdot}8 - 0{\cdot}314 + IR$$

$$= 1{\cdot}29 + IR \text{ V}$$

where IR is the voltage drop due to the cell resistance. For each ten fold change in the copper concentration the decomposition potential is changed by 0·03 V. Thus for a 10 ppm solution the calculated decomposition potential is 1·38 V. Thus, as in most of the experiments a potential difference of 2·0 V was used, it is assumed that the decomposition potential for the cell was exceeded and that electrolysis was occurring.

It is thought that a number of effects could give rise to this change in absorbance. These include

1. distortion of the electrodes on applying the potential difference,
2. obstruction of the light beam by material deposited on the electrode surface,
3. scattering of light by gas bubbles or colloidal metal,
4. changes in the absorbance of the solution due to migration of the background electrolyte or reducible

metal ions,

5. change in reflectivity of the electrode surface,
6. absorption of light by a chemical species involving the metal ion generated during electrolysis,
7. absorption by a species not containing the metal ion or by a species generated in a secondary reaction.

Factor 1 may be discounted as there is no change in absorbance in the absence of the copper ions. As the absorbance decreases when the potential difference reverts to zero, there can be no permanent physical obstruction of the light path, also the change in absorbance is dependent on wavelength and thus factor 2 may be discounted. The dependence on wavelength also indicates that the light is not being scattered, and so factor 3 may be discounted as if scatter were occurring it would be expected that the change in absorption would increase with decreasing wavelength (54).

It is thought unlikely that light reflected from the surface of the cathode would enter the monochromator and so changes in reflected light intensity would not be monitored. In addition the effect observed here is about two orders of magnitude greater than for typical electroreflectance effects (6), and thus factor 5 may be discounted.

The experimental evidence discussed so far indicates that the change in absorbance observed is not due to a physical effect and must therefore be due to absorption

of light by a chemical species. If the change in absorbance were due to the migration of the background electrolyte under the action of the electric field generated when the potential difference is applied between the electrodes, then the effect would be observed in the absence of the reducible copper ions. The migration of the reducible species is eliminated by the presence of the large excess of background electrolyte and its arrival at the electrode is controlled by diffusion across a concentration gradient created by depletion of the species at the electrode surface by reduction. Thus in the vicinity of the electrode surface the concentration of the electroactive species is lower than that in the bulk solution, and if the analysing light beam only passes through this region then a decrease in absorbance would be observed. However, it is thought that the thickness of the diffusion layer is small compared with the thickness of solution that the light beam passes through, and so the concentration of reducible species in the light beam is virtually unchanged during electrolysis. Thus, on the basis of this argument, factor 4 may be discounted.

It would appear, then, that the reduction in light intensity is due to absorption of light by a chemical species generated during electrolysis. As only one metal ion has been studied so far, it is not possible to distinguish between factors 6 and 7 at this stage.

A similar discussion to that presented here is used

by Walker and Kenney (55) in their interpretation of the results of an experiment in which the absorbance of He/Ne laser light spiralled round the inside of a polished elliptical silver cathode is monitored during the electrolysis of a sodium sulphate solution. In their case, though, the results are interpreted as being due to the formation of hydrated electrons next to the cathode. The possibility of hydrated electrons being involved in the electrode process observed here will be discussed later (see Section 5.3).

In order to continue the study of the absorption phenomena observed in these preliminary experiments, the use of the Varian Techtron model 1000 instrument was discontinued and apparatus was assembled from individual components. The design and development of this apparatus and the experiments performed with it are discussed in the next chapters.

3. INSTRUMENTATION

3.1 Apparatus

From the preliminary experiments, it was apparent that the apparatus required was a single beam uv/visible spectrophotometer i.e. light source, cell, monochromator, photodetecting device and readout, together with a siutable source of potential difference. The cell would contain the electrodes and suitable means of removing the solutions by suction and introducing nitrogen to deaerate the solutions.

As the absorption spectrum of the species generated in the copper solutions was fairly broad, it was decided that the hollow cathode lamps used in the preliminary experiments were not necessary and that a continuum source would be satisfactory.

A means of varying the position of the light beam with reference to the cathode was also required. The source of potential difference and related circuitry needed no modification from that already described. The first instrument that was assembled is shown schematically in Figure 3.1. The light source was a quartz halogen lamp (Philips type 12336) which was run from a regulated power supply (APT Electronic Industries type TCU 550). A 2 cm silica cell was used with slits in front and behind. Three silical lenses were incorporated into the optical system. All the optical components were mounted on an

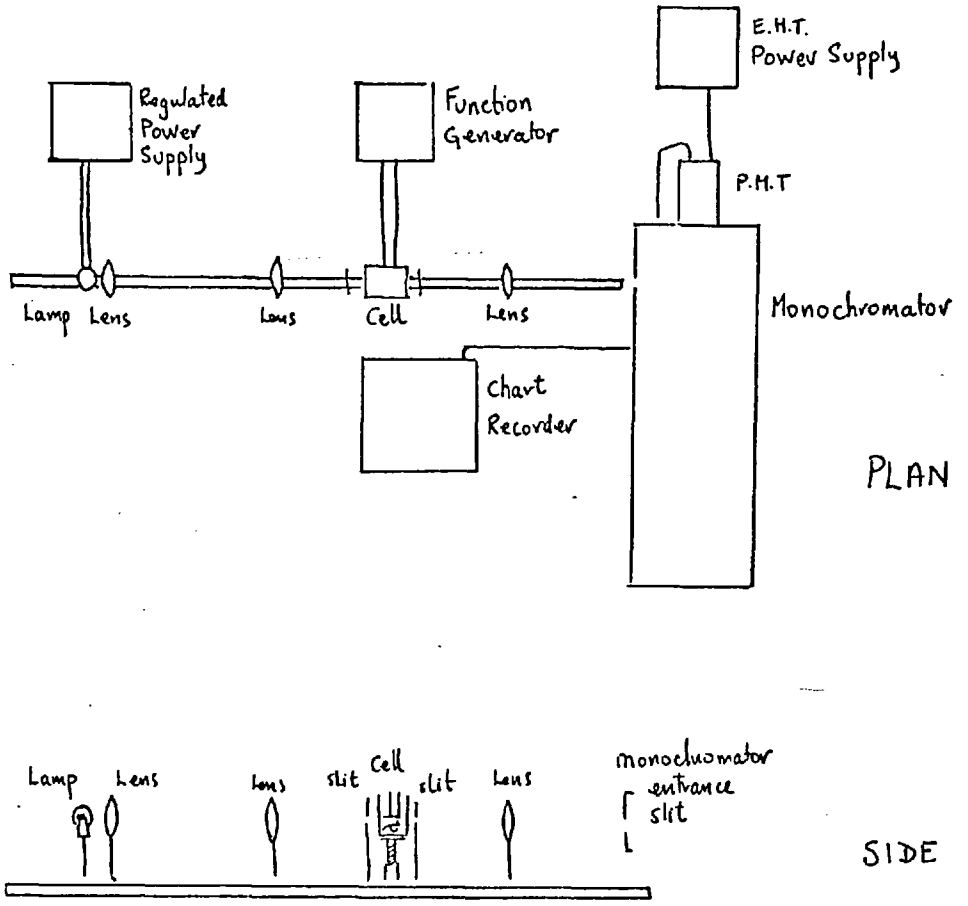

Figure 3.1 Schematic Diagram of Apparatus

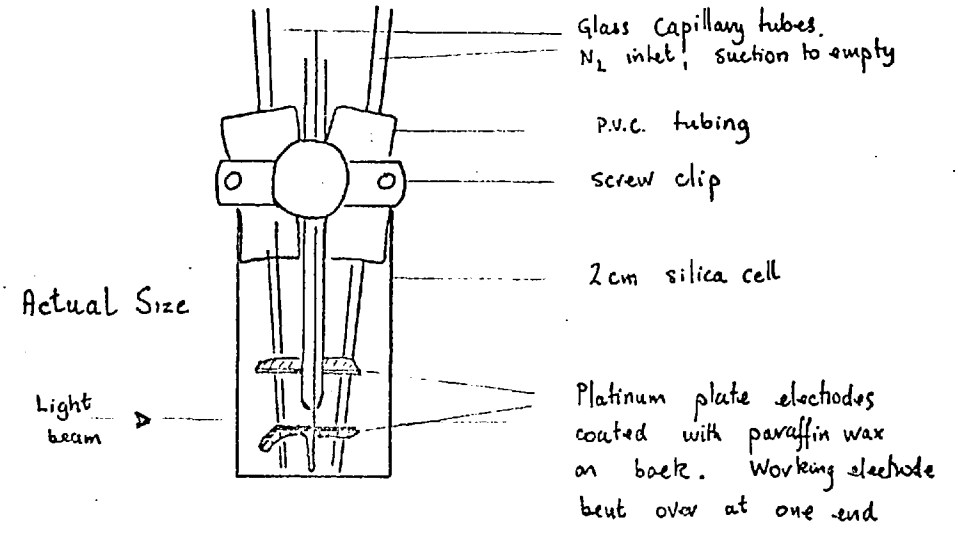

Figure 3.2 Cell and Electrode Assembly

optical bar (Ealing Beck 'Trirack') and could be moved along the bar by means of a rack and pinion mechanism. The cell holder was mounted on vertical and lateral (right angles to the direction of the optical bar) racking devices. The monochromator used was an Optika CE 4. The light intensity was monitored by a photomultiplier tube (E.M.I. type 6265B) with a Brandenburg type 475R e.h.t. power supply. The resulting photo-current was passed through a standard resistor and the voltage drop monitored by a chart recorder (Smiths 'Servoscribe type RE 511.20). The electrodes were mounted in the cell as shown in Figure 3.2. The potential difference was supplied by a function generator (Hewlett Packard type 3310A).

The optical components were set up with the cell removed so as to get as much light as possible into the monochromator. The cell containing the electrodes was then mounted in the light path and by adjusting the position of the cell in the vertical plane, the amount of light passing over the electrode surface could be varied. Lateral adjustment of the cell position ensured that light passed only over the surface of the electrode.

3.2 Study of Copper Solutions

The experimental technique used in most of these experiments is set out below.

1. The function generator was set to give the required potential difference (2·0 V) when switched on.
2. A 5 ml aliquot of the solution was placed in the cell and deaerated with 'white spot' nitrogen for two minutes.
3. The required wavelength was set on the monochromator.
4. The 0% absorption and 100% absorption readings on the chart recorder were set.
5. The chart recorder was started and the potential difference was applied. The absorption was recorded until a maximum was reached.
6. The solution was removed from the cell by suction.
7. With the suction still applied, a potential of 5 V was applied so that the electrode in the light path became the anode, the cell was then washed through with background electrolyte solution and rinsed with distilled water. This method of cleaning the working electrode of any metal plated onto it during the electrolysis by anodic stripping was preferred to that of washing with concentrated nitric acid used previously as nitrate has a strong absorption band centered at 203 nm ($\epsilon = 10^4$ l mole^{-1}cm^{-1}) and traces of acid left in the cell produced spurious signals.
8. The procedure was repeated as required.

3.2.1 Variation of Absorbance with Wavelength

Using the method outlined above the variation of absorbance with wavelength was studied, i.e. the concentration of the solution in step 2 was kept the same but the wavelength setting in step 3 was altered each time.

The spectrum obtained with a 30 ppm Cu^{2+} solution in 0·1 M KCl is shown in Figure 3.3 and it can be seen that it is essentially similar to that obtained in the preliminary experiments (see Figure 2.5).

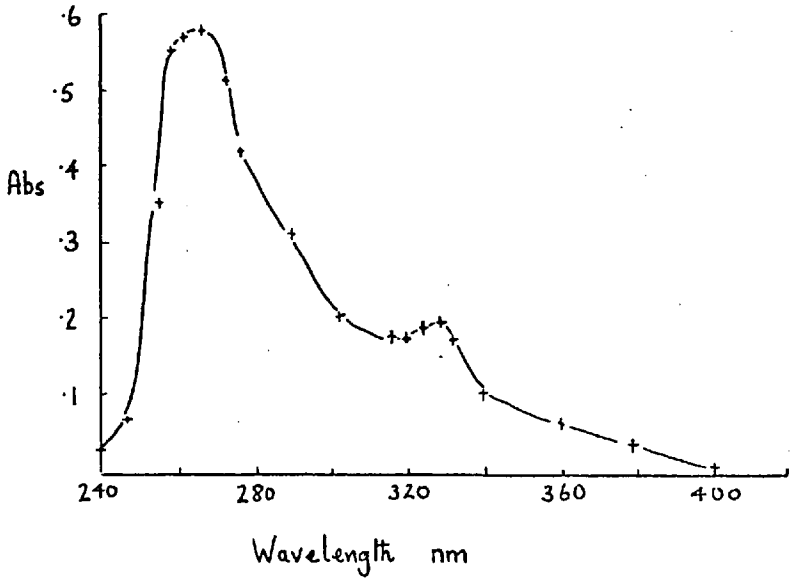

Figure 3.3 Absorption Spectrum for 30 ppm Copper

It is thus concluded that the same effect is being produced and monitored with this apparatus as in the preliminary experiments.

3.2.2 Variation of Absorbance with Distance from the Electrode Surface

Starting with the working electrode raised into the light beam as far as possible consistent with settings of 0% absorption and 100% absorption being obtainable on the chart recorder, the absorption obtained on applying a potential difference of 2·0 V between the electrodes was found for a given concentration of copper (20 ppm in 0·1 M KNO_3) at a fixed wavelength (270 nm). The height of the light beam above the electrode surface was increased by lowering the electrode out of the light beam. The absorption was measured for successive new positions of the electrode.

The results of the experiment are shown in Table 3.1 and the variation of absorption with time for certain positions of the electrode is shown in Figure 3.4.

As the electrode is raised into the light path, the e.h.t. supply to the photomultiplier tube had to be increased so that a reading of 0% absorption could be obtained on the chart recorder before the potential difference was applied. At e.h.t. values greater than 1·2 kV, the signal recorded was noisy and also because of stray light entering the monochromator, a value of 100% absorption was not obtained when the light beam was interrupted by an opaque material. It was found preferable to keep the e.h.t. supply fixed at approximately 1 kV and to change the gain of the system using the voltage range

Table 3.1 Absorbance as a Function of Distance from the Electrode Surface

Vertical scale reading. mm	% absorption	Time before first abs. observed. sec
26·1	62·0	0
26·0	63·1	0
25·9	61·0	0
25·7	52·4	0
25·6	41·9	0
25·5	35·1	0
25·3	32·2	7
25·1	30·1	11
25·0	32·0	22
24·5	13·0	38
24·0		60
23·5		74
23·0		88

With the last three positions of the electrode no maximum absorption was recorded.

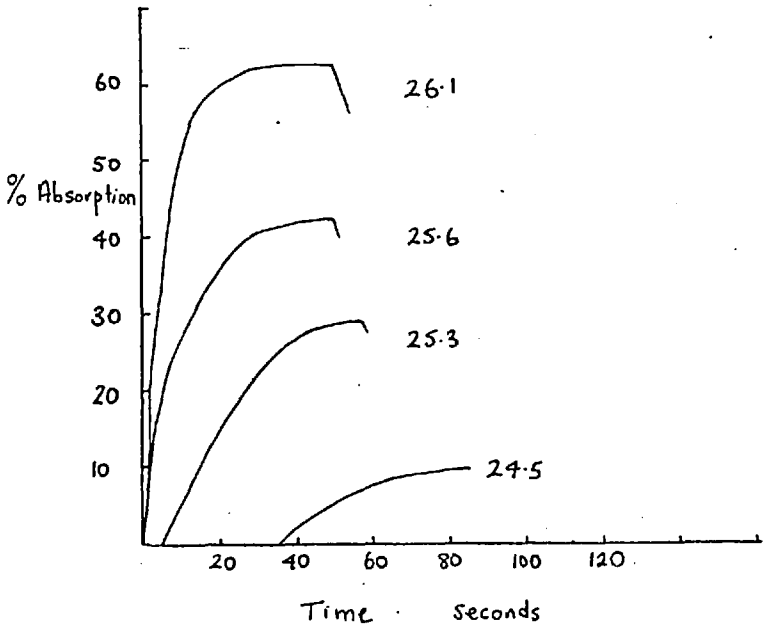

Figure 3.4 Absorption-Time Curves

controls on the chart recorder.

From the results it can be seen that the effect is only detectable within approximately 2·5 mm of the cathode surface. Also because of the delay in the start of the absorption, which occurs when the light beam passes above the electrode surface, it would seem that the absorbing species is being produced at the cathode surface and then diffusing out into the solution and is not arriving in the light path by some transport process from the bulk solution.

3.3 Study of Other Elements: Cadmium, Silver and Mercury

After some initial difficulty, absorption signals were obtained for solutions of cadmium in a background electrolyte of 0·1 M KCl. The absorption spectrum obtained was similar to that obtained with the copper solutions, with a maximum at 250 nm. A plot of absorbance against concentration was linear over the range 0-25 ppm.

With silver solutions, a decrease in absorption was recorded on applying a potential difference, but the absorbance did not vary with wavelength and remained at approximately 0·2 over the range 220-550 nm for a 50 ppm solution and a potential difference of 2·0 V. This change in absorption was attributed to scatter.

No change in absorption was observed when a potential difference was applied using solutions of mercuric ions. A large range of wavelengths was tried and three background

electrolytes were used, potassium sulphate, chloride and nitrate, without success.

3.4 Study of Chloride, Bromide and Iodide Solutions

With only 0·1 M potassium chloride background electrolyte in the cell, it was found that large absorption signals were observed when the electrode in the light path was made the anode i.e. was positively charged with respect to the other electrode so that oxidation reactions would occur in the light path. The absorption was observed at potential differences greater than 1·0 V and covered the wavelength range 220-380 nm with a maximum at 300 nm (see Figure 3.5). In addition, if, after the absorbance observed during oxidation had been recorded, the polarity of the electrodes was reversed so that the electrode in the light path became the cathode, a second absorbance peak was observed having a similar spectral distribution as the first peak. However, as has been reported earlier, no absorbance was observed if the electrode in the light path was made the cathode first. Solutions of potassium bromide and potassium iodide were also investigated and found to give strong absorption signals at potential differences greater than 0·7 V and 0·5 V respectively when the electrode in the light path was made the anode. No absorption was observed when the polarity was reversed (unlike the potassium chloride solutions). The spectral distributions are shown in

Figure 3.5.

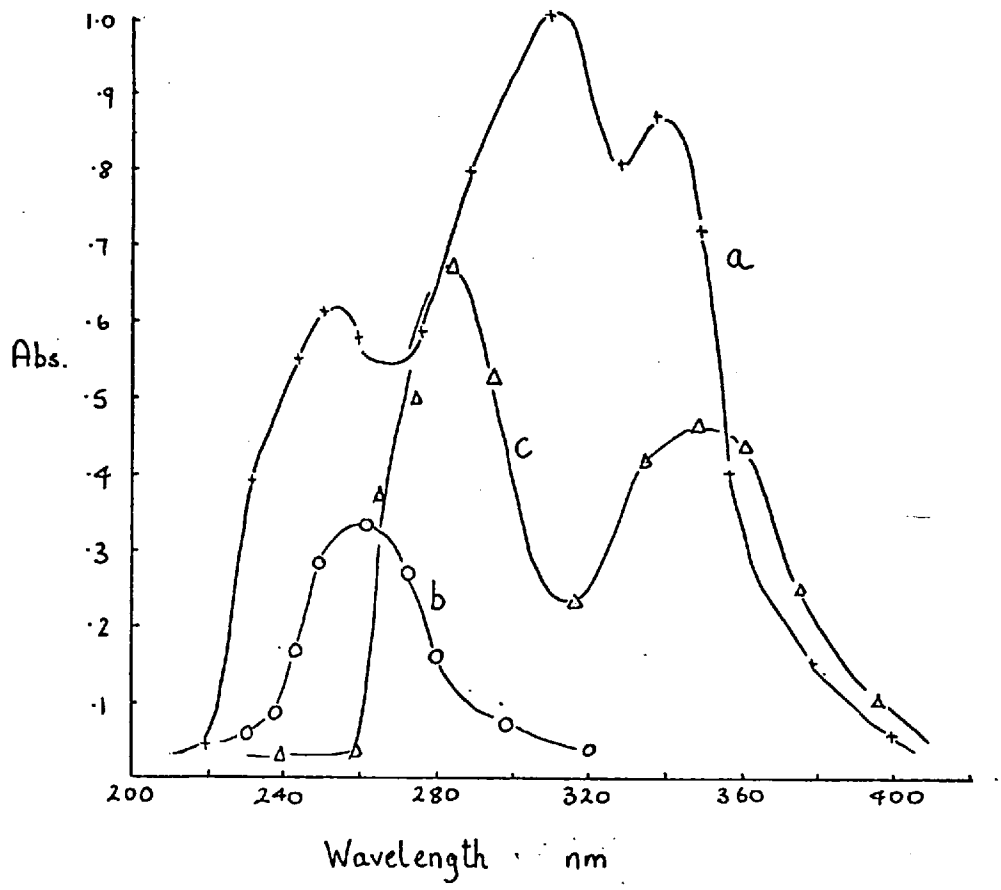

Figure 3.5 Absorption Spectra Obtained on Oxidizing a, KCl. b, KBr. c, KI Solutions

When the potential difference was switched on, a green-brown coating formed on the electrode in the light path in the case of bromide and a brownish coating was observed in the case of iodide. No coating was seen on the electrode in the case of chloride. By comparing the spectra obtained with those of a hypochlorite solution, a solution of bromine in water and a solution of iodine

in water, it was deduced that the absorbance was due to the formation of chlorine, bromine and iodine respectively on the electrode surface. The absorbance observed on reversing the polarity in the case of chloride is explained by the reduction of hypochlorite formed by the hydrolysis of chlorine. Bromine and iodine do not hydrolyse to the same extent (56). The proposed reaction scheme is as follows.

1. $2Cl^- \longrightarrow Cl_2 + 2e^-$

oxidation of chloride to chlorine

2. $Cl_2 + H_2O \longrightarrow H^+ + Cl^- + HOCl$

disproportionation to chloride and hypochlorous acid

3. $2HOCl + 2e^- \longrightarrow Cl_2 + 2OH^-$

reduction of hypochlorous acid to chlorine

In addition it appears that the solution is not basic in the vicinity of the electrode as bromine dissolves fairly rapidly to give bromate and iodine dissolves extremely rapidly to give iodate quantitatively (56). The spectra recorded do not resemble those of bromate or iodate.

When the concentration of halide was reduced to 50 ppm and the solutions made up in 0·05 M potassium sulphate, no absorbance was detected for chloride or iodide but with bromide an absorbance of 0·04 was obtained at 270 nm with a potential difference of 2·0 V.

3.5 Problems in the Study of Iron Solutions

The main difficulty with ferrous iron solutions was the prevention of oxidation to ferric iron by dissolved atmospheric oxygen followed by hydrolysis to give ferric hydroxide or hydrous ferric oxide. All solutions were deoxygenated with nitrogen and kept under a nitrogen blanket. With ferric solutions the pH had to be low (about 3) to avoid hydrolysis and precipitation of ferric hydroxide. This increase in the concentration of hydrogen ions meant that hydrogen was more easily discharged and consequently the potential range accessible was reduced.

It was found that absorption signals could be obtained from both ferrous and ferric solutions. The absorption showed the same sort of variation with wavelength and concentration as had been observed with copper and cadmium However, it was noted with the ferric solutions which were made up in 0·1 M KCl as background electrolyte, that at potential differences less than 1·4 V an increase in the transmission of the solution was observed when the potential was first applied. As the solutions were acid and contained a large excess of chloride, it was thought that the iron might be complexed predominantly as an anionic species such as $FeCl_4^-$ and thus when a negative charge was applied to the electrode in the light path, such a negatively charged species would be repelled. In order to see whether there was any relation between the absorption spectrum of the species being removed from the light path

(thus causing an increase in transmission) and the species existing in an acid solution of ferric ions in the presence of excess chloride, the absorption of the ferric solution was obtained using a Perkin Elmer model 402 recording instrument and using the experimental apparatus. As the experimental apparatus is only single beam and the cell is essentially fixed in the light path, the method of recording the spectrum was as follows.

1. The clean cell was filled with distilled water.
2. The voltage range on the chart recorder was fixed.
3. The wavelength was set at the required value.
4. The e.h.t. to the photomultiplier tube was varied until 100% transmission was obtained on the chart recorder. This value of the e.h.t. was noted.
5. Steps 3 and 4 were repeated until the desired wavelength range was covered.
6. The distilled water was replaced by the ferric solution
7. The wavelength was set to the required value and the e.h.t. value noted in step 4 set.
8. The absorption was recorded.
9. Steps 7 and 8 were repeated until the desired spectral range had been covered.

The spectrum recorded in this manner and that recorded on the Perkin Elmer model 402 are shown in Figure 3.6. As there was a discrepancy between these two spectra, the spectrum of a dilute potassium permanganate solution was obtained on each instrument and compared. The spectra

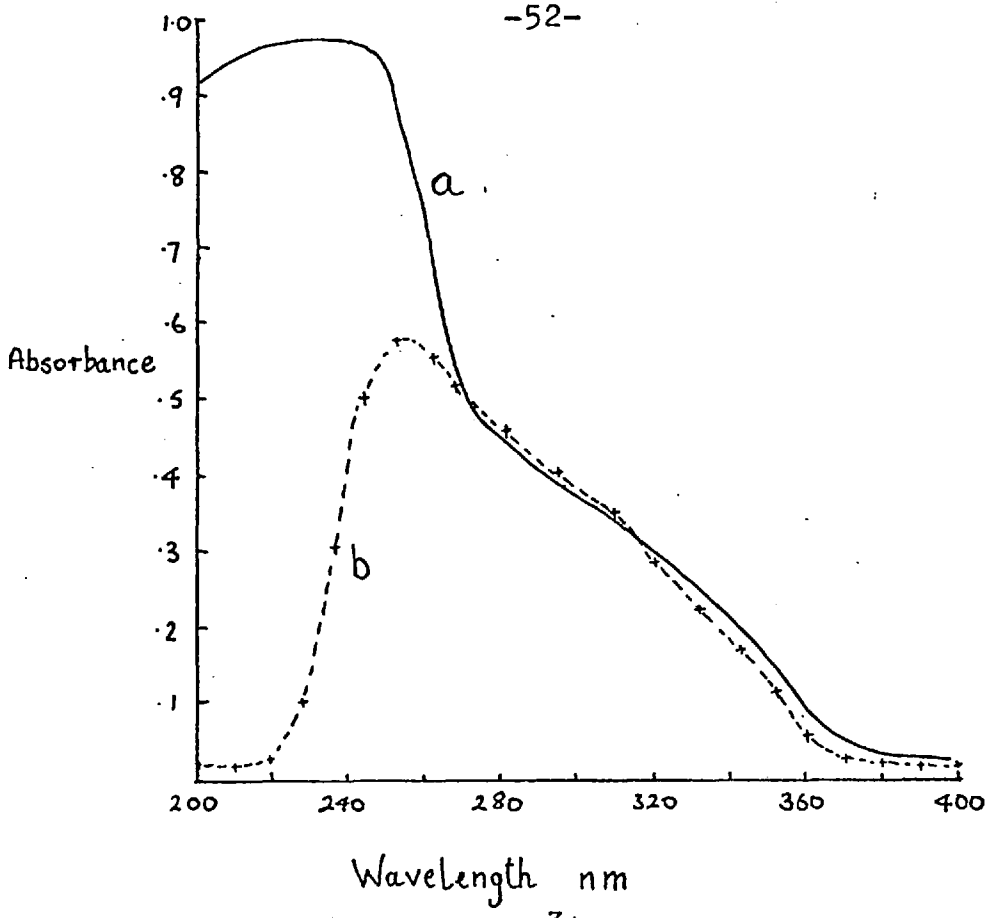

Figure 3.6 Comparison of Fe^{3+} Absorption Spectra.
a, Perkin Elmer 402 b, experimental apparatus.

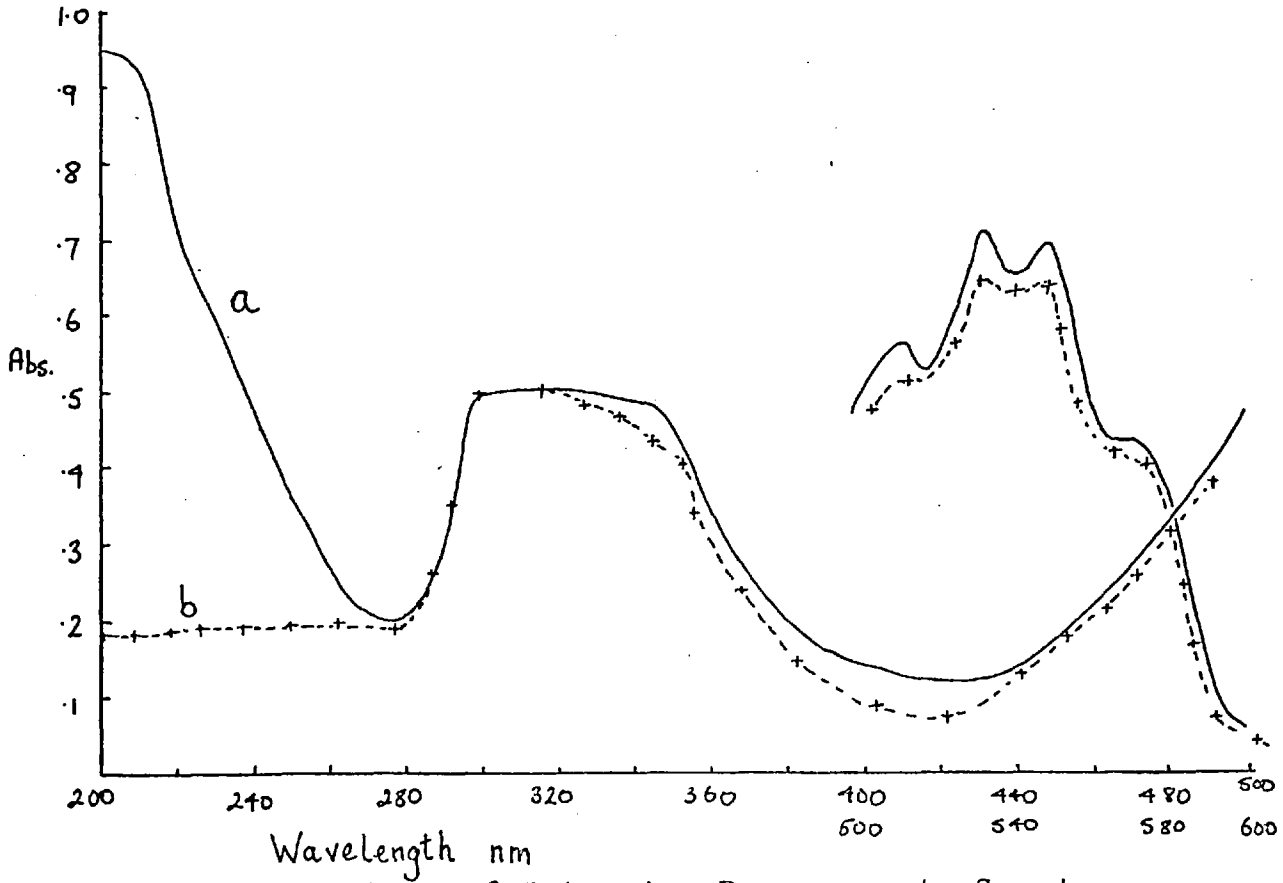

Figure 3.7 Comparison of Potassium Permanganate Spectra
a, Perkin Elmer 402. b, experimental apparatus.

are shown in Figure 3.7. From these two sets of spectra, it was apparent that below 280 nm incorrect absorption values were being obtained, possibly because no light of these wavelengths was being emitted by the source.

3.6 Modification of Apparatus

The light source was changed for a hydrogen lamp and tungsten filament lamp (Unicam SP 500 lamp supply). Both lamps were mounted in a single housing containing a movable concave mirror, so that light from either lamp could be directed along the optical path. The tungsten filament lamp was run from the regulated power supply that had been previously used to run the quartz halogen lamp, and the hydrogen lamp was run from a Unicam 220 watt power supply. The spectrum of a dilute acetone solution obtained using the quatrz halogen lamp, the hydrogen lamp and the Perkin Elmer 402 are shown in Figure 3.8, from which it can be seen that the spectrum obtained with the hydrogen lamp agrees with that obtained on the Perkin Elmer 402.

The Hewlett Packard function generator was changed for a Chemtrix type 804 potentiostatic waveform source. This had the advantages over the Hewlett Packard component of 1) having the facility to incorporate a third, reference electrode into the circuit, 2) having a single-shot facility as well as a repetitive mode of operation and 3) having a built-in voltmeter/milleammeter. A centre-zero voltmeter was connected across the electrodes. The

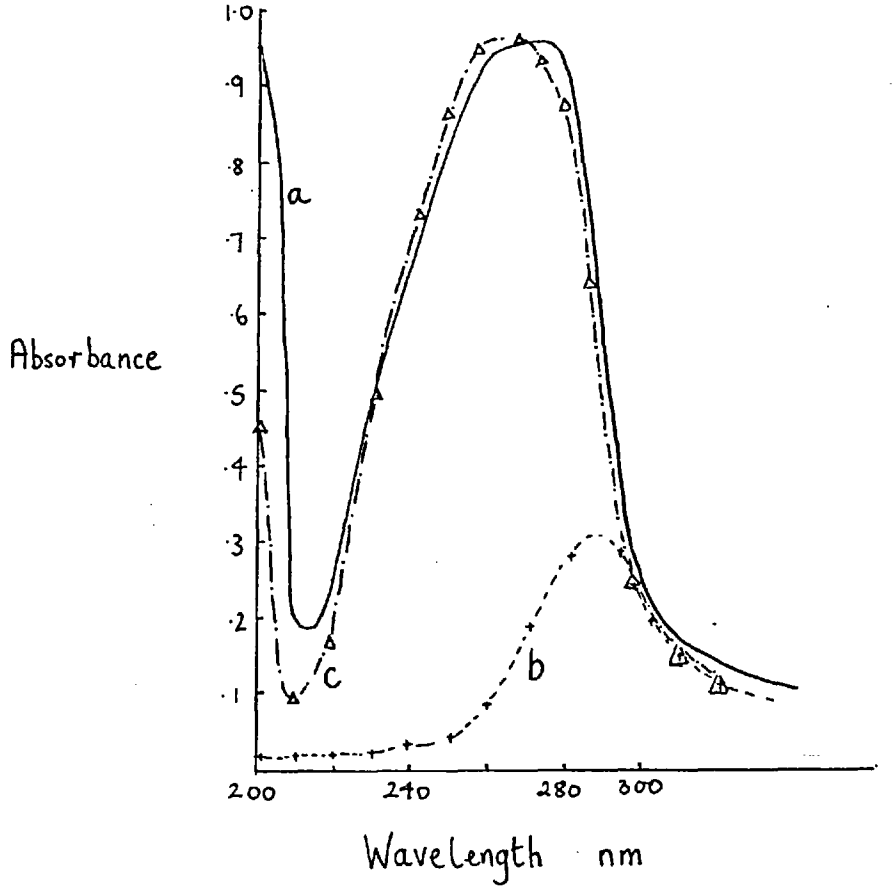

Figure 3.8 Comparison of Acetone Spectra.
a, Perkin Elmer 402. b, experimental apparatus quartz halogen lamp. c, experimental apparatus hydrogen lamp.

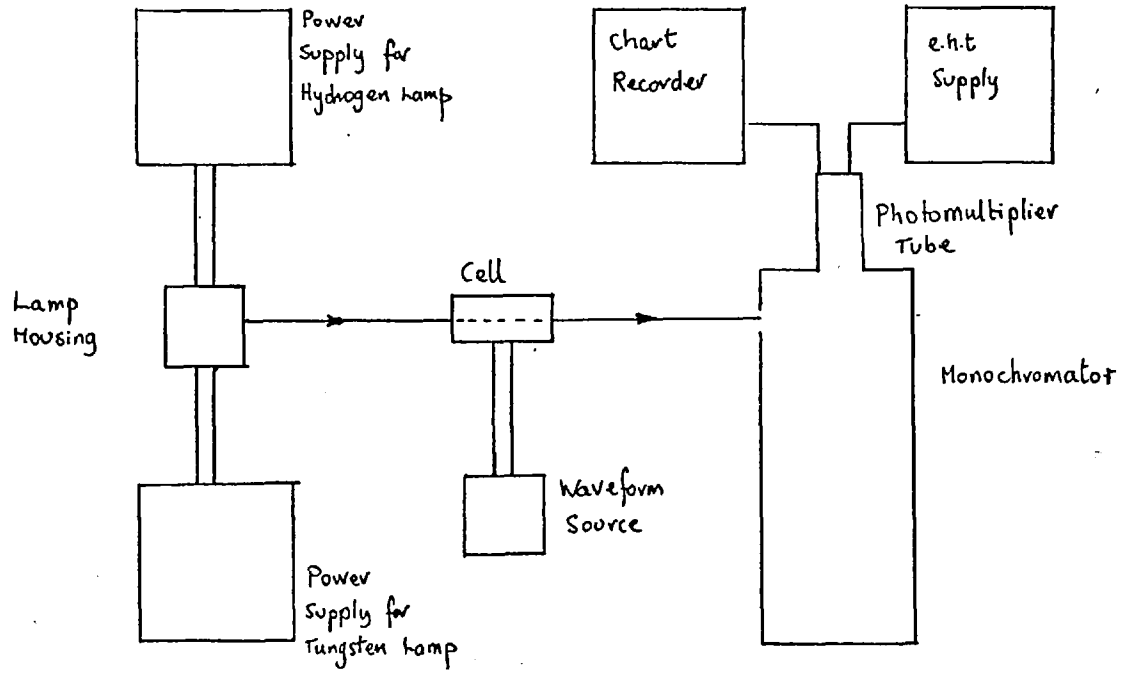

Figure 3.9 Schematic Diagram of Apparatus

modified apparatus is shown schematically in Figure 3.9 and was used with only one minor alteration (change of the hydrogen lamp for a deuterium lamp) for the rest of the experimental work. A calomel reference electrode was included for some of the current-voltage studies involving cadmium described later (see Chapter 6).

4. SYSTEMATIC STUDY OF METAL ION SOLUTIONS

4.1 Introduction

Having resolved the problems associated with the apparatus, attention was turned to the study of the absorption phenomenon itself. It was decided that the best approach to the problem would be to study the effect on the absorption signal of varying the relevant parameters in turn while keeping the others fixed. In the preliminary experiments some of these parameters have already been mentioned in connection with copper (see Section 2.3) and it seems likely that the parameters involved are:-

1. nature of the metal ion
2. nature of the background electrolyte
3. dissolved oxygen content
4. pH of the solution
5. wavelength
6. potential difference
7. concentration of reducible species
8. distance above the electrode surface and
9. nature of the electrode surface.

As it is desired to study the possible analytical applications of the phenomenon, the approach chosen was to change the metal ion and study the effect of varying wavelength, potential difference and concentration on any absorption signal obtained. The method used was to prepare a dilute solution of the metal ion (about 20 ppm)

in an inert background electrolyte, and by a series of trial experiments to find a wavelength at which absorption signals could be obtained. At this wavelength, the pretreatment and voltage conditions necessary to obtain reproducible signals were found and under these conditions, the variation of absorbance with wavelength was obtained. At the absorbance maximum, the variation of absorbance with voltage and with concentration of the metal ion were investigated.

4.2 Preparation of Solutions

Stock metal ion solutions containing 1% (10,000 ppm) of the metal were prepared by dissolving the appropriate amount of the AnalaR grade salt in 100 ml of distilled water. Usually the chloride or sulphate was used. The solutions were stored in polythene bottles except silver, which was stored in a brown glass bottle, and ferrous iron, which was stored under a nitrogen blanket in a volumetric flask. Stock 1 M potassium chloride and 0·3 M potassium sulphate were prepared by dissolving the appropriate amount of the AnalaR grade salt in 1 litre of distilled water. Metal ion solutions (100 ppm) were prepared by diluting 1 ml of the stock solutions to 100 ml with distilled water and a further dilution was made to give the required working solutions. The appropriate amount of background electrolyte was added, so that on finally making up to the mark, the solution was 0·1 M with

respect to potassium chloride or 0·03 M with respect to potassium sulphate. These two solutions have the same ionic strength. The 100 ppm metal ion solutions were made up every two to three days and the more dilute solutions were made up every day.

4.3 Copper

The absorption spectrum at 2·0 V of a 10 ppm solution in 0·1 M KCl was obtained. As the absorption maximum appeared to be stable for a considerable time, the method used was similar to that described in Section 3.5. The variation of absorbance with potential difference was obtained at 235 nm for a 10 ppm solution in 0·03 M K_2SO_4 and also the variation of absorbance with concentration. The results are shown in Figure 4.1. It can be seen from the Figure that there is a marked difference between the absorption spectrum obtained with the hydrogen lamp and that obtained with the quartz halogen lamp (which was similar to that obtained in the preliminary experiments using a copper hollow cathode lamp). It has been shown that the quartz halogen lamp had very little uv component and it seems possible that a similar effect was also obtained with the Varian Techtron instrument.

4.4 Cadmium

The absorption spectrum for 10 ppm cadmium in both 0·1 M KCl and 0·03 M K_2SO_4 background electrolyte solutions were recorded and are shown in Figure 4.2.

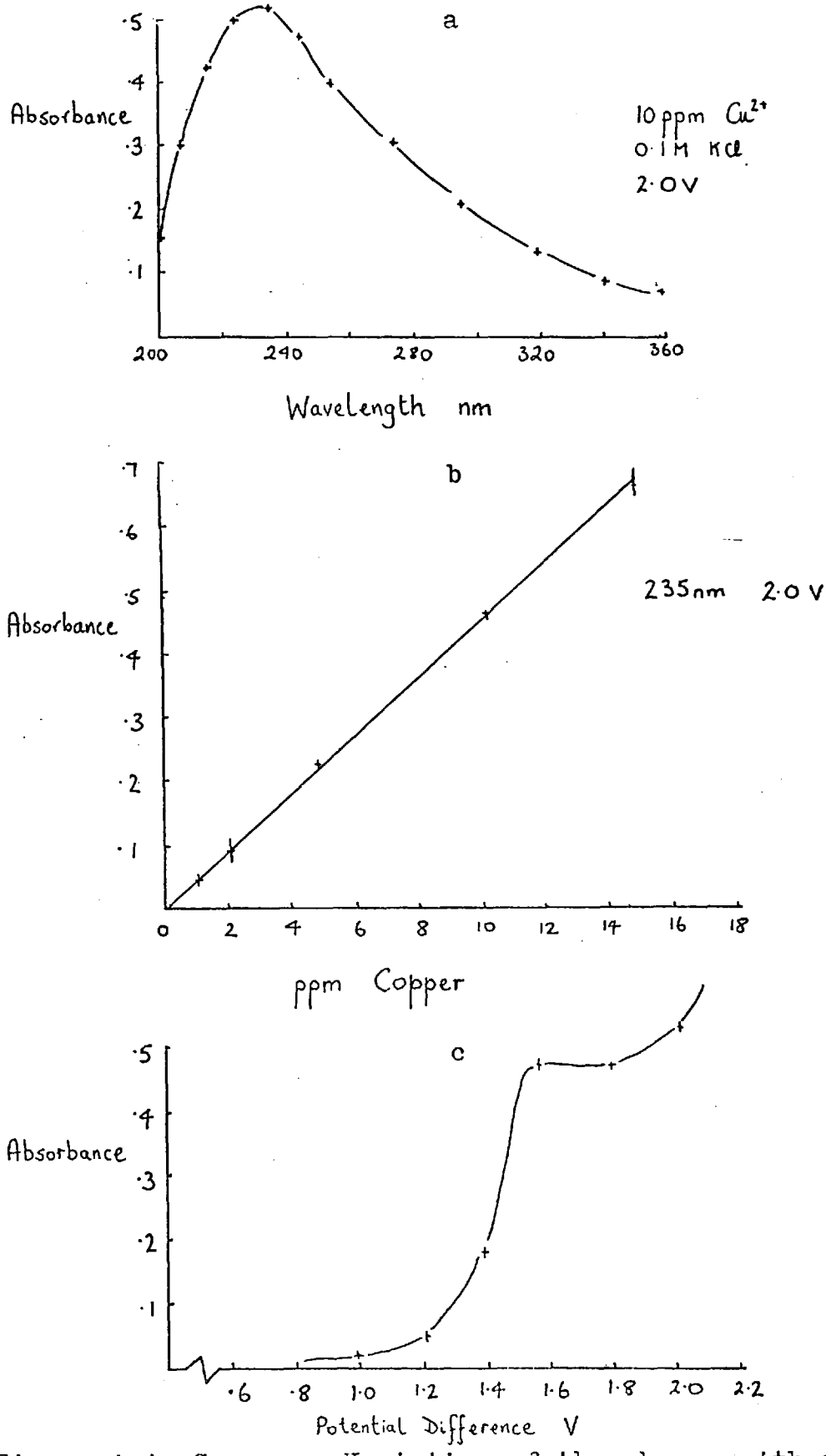

Figure 4.1 Copper. Variation of Absorbance with a, Wavelength b, Concentration c, potential

The variation of absorbance with concentration in 0·1 M KCl solutions is also shown in the Figure.

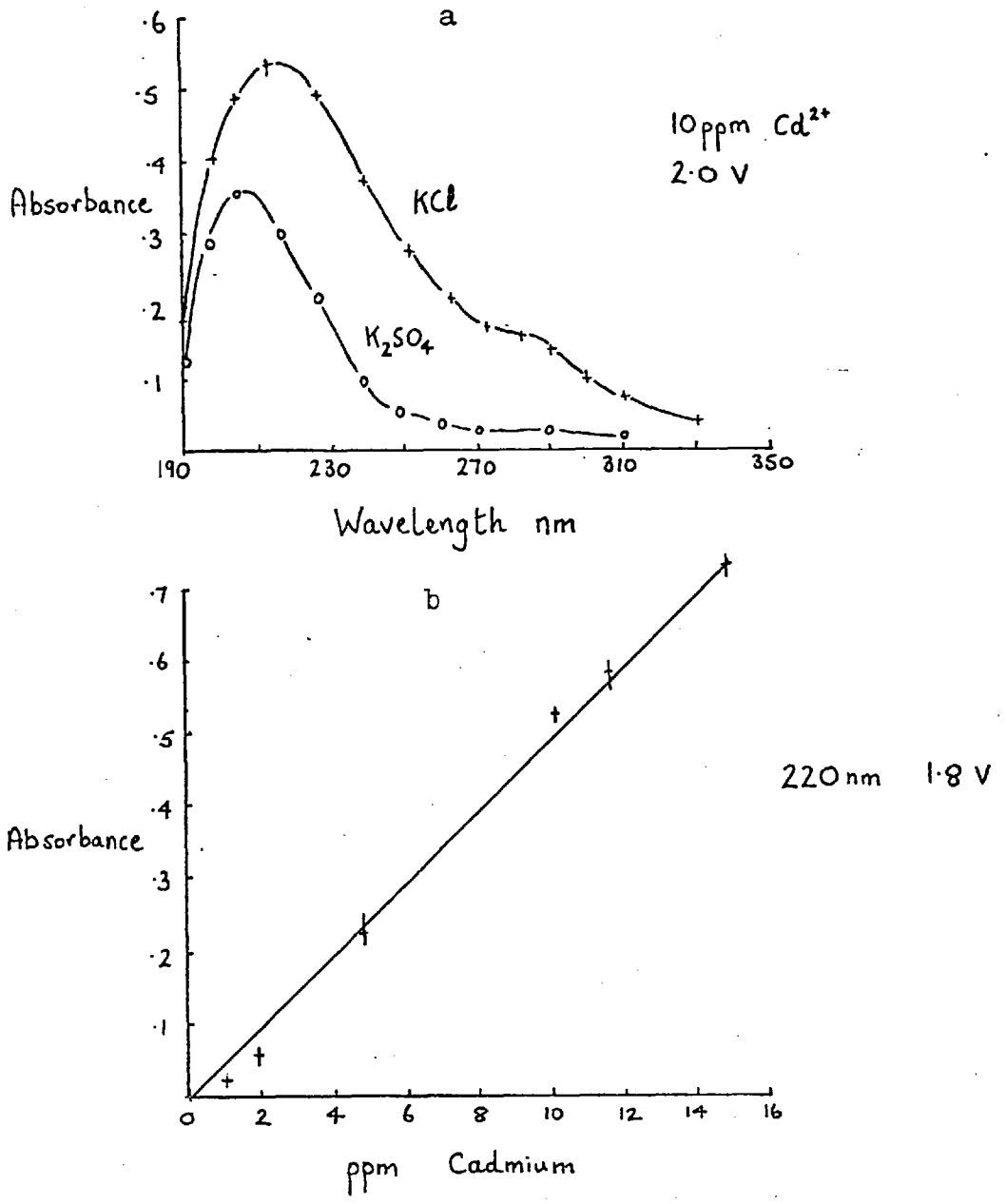

Figure 4.2 Cadmium. Variation of Absorbance with a, wavelength b, concentration.

4.5 Mercury

As before (Section 3.3) no inrease in absorption was detected on applying a potential difference. However, at a potential difference of 0·8 V a decrease in absorption was observed. A comparison between the spectral distribution of this decrease and the absorption spectrum of the mercury solution in 0·03 M K_2SO_4 with respect to 0·03 M K_2SO_4 suggested that the decrease could be due to a migration of mercury species out of the light path when the potential difference was applied. As mercury has a more positive standard electrode potential than copper (0·85 V and 0·337 V respectively), it would be expected that mercuric ions would be easier to reduce than cupric ions and thus under potential conditions at which copper is reduced, mercury would also be reduced. It is concluded that in the reduction of mercuric ions at a platinum electrode absorbing species analogous to those obtained with copper and cadmium are not formed.

4.6 Iron

The main problem associated with ferric iron solutions has already been outlined in Section 3.5 i.e. hydrolysis. As the stock solution was made up in hydrochloric acid, dilution produced an increase in pH and it appeared that, in 0·1 M KCl, solutions containing 40 ppm or more iron were stable with respect to hydrolysis. The pH of a 40 ppm solution was calculated to be 3·0. The variation of

absorbance with wavelength and absorbance with concentration (at 255 nm) was obtained. The results are shown in Figure 4.3

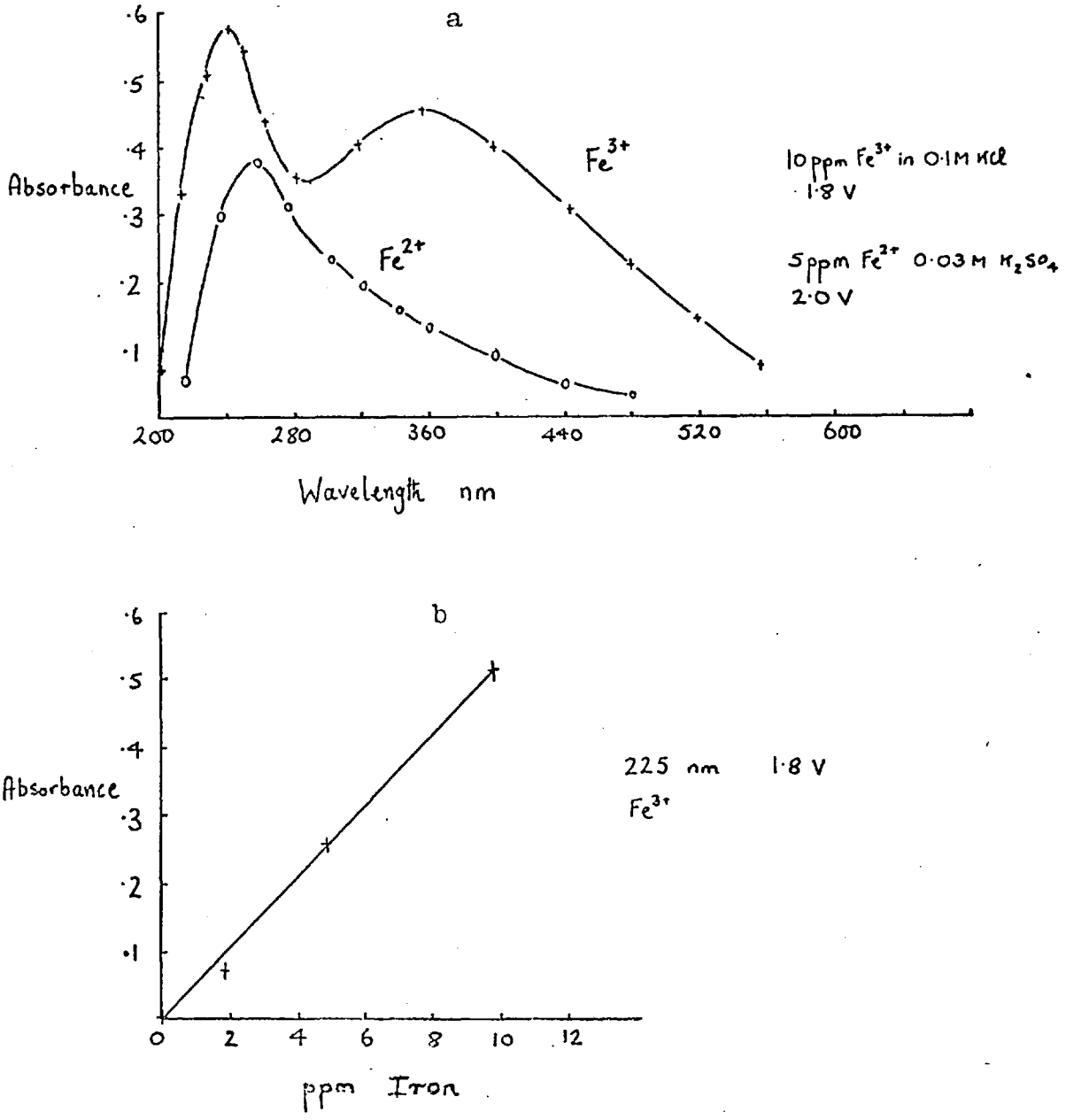

Figure 4.3 Iron. Variation of Absorbance with a, wavelength b, concentration

Attempts to produce absorption signals from solutions in which the pH was controlled by the addition of a buffer were not successful. A pH 2·4 buffer made from potassium hydrogen phthalate and hydrochloric acid produced a green precipitate when added to ferric solutions and a pH 2·6 buffer made from disodium hydrogen orthophosphate and citric acid produced a green colouration on adding to the iron solutions. With the latter, no change in absorbance was observed on applying a potential difference that was not due to the evolution of hydrogen. These results are interpreted as being due to complex formation between the iron and the organic component of the buffer solutions.

The results obtained for ferrous iron before the final modification of the apparatus are also shown in Figure 4.3. It should be borne in mind that the absorption values below 270 nm do not have much significance and the absorption maximum at around 270 nm is most likely an instrumental artifact.

4.7 Lead

A stock solution of 1% Pb^{2+} as lead acetate in dilute acetic acid was used. The variation of absorbance with wavelength for a 20 ppm solution in 0·1 M KCl at a potential difference of 2·0 V is shown in Figure 4.4. At this point problems were encountered with the electrode assembly and it was eventually found that one of the platinum wires had fractured just below the electrode

and only intermittent contact was being made. After this had been repaired the sensitivity was reduced and although the absorption spectrum obtained was the same, the magnitude of the absorbance was reduced. The variation of absorbance with concentration at 270 nm and a potential difference of 1·9 V is also shown in Figure 4.4.

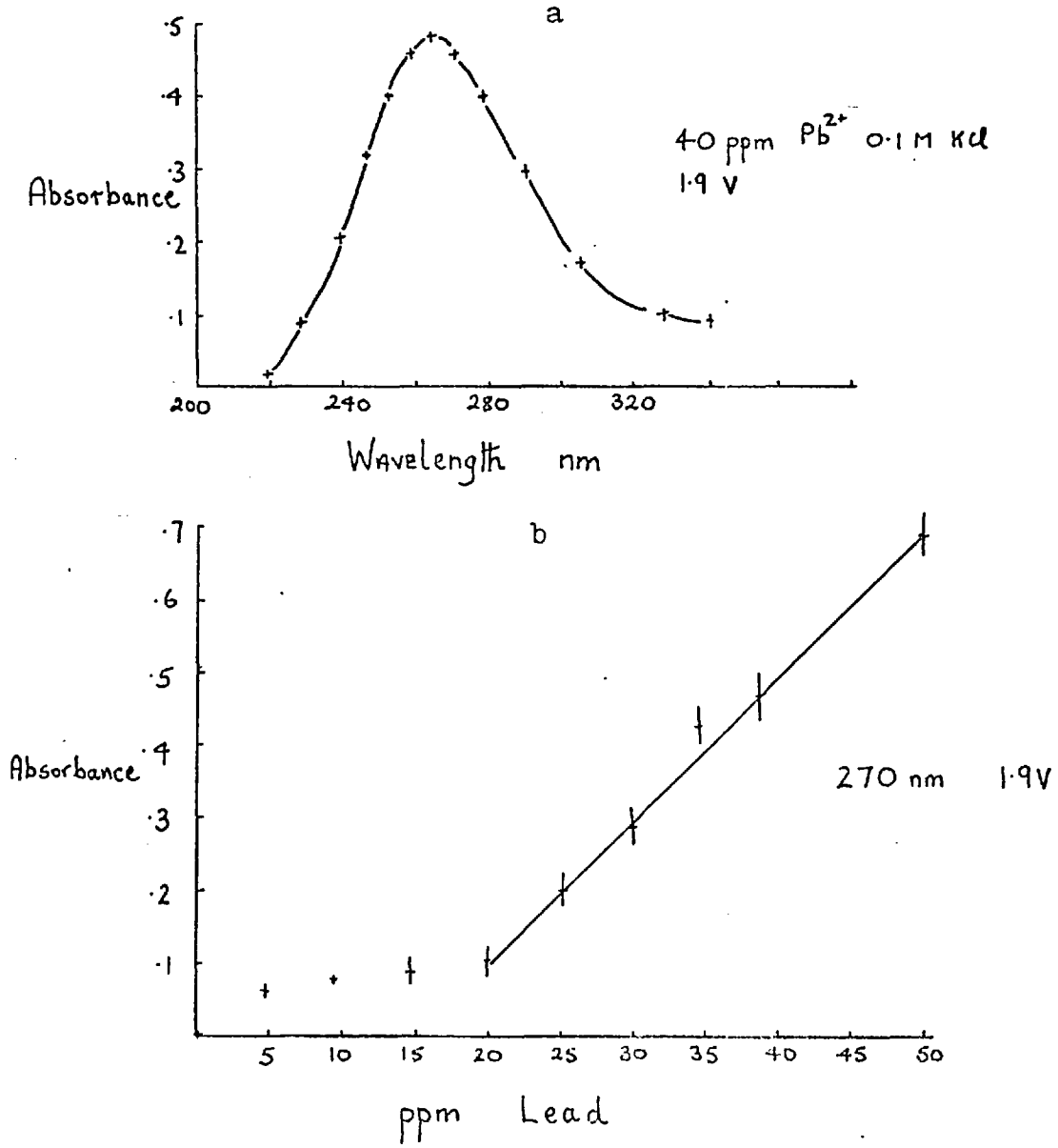

Figure 4.4 Lead. Variation of Absorbance with a, wavelength b, concentration.

Although the agreement between replicates was poor, giving a wide range of absorbance values for certain solutions, there was no doubt that increasing the concentration of lead increased the magnitude of the absorbance. Certainly, an analytical working curve based on these results would be of little use. However, as the purpose of the study was to investigate a number of metal ions, it was considered more important to proceed to the study of another metal than to try to improve the precision for lead.

4.8 Zinc

No difficulty was found in obtaining absorption signals from a solution containing 20 ppm zinc. Both potassium chloride and sulphate were used as background electrolytes and it was found that sulphate gave the more reproducible signals. The variation of absorbance with voltage for a 5 ppm solution of zinc in 0·03 M K_2SO_4 is shown in Figure 4.5a. With chloride as background electrolyte, the variation was essentially similar, but the sharp increase in the absorbance due to the evolution of hydrogen occurred at a smaller potential difference. The variation of absorbance with wavelength for a 10 ppm solution in 0·03 M K_2SO_4 at a potential difference of 1·4 V is shown in Figure 4.5b, and finally, the variation of absorbance with concentration is shown in Figure 4.5c. The potential difference was 1·4 V and the wavelength was set at 207 nm.

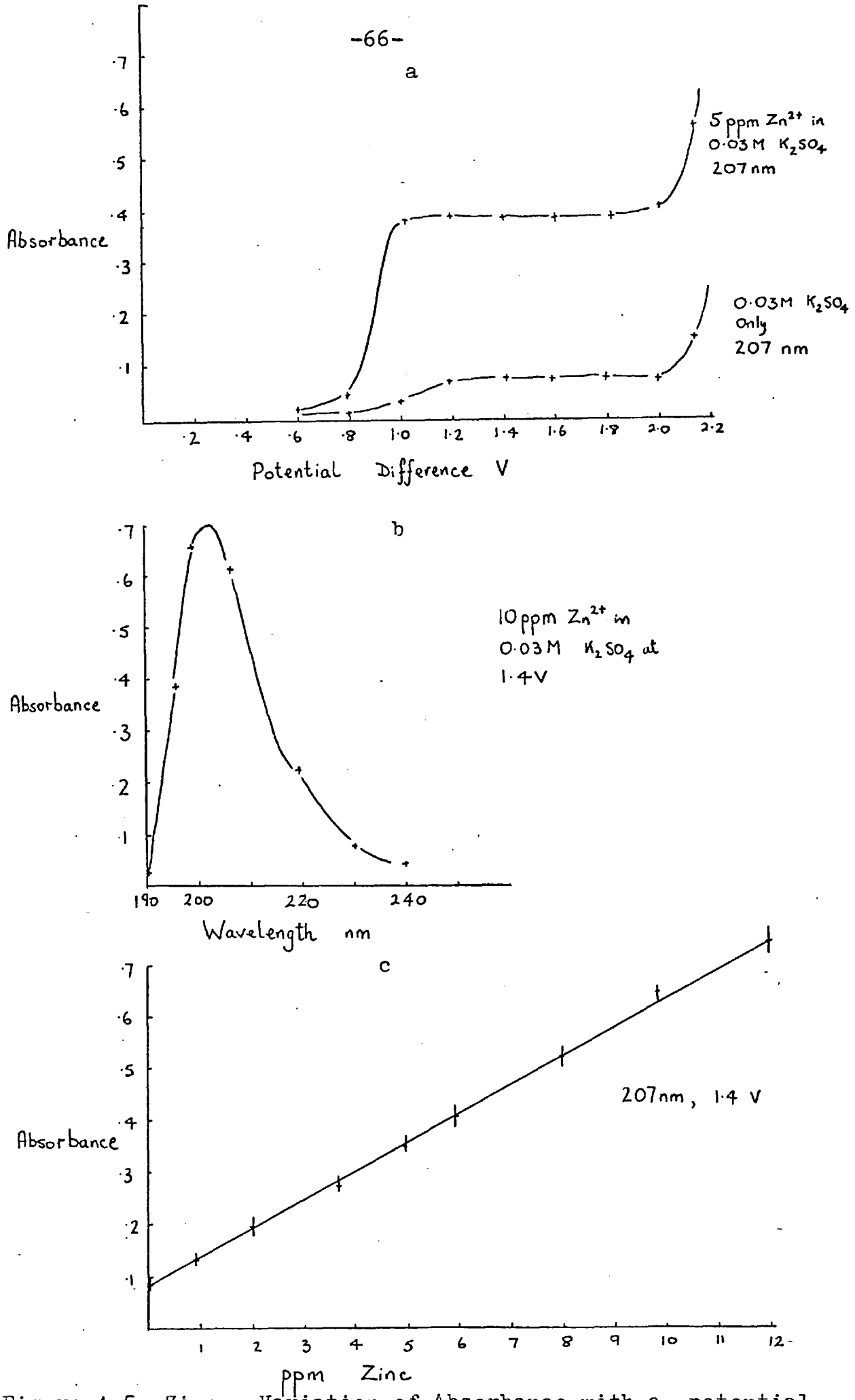

Figure 4.5 Zinc. Variation of Absorbance with a, potential difference b, wavelength and c, concentration

The cleaning step in the electrode pretreatment meant that the working electrode was in an oxidized state before the signals were obtained. If the pretreatment included a reducing step after the anodic stripping cleaning stage, then much smaller signals were obtained at the same potential difference. If, however, the potential difference was increased to 2·0 V, then signals of a similar magnitude were obtained. The effect of the electrode pretreatment on the signals will be dealt with later (Section 4.14)

4.9 Tin

No absorption signals could be obtained from stannous solutions. A variety of concentrations, wavelengths and pretreatment conditions were tried. Both potassium chloride and potassium sulphate were used as background electrolytes but the only increase in absorption observed was due to evolution of hydrogen from the cathode.

4.10 Cobalt

From a preliminary study, absorption signals from a 10 ppm cobalt solution in 0·03 M K_2SO_4 were found to have maximum values at 207 and 225 nm. The potential difference used was 1·4 V. The variation of absorbance with voltage for a 10 ppm solution in 0·03 M K_2SO_4 at 225 nm is shown in Figure 4.6a. The variation of absorbance with wavelength at a potential difference of 2·0 V is

shown in Figure 4.6b and the analytical growth curve at 2·0 V and 210 nm in potassium sulphate solutions is shown in Figure 4.6c.

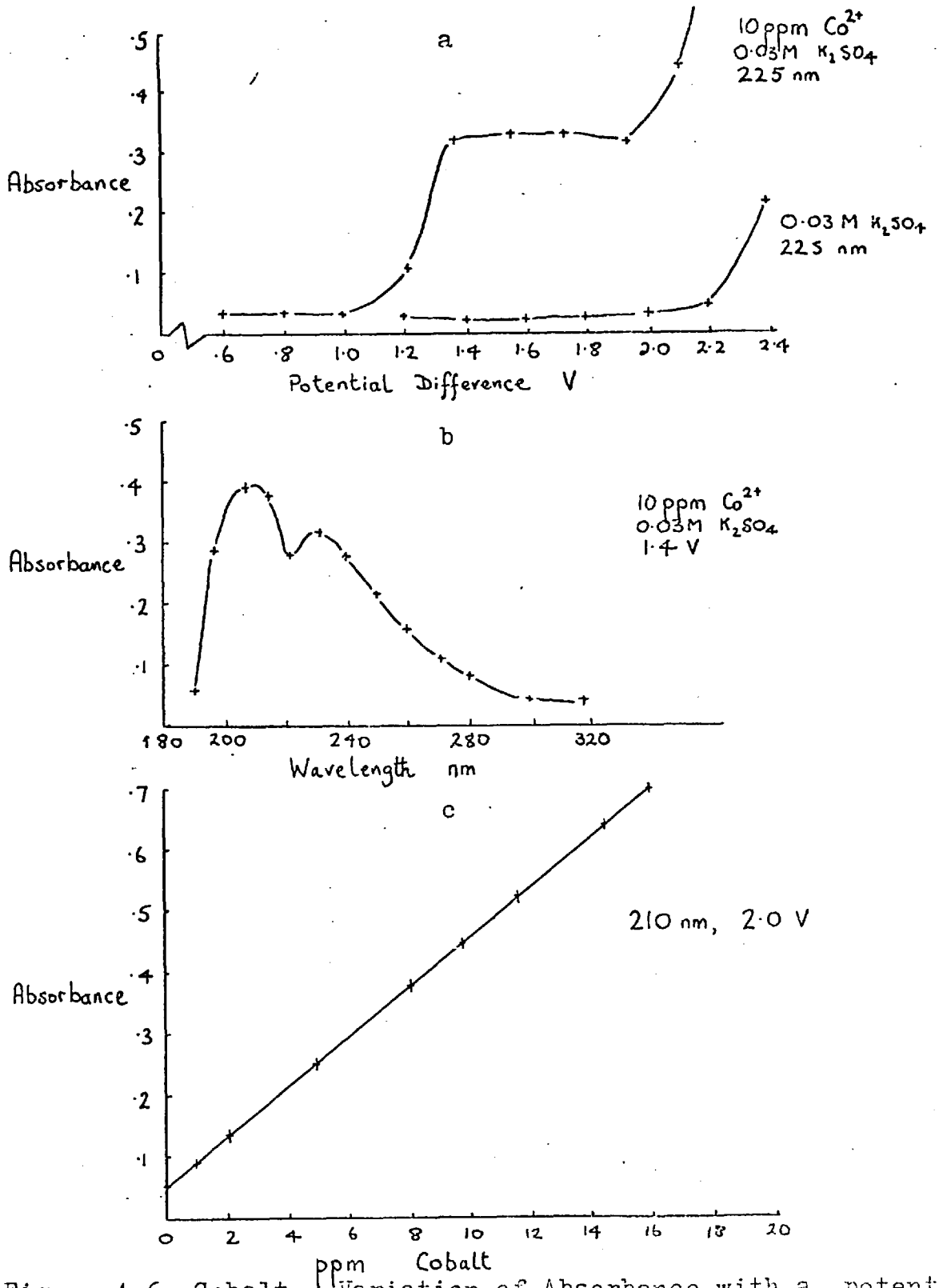

Figure 4.6 Cobalt. Variation of Absorbance with a, potential difference b, wavelength c, concentration.

The background electrolyte was changed for 0·1 M potassium chloride and the variation of absorbance with potential difference, wavelength and concentration obtained is shown in Figure 4.7.

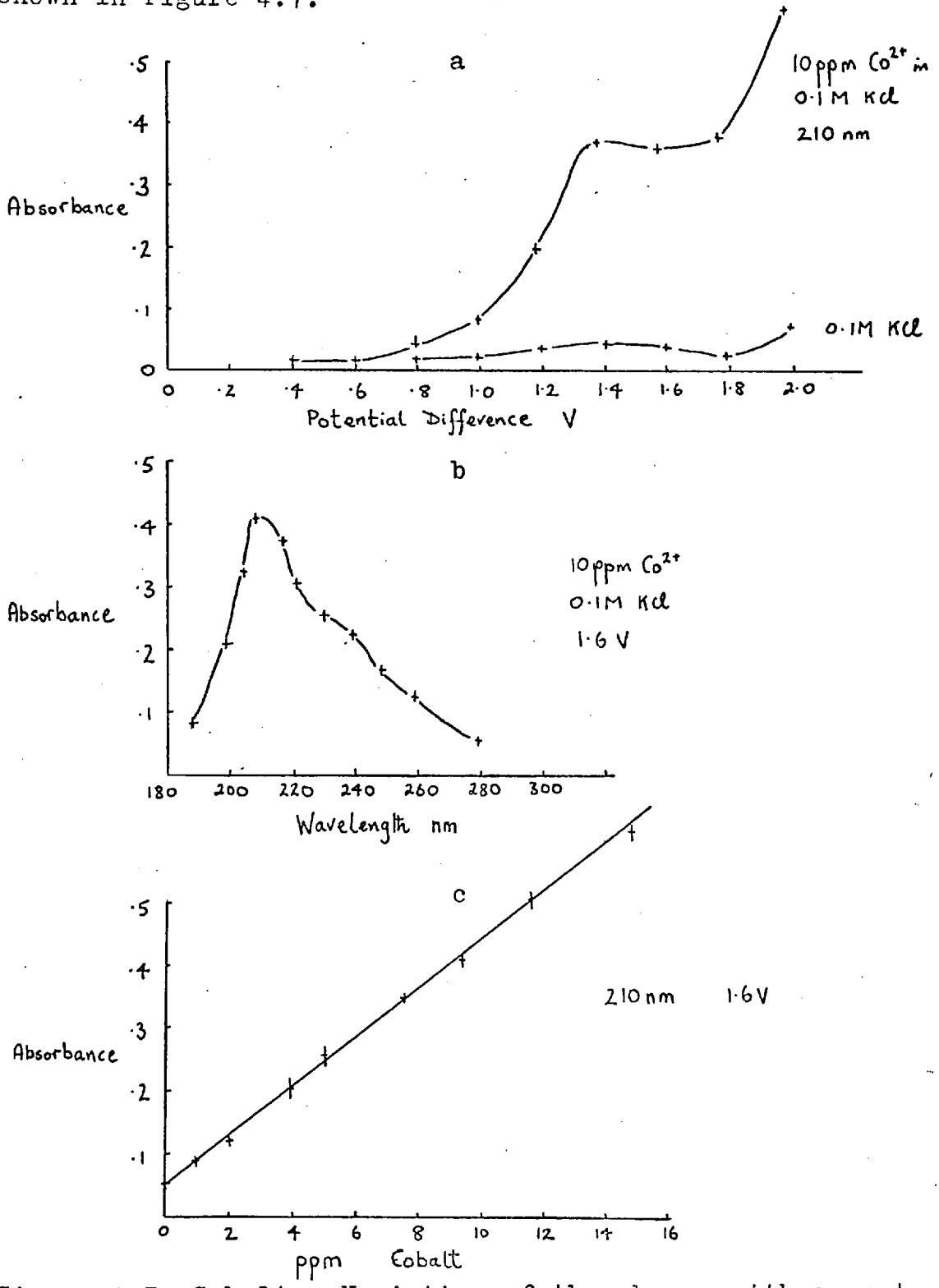

Figure 4.7 Cobalt. Variation of Absorbance with a, potential difference b, wavelength c, concentration Chloride background electrolyte

The similarity between the results shown here and in Figure 4.6 suggest that there is no difference between the species generated in the presence of sulphate and that generated in the presence of chloride.

4.11 Nickel

The variation of absorbance with wavelength is shown in Figure 4.8. A potential difference of 2·0 V was applied to a 10 ppm solution in 0·03 M potassium sulphate. The absorbance obtained from a blank solution (i.e. 0·03 M potassium sulphate only) is also shown. The variation of absorbance with voltage for nickel solutions and blank solutions at 198 nm (the absorbance maximum without correction for blank values) and 207 nm (the absorbance maximum corrected for blank values) is shown in Figure 4.9.

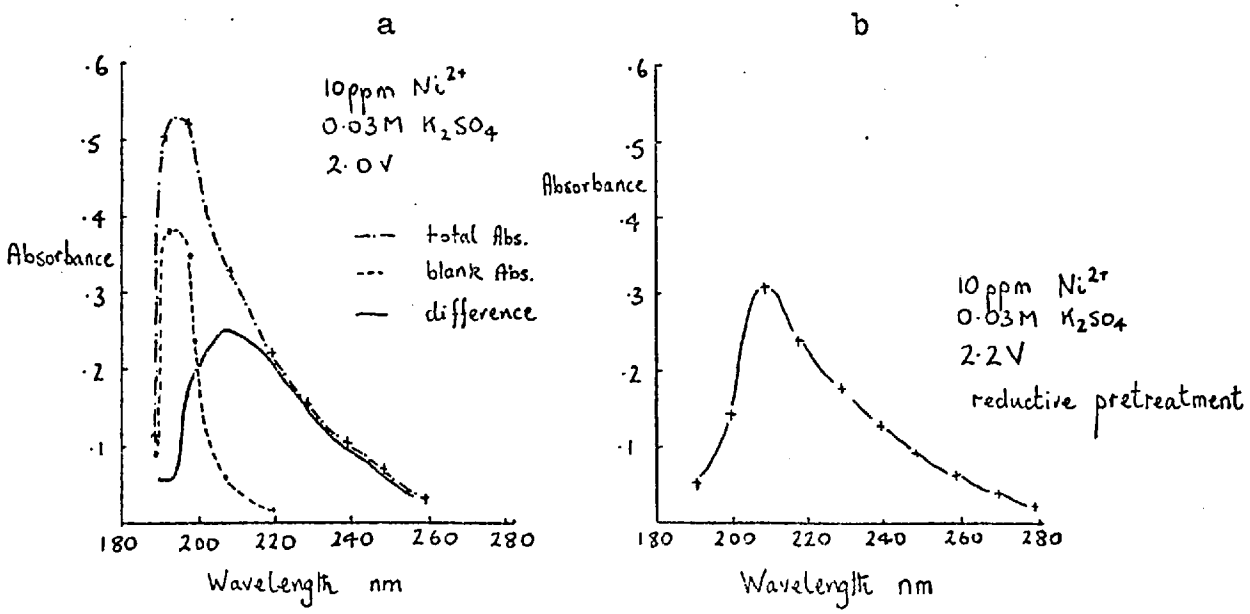

Figure 4.8 Nickel Absorption Spectra. a, oxidative pretreatment b, reductive pretreatment

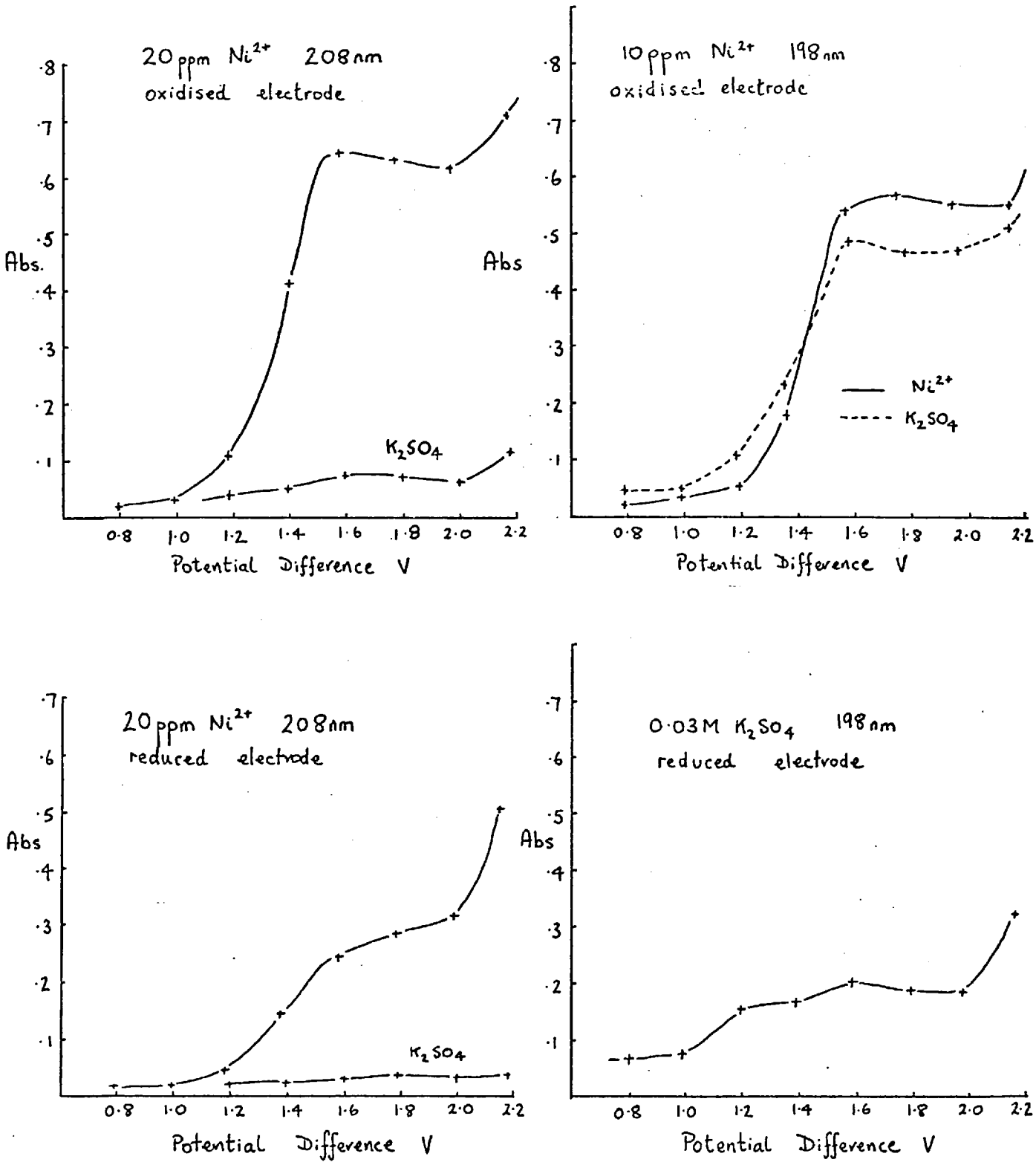

Figure 4.9 Nickel. Effect of Pretreatment and Wavelength on the Variation of Absorbance with Potential Difference

The effect of pretreating the electrode at different potentials is also shown. It can be seen that the best results are obtained with an anodic pretreatment of the working electrode and a wavelength of 208 nm. The absorbance spectrum obtained using the maximum potential difference without the evolution of hydrogen (2·2 V) is shown in Figure 4.8.

The effect of the nature of the potential difference applied was studied for a 20 ppm nickel solution in 0·03 M potassium sulphate. For most of the metals studied so far, a simple step function had been used, i.e. the potential difference was stepped from zero to the preset required value and maintained until a maximum in the absorbance signal had been recorded. In this study the repetitive mode of operation of the waveform source was used and both positive and negative potentials were applied, i.e. the electrode in the light path was made the anode and the cathode alternately. For simplicity of representation, a minus sign will be used when the electrode in the light path was negative with respect to the other (and thus the cathode) and a plus sign will be used when the electrode was positive with respect to the other (i.e. was the anode). Thus, for example, a potential difference of -1·6, +1·0 V with 30 sec pulses means that a potential difference of 1·6 V was applied so that the electrode in the light beam was the cathode for 30 seconds, then a potential difference of 1·0 V was applied so that this electrode

was the anode for 30 seconds. The process would then be repeated. The results for a variety of waveforms are given in Table 4.1. The figures quoted in the results column are percentage absorption.

Table 4.1 Repetitive Potential Functions

Amplitude V	Pulse Length sec	Results
-1·6, 0·0	30	max at 68%, decays with a number of smaller max to zero
-1·6, 0·0	16	smooth increase to 71%, decay in series of steps
-1·6, 0·0	4·7	smooth increase to max at 73%, decay in series of sawtooth peaks
-1·6, 0·0	3·5	identical to previous run max at 73%
-1·6, 0·0	0·5	smooth curve with max at 71%
-1·6, 0·0	0·05	broader peak, max at 67% voltmeter shows -0·9 V
-1·6, 0·0	0·005	max at 8%
-0·9	held till max	max at 5%
-1·6,+1·6	50	first peak largest at 70%
-1·6,+1·6	32	series of peaks, second one largest at 74%, subsequent ones decreased
-1·6,+1·6	17	second peak largest at 70% subsequent ones steady at 67%
-1·6,+1·6	9	rapid increase to 70%, more gradual increase to 84%, no max
-1·6,+1·6	5	levels off at 70%, then increases
-1·6,+1·6	0·05	levels off at 74%
-1·6,+1·6	0·005	levels off at 33%

Table 4.1 continued

Amplitude V	Pulse Length sec	Results
-1·6, +0·5	5	max at 79%, no reversal of signal on ascending side
-1·6, +0·6	5	max at 74%
-1·6, +0·8	5	max at 77%, decreased to 66%, then increased steadily
-1·6, +1·0	5	max at 75%, decreased to 73% then increased steadily, reversal of signal obtained on ascending side
-1·6, +1·2	5	max at 74%, decreased to 68% then levelled off at 73%
-1·6, +1·5	5	levelled off at 78%
-1·6, +2·0	5	levelled off at 77%
-1·6, +2·0	0·5	smooth increase to plateau at 82%
-2·0, +1·0	5	max at 77% decreased to 69%
-2·0, +1·0	0·5	max at 72% decreased to 64%
-2·0, +1·6	5	broad peak with max at 83%
-2·0, +2·0	5	levelled off at 77%

Blank solutions were also run and it was found that large signals were produced at -1·6, +2·0 V with 0·5 sec pulses and also at -1·6, +1·6 V with a reductive pretreatment of the electrode. With an oxidative pretreatment of the electrode, values of about 20% absorption were recorded. These values were comparable to those obtained with a

steady potential of -1·6 V.

From the Table it is seen that the absorption signals were obtained with a pulse length as short as 0·05 sec (i.e. the frequency of the oscillation was 10 Hz). When a symmetric alternating potential was applied (-1·6, +1·6 V), the net result was not zero absorbance, but the production of the absorption signal in the usual manner, except that as the frequency of the oscillation increased, the curve tended to level off instead of passing through a maximum. On the ascending side of the absorption curve, the reversal of polarity did not cause a reversal in absorption until the positive potential was +1·0 V, even at -1·6, +2·0 V the reversal of the absorption was not complete and the signal built up. This shows that the change in absorbance was not due to the movement of ions under the action of the electric field; if it were, the net effect of an alternating potential would be zero absorption. It can also be seen that to maintain the maximum absorption at a plateau, the alternating potential must have a positive excursion of at least 1·0 V and a frequency in excess of 0·1 Hz.

The absorption spectrum of a 1% nickel solution is shown in Figure 4.10. If the absorption at 208 nm were due to migration of Ni^{2+} species into the light path, then a corresponding increase should have been observed at 405 nm. The results obtained at the two wavelengths are shown in Table 4.2.

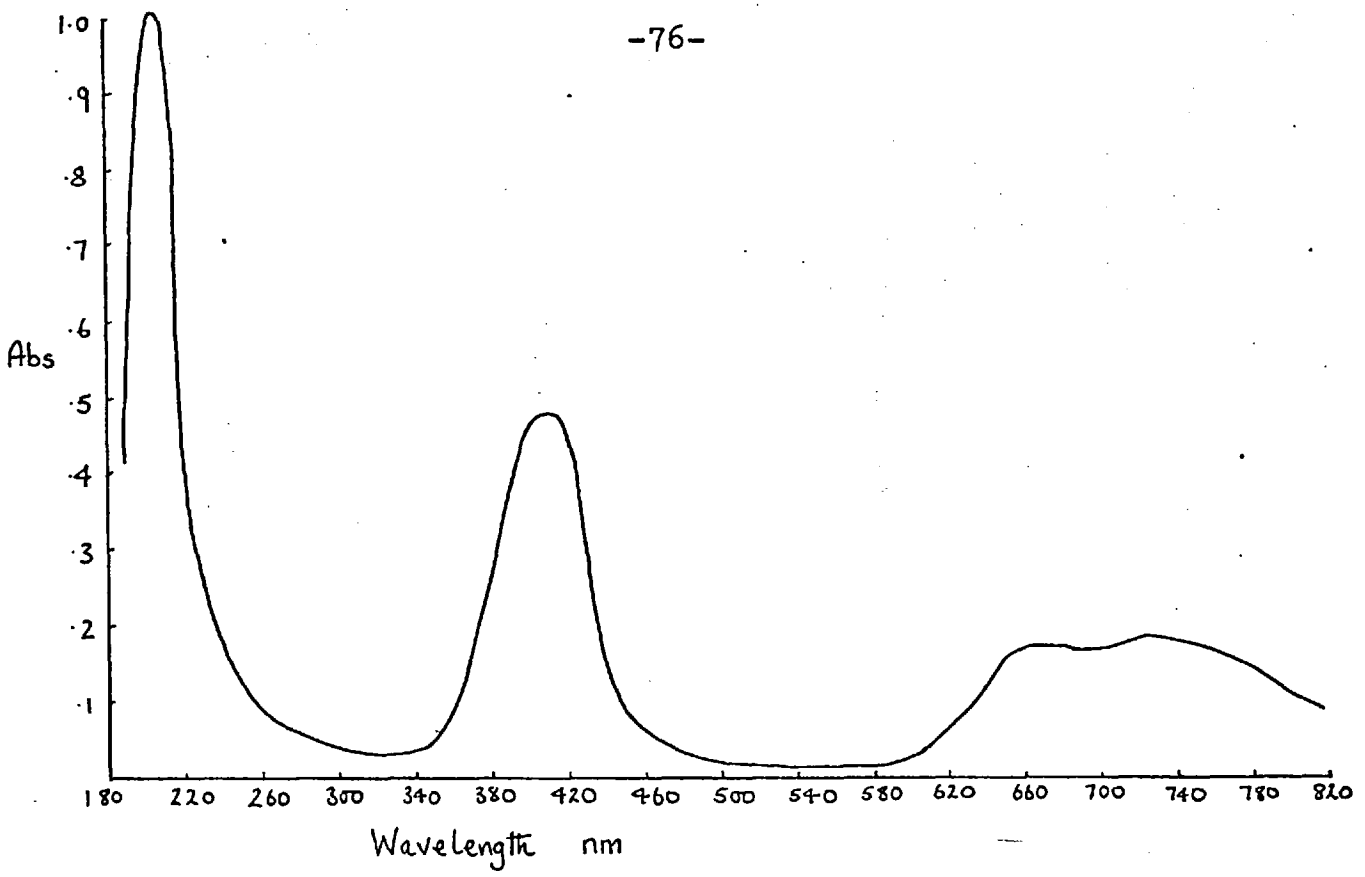

Figure 4.10 Absorption Spectrum of 1% Nickel Solution

Table 4.2 Absorption Signal from 20 ppm Ni^{2+} at Cathode

Wavelength nm	Absorbance
208	0·46
405	0·03
420	0·03
370	0·03
300	0·04

If the absorption were due to Ni^{2+}_{aq}, then an absorbance of 0·18 should have been obtained at 405 nm. Furthermore, in about 10 sec the concentration in the light path would have to have increased by approximately 100 times to account for the magnitude of the signal on the basis of the rather weak absorption of Ni^{2+}_{aq}.

4.12 Manganese

A stock solution of manganese was prepared by dissolving the appropriate amount of $MnCl_2.4H_2O$ in distilled water. A 20 ppm solution in 0·03 M potassium sulphate was used as a test solution. It was found that absorption occurred when the working electrode was the anode as well as the cathode. During the anodic part of the cycle, the electrode was seen to be coated with a red layer. No coloured deposit was observed during the cathodic part of the cycle. No difference in precision was observed between potassium chloride and potassium sulphate as background electrolytes. It was found that larger and more reproducible signals were obtained with a reduced electrode surface, whereas for most of the metals already described, better signals were obtained with an oxidized surface. Accordingly, the cleaning and pretreatment procedure used was to wash the electrodes while a potential difference of +5·0 V was applied with 0·03 M potassium sulphate and then to repeat the process with a potential difference of -5·0 V. After rinsing with distilled water, the electrodes were ready for use.

The variation of absorbance with wavelength, potential difference and concentration is shown in Figure 4.11. It can be seen that the plateau region on the absorbance-potential difference curve is poorly defined and it would appear that manganese represents the limit, in terms of reduction potential, that can be reached in the aqueous

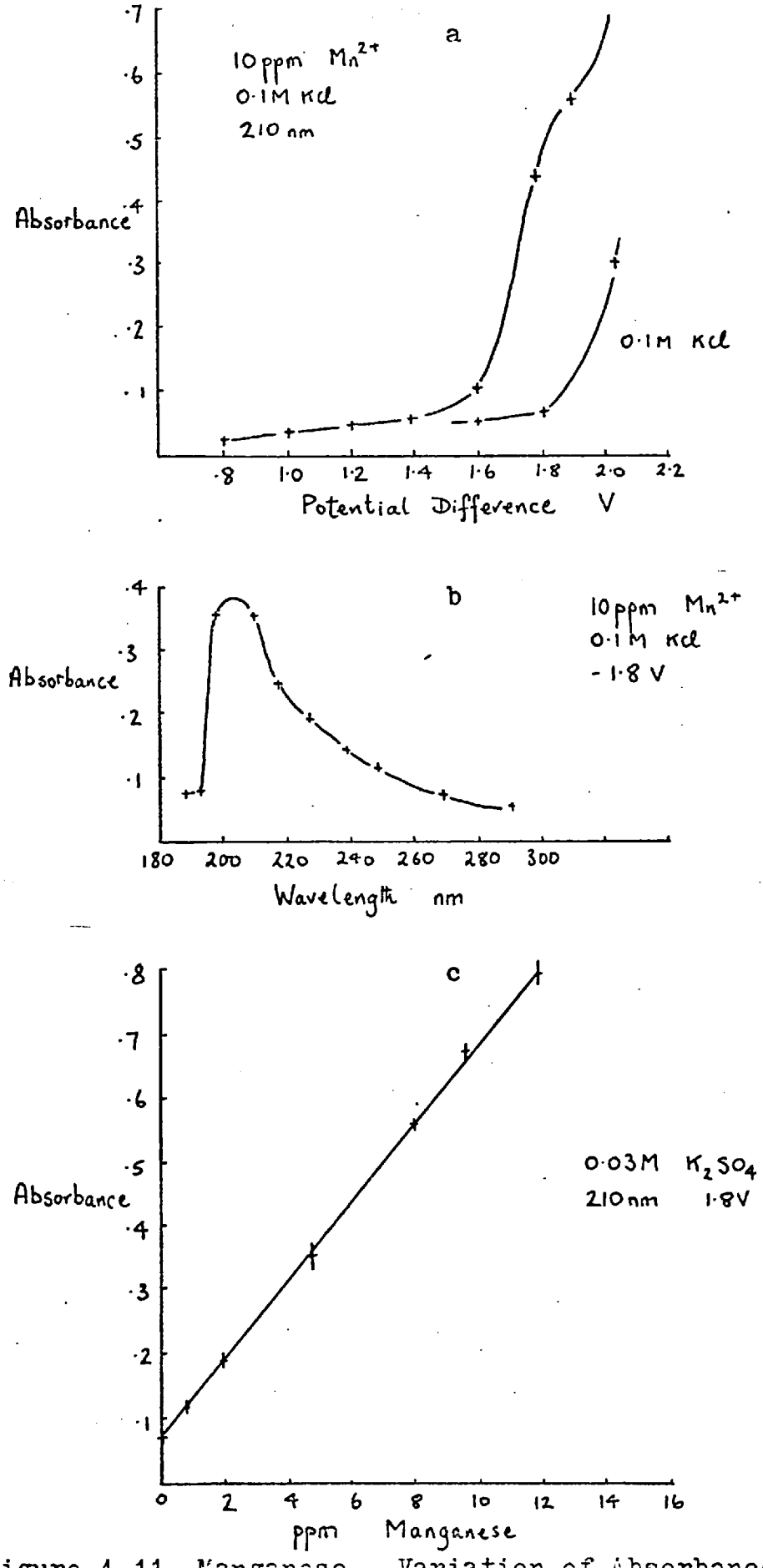

Figure 4.11 Manganese. Variation of Absorbance with a, potential difference b, wavelength c, concentration

solutions employed here. The standard electrode potential for the couple Mn^{2+}/Mn is -1·18 V, the most negative value of all the metals that have been studied so far.

With manganese as permanganate (i.e. Mn VII), a somewhat erratic increase in absorbance was obtained when a potential difference of -1·8 V was applied. At wavelengths between 200 and 300 nm, a rapid decrease in absorbance was observed when the potential was first applied. This was interpreted as movement of the strongly absorbing MnO_4^- ions during the double layer charging stage. During the electrolysis the electrode became coated with a brown layer, which was thought to be manganese dioxide. No well defined absorption signals could be obtained.

4.13 Chromium

A stock solution of Cr^{3+} was prepared from $CrCl_3.6H_2O$. The signals were recorded at a potential difference of 1·8 V with an oxidative electrode pretreatment. The application of a positive potential to the electrode in the light path resulted in an increase in absorbance which meant that as signals were being produced on oxidation, an alternating potential difference (as in the case of nickel, Section 4.11) could not be used. The variation of absorbance with potential difference is shown in Figure 4.12. The variation with wavelength for a 10 ppm solution in 0·03 M potassium sulphate as background electrolyte is also shown in Figure 4.12. In

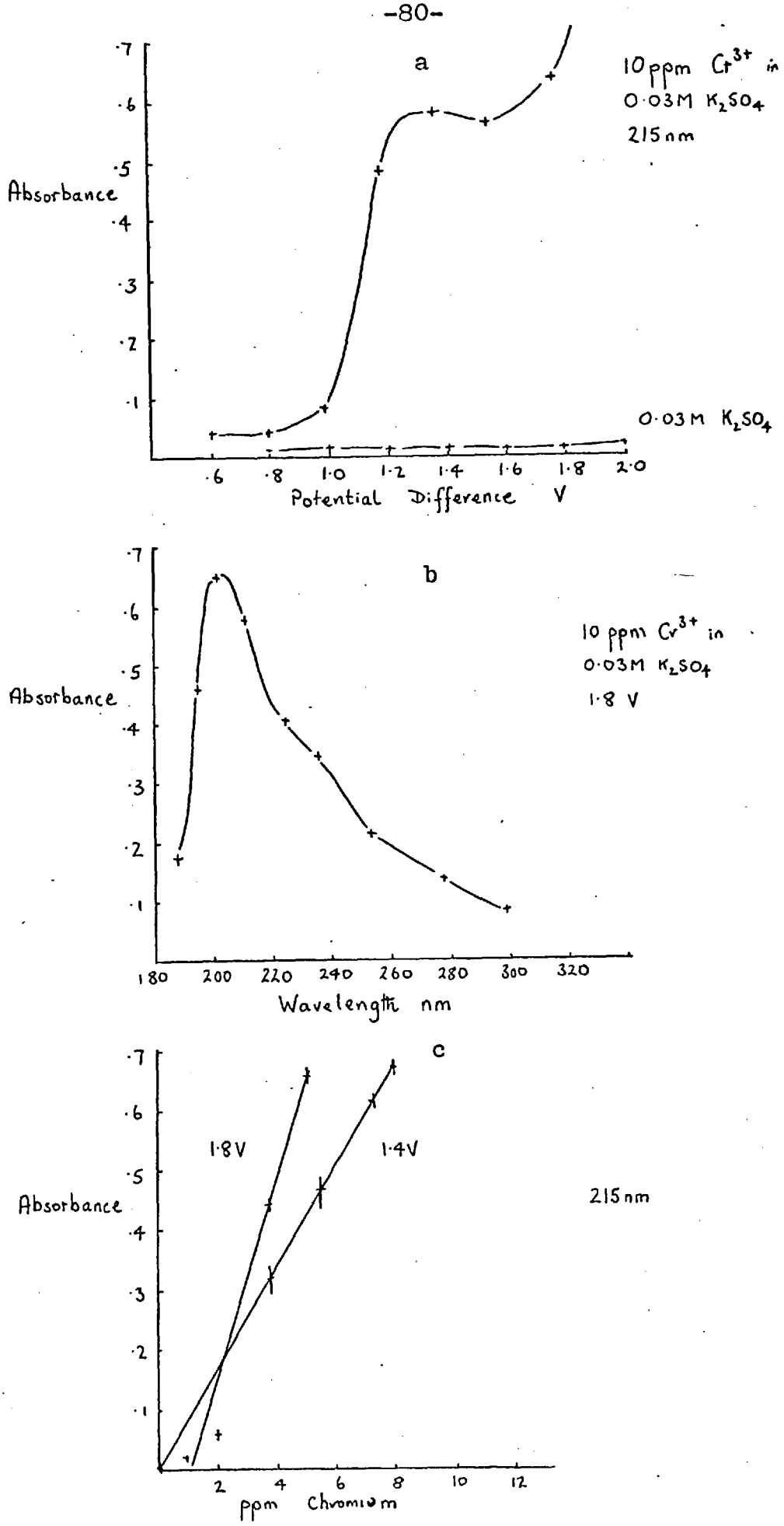

Figure 4.12 Chromium. Variation of Absorbance with a, potential difference b, wavelength

plotting the analytical growth curve, potential differences of 1·4 and 1·8 V were used. However at both these potentials, the precision was poor, and it was found difficult to improve this for solutions containing less than 5 ppm chromium. The variation of absorbance with concentration is also shown in Figure 4.12.

4.14 Blank Signals and the Effect of Electrode Pretreatment

It is well known that a platinum electrode is not electrochemically inert (57) and various potential regions corresponding to hydrogen adsorption, oxygen adsorption or oxide formation can be identified (58). It is apparent that the conditions employed here to clean the electrode leave the surface covered with a layer of adsorbed oxygen and platinum oxide. The effect of the pretreatment of the electrode on the absorption signals for zinc is shown in Table 4.3.

Table 4.3 Effect of Pretreatment on Zinc Signals

Wavelength nm	Pretreatment Cycle V	Solution	Absorbance at -1·4 V
205	±2·0	20 ppm Zn	0·025
205	±3·0	20 ppm Zn	0·029
205	±3·5	20 ppm Zn	0·029
205	±4·0	20 ppm Zn	0·141
205	+4·0	20 ppm Zn	>1
205	+5·0	20 ppm Zn	>1
205	+5·0	10 ppm Zn	0·78
205	+5·0	blank	0·14

The sharp increase in absorbance that is obtained when the pretreatment does not include a reducing stage can be clearly seen from the Table. The effect of the pretreatment on the absorption produced from the background electrolyte alone (in this case 0·1 M potassium chloride) at 200 nm is shown in Table 4.4.

Table 4.4 Effect of Pretreatment on Blank Signals

Pretreatment Cycle V	Absorbance at -1·4 V
0·0	0·019
+1·0	0·036
+2·0	0·053
+3·0	0·080
+4·0	0·152
+5·0	0·167
+5·0, -0·5	0·165
+5·0, -1·0	0·104
+5·0, -1·5	0·035
+5·0, -2·0	0·028

It can be seen from the Table that the absorbance increased with increasing anodic potential (and presumably increasing oxide covering) and decreased as the cathodic potential was increased for a given anodic potential. The absorption spectra for the blank solutions are shown in Figure 4.13. The effect of deaeration of the solution with 'white-spot' nitrogen is also shown.

Most of the other metals studied showed an effect similar to that of zinc i.e. an oxidised electrode surface gave rise to larger signals than a reduced surface, though

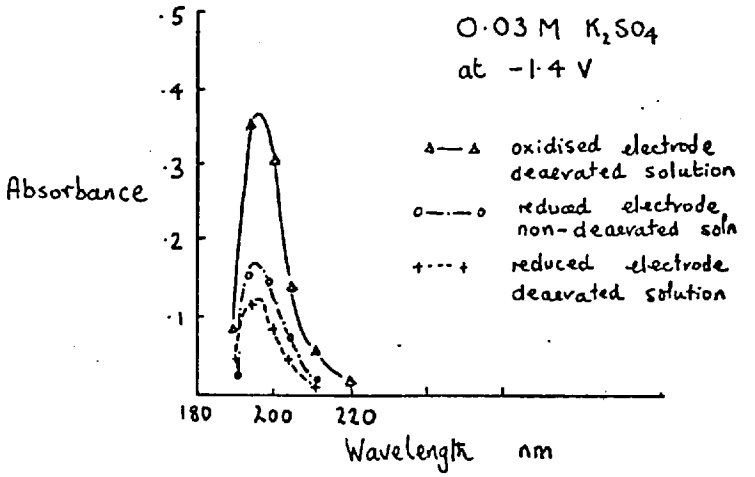

Figure 4.13 Effect of Electrode Pretreatment on Blank Signals

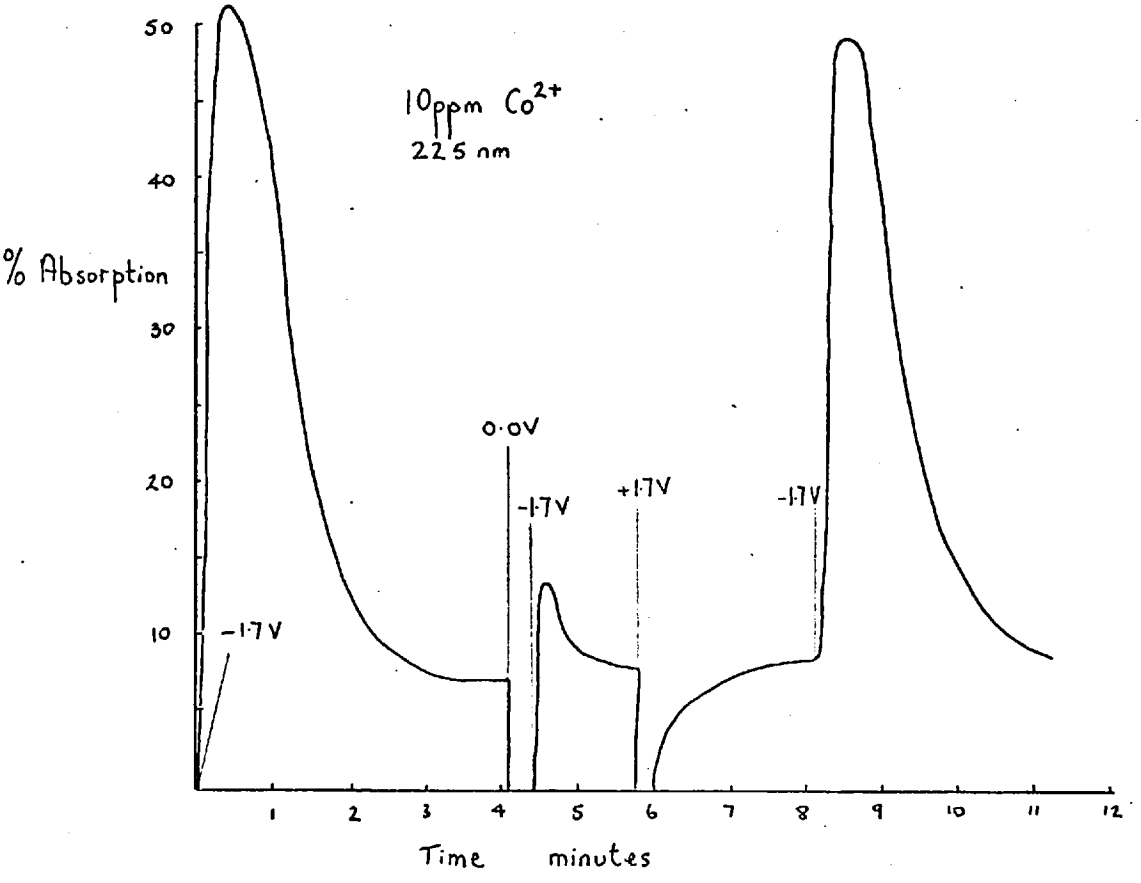

Figure 4.14 Effect of Nature of the Electrode Surface on Cobalt Absorption

the blank values were also larger. This effect is shown for cobalt in Figure 4.14. A 10 ppm solution was electrolysed at -1·7 V and after the signal decayed, the potential difference was switched off and then on again. An absorption signal of the same magnitude as the initial signal was only obtained after an anodic potential had been applied to the electrode.

With zinc, signals of similar magnitude to those produced after an oxidising pretreatment were obtained with a reduced electrode surface by applying a larger potential difference. The spectral distribution of this absorption is shown in Figure 4.15. From a comparison with Figure 4.5 (oxidised pretreatment and potential difference of -1·4 V), it is seen that the species generated in each case is the same, indicating that the state of the electrode surface does not appreciably affect the nature of the species produced.

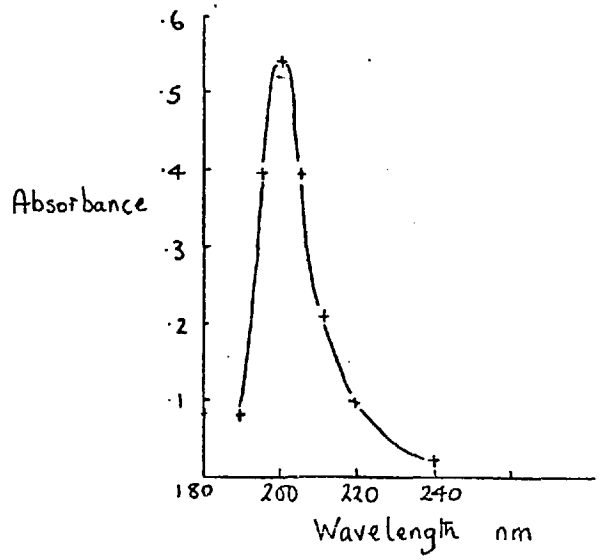

Figure 4.15 Zinc. Variation of Absorbance with Wavelength. Reduced Pretreatment

4.15 Summary of Results

The absorption spectra of the nine metal ions that gave an absorption signal at the cathode during electrolysis are shown in Figure 4.16. The spectra were all obtained with 10 ppm solutions apart from ferrous iron, for which a 5 ppm solution was used. The other results are summarized in Table 4.5.

Table 4.5 Summary of Results

Metal Ion	Plateau Region V	E^o V	Abs. Max. nm	Sens. ppm	AA line nm
Cu^{2+}	1·6-2·0	+0·337	235	0·10	226·6
Cd^{2+}	2·0 used	-0·403	215	0·09	228·8
Fe^{2+}	2·0 used	-0·440	270	0·07	248·3
Fe^{3+}	1·8 used	-0·040	270, 364	0·09	248·3
Zn^{2+}	0·9-1·8	-0·736	207	0·08	213·9
Pb^{2+}	2·0 used	-0·126	270	0·35	283·3
Cr^{3+}	1·4-1·8	-0·740	215	0·05	357·9
Ni^{2+}	1·6-2·0	-0·250	208	0·16	232·0
Mn^{2+}	1·9-2·0	-1·180	210	0·08	210·9
Co^{2+}	1·4-2·0	-0·227	210	0·11	240·7

The sensitivities are the concentrations in ppm that would give 1% absorption. It can be seen that although the absorption spectra are similar, they are not identical and the variation of absorbance with potential difference suggests that the absorption is characteristic of the metal ion, and arises from a species containing the metal produced in

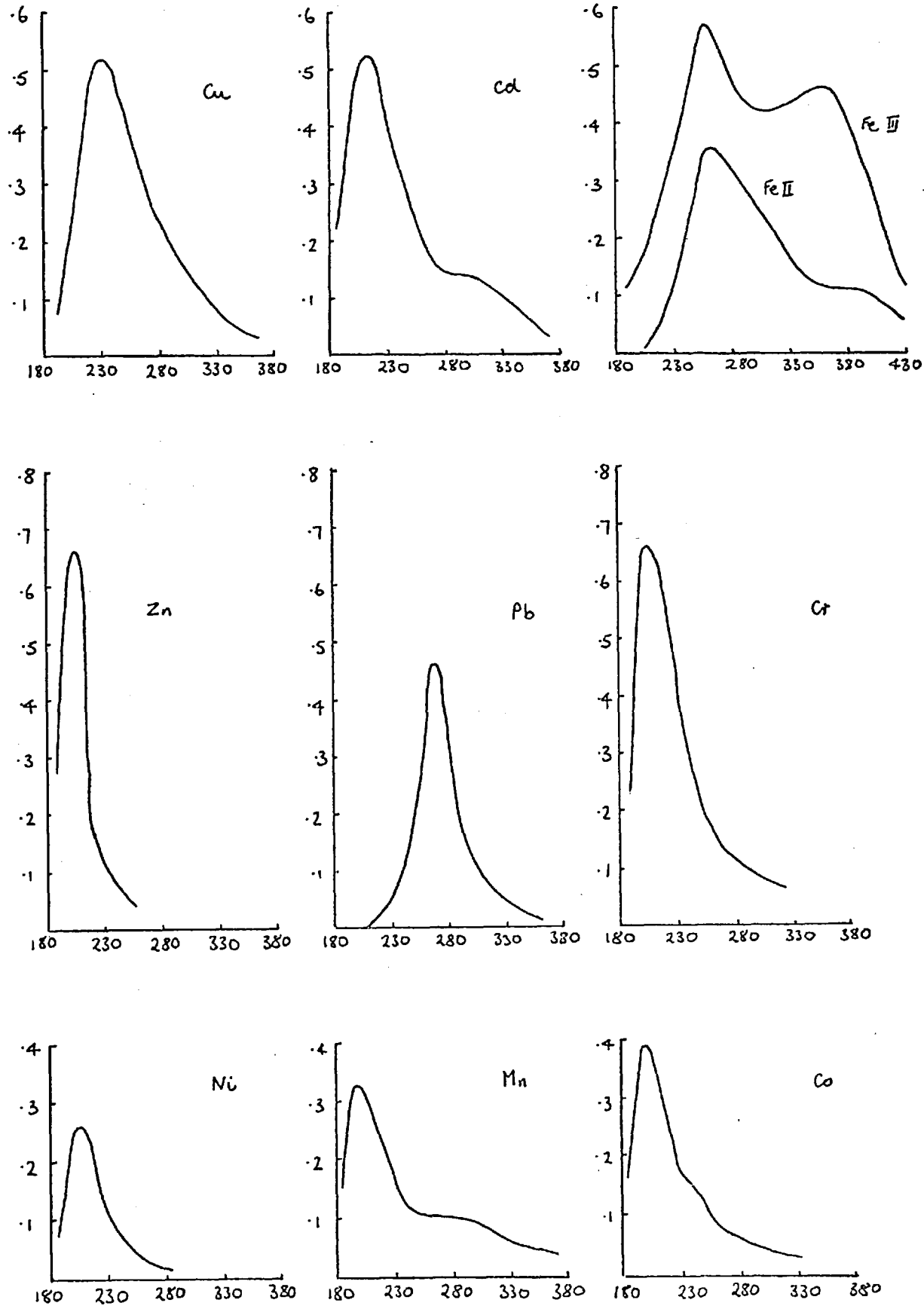

Figure 4.16 Absorption Spectra of Species Produced during Electrolysis, Plots of Absorbance vs Wavelength nm

the electrolysis. Incidentally, no absorption signals could be obtained from solutions of magnesium (E^{o} -2·37 V) or aluminium (E^{o} -1·66 V) at the potential differences accessible in the aqueous solutions used. It appears that the process involves a reaction at the electrode, as the results with the nickel solutions (Section 4·11) strongly suggest that the movement of ions under the action of the electric field is not responsible for the change in absorption observed. The wavelength of an atomic line used in conventional AAS is shown for each element in Table 4.5. It can be seen that there is possibly a weak correlation between this value and the value for the absorption maximum of the species obtained at the electrode surface. It is also apparent that the nature of the electrode surface somehow affects the absorption signal.

In this Chapter, the absorption phenomenon has been studied from the point of view of variation of the reducible metal ion and the study of how the absorbance varies with potential difference, wavelength and concentration of the metal. For some metals the effect of the nature of the pretreatment of the working electrode and of an alternating potential difference have also been studied. However, at the beginning of this Chapter, a number of other parameters were also mentioned as possibly having an effect on the absorption signal. These will be discussed in Chapter 6.

5. THEORETICAL CONSIDERATIONS

A considerable amount of experimental results have been compiled for the absorption signals produced during the electrolysis of a number of dilute metal ion solutions. In particular, the variation of the absorbance with wavelength, potential difference, concentration and, in certain cases, electrode pretreatment have been investigated. If the nature of the phenomenon is to be determined, it will be of value to examine some relevant aspects of the chemical theory.

5.1 Mechanism of Electrodeposition of Metals

In a review of this title, Bockris and Damjanovic (59) consider the subject under the two broad headings of monolayer deposition and multilayer deposition. As the amount of metal deposited in the experiments under consideration here is probably of monolayer or sub-monolayer amounts, only monolayer deposition will be discussed here. They consider two general mechanisms on the basis of energy considerations for the various steps involved, namely 1, direct transfer of an ion from its fully hydrated state in solution to a surface vacancy, or 'hole' site, from which it migrates no further, or 2, transfer to a surface plane followed by surface diffusion through the adsorbed water layer to a growth site, accompanied by

successive diminution in the number of water molecules in the hydration shell and successive increase in the number of metal ions which co-ordinate the particle under consideration. From a consideration of the results of a number of other workers (60,61,62,63), the following conclusions are reached.

1. Transfer occurs at planes, as direct transfer to growth sites requires more energy to distort the ionic hydration shell when the final state involves high co-ordination by metal lattice ions.
2. The transferred particle is an 'adion', i.e. an adsorbed ion, not an 'adatom', because the energy of activation for transfer from a hydrated ion in solution to an uncharged species is too large to allow appreciable transfer rates.
3. Electrons are transferred one at a time, as the activation energy in a transfer reaction in which n electrons take part is so much greater than that of a reaction in which only one electron takes part.
4. At low current densities, surface diffusion is likely to be the rate determining step, whereas at high current densities, charge transfer will be rate determining.

Their discussion which follows, based on the above conclusions is mainly concerned with the kinetics of the deposition process and it is difficult to obtain from the discussion a chemical model of the processes involved

in particular, as to what is happening on the solution side of the electrode surface during deposition. Although it would appear that there is no process occurring in the reduction whereby a change in the absorbance in the experiments described previously would be expected, there is very little discussion of the mechanism of charge transfer.

5.2 Mechanism of Charge Transfer

The contributions to this aspect of electrochemistry over the last 40 years are comprehensively reviewed by Matthews and Bockris (64). The foundations of present ideas on charge transfer were laid down by Gurney (65) over 40 years ago, in an attempt to rationalise results obtained by Bowden (66) on hydrogen overpotential. Gurney's theory, which involved the transfer of electrons by quantum mechanical tunneling, was, however, largely ignored, and it was not until the 1960's that the quantum mechanics of electrode processes were rediscovered (67). The tunneling of electrons through potential barriers, rather than surmounting them, is a consequence of the quantum mechanical nature of the electron.

The probability of finding the electron at a given place and time is given by the square of the probability amplitude, ψ, whose variation with distance and time is given by the Schrödinger equation. When this is solved for an electron in a uniform field, the probability amplitude varies as $e^{-i\omega t}$. From which it can further be

deduced that ψ varies as $e^{-i(\omega t - \dot{k}x)}$ where ω is the angular frequency given in terms of the conventional frequency, ν, by

$$\omega = 2\pi\nu$$

and $\dot{k}$, the wavenumber or propogation constant, is given by

$$\dot{k} = \frac{2\pi}{\lambda}$$

By using Planck's equation,

$$E = h\nu$$

and de Broglie's relation

$$p = \frac{h}{\lambda}$$

where h is Planck's constant, p is the momentum, E is the total energy and λ is the wavelength,

then ψ varies as

$$\exp -\frac{2\pi i}{h}(Et - px)$$

E, the total energy, is the sum of the kinetic and potential energies, i.e.

$$\begin{aligned} E &= E_k + E_p \\ &= \frac{mv^2}{2} + E_p \\ &= \frac{p^2}{2m} + E_p \end{aligned}$$

from which ψ varies as

$$\exp -\frac{2\pi i}{h}\left[\left(\frac{p^2}{2m} + E_p\right)t - px\right] \qquad 5.1$$

If the case of a metal-vacuum interface is considered, for which at $x<0$* (i.e. inside the metal) the potential energy of the electron is V_1 and at $x>0$ (in the vacuum) the

* where x is the distance from the vacuum-metal interface

potential energy is V_2. This situation is shown in the diagram.

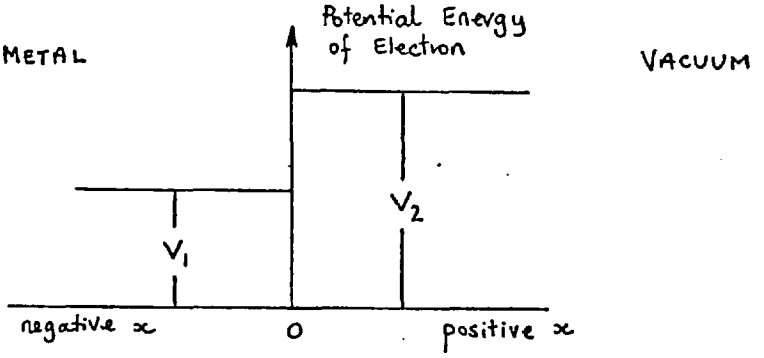

The total energy of the electron in the metal, E_1, is given by

$$E_1 = \frac{p_1^2}{2m} + V_1$$

and in the vacuum

$$E_2 = \frac{p_2^2}{2m} + V_2$$

for a radiationless transition $E_1 = E_2$

i.e. $$\frac{p_2^2}{2m} = \frac{p_1^2}{2m} - (V_2 - V_1)$$

If the potential energy of the electron in the metal, $p_1^2/2m$, is less than the height of the potential barrier, $V_2 - V_1$, then

$$\frac{p_2^2}{2m} < 0$$

and as 2 and m are both positive, it follows that p_2^2 is negative. This result is clearly untenable on a classical basis, from which it is concluded that no transfer of electrons can take place. If, however, the argument is continued on the basis of the probability of finding the

electron outside the metal, a different result is obtained.

If p'_2 is the real part of the electron momentum, then $p_2 = ip'_2$. Substituting in Equation 5.1 gives

$$\psi_2 \text{ varies as } \exp -\frac{2\pi i}{h}\left\{\left[\frac{(ip'_2)^2}{2m} + V_2\right]t - ip'_2x\right\}$$

If only the space variation of ψ_2 is considered, then

$$\psi_2 \text{ varies as } \exp \frac{-2\pi p'_2 x}{h}$$

and thus as the quantities π, p'_2 and h are all real, ψ_2 has a real dependence on x and thus there is a finite probability of finding the electron at a distance x in the vacuum of

$$P = |\psi_2|^2 = \exp \frac{-4\pi p'_2 x}{h}$$

If the barrier is made finite and quite small, and by having molecular entities with possible energy states for the electron equal to those which the electrons have in the metal, then the condition for radiationless tunneling can be fulfilled at a distance small enough for $|\psi_2|^2$ to have values large enough to account for the currents which are observed to flow at electrodes at room temperatures. It is known that electrons only go over barriers (thermionic emission) at high temperatures.

5.2.1 The Hydrogen Evolution Reaction

The shape of the barrier can be obtained from a consideration of how the energy changes as the electron moves away from the metal, and how it changes as the

electron moves away from a hydrogen ion (68). The former of these is given by $-e^2/4x^2$ and the latter may be assumed due to coulombic attraction given by e^2/x^2. The combination of these two profiles is shown in Figure 5.1

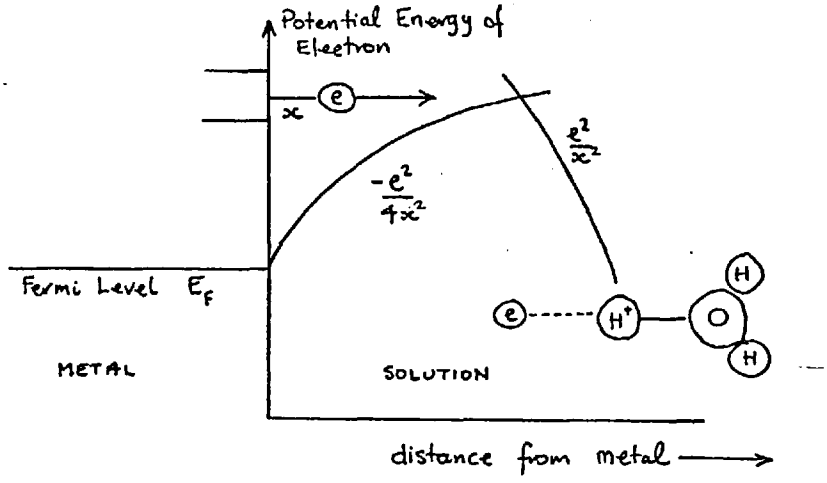

Figure 5.1 Shape of the Potential Barrier

For electron tunneling to occur then

$$\phi \leq E_R$$

where ϕ is the work function of the metal, i.e. the energy required to bring an electron from infinity to the Fermi level in the metal and E_R is the energy required to bring an electron from infinity to a vacant acceptor state in the hydrated proton near the metal. This condition is shown in Figure 5.2.

To find E_R consider the reverse process in four stages.

1. The atom is removed from its interaction with the metal. This involves the heat of adsorption, A.
2. The hydrogen atom reacts repulsively with the neighbouring oxygen of the water. If the work done in overcoming

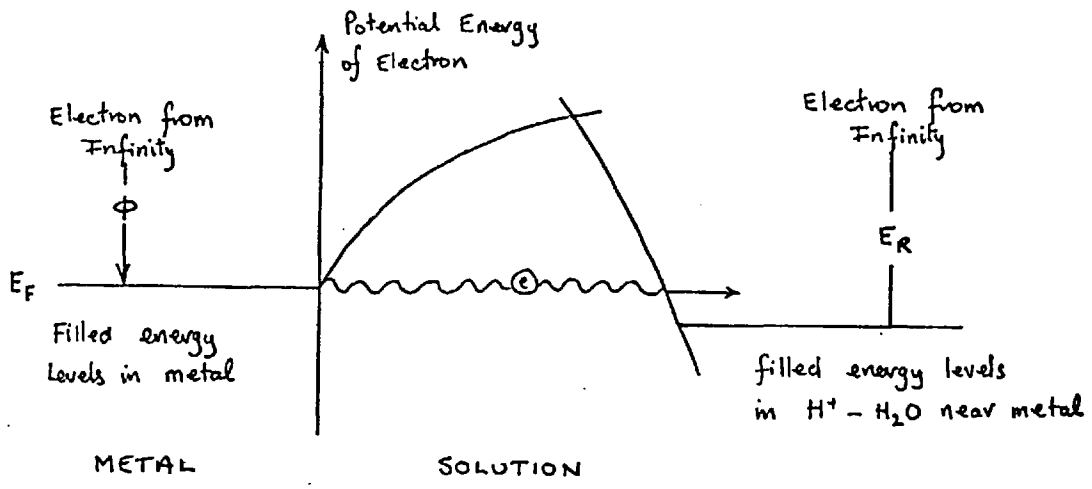

Figure 5.2 Electron Tunneling Condition

the associated energy is R, then R + A gives a free atom.

3. This atom is now ionised to get an electron at infinity and a proton. The energy involved is the ionization energy, I.
4. The proton is returned to the solution, involving solvation energy, L.

Thus,

$$E_R = R + A + I + L$$

snd the electron tunneling condition becomes

$$\Phi \leq R + A + I + L$$

If a check on the comparative magnitudes of R, A, I, L and Φ is made, then it is found that generally the transfer condition is not obtained. The situation can be improved by increasing the cathodic potential of the metal with respect to the solution. The energy of the electron in the metal becomes $\Phi + F\psi^m$ and in the solution becomes $R + A + I + L + F\psi^s$ where ψ is the outer potential

of the given phase. At a charged electrode, the tunneling condition becomes

$$\phi + F\Delta\psi \leq R + A + I + L$$

If the tunneling condition is rewritten as

$$-(R + A) \leq I + L - \phi - F\Delta\psi$$

then the right hand side of the inequality gives the energy of an electron in the metal and a hydrated proton i.e. $e_M + H^+—H_2O$, and the left hand side gives the energy of an adsorbed hydrogen atom and a water molecule i.e. $M—H + H_2O$. These two energies vary as the proton oscillates between the metal and the water molecule and as the hydrogen atom oscillates between the metal and the water molecule respectively. The variation of the appropriate energies is shown in Figure 5.3.

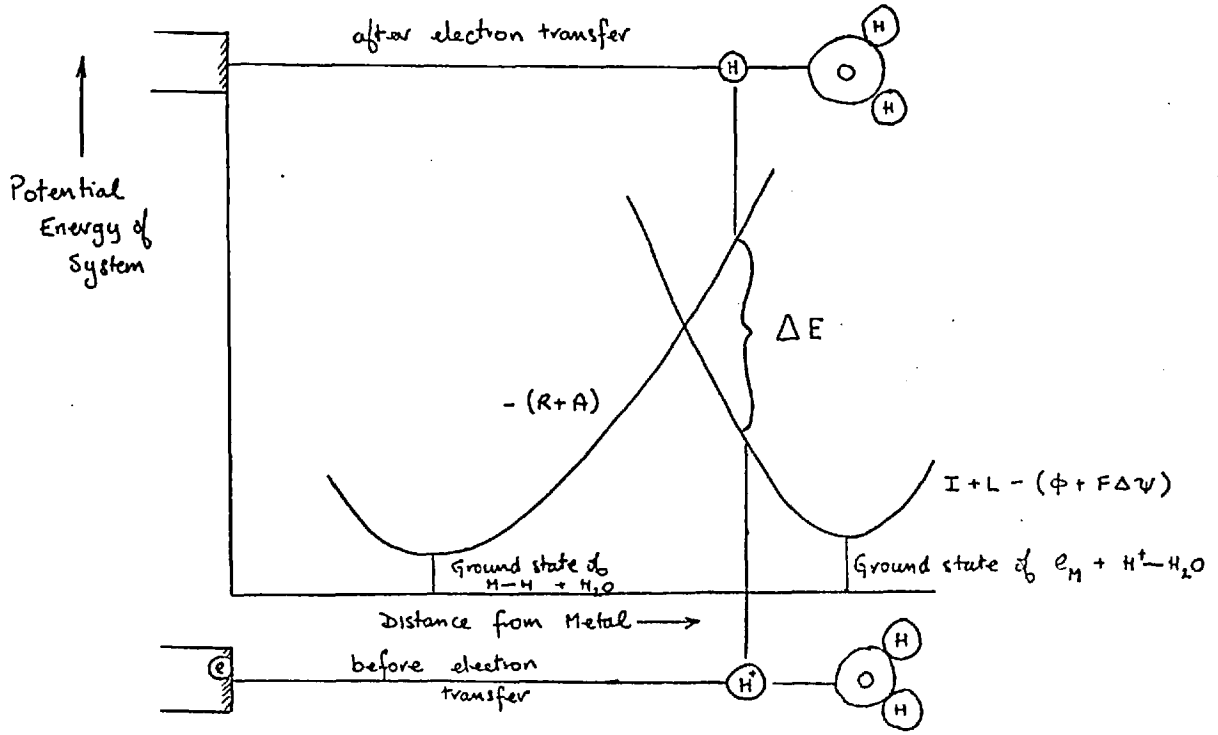

Figure 5.3 Energy Profiles

It can easily be seen that charge transfer cannot occur to the hydrated proton in the ground state and will not occur until the $H^{+}\!\!-\!\!-H_2O$ bond has stretched so that $\Delta E \leqslant 0$. Immediately after transfer occurs, the relevant curve becomes the $-(R + A)$ curve and the repulsion of the water molecule and attraction of the metal set in to make the hydrogen atom adsorb on the metal.

The model that emerges from this theory, which is a combination of that given by Matthews and Bockris (64) and Bockris and Reddy (69), for the reduction of H_3O^+ is as follows.

1. The hydrated proton reaches the electrified interface by conventional means of transport diffusion and conduction.
2. The bond between the proton and the water molecule stretches as the proton vibrates.
3. When the electron tunneling condition is achieved, transfer of an electron occurs.
4. The hydrogen atom moves on to its final state i.e. adsorption on the electrode surface.

Incidentally, it was Gurney's assumption that there was no interaction between the atom and the metal that led to the theory's rejection, as it was markedly discrepant with the order of magnitude of the heat of activation observed for some electrochemical reactions.

5.2.2 Other Electrochemical Reactions

As pointed out by Bockris and Matthews (68), there exists no single unified theory of charge transfer from electrodes in electrolyte solution. Parts of their treatment of the hydrogen evolution reaction are incorporated in the model given here.

According to Bockris and Reddy (69), there is no reason why the model for the hydrogen evolution reaction cannot be applied to the reduction of a hydrated metal ion, leading to the deposition of the metal on the electrode, eg.

$$[Ag(H_2O)_n]^+ + e_M^- \longrightarrow M\text{—}Ag + nH_2O$$

The silver ion is enveloped in a solvation sheath of n water molecules rather than one (as in the case of H_3O^+), which is an added complication, though the tunneling condition is achieved in a similar manner by the displacement of the ion from the surrounding water molecules until the electron energy is equal to the energy in the Fermi level in the electrode. On the basis of this model, electron transfer and dehydration occur simultaneously, however, from the discussion in Section 5.1, it would appear unlikely that the two processes do occur together.

The same sort of model applies to redox reactions of the type

$$M^{(z+1)+}(H_2O)_n + e_M^- \longrightarrow M^{z+}(H_2O)_m + n\text{-}mH_2O + M$$

where both ions remain dissolved in the electrolyte, and the interaction with the surface is much less than of, say,

the proton discharge reaction. This type of reaction has been discussed by Gerisher (67), who considers that the $M^{(z+1)+}(H_2O)_n$ represent 'empty' terms and the $M^{z+}(H_2O)_m$ 'full' terms. The position of the empty terms on the energy scale is given by the work done in bringing an electron from infinity into the electron state of the ion. Each ion has a solvation sheath that is different on a time average and which constantly fluctuates because of thermal energy. Thus the energies of the two kinds of ion form a distribution of energy states analogous to the distribution of electrons in the metal. Electron exchange takes place in the immediate region of the Fermi level, indicating that the solvation sheath of the ion favoured for electron transfer has a structure between the most probable states of the individual components. Transfer only occurs when the ions have reached a favourable configuration.

The question still arises of what the various stages are in the deposition of a doubly (or higher) charged solvated metal ion.

5.2.3 Deposition of Doubly Charged Ions

Most authors appear careful to avoid general discussion of the mechanism of the deposition of doubly charged ions and confine themselves to the specific cases of iron and copper, on which most experimental work has been done. However, if the various models developed earlier are put together, then a possible mechanism emerges.

As the simultaneous transfer of more than one electron is extremely unlikely, the first stage in the deposition must be the tunneling of one electron to the ion in solution to give a singly charged ion with a different solvation sheath (Gerisher's theory) near the electrode surface but in solution. This is then followed by transfer of a second electron, which results in the formation of a partially hydrated adion on the surface of the electrode (Bockris and Damjanovic's theory). The ion is transferred to a planar site and then undergoes a two dimensional random walk process until the remaining molecules of water in the solvation sheath are gradually replaced by co-ordinating metal ions. This process is shown diagrammatically in Figure 5.4.

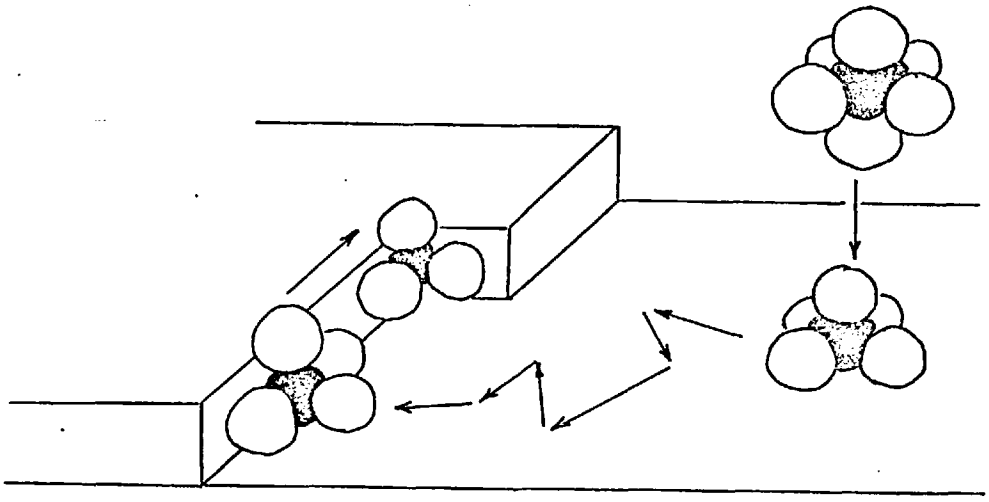

Figure 5.4 Initial Stages of Electrodeposition

The final step in the incorporating of the surface species into the electrode metal lattice is the contribution of an electron to the free electron 'flux' in the electrode. An alternative mechanism is if the step-wise transfer of two electrons to an ion in solution did not occur, but after transfer of the first had occurred, a surface adion was formed. The second electron would be transferred to a species on the surface. Then, after the successive dehydration process, an electron would be 'given back' to the metal. The overall result is that a divalent metal ion would be deposited with only the transfer of one electron across the electrode-solution interface.

The metal ion which has been investigated most extensively is copper (60,63,70,71), though the analysis has always been from a kinetic viewpoint to try and elucidate the rate determining step, rather than to build up a picture of the process occurring. However, the mechanisms proposed are not inconsistent with the model discussed here. It may be that every metal is electrodeposited from aqueous solution via a different mechanism, and that it is not possible to generalise to any great extent. Bockris, in one of his most recent contributions to dicussions of the nature of deposition (72), adopts a more comprehensive and unified approach to the problem, and for the first time in any of his contributions to this field, discusses the specific case of the discharge of divalent metal ions. He considers four possible

mechanisms, namely:-

1. $M^{2+} + 2e^- \rightleftharpoons M$

2. $M^{2+} + e^- \rightleftharpoons M^+$; $M^+ + e^- \rightleftharpoons M$

3. $M^{2+} + M \rightleftharpoons 2M^+$; $M^+ + e^- \rightleftharpoons M$

4. $M^{2+} + e^- \rightleftharpoons M^+$; $2M^+ \rightleftharpoons M^{2+} + M$

and considers the results of various workers for copper, cadmium, zinc and iron (though iron is treated as something of a special case) and states that there is good experimental evidence that mechanisms involving univalent intermediates prevail, i.e. mechanisms 2 and 4 above.

It is interesting to speculate on the fate of the species produced after the first electron has been transferred to the ion in solution. If the potential of the electrode is insufficiently cathodic, then the electron tunneling condition may not be achieved for the second electron and the resultant hydrated ion would diffuse away from the electrode surface (eg $Fe^{3+} \longrightarrow Fe^{2+}$). If, however, the potential is sufficiently negative so that transfer of a second electron is possible, then there are a number of possible reactions when the singly charged species is thermodynamically unstable and there is the possibility of electron transfer in a homogeneous redox reaction in the solution (73,74,75). For a divalent ion M^{2+}_{aq} the following reactions could occur (the subscript 'aq' represents a variable number of water molecules in the solvation sheath).

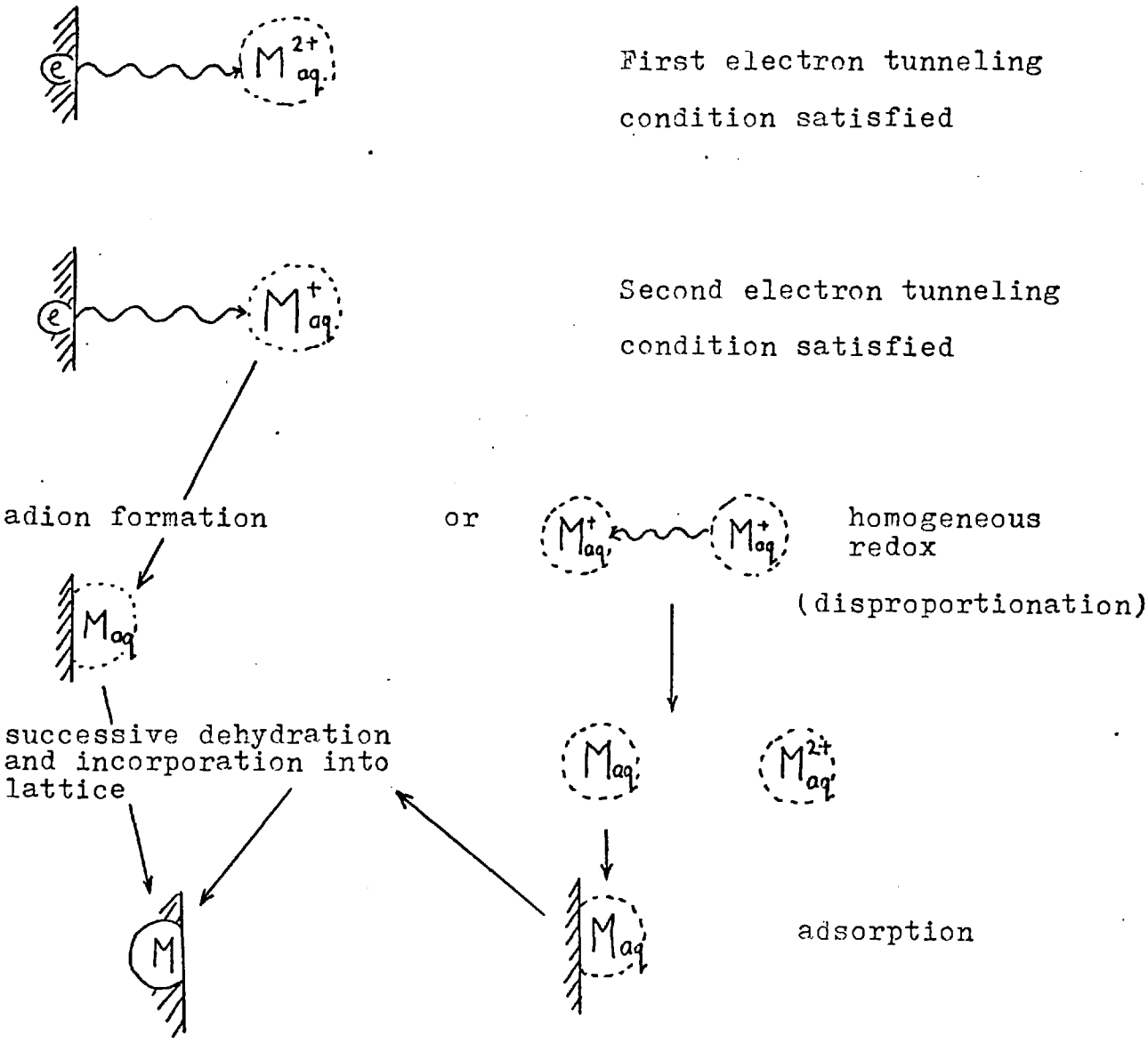

It can be seen that there is a possibility of producing reduced species such as M^{+}_{aq} or even M_{aq}. The extent to which the various pathways above will occur will depend on the relative probabilities for the various electron tunnelings (which, in turn, depend on the shape of the barrier). If these reduced species had sufficient lifetimes, then it is possible that they could diffuse far enough from the electrode and in sufficient concentrations

to interact measureably with the analysing light beam that is passing through the solution in the experiments described in Chapter 4.

Finally, there is one further consideration that is of interest, and that is the possibility of the solvent molecules orientating themselves to produce an energy level such that electrons can tunnel from a suitably charged electrode into the solution to form hydrated electrons.

5.3 Hydrated Electrons in Aqueous Electrochemical Reactions

The existance of hydrated electrons, first discovered in studies on the radiolysis of water, in aqueous media is now established beyond doubt. The species has been as extensively studied as any other ionic species in solution from the point of view of structure (76), and of reaction with both inorganic and organic compounds (77). In recent years, numerous comprehensive reviews have appeared (78,79,80,81,82,83). Two (84,55) are of particular interest here, as they approach the problem of the involvement of hydrated electrons in aqueous electrochemical reactions from different viewpoints. Kenney and Walker (55), in a very lucid discussion, argue in favour of solvated electrons being involved in aqueous electrochemical reactions, particularly as a precursor in the hydrogen evolution reaction, an idea supported by other workers (85,86). Conway (84), on the other hand, in a more

to interact measureably with the analysing light beam that is passing through the solution in the experiments described in Chapter 4.

Finally, there is one further consideration that is of interest, and that is the possibility of the solvent molecules orientating themselves to produce an energy level such that electrons can tunnel from a suitably charged electrode into the solution to form hydrated electrons.

5.3 Hydrated Electrons in Aqueous Electrochemical Reactions

The existance of hydrated electrons, first discovered in studies on the radiolysis of water, in aqueous media is now established beyond doubt. The species has been as extensively studied as any other ionic species in solution from the point of view of structure (76), and of reaction with both inorganic and organic compounds (77). In recent years, numerous comprehensive reviews have appeared (78,79,80,81,82,83). Two (84,55) are of particular interest here, as they approach the problem of the involvement of hydrated electrons in aqueous electrochemical reactions from different viewpoints. Kenney and Walker (55), in a very lucid discussion, argue in favour of solvated electrons being involved in aqueous electrochemical reactions, particularly as a precursor in the hydrogen evolution reaction, an idea supported by other workers (85,86). Conway (84), on the other hand, in a more

thorough discussion of the problem, argues against their involvement in this type of reaction.

The electron tunneling condition (see Section 5.2) may be written as

$$\phi_{e,s} = \phi_e + V_{M,soln} - G_{s,e}$$

where $\phi_{e,s}$ is the work function relevant to the escape of an electron into the solution, ϕ_e is the work function for the metal-vacuum interface, $V_{M,soln}$ is the metal-solution potential difference at a given measured electrode potential and $G_{s,e}$ is the free energy of solvation of the electron from its state in the vacuum (87).

Substitution of the appropriate values (88) yields a value for the potential at a platinum electrode (with respect to the reversible hydrogen electrode) of -2·8 V. Under these conditions, the normal evolution mechanism involving H^+_{aq} and e^- in the metal (see previous Section) would yield a current many orders of magnitude greater than the current for direct production of hydrated electrons. The value of the standard electrode potential for aqueous media has been the subject of some discussion (89,90,91,92), but is currently estimated to be -2·67 V. Thus, the hydrated electron is a stronger reducing agent than either the hydrogen atom (-2·1 V) or the solvated electron in ammonia (-1·95 V).

Kenney and Walker get round this problem by the following arguments. In the conventional manner, the

standard potential of e^-_{aq} should be equal to the standard free energy change for the reaction

$$H^+_{aq} + e^-_{aq} \longrightarrow \tfrac{1}{2}H_{2(g)} \qquad 5.1$$

for which Baxendale (89) calculated $\Delta G^\circ_1 = -61{\cdot}5$ kcal mole^{-1}. For the reaction

$$H^+_{aq} + e^-_{Pt} \longrightarrow \tfrac{1}{2}H_{2(g)} \qquad 5.2$$

ΔG°_2 is arbitrarily taken as zero; but, argue Kenney and Walker, it cannot be concluded that by difference ΔG°_3 for the reaction

$$e^-_{Pt} \longrightarrow e^-_{aq} \qquad 5.3$$

is +61·5 kcal mole^{-1} because ΔG°_1 is on an absolute basis and is not directly related to $\Delta G^\circ_2 = 0$. They further argue that the free energy of Reaction 5.3 above may not constitute an energy barrier in the hydrogen evolution reaction because the potential required (-2·1 V) to form hydrogen atoms in the reaction

$$H^+_{aq} + e^-_{Pt} \longrightarrow H_{ads} \qquad 5.4$$

does not represent an energy barrier, as the hydrogen atoms remain adsorbed on the surface (the electrode is actually reversible to hydrogen gas) and possibly a mechanism involving pairing such as

$$e^-_{aq} + e^-_{aq} \longrightarrow H_2 + 2OH^-_{aq} \qquad 5.5$$

makes the electrode reversible to $H_{2(g)}$ and that the nature of the intermediate is irrelevant; the reversible potential being given by the activity of the hydrogen gas

in equilibrium with the electrode.

They make one further point that, in practice, the electrode could never be made reversible with respect to such a highly reactive and mobile species as e^-_{aq}, and that electrons becoming hydrated 3-10 nm from the surface cannot again surmount the high field gradient of the double layer, and that the only meaningful concentration at the surface which affects the potential at which e^-_{aq} is generated may be so small that there is essentially no thermodynamic barrier to its formation.

Conway considers the non-equilibrium situation arising from annihilation and concludes that "the thermodynamic conclusions regarding electrochemical production of e^-_{aq} are not invalidated by the fact that non-equilibrium conditions are obtained in water and acid solutions".

The conviction that hydrated electrons are involved in the hydrogen evolution reaction is, of course, based on experimental evidence. Hills and Kinnibrugh (86) suggested that the negative volume of activation in the kinetics of the hydrogen evolution reaction at high pressures supports the view that e^-_{aq} is involved, as it would be expected that the electron would have a large positive molal volume in water as it has in ammonia (93). Subsequent examination of the experiment by Conway (94) and Kristalik (95) showed that the pressure dependence of the emf of the reference electrode and the reversible hydrogen electrode had not been taken into account correctly, and that the activation

volume was, in fact, positive and entirely consistent with the normal H^+ neutralization mechanism.

Walker presents evidence on the basis of experiments with scavengers (96), this is countered by Conway, who argues that only in the case of dissolving base metals or strong amalgams does it seem possible that a process of direct electron injection to form e^-_{aq} might occur to a small extent as a parallel reaction with the normal hydrogen evolution as the main cathodic partial process.

Walker (37) also produces spectrophotometric evidence in an experiment in which a He/Ne laser is shone tangentially round the inside of a polished silver elliptical 'cylinder' and the absorbance at 632·8 nm measured. The decrease in absorbance when the cylinder is made the cathode in an electrolyte solution of 0·25 M sodium sulphate adjusted to pH 1 with sulphuric acid with a silver wire anode, is interpreted as being due to absorption by solvated electrons (λ_{max} 720 nm, ϵ_{633} $1{\cdot}25\times10^4$ l mole^{-1} cm^{-1}). This interpretation of the result of the experiment has been criticised by Conway (84,97) and McIntyre (98) who regard the effect observed by Walker to be due to a combination of ionic and electronic electroreflectance effects. Schindewolf (99) could find no evidence for the production of e^-_{aq} at a silver cathode. Walker, however, has replied to these criticisms (100) and the discussion continues.

An experiment whose results are harder to interpret is that of Yurkov (101) who produced a layer of colloidal

copper metal at distances of 0·1 to 1 mm from a cathode surface when a solution of sodium nitrate was electrolysed at high current density (2 A cm^{-2}) using a copper anode and almost any other metal as the cathode. The electrodes were about 1·5 mm apart and of 0·2 mm^2 cross-sectional area. Conway is unable to explain the result, but Kenney and Walker propose that the entity responsible for the reduction is a solvated dielectron, $(e_2^{2-})_{aq}$, which has sufficient lifetime to diffuse away from the cathode (e_{aq}^- has far too short a lifetime, 10^{-11} sec, to be responsible). They further suggest that this species is responsible for the results obtained by Uhlig and Krutenat (102) who detected a reducing species in solution near a platinum or tin cathode in the electrolysis of sodium chloride solutions at pH 10. This species, which had an average half life of 5 min was interpreted by them as hydrogen atoms.

Conway discusses the thermodynamic difficulties in the evaluation of E^o for the hydrated electron and also discusses the problems which arise from a consideration of the principle of microscopic reversibility, whereby H would have to give e_{aq}^- spontaneously. He further points out that electrochemically adsorbed H can be controllably produced at a number of noble metals such as Pt, Rh or Ir (103,104) and shows an independence of pH at variance with what would be expected if e_{aq}^- were the precursor (105). Conway also points out that one of the characteristics of the kinetics of the hydrogen evolution reaction is a strong

dependence on the cathode material, the ejection of electrons into the solution would not give this dependence.

None of the authors who favour the hydrated electron mechanism for hydrogen evolution, actually go as far as to suggest that the first stage in metal deposition is the formation of e^-_{aq} (though there is no reason why the hydrogen evolution reaction should be unique in this way) which then reacts with a hydrated metal ion in the double layer.

And so, it must be concluded that, with the possible exception of Yurkov's work, all the evidence points to the fact that solvated electrons are not involved in aqueous electrochemical reactions, apart from the dissolution of strong amalgams.

There is, though, one experimental condition under which electrons are ejected from the cathode into aqueous solution, and that is when the cathode is illuminated.

5.3.1 Photoassisted Electron Ejection from Cathodes

Photoeffects on electrode potentials in the absence of electronically excitable, electrochemically active molecules were first characterised by Bowden (106). The effect was first studied quantitatively by Heýrovsky (107). Barker *et al* (108,109,110) examined the effect of scavengers for hydrated electrons on the photocurrent behaviour of mercury electrodes and showed that the rate constants for the scavenging processes were the same as those evaluated in pulse radiolysis experiments where hydrated electrons are

well characterised, and concluded that the photoemitted species were electrons. Similar conclusions were reached by Delahay and Srinivasan (111) from coulostatic experiments.

The basic equations for electrochemical photoeffects were given by Bockris (112) who showed that the provision of photoassistance lowers the work function of the metal, and thus lowers the potential necessary to satisfy the electron tunneling condition, by $300h\nu/e$. In practice, at a mercury electrode, photocurrents of the order of $0{\cdot}2\ \mu A$ are obtained with a 1 kW mercury arc source, the currents being proportional to intensity at a given wavelength. Barker (108,109) envisaged the formation of hydrated electrons some distance from the surface in three steps.

1. Ejection of the electron from the electrode.
2. Thermalization.
3. Hydration, an appreciable fraction returning to the electrode before hydration occurs.

He concluded that hydrated electrons were formed at 3 to 30 nm from the electrode but did not calculate a concentration. Walker (113) calculated that if hydrated electrons were formed, then they would exist within a distance of 170 nm of the surface at a concentration of about 8×10^{-7} M. This distance is an order of magnitude greater than that calculated by Pyle and Roberts (85). Conway (84) suggests that photoassisted emission could be responsible for the production of solvated electrons in Walker's experiment with the laser and the silver cathode (37), though he

questions whether the intensity of the illumination was sufficient to produce the effects observed.

From this discussion, it seems unlikely that electrons are being photo-ejected from the platinum cathode in the experiments described in Chapter 4 (the power of the deuterium lamp was 24 W), furthermore, as the layers of solution approximately 0·1 mm above the cathode surface were being monitored, it seems unlikely that any process occurring within 200 nm (or less) of the surface will have any measurable interaction with the light beam.

If the effect being observed were the interaction of hydrated electrons with the cations in solution, then it would be expected that the results obtained would be similar to those produced in radiolysis experiments, where radiolytically generated hydrated electrons react with metal ions in solution. Such a study was made by Baxendale *et al* (114), who recorded the uv/vis. absorption spectra of species generated when metal ions (including Cu^{2+}, Cd^{2+}, Ni^{2+}, Co^{2+}, Zn^{2+}, Pb^{2+}, and Ag^{+}) reacted with hydrated electrons produced by a 2 μsec pulse of 4 MeV electrons from a linear accelerator. They found that all the spectra of the transient species produced were similar, with an absorbance maximum around 310 nm. They conclude that this is due to charge transfer of the type,

$$M^{+}:H_2O \longrightarrow M^{2+}.H_2O^{-}$$

i.e. from the metal to the ligand. In the case of copper, the absorption was interpreted as being due to Cu^{3+}. The

spectra obtained in the experiments described in Chapter 4 all have a maximum around 210 nm, and it would appear that the spectra are not due to the formation of species of lower oxidation state.

5.4 Other Reducing Species in Solution

In 1930, Kobosev and Nekrasov (115) reported that they had observed the reduction of yellow WO_3 particles in suspension in 2 M sulphuric acid above a platinum cathode to blue W_2O_5. They suggested that the reducing agent was dissolved atomic hydrogen. Other workers were unable to repeat this experiment and did not observe any colour change unless the particles were actually touching the electrode surface (116).

Uhlig and Krutenat (102,117) in an investigation of a temporary reducing species produced in solution when a magnesium anode dissolved, a phenomenon first reported by Petty et al.(118), also discovered that a similar reducing species was produced near a platinum or tin cathode. From a comparison with atomic hydrogen generated by creating a discharge in a stream of gaseous hydrogen, they concluded that the species being investigated was dissolved atomic hydrogen. They further deduced that at a distance of 0·5 mm from the electrode surface a concentration of atomic hydrogen of about 5×10^{-4}M was obtained. They measured the half life of the species to be 5-6 min and accounted for its failure to reduce WO_3 to W_2O_5 as being due to the

reaction of atomic hydrogen to give molecular hydrogen $H_2(aq)$ in preference to reducing the oxide.

As has already been mentioned, this interpretation of the experimental results has been questioned by Kenney and Walker (55) who suggested that a hydrated dielectron was the species involved.

The experimental conditions employed in Chapter 4 are similar to those used by Uhlig and Krutenat and it is possible, therefore, that a reduced metal species is being formed by the reduction of the metal ions by dissolved atomic hydrogen, which has sufficient life time to achieve a concentration comparable to that of the bulk metal ion solution at a distance from the electrode surface sufficient for any products of the reaction to interact with the analysing light beam.

5.5 Decomposition Potential

The calculation of the potential which must be applied to the electrodes to cause the deposition of a metal from solution involves a knowledge of how the potentials of the anode and cathode reactions vary with concentration, of the overpotential for the evolution of oxygen (at the anode) and of the IR drop across the cell. If the Nernst equation is used to calculate the electrode potentials then the decomposition potential is given by (see Section 2.4).

$$E_{app} = E_{cell} + IR + \omega_{anode}$$

$$= 0{\cdot}804 - \left\{E^{o}_{M} + \frac{0{\cdot}059}{n} \log\left[M^{n+}\right]\right\} + IR + \omega_{anode}$$

As the maximum potential appears to be about 2·2 V for a solution of 0·03 M potassium sulphate at pH 6, then

$$E_{app} = 0{\cdot}804 - (0 - 0{\cdot}36) + IR + \omega_{anode}$$

$$2{\cdot}2 = 0{\cdot}804 + 0{\cdot}36 + IR + \omega_{anode}$$

Thus the sum of the IR drop and the overpotential effects is 1·04 V and the potential required for decomposition is given by

$$E_{app} = 1{\cdot}844 - \left\{E^{o} + \frac{0{\cdot}059}{n} \log[M^{n+}]\right\}$$

The decomposition potentials for the metal ions investigated are given in Table 5.1.

Table 5.1 Decomposition Potentials

Metal Ion 10^{-4} M	E^{o} V	E_{app} V	E_{sce} V
Hg^{2+}	+0·85	1·21	+0·38
Ag^{+}	+0·80	1·16	+0·43
Cu^{2+}	+0·34	1·62	-0·03
Fe^{3+}	-0·04	1·96	-0·37
Pb^{2+}	-0·13	2·09	-0·50
Sn^{2+}	-0·14	2·10	-0·51
Ni^{2+}	-0·25	2·21	-0·62
Co^{2+}	-0·28	2·24	-0·65
Cd^{2+}	-0·40	2·36	-0·77
Fe^{2+}	-0·44	2·40	-0·81
Zn^{2+}	-0·76	2·72	-1·13
Mn^{2+}	-1·18	3·24	-1·65
H^{+} pH 6	0·00	2·20	-0·61
pH 9	0·00	2·38	-0·79
pH 11	0·00	2·50	-0·91

The last column in the Table gives the potential of the cathode with respect to a saturated calomel reference electrode.

The values for the potential required to cause deposition of the metals show that, on the basis of this calculation, the following metals would not be deposited before hydrogen was evolved:- Ni, Co, Cd, Fe(II), Zn, Mn. It has long been known, however, that if the amount of metal deposited on an inert electrode is of monolayer or sub-monolayer quantities the form of the Nernst equation used above no longer holds, and an additional term must be introduced to allow for the activity of the deposit via the energy changes at the deposit-electrode interface (119). The result predicted by this unabridged form of the Nernst equation is that monolayer or sub-monolayer amounts of metal are deposited at potentials more anodic than for deposition of bulk material. This underpotential has been dealt with theoretically (120,121), and has been investigated experimentally by a number of techniques, mainly electrochemical such as the twin electrode thin layer cell developed by Schmidt et al (122,123,124), rotating electrode systems (125,126), potentiostatic pulse techniques, cyclic or linear sweep voltammetry (127,128). A particularly well presented discussion of the deposition of copper on platinum is given by Breiter (129). More recently, the phenomenon has been studied optically by specular reflection spectroscopy (130,131,132,133), this technique is of particular interest in that it enables

in situ measurements to be made of the electrode surface and it is possible to monitor the transition from an atomic to a metallic state (134). A recent discussion of the theory of the phenomenon and a brief review of the methods used to study it is given by Lorenz et al (135). The use of thin films in analytical chemistry has been reviewed by Brainina (136).

The results of the above workers indicate that for a number of inert electrodes such as silver, platinum and gold, underpotentials of between 0·3 and 0·6 V are observed, i.e. monolayer and sub-monolayer deposits are formed at potentials between 0·3 and 0·6 V more anodic than the potential for deposition of the bulk metal. Thus, the values of E_{app} calculated in Table 5.1 may be too high by 0·6 V. If this were so, it would bring the potential required to deposit a monolayer of nearly all the metals studied within the accessible potential range (approximately 2·2 V).

5.6 Diffusion to Plane Electrodes

For a reaction of the type

$$Ox + ne^- \longrightarrow Red$$

where both the species Ox and Red are soluble, the concentrations of the oxidised and reduced species, C_O and C_R respectively, are functions of both time, t, and distance from the electrode surface, x. The variation with distance is given by Fick's first law, provided that the cell is free from

thermal and mechanical disturbances and that the solution contains an excess of supporting electrolyte, as follows.

$$\frac{dN}{dt} = D_o A \frac{\partial C_o}{\partial x}$$

where N is the number of moles, D_o is the diffusion coefficient of the oxidised species, A is the cross-sectional area and C_o is the concentration of the oxidised species.

The flux of material, q, being the number of moles diffusing per unit time through unit area, is given by

$$q = \frac{1}{A}\frac{dN}{dt} = D_o \frac{\partial C_o}{\partial x} \qquad 5.2$$

The change in C_o with time between two planes at distances x and x + dx from the electrode surface (x = 0) is the difference between the number of moles entering at plane x + dx and leaving at plane x. If the process is considered on a unit area of flux basis, then

$$\frac{\partial C_o}{\partial t} = [q(x + dx) - q(x)]/dx$$

The right hand side of this equation is $\frac{\partial q}{\partial x}$ as $x \longrightarrow 0$

$$\frac{\partial C}{\partial t} = \frac{\partial q}{\partial x}$$

But $$q = D_o \frac{\partial C_o}{\partial x}$$ from Equation 5.2

$$\therefore \quad \frac{\partial C}{\partial t} = D_o \frac{\partial^2 C_o}{\partial x^2}$$

This is Fick's second law.

The following boundary conditions apply for the solution in this case.

at t = 0; $C_o^e = C_o^b$

$C_R = 0$

where the superscripts e and b indicate at the electrode surface and bulk respectively.

At $t > 0$; $\quad C_o^e = 0$

and $C_o \longrightarrow C_o^b$ as $x \longrightarrow \infty$

The standard treatment of the problem (137,138) gives

$$C_o(x,t) = \frac{C_o^b 2}{\pi^{\frac{1}{2}}} \int_0^{\frac{x}{2D^{\frac{1}{2}}t^{\frac{1}{2}}}} e^{-y^2} dy \qquad 5.3$$

The integral

$$\frac{2}{\pi^{\frac{1}{2}}} \int_0^z e^{-y^2} dy$$

is known as the error function of z, abbreviated as erf(z). The integral is evaluated numerically and can be found in standard tables.

Thus $$C_o(x,t) = C_o^b \, \mathrm{erf}(z) \qquad 5.4$$

where $$z = \frac{x}{2D^{\frac{1}{2}}t^{\frac{1}{2}}} \qquad 5.5$$

For the production of Red, the corresponding equation is

$$C_R(x,t) = C_o^b \, \mathrm{erfc}(z) \qquad 5.6$$

where erfc(z), the error function complement, is given by

$$\mathrm{erfc}(z) = 1 - \mathrm{erf}(z)$$

A more rigorous treatment may be found in Delahay (139). By introducing a number of simplifying assumptions namely that $C_O(0,t) = 0$ and that $D_R = D_O$, the equations given there reduce to the form used here.

The concentration-distance profile for the species formed during electrolysis is shown in Figure 5.5.

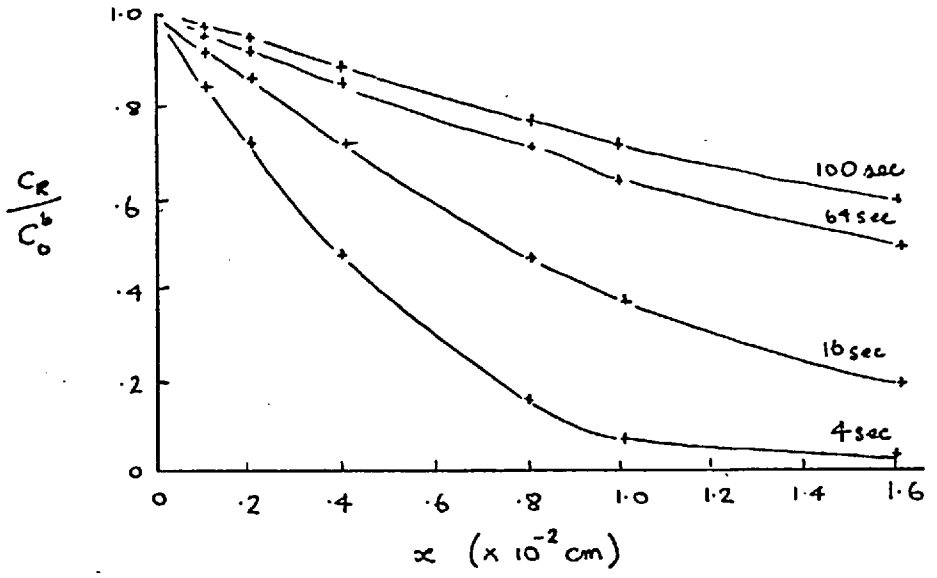

Figure 5.5 Concentration - Distance Profiles

It can be seen from the Figure that as the system evolves with time, the diffusion layer moves out from the electrode surface into the solution. If the thickness of the diffusion layer is defined as that distance from the electrode surface at which $C_o = C_o^b$, the numerical values may be calculated for given times from Equations 5.4 and 5.5. In fact, the value of z which gives erf(z) = 1 is ∞, and for all practical purposes the value of erf(z) may be taken as unity for values of $z \geqslant 2$. Table 5.2 shows the variation with time for $D = 10^{-5}$ cm^2 sec^{-1} and z = 2.

It can be seen that the diffusion layer extends a considerable distance into the solution. It would thus be expected that if the electrode process being monitored in the experiments described in Chapter 4 were of the type discussed here, where the movement of species in the solution is governed by semi-infinite linear diffusion, then the species produced at the electrode surface would diffuse a sufficient distance from the electrode to

Table 5.2 Diffusion Layer Thickness as a Function of Time

Time sec	10^2x cm
0	0·0
1	1·26
4	2·54
9	3·81
16	5·08
25	6·85
36	7·62
49	8·89
64	10·16

interact with the analysing light beam.

5.7 Ultra-Violet Spectra of Complex Compounds

In a theoretical discussion of atomic energy levels, the final levels are obtained by a process of successive approximations, except in the simplest case of the hydrogen atom. For a poly-electronic atom (or ion) the various forces acting within the atom are assessed and placed in order of magnitude and the calculations are then carried out one stage at a time starting with the treatment of the largest force. In general, these forces are divisible into three main classes, 1) central field forces (electrostatic), 2) inter-electronic repulsion forces (electrostatic) and 3) spin-orbit coupling forces (magnetic). The central field forces, involving attraction of the electrons by a central positively charged nucleus, are

much larger than the others (as is necessary for the atom to be stable). The hydrogen atom is the prototype for this part of the problem and the solution of the Schrödinger equation for this atom provides a scheme of one-electron orbitals into which the electrons may be placed according to the aufbau and Pauli principles. Further refinement to this zeroth order set of orbitals is then made depending on the relative magnitude of forces 2 and 3 above. If 2 is very much greater than 3, then the final levels are found from the Russell-Saunders or LS coupling scheme. If 3 is very much greater than 2 (as is the case for atoms with atomic number greater that 30), then the final levels are found from the so-called jj coupling scheme. Intermediate cases arise when the magnitudes of the forces are approximately equal. The validity and correctness of the various approximations are, of course, established by accounting for the atomic spectra observed, the lines of which are a direct measure of the energy difference between two levels. A detailed treatment would be out of place here, but several excellent monographs have been written on the subject, eg (140,141). Only the outer or valence shell electrons give rise to transitions in the uv or visible region of the spectrum (140), and theories of the origin of atomic spectra need only consider the energy states of these electrons. Filled shells always give rise to the same spectroscopic state, namely $^1S_0$ (140).

When the atom is placed in an environment where chemical

combination may take place, an exchange of electrons between the atom and the surrounding chemical entities will occur governed by the thermodynamics of the system, until a free energy minimum is established. In this state, the original electron energy levels will have been further perturbed and the central nucleus of the atom will, in general, have a different number of electrons associated with it (the change being in the outer or valence shell).

These further perturbations have been considered by:-

1. The crystal field theory, where the effect of the ligands is considered to be purely electrostatic and the field arising is calculated to be due to point negative charges (or dipoles as a refinement).
2. The ligand field theory, in which a certain amount of covalent bonding is assumed between the metal and the ligands; molecular orbitals are formed from the linear combination of the appropriate orbitals from the ligand and the metal, to give bonding and antibonding orbitals.

The levels are further perturbed by vibrational effects, the Jahn-Teller effect, ligand inequivalencies etc, and so, in solution, the spectra appear as a series of broad bands of varying intensity. The bands arising from transitions between perturbed levels in the metal ion are usually weak, because they are Laporte forbidden, and occur in the visible part of the spectrum. A discussion of the origin of these spectra and of crystal and ligand field theories may be found in any advanced textbook of inorganic chemistry

as a preface to the section on transition metal compounds (56,142), or in any textbook on co-ordination chemistry (143).

Strong absorbances i.e. Laporte allowed transitions, are often observed in the uv part of the spectrum and are often referred to as charge transfer bands. These can arise in a number of ways as follows.

1. When the excited level has a principal quantum number greater than that of the electrons making up the valence shell, thereby retaining certain atomic characteristics rather that being concerned with binding or having antibonding properties (Rydberg spectra).
2. When transfer occurs to orbitals of the ligand not mixed much with those of the metal (metal oxidation spectra).
3. When an electron is transferred to the central metal ion from a specific ligand, if the ligands are different, or from a ligand molecular orbital if the ligands are equivalent (metal reduction spectra).
4. When the ligand is a polyatomic group and the transitions are between molecular orbitals of the ligand alone (intra-ligand spectra).
5. When the source of the electron is outside the primary ligand sphere(ion pair spectra).
6. When in a bi-nuclear complex with metal ions in different oxidation states transfer occurs between the metal ions. This can occur even if the ions are separated by another atom (such as oxygen) if there is a large amount of electron delocalization. Usually the bands are shifted to

longer wavelengths i.e. into the visible part of the spectrum.

From the intensity and position in the spectrum of the absorbances measured in the experiments described in Chapter 4, it is clear that the spectra are of the charge transfer type rather than being due to transitions within the electron energy levels of the metal ion.

5.8 Summary

The examination of the thoeries of metal deposition shows that the phenomenon of electrodeposition of metal ions on inert substrates, particularly in monolayer or sub-monolayer amounts, is not yet well understood in mechanistic terms. In this Chapter a model composed of features from a number of other models is presented as a possible general mechanism for the discharge of divalent metal ions from aqueous solution. This model gives rise to the possible formation of reduced hydrated metal species at macro distances (in terms of the charge transfer distance) from the cathode surface. It seems unlikely that hydrated electrons are involved in the electrode process (by either field or photo assisted ejection) but the possibility of dissolved atomic hydrogen being present near the cathode cannot be ruled out.

A consideration of the electrode potentials for the various metals studied indicates that, if a reduced metallic state is produced as the final state in the electrode

process, the transfer of electrons must be occurring at underpotential, a phenomenon which, though apparently not widely appreciated at present, is being extensively studied, particularly by the recent powerful combination of electrochemical and optical techniques such as specular reflection spectroscopy and ellipsometry.

An examination of the semi-infinite linear diffusion process shows that a species produced at the electrode surface could diffuse well into the light beam on the time scale of the experiments described in Chapter 4. Finally, the spectra obtained suggest that the absorbing species is one in which charge transfer transitions give rise to the absorbances observed.

6. NATURE OF THE ELECTRODE PROCESS

The experiments described in this Chapter continue the investigation of the absorption phenomena with respect to the parameters discussed at the start of Chapter 4 in the light of the theory discussed in the previous Chapter. Experiments were also performed to investigate some of the electrochemical properties of the process, and to try and determine the nature of the process occurring at the electrode surface and the identity of the absorbing species.

6.1 Variation of Current with Time (Chronoamperometry)

If the electrode process is controlled by semi-infinite linear diffusion (see Section 5.6), then the instantaneous current, i_t, will be proportional to the flux at the electrode surface (i.e. at x = 0).

Thus

$$i_t = n\ F\ A\ q(0,t)$$

where n is the number of electrons, F is the Faraday, A is the electrode area (in cm^2) and q is the number of moles diffusing per unit time through unit area.

Therefore from Equation 5.2

$$i_t = nFAD_o\left(\frac{\partial C}{\partial x}\right)_{0,t} \qquad 6.1$$

The value of the concentration gradient at the electrode surface, $\left(\frac{\partial C}{\partial x}\right)_{0,t}$ is obtained by differentiating Equation 5.3

and evaluating at x = 0.

Now

$$\frac{d}{du}\,\mathrm{erf}[\lambda(u)] = \frac{2}{\pi^{\frac{1}{2}}} e^{-[\lambda(u)]^2} \cdot \frac{d}{du}\lambda(u) \qquad 6.2$$

In this case

$$\lambda(u) = \frac{x}{2D_o^{\frac{1}{2}} t^{\frac{1}{2}}}$$

Therefore

$$\left(\frac{\partial C_o}{\partial x}\right)_{x,t} = C_o^b \frac{2}{\pi^{\frac{1}{2}}} e^{-x^2/4D_o t} \cdot \frac{1}{2D_o^{\frac{1}{2}} t^{\frac{1}{2}}}$$

at x = 0

$$\left(\frac{\partial C_o}{\partial x}\right)_{0,t} = \frac{C_o^b}{\pi^{\frac{1}{2}} D_o^{\frac{1}{2}} t^{\frac{1}{2}}} \qquad 6.3$$

Therefore

$$i_t = \frac{nFAD_o^{\frac{1}{2}} C_o^b}{\pi^{\frac{1}{2}} t^{\frac{1}{2}}} \qquad 6.4$$

It can be seen from Equation 6.4, that for a given system the product $i_t . t^{\frac{1}{2}}$ is a constant and that if the value of the diffusion coefficient, D, is known a value for the electrochemical area may be calculated.

The cell assembly was modified by including a saturated calomel reference electrode into the circuit connected to the cell by a saturated KCl/agar salt bridge. The bridge was drawn out to a capillary and the tip placed close to the working electrode. As recommended in the instruction manual for the function generator, the working electrode was earthed and the effect of a negative going potential was obtained by applying a positive going potential to the counter electrode. To monitor the current flowing

through the cell, the chart recorder was used as a recording ammeter by incorporating a standard resistance in the circuit and measuring the potential drop across it, in exactly the same way as the absorption of the solution was measured by passing the current output from the photomultiplier tube through a standard resistance and recording the voltage drop across it. A schematic diagram of the circuit is shown in Figure 6.1.

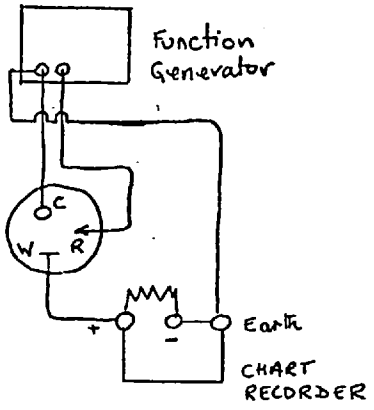

Figure 6.1 Schematic Circuit Diagram

A potential step from +1·2 to -0·6 V vs SCE was applied to the working electrode and the variation of current with time was recorded for a blank solution of 0·03 M potassium sulphate and a solution of 10 ppm Cd^{2+} in 0·03 M potassium sulphate. The results obtained are given in Table 6.1 in which the value of i is corrected for the residual charging current flowing in the absence of the cadmium. It can be seen that over the first sixteen seconds of the electrolysis, ~~that~~ the value of the product

Table 6.1 Current - Time Variation

t sec	i μamp	$it^{\frac{1}{2}}$	t sec	i μamp	$it^{\frac{1}{2}}$
1	40·5	40·50	9	17·0	51·00
2	34·0	47·95	10	14·5	45·80
3	28·0	48·45	11	14·0	46·50
4	25·0	50·00	12	14·0	48·45
5	23·0	50·15	13	14·0	50·55
6	20·0	49·00	14	12·5	46·80
7	19·0	50·35	15	12·0	45·95
8	18·0	50·95	16	11·5	46·00

$it^{\frac{1}{2}}$ is approximately constant. Using a value for the diffusion coefficient of Cd^{2+} of $7{\cdot}2\times10^{-6}$ cm^2 sec^{-1} (144), the area of the electrode was calculated to be 1·86 cm^2. The physical area of the electrode was approximately 1 cm^2, showing that the application of this theory gives a result of the correct order of magnitude.

6.2 Variation of Absorbance with Time

6.2.1 Absorbance Measured Normal to the Electrode Surface

Method 1.

The total charge that has been passed at any given time t, can be found by integration.

Thus

$$Q(t) = \int_0^t i_t \, dt$$

From Equation 6.4

$$Q(t) = \frac{nFaD_o^{\frac{1}{2}}C_o^b}{\pi^{\frac{1}{2}}} \int_0^t t^{-\frac{1}{2}} \, dt$$

where a is the surface area of the electrode

$$Q(t) = \frac{2nFaD_o^{\frac{1}{2}}C_o^b t^{\frac{1}{2}}}{\pi^{\frac{1}{2}}} \qquad 6.5$$

From Faraday's laws, the weight of material 'deposited', w, is given by

$$w(t) = \frac{Q(t)E}{F}$$

where E is the equivalent weight, given by

$$E = \frac{M}{n}$$

where M is the molecular weight.

If the volume of the solution in which the material is dissolved is V(t), then

$$C_R(t) = \frac{w(t)}{EV(t)} = \frac{Q(t)}{nFV(t)}$$

where $C_R(t)$ is the concentration of the reduced species. The volume is a function of time as the reduced species is diffusing out into the solution.

$$\therefore \qquad C_R(t) = \frac{2aD_o^{\frac{1}{2}}C_o^b t^{\frac{1}{2}}}{\pi^{\frac{1}{2}}V(t)}$$

Now if the absorbance is measured at right angles to the surface of the electrode, then

$$A(t,\lambda) = \epsilon_R(\lambda)l(t)C_R(t)$$

The pathlength, as well as the concentration, is a function of time.

If this pathlength is taken as the volume, V(t), divided by the electrode surface area, a, then

$$A(t,\lambda) = \epsilon(\lambda)\frac{V(t)}{a}.\frac{2aD_o^{\frac{1}{2}}C_o^b t^{\frac{1}{2}}}{\pi^{\frac{1}{2}}V(t)}$$

$$A(t,\lambda) = \epsilon(\lambda)\frac{2D_o^{\frac{1}{2}}t^{\frac{1}{2}}C_o^b}{\pi^{\frac{1}{2}}} \qquad 6.6$$

Thus a plot of absorbance vs $t^{\frac{1}{2}}$ would be a straight line, from whose slope $\epsilon_R(\lambda)$ could be found if D_o and C_o^b were known.

A similar derivation of the relationship is given by Strojek and Kuwana (12), though the argument is very poorly presented. Confusion arises because of their use of the same symbol for absorbance and electrode area. The result is also identical to that derived by the method of Laplace transforms on Fick's equations with the appropriate boundary conditions (4).

It should be noted that although Equations 6.5 and 6.6 are similar, kinetic complications which occur within the diffusion layer will affect the A-t and Q-t behaviour quite differently, as absorbance is characteristic of the integrated concentration of the reduced species, whereas charge is characteristic of the integrated flux of the oxidised species at the electrode surface.

Method 2.

As the pathlength and the concentration both vary with time for absorbance measured normal to the electrode surface, then

$$A = \epsilon_R \int C_R(x)\, dx$$

and, from Equation 5.6,

$$C_R = C_o^b \operatorname{erfc}(z)$$

where $$z = \frac{x}{2D_o^{\frac{1}{2}}t^{\frac{1}{2}}}$$

Thus the absorbance is given by

$$\underset{h\to\infty}{A} = \epsilon_R C_o^b \int_o^h \text{erfc}(z)\, dx$$

Now let

$$I = \int_o^h \text{erfc}(z)\, dx$$

$$\therefore \quad I = \int_o^h [1 - \text{erf}(z)]\, dx$$

$$= \int_o^h dx - \int_o^h \text{erf}(z)\, dx$$

$$= h - \int_o^h \text{erf}(z)\, dx$$

Let $J = \int_o^h \text{erf}(z)\, dx$

and integrate by parts

i.e. $$\int u \frac{dv}{dx}\, dx = uv - \int v \frac{du}{dx}\, dx$$

where $u = \text{erf}(z)$, $v = x$

$$\frac{du}{dx} = \frac{2}{\pi^{1/2}} e^{-x^2/4Dt} \cdot \frac{1}{2D^{1/2}t^{1/2}} \qquad \text{from Equation 6.2}$$

$$\frac{dv}{dx} = 1$$

$$\therefore \quad J = \left[x\,\text{erf}(z)\right]_o^h - \int \frac{x\, e^{-x^2/4D_o t}}{\pi^{1/2} D_o^{1/2} t^{1/2}}\, dx$$

now $$\frac{d(e^{-x^2/4D_o t})}{dx} = \frac{-2x}{4Dt} e^{-x^2/4D_o t}$$

$$\therefore \quad J = h\,\text{erf}\frac{h}{2D_o^{1/2}t^{1/2}} + \frac{4Dt}{2\pi^{1/2}D_o^{1/2}t^{1/2}} \int_o^h \frac{-2x}{4D_o t} e^{-x^2/4D_o t}\, dx$$

$$= h\,\text{erf}\frac{h}{2D_o^{1/2}t^{1/2}} + \frac{2D_o^{1/2}t^{1/2}}{\pi^{1/2}} \left[e^{-x^2/4D_o t}\right]_o^h$$

$$J = h.\mathrm{erf}\frac{h}{2D_o^{\frac{1}{2}}t^{\frac{1}{2}}} + \frac{2D_o^{\frac{1}{2}}t^{\frac{1}{2}}}{\pi^{\frac{1}{2}}}\, e^{-h^2/4D_ot} - \frac{2D_o^{\frac{1}{2}}t^{\frac{1}{2}}}{\pi^{\frac{1}{2}}}$$

$$\therefore \quad I = h - h.\mathrm{erf}\,\frac{h}{2D_o^{\frac{1}{2}}t^{\frac{1}{2}}} - \frac{2D_o^{\frac{1}{2}}t^{\frac{1}{2}}}{\pi^{\frac{1}{2}}}\, e^{-h^2/4D_ot} + \frac{2D_o^{\frac{1}{2}}t^{\frac{1}{2}}}{\pi^{\frac{1}{2}}}$$

$$I = h.\mathrm{erfc}\,\frac{h}{2D_o^{\frac{1}{2}}t^{\frac{1}{2}}} - \frac{2D_o^{\frac{1}{2}}t^{\frac{1}{2}}}{\pi^{\frac{1}{2}}}\, e^{-h^2/4D_ot} + \frac{2D_o^{\frac{1}{2}}t^{\frac{1}{2}}}{\pi^{\frac{1}{2}}}$$

Now as $h \longrightarrow \infty$

$$\mathrm{erfc}\,\frac{h}{2D_o^{\frac{1}{2}}t^{\frac{1}{2}}} \longrightarrow 0 \quad \text{and} \quad e^{-h^2/4D_ot} \longrightarrow 0$$

$$A = \frac{\epsilon_R C_o^b 2D_o^{\frac{1}{2}}t^{\frac{1}{2}}}{\pi^{\frac{1}{2}}}$$

This result is identical to that obtained by the first method (see Equation 6.6).

It should be noted that the product of the pathlength and the concentration, that a light beam normal to the electrode surface passes through, varies linearly with the square root of the time. This result means that the situation is exactly equivalent to that in which the concentration is uniform up to a sharp boundary (beyond which it is zero) which moves out into the solution linearly with $t^{\frac{1}{2}}$. This fact is used in the next Section to derive an expression for the variation of absorbance, measured parallel to the electrode surface, with time.

6.2.2 Absorbance Measured Parallel to the Electrode Surface

This is the situation that is used in the experiments described in Chapter 4. The pathlength on the electrode surface, l, is fixed and the reduced species moves out into a light beam of finite height, h.

Now from Equation 6.6 the absorbance normal to the electrode surface, $A_\perp$, is given by

$$A_\perp = \frac{\epsilon_R 2 D_o^{\frac{1}{2}} t^{\frac{1}{2}} C_o^b}{\pi^{\frac{1}{2}}}$$

this may be written as

$$A_\perp = \epsilon_R l_{eq} C_R$$

where l_{eq} is the path length in which the concentration of the reduced species, C_R, may be considered uniform such that for $x < l_{eq}$, the concentration of reduced species is C_R and for $x > l_{eq}$ the concentration is zero; and such that

$$l_{eq} C_R = \frac{2 D_o^{\frac{1}{2}} C_o^b t^{\frac{1}{2}}}{\pi^{\frac{1}{2}}} \qquad 6.7$$

Now a light beam parallel to the electrode surface 'sees' a concentration given by

$$C_R' h = C_R l_{eq}$$

i.e.

$$C_R' = \frac{C_R l_{eq}}{h} \qquad 6.8$$

This is illustrated in Figure 6.2.

Now the absorbance parallel to the electrode surface, $A_\parallel$, is given by

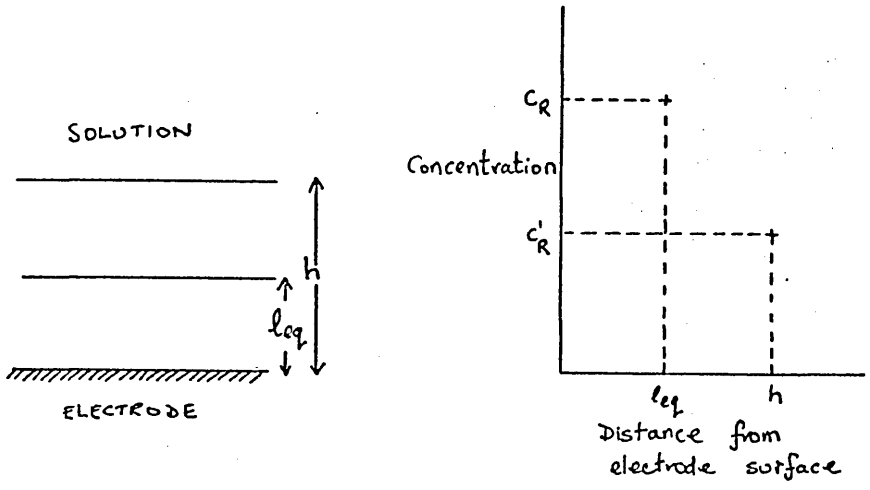

Figure 6.2 Cross Section Through Electrode-Solution Interface

$$A_{\parallel} = \epsilon_R l C'_R$$

from Equation 6.8

$$A_{\parallel} = l \frac{C_R l_{eq}}{h} \qquad 6.9$$

and from Equation 6.7

$$A_{\parallel} = \frac{\epsilon_R l 2 D_o^{\frac{1}{2}} C_o^b t^{\frac{1}{2}}}{h \pi^{\frac{1}{2}}} \qquad 6.10$$

Thus a plot of absorbance against the square root of the time would be a straight line from which ϵ_R could be found if l, D_o, C_o^b and h were known.

In the foregoing treatment of the variation of absorbance with time it has been assumed that only the reduced species absorbs at the wavelength chosen. However, if both the oxidised and reduced species absorb, then the expression must be expanded to include the decrease in absorbance of the oxidised species.

As the electrode reaction has been formulated as

$$Ox + ne^- \longrightarrow Red$$

i.e. for every molecule of Red that appears, one molecule of Ox disappears, then in any given volume

$$C_o' + C_R' = C_o^b$$

where C_o' is the concentration of the oxidised species that the light beam parallel to the electrode surface 'sees'. Now

$$A_{o,\parallel}(t) = \epsilon_o l\, C_o'(t)$$

where $A_{o,\parallel}(t)$ is the absorbance of the oxidised species measured parallel to the electrode surface at time t. The notation indicating that A and ϵ are both functions of wavelength is omitted for clarity.

$$A_{o,\parallel}(t) = \epsilon_o l\left[C_o^b - C_R'(t)\right]$$

$$= \epsilon_o l\, C_o^b - \epsilon_o l\, C_R'(t)$$

from Equation 6.8, $$= A_{o,\parallel}(0) - \frac{\epsilon_o l\, C_R l_{eq}}{h}$$

and from Equation 6.7,

$$A_{o,\parallel}(t) = A_{o,\parallel}(0) - \frac{\epsilon_o l.2D_o^{\frac{1}{2}} C_o^b t^{\frac{1}{2}}}{h\pi^{\frac{1}{2}}} \qquad 6.11$$

The experimental situation is shown in Figure 6.3.

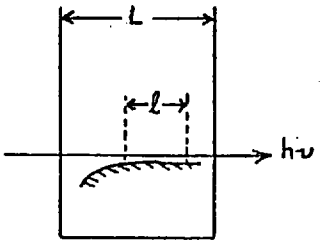

Figure 6.3 Schematic Diagram of Cell

It can be seen from the Figure that the pathlength on the electrode does not equal the pathlength of the cell. If the oxidised form absorbs, then the final equation must include a term to account for the absorbance due to the solution at each end of the electrode. During electrolysis, the absorbance measured is made up of three components;

1. the absorbance of the oxidised species outwith the ends of the electrode,
2. the absorbance of the oxidised species within the path length on the electrode surface,
3. the absorbance of the reduced species within the path length on the electrode surface.

Thus

$$A = \epsilon_o C_o^b (L - l) + \epsilon_o C_o' l + \epsilon_R C_R' l$$

$$A = \epsilon_o (L - l) C_o^b + \epsilon_o C_o^b l - \frac{2\epsilon_o l D_o^{\frac{1}{2}} C_o^b t^{\frac{1}{2}}}{h\pi^{\frac{1}{2}}} + \frac{2\epsilon_R l D_o^{\frac{1}{2}} C_o^b t^{\frac{1}{2}}}{h\pi^{\frac{1}{2}}}$$

$$= \epsilon_o L C_o^b + \frac{2 l D_o^{\frac{1}{2}} C_o^b t^{\frac{1}{2}} (\epsilon_R - \epsilon_o)}{h\pi^{\frac{1}{2}}}$$

$$= A(0) + \frac{2 l D_o^{\frac{1}{2}} C_o^b t^{\frac{1}{2}} (\epsilon_R - \epsilon_o)}{h\pi^{\frac{1}{2}}}$$

As the initial absorbance, A(0), is always set equal to zero,

$$A = \frac{2 D_o^{\frac{1}{2}} (\epsilon_R - \epsilon_o) . l . C_o^b t^{\frac{1}{2}}}{h\pi^{\frac{1}{2}}} \qquad 6.12$$

Thus the absorbance is a linear function of the square root of the time and the product $At^{-\frac{1}{2}}$ should be a constant. It can be seen from the equation that the absorbance only increases during electrolysis if $\epsilon_R > \epsilon_o$ and that if $\epsilon_o = 0$,

the expression reduces to Equation 6.10. It is noted that the maximum value that the absorbance can have is given by

$$A_{max} = (\epsilon_R - \epsilon_o)\ l\ C_o^b$$

This occurs when

$$\frac{2D_o^{\frac{1}{2}} t^{\frac{1}{2}}}{h\pi^{\frac{1}{2}}} = 1$$

For values of $D_o = 10^{-5}$ cm^2 sec^{-1} and h = 0·02 cm, t = 31·5 sec

A plot of A vs t is shown in Figure 6·4 for the following values, $D_o = 10^{-5}$ cm^2 sec^{-1}, $C_o^b = 10^{-4}$ M, $\epsilon_R = 5000$ l mole^{-1} cm^{-1}, $\epsilon_o = 0$, l = 1 cm and h = 0·02 cm. The curve obtained on electrolysing a 10 ppm solution of Co^{2+} in 0·1 M KCl at 1·6 V is also shown. The wavelength used was 210 nm.

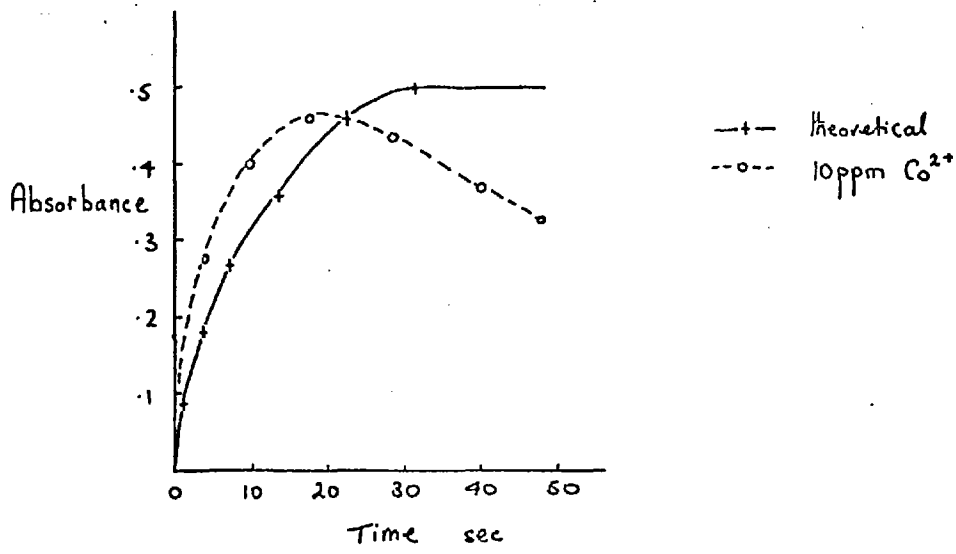

Figure 6.4 Variation of Absorbance with Time

The variation of absorbance with time obtained with a 20 ppm Ni^{2+} solution in 0·03 M potassium sulphate, and with a 10 ppm Cd^{2+} solution also in potassium sulphate are shown in Table 6.2. The wavelengths used were 208 and 220 nm respectively.

Table 6.2 Absorbance - Time Variation

Nickel

t sec	A	$At^{-\frac{1}{2}}$
2	0·113	0·080
4	0·209	0·105
6	0·276	0·113
8	0·326	0·115
10	0·367	0·119
12	0·403	0·116
14	0·426	0·117
16	0·446	0·110
18	0·457	0·108
20	0·466	0·104
22	0·470	0·100

Cadmium

t sec	A	$At^{-\frac{1}{2}}$
1	0·056	0·056
2	0·122	0·087
3	0·168	0·097
4	0·201	0·100
5	0·228	0·102
6	0·248	0·101
7	0·268	0·101
8	0·284	0·100
9	0·293	0·098
10	0·305	0·098
11	0·313	0·094
12	0·321	0·093
13	0·329	0·091
14	0·334	0·089
15	0·338	0·087
16	0·344	0·080

It can be seen from the Table that the value of the product $At^{-\frac{1}{2}}$ is approximately constant for these two metals. It is suggested that the absorbance - time variation over the initial 16 seconds or so is governed largely by

a diffusional process. As the absorbance passes through a maximum and then decreases, it is obvious that diffusion from the electrode surface is not the only process involved.

6.2.3 Approximate Methods

1. Diffusion Layer Concept

According to Nernst (145) the shape of the C_o - distance profile can be approximated to a straight line over a distance δ from the electrode surface and the slope of this line is given by $\left(\frac{\partial C_o}{\partial x}\right)_{x = 0}$

This is shown in Figure 6.5.

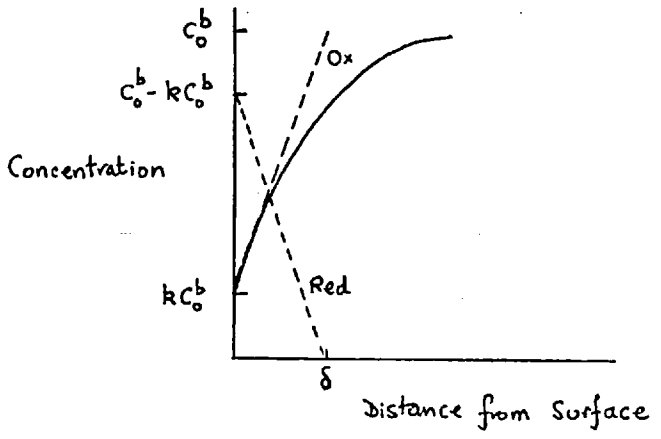

Figure 6.5 Concentration - Distance Profile

Now from Equation 6.3

$$\left(\frac{\partial C_o}{\partial x}\right)_{x = 0} = \frac{C_o^b}{\pi^{\frac{1}{2}} D_o^{\frac{1}{2}} t^{\frac{1}{2}}}$$

If the concentration of the oxidised species at the electrode surface is kC_o^b at time t (see Figure 6.6), then the slope

of the line is given by

$$\frac{C_o^b - kC_o^b}{\delta}$$

$$\therefore \quad \frac{C_o^b - kC_o^b}{\delta} = \frac{C_o^b}{\pi^{\frac{1}{2}} D_o^{\frac{1}{2}} t^{\frac{1}{2}}}$$

$$\therefore \quad \delta = (1 - k)\pi^{\frac{1}{2}} D_o^{\frac{1}{2}} t^{\frac{1}{2}}$$

and the average concentration of the reduced species is $\frac{1}{2}(C_o^b - kC_o^b)$.

Thus a light beam of height h 'sees' a concentration given by

$$h\, C_R' = (1 - k)\pi^{\frac{1}{2}} D_o^{\frac{1}{2}} t^{\frac{1}{2}} \tfrac{1}{2} C_o^b (1 - k)$$

Now the absorbance is given by

$$A = \epsilon_R l\, C_R'$$

$$= \frac{\epsilon_R l\, (1 - k)^2 \pi^{\frac{1}{2}} D_o^{\frac{1}{2}} C_o^b\, t^{\frac{1}{2}}}{2h}$$

For this to be euivalent to Equation 6.10

$$\pi^{\frac{1}{2}} \frac{(1 - k)^2}{2} = \frac{2}{\pi^{\frac{1}{2}}}$$

$$\therefore \quad (1 - k)^2 = \frac{4}{\pi}$$

$$\therefore \quad 1 - k = \frac{2}{\pi^{\frac{1}{2}}}$$

$$\therefore \quad k = -0{\cdot}128$$

A negative value of k is clearly untenable as a solution, showing that the diffusion layer concept is not a valid approximation in this case. The best approximation would be to take k = 0 which gives

$$A = \frac{\pi^{\frac{1}{2}} \epsilon_R l D_o^{\frac{1}{2}} C_o^b\, t^{\frac{1}{2}}}{2h}$$

($2\pi^{-\frac{1}{2}} = 1{\cdot}128$, $0{\cdot}5\,\pi^{\frac{1}{2}} = 0{\cdot}887$).

2. Single Distance from the Electrode Surface

The assumption here is that the absorbance monitored by the light beam of thickness h may be considered equivalent to that at a single distance, m, from the surface.

The values of C_o and C_R are now given by Equations 5.4 and 5.6

$$\text{i.e.} \quad C_o = C_o^b \, \text{erf}(z)$$

$$C_R = C_o^b \, \text{erfc}(z)$$

where

$$z = \frac{m}{2 D_o^{\frac{1}{2}} t^{\frac{1}{2}}}$$

and $\text{erfc}(z) = 1 - \text{erf}(z)$

If it is assumed that both species absorb, then referring to Figure 6.4, the absorbance may be written as

$$\begin{aligned} A &= \epsilon_o C_o^b (L - l) + \epsilon_o C_o l + \epsilon_R C_R l \\ &= \epsilon_o C_o^b L - \epsilon_o C_o^b l + \epsilon_o l C_o^b \text{erf}(z) + \epsilon_R l C_o^b \text{erfc}(z) \\ &= A(0) - \epsilon_o C_o^b l + \epsilon_o l C_o^b \text{erf}(z) + \epsilon_R l C_o^b \text{erfc}(z) \\ &= A(0) - \epsilon_o C_o^b l \left[1 - \text{erf}(z)\right] + \epsilon_R l C_o^b \text{erfc}(z) \\ &= A(0) - \epsilon_o C_o^b l \, \text{erfc}(z) + \epsilon_R l C_o^b \text{erfc}(z) \\ &= A(0) + l C_o^b \text{erfc}(z) (\epsilon_R - \epsilon_o) \end{aligned}$$

As the initial absorbance is set to zero

$$A = l C_o^b \text{erfc}(z) (\epsilon_R - \epsilon_o) \qquad 6.13$$

For Equation 6.13 to be equivalent to Equation 6.12 then

$$\text{erfc}(z) = \frac{2 D_o^{\frac{1}{2}} t^{\frac{1}{2}}}{h \pi^{\frac{1}{2}}}$$

As $$z = \frac{m}{2D_o^{\frac{1}{2}}t^{\frac{1}{2}}}$$

m cannot have a unique value and must vary with time so that $t^{-\frac{1}{2}}\text{erfc}(z)$ is a constant equal to $2D_o^{\frac{1}{2}}/h\pi^{\frac{1}{2}}$. Table 6.3 shows the variation of m with time for $D_o = 10^{-5}$ cm^2 sec^{-1}, and h = 0·05 cm.

Table 6.3 Variation of m with Time

t sec	10^3m cm
1	8·09
4	13·00
9	16·58
16	19·00
25	20·20
36	20·85
49	20·83
64	20·22

It can be seen that if m was taken as constant over the first 16 sec of electrolysis, then considerable error would result.

As was noted at the end of Section 6.2.1, it is the product of diffusion layer thickness and concentration that varies linearly with the square root of the time. Thus, the concentration may be considered as fixed at some value (less than C_o^b) and thus the diffusion layer thickness varies linearly with $t^{\frac{1}{2}}$; or the diffusion layer thickness may be considered as fixed and the concentration

then varies linearly with $t^{\frac{1}{2}}$. If suitable values of concentration or diffusion layer thickness are taken, then the resulting equation for the absorbance-time variation will be the same as Equation 6.10. For example, if it is assumed that at a distance of $4D_o^{\frac{1}{2}}t^{\frac{1}{2}}/\pi^{\frac{1}{2}}$ from the electrode surface the concentration, C_R, is $0{\cdot}5C_o^b$, then Equation 6.10 results for the variation of absorbance with time. This approximation is shown in Figure 6.6.

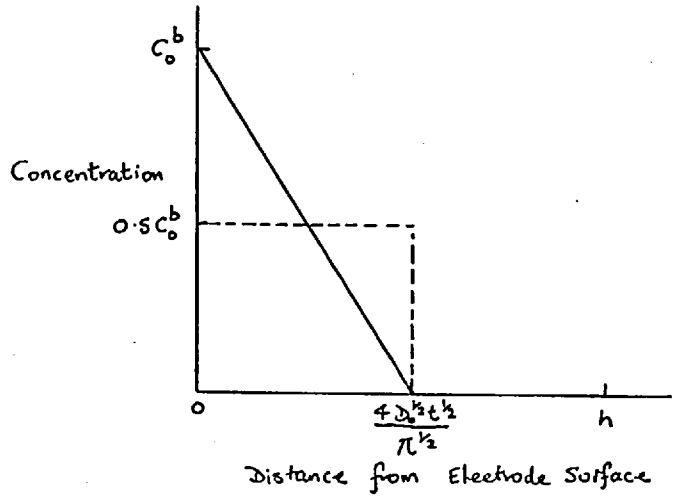

Figure 6.6 Variation of Concentration with Distance

A linear variation of concentration with distance gives $C_R = 0{\cdot}5\ C_o^b$.

6.2.4 Summary

Assuming that for an electrode reaction of the type

$$Ox + ne^- \longrightarrow Red$$

only the reduced form absorbs at the wavelength at which

the absorbance is being monitored and that the movement of the species is controlled only by diffusion, an expression for the variation of absorbance measured normal to the electrode surface with time has been derived by two methods (Equation 6.6). From this, an expression relating the absorbance parallel to the electrode surface with time has been derived (Equation 6.10). The variation of absorbance measured under the conditions used in the experiments described in Chapter 4 (see Figure 6.3) with time, taking into account the fact that the oxidised species may also absorb at the wavelength being used, is then derived (Equation 6.12). The variation of absorbance with time for two metals is shown (Table 6.2) from which it can be seen that there is good agreement between the predicted variation and that observed in practice. Finally, two approximate methods for deriving the absorbance-time variation are discussed.

6.3 Variation of Absorbance with Distance from the Electrode Surface

At any given time, t, the variation of absorbance with distance from the electrode surface, x, is given by Equation 6.13.

$$A = lC_o^b \operatorname{erfc}(z)\ (\epsilon_R - \epsilon_o)$$

where

$$z = \frac{x}{2D^{\frac{1}{2}}t^{\frac{1}{2}}}$$

However, as has already been discussed, the experiments employ a light beam of finite width, h, grazing the electrode surface. The variation of absorbance with h is given by Equation 6.12 i.e.

$$A = \frac{2D_o^{\frac{1}{2}}(\epsilon_R - \epsilon_o)\, l\, C_o^b\, t^{\frac{1}{2}}}{\pi^{\frac{1}{2}}} \frac{1}{h}$$

and thus for any given time, a plot of A vs h will be one half of a rectangular hyperbola. However, as was noted in conjunction with Equation 6.12 for the absorbance-time variation, there is a limit to the absorbance given by

$$A_{max} = \epsilon_R C_o^b l$$

In this case, this limit will have the effect that for values of h below a certain limit, the absorbance will be independent of h.

Plots of A vs h for various times after the start of the electrolysis are shown in Figure 6.7 for the following values, $D_o = 10^{-5}$ cm^{2}sec^{-1}, $\epsilon_R = 5000$ l mole^{-1} cm^{-1}, $\epsilon_o = 0$, $l = 1$ cm and $C_o^b = 10^{-4}$ M.

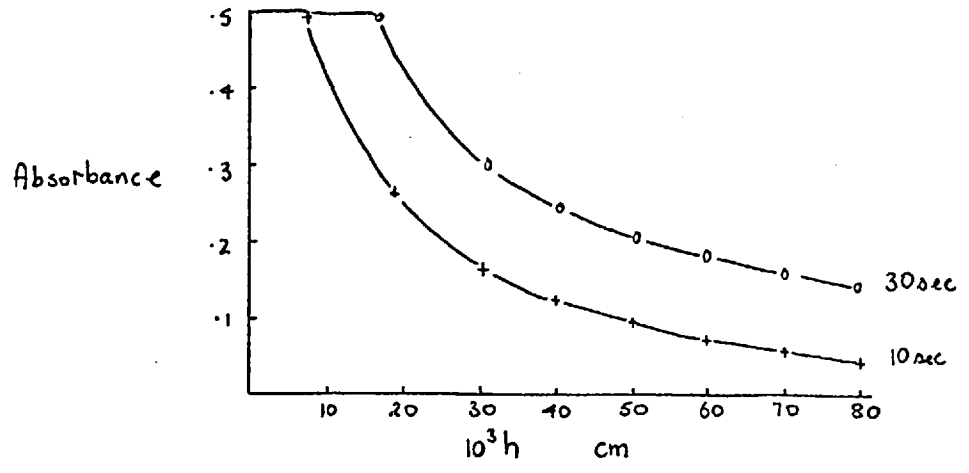

Figure 6.7 Variation of Absorbance with Distance

The variation with distance was studied for two metal ion solutions, namely copper and cobalt. With copper, a 20 ppm solution in 0·1 M KCl was used. The gain of the system was altered by changing the e.h.t.supply to the phctomultiplier tube and the change in absorbance obtained on applying a potential difference was observed as the electrode was lowered, stepwise, out of the light path. The height of the electrode was read from an arbitrary scale on the vertical slide. The results of the experiment have already been given in Table 3.1. From the Table it can be seen that as the electrode is lowered out of the light path and the height of the light beam increases, the signal gradually decreases. As the light beam moves clear of the electrode surface, there is a time lag before the signal appears. After the light beam is more than 1 mm above the surface of the electrode no maximum is observed and the change in absorbance is very small.

An exactly similar experiment was performed with cobalt. A 10 ppm solution in 0·1 M KCl was used and a potential difference of 1·6 V was applied to the electrodes. The results are shown in Figure 6.8. Comparing the results with those for the copper solutions (see Figure 3.4), shows that an exactly similar process is being observed, and it would appear that for layers of solution up to 0·2 mm above the electrode surface, the maximum absorbance obtained on electrolysis is independent of the height of the light beam. With a beam of light greater than 0·2 mm in height, the

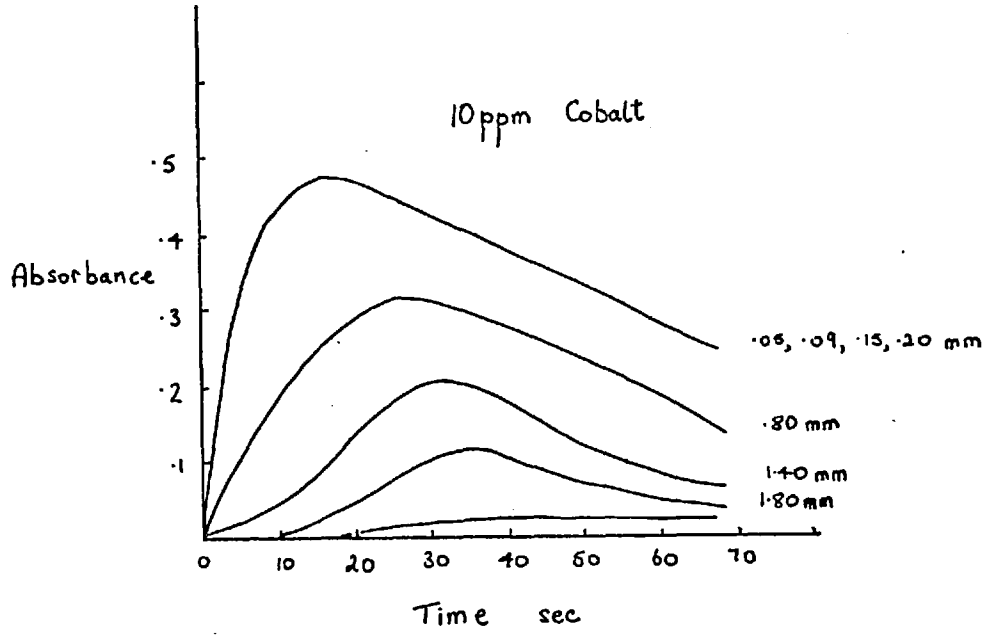

Figure 6.8 Cobalt. Variation of Absorbance with Time

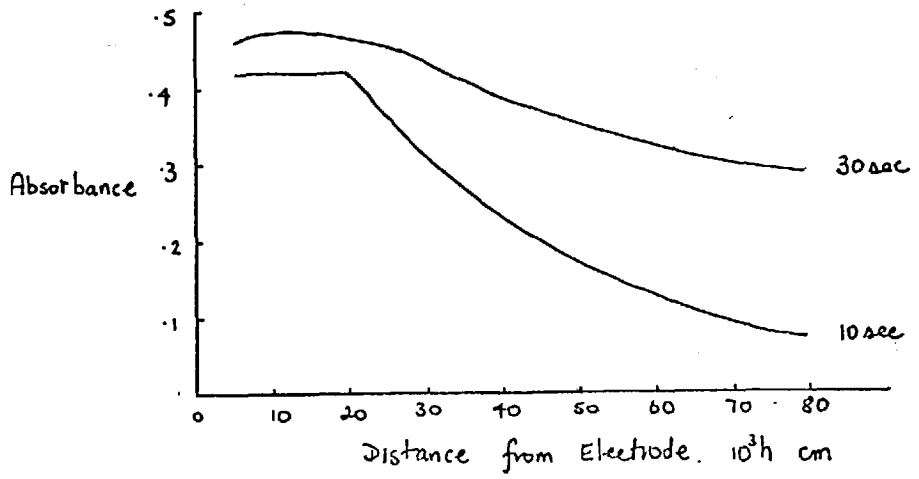

Figure 6.9 Cobalt. Variation of Absorbance with Height of the Light Beam

absorbance decreases until with a beam of light 0·8 mm in height, 0·8 mm clear of the electrode surface, only a very slight increase in absorbance is observed.

The variation of absorbance with distance is shown in Figure 6.9 for various times after the start of the electrolysis. From a comparison between these curves and the theoretical ones shown in Figure 6.8, it can be seen that there is poor agreement between the calculated and experimental curves. By choosing different values of D_o, ϵ_R, l etc a better fit could probably be obtained. Also the value for h over the first few readings may be considerably in error as the scale on the slide was only calibrated to the nearest mm. The two sets of curves are similar in that an absorbance maximum, independent of h, is observed, after which the absorbance decreases. If the pathlength on the electrode surface, l, were known then a value for ϵ_R could be calculated from the relation

$$A_{max} = \epsilon_R l\, C_o^b \qquad \text{(assuming } \epsilon_o = 0\text{)}$$

It is also possible that diffusion is not the only form of mass transport operating, and that convection, etc could cause the absorbance to be independent of h over a wider range of values. Also the conditions under which semi-infinite linear diffusion is obtained are not being rigidly adhered to in the experimental set up used here.

6.4 Variation of Current and Absorbance with Potential

By using the function generator in the 'triangular' mode, a potential difference between the working and the reference electrodes which varied linearly with time was obtained. The circuit used was identical to that shown in Figure 6.1 with the chart recorder set to record the variation of current with time. As the chart speed was constant and the potential varied linearly with time, the 'time' could be replaced directly with potential, so that the chart recording provided a record of the current-voltage variation. This technique of linear sweep voltammetry has, of course, been extensively applied in electrochemistry. It is interesting to note that the technique is proving very powerful in elucidating the nature of species adsorbed or deposited on the electrode surface, eg (129), particularly when coupled with an optical technique which monitors changes in the electrode surface such as ellipsometry (146) or specular reflection spectroscopy (131).

The variation of current with voltage for a solution containing 0·03 M potassium sulphate only (i.e. no reducible metal ion) is shown in Figure 6.10. The pH of the solution (unbuffered) was approximately 5·5 and a potential scan rate of 40 mV sec^{-1} was used. The regions of hydrogen adsorption and desorption and 'oxide' formation and reduction (147,148) can clearly be seen. Here two peaks were seen in the oxide reduction region, whereas

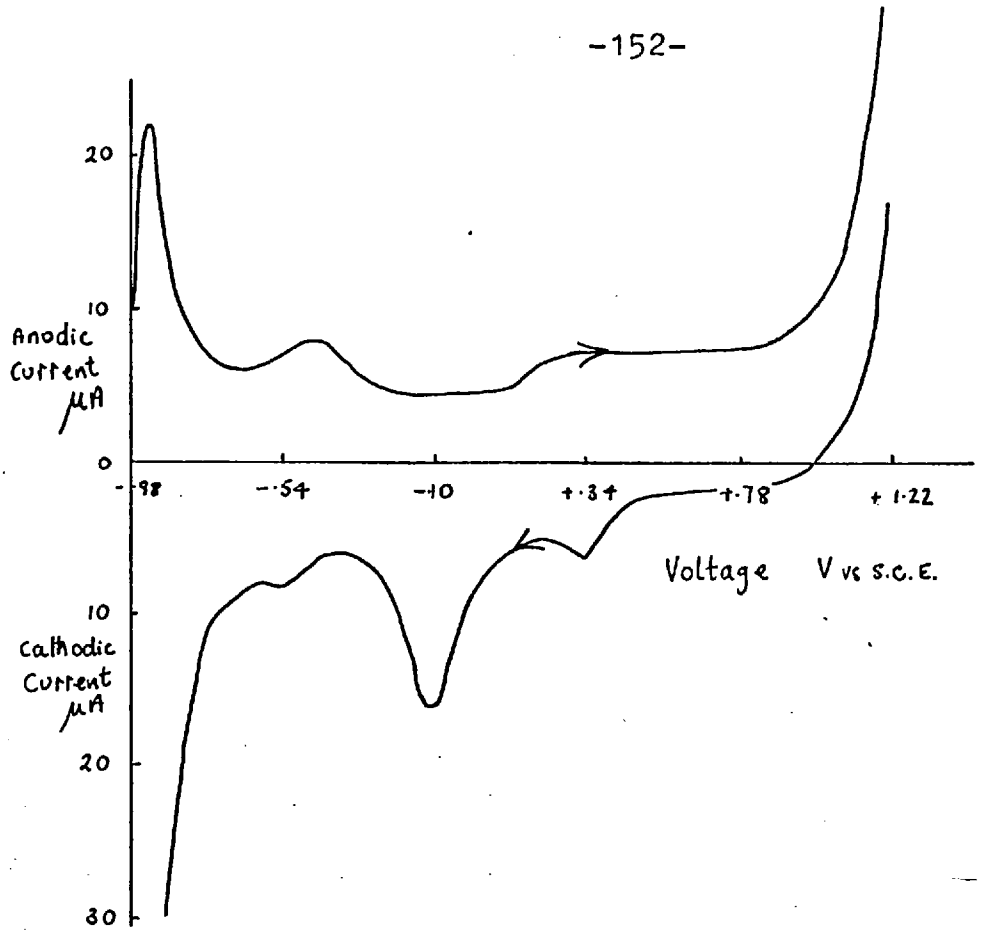

Figure 6.10 Variation of Current with Voltage. 0·03 M Potassium Sulphate at pH 5·5

most other workers have only observed one (147). It is possible that the appearance of this second peak is a function of the pH of the solution. Other workers have usually used 1 M acid (sulphuric or perchloric) or 1 M alkali (potassium hydroxide). The potentials at which the various regions occur are obviously functions of pH (148).

The variation of absorbance with voltage for a 10 ppm cadmium solution in 0·03 M potassium sulphate at 220 nm and for 0·03 M potassium sulphate only at 195 nm are shown in Figure 6.11. The variation of current with the same voltage scan for the solutions is also shown in the Figure.

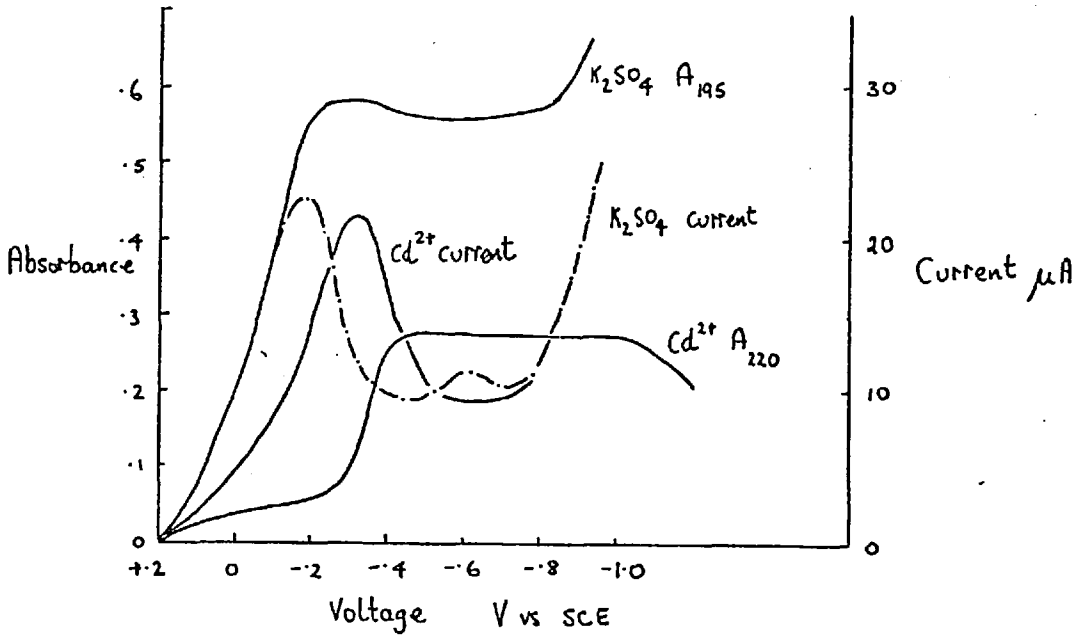

Figure 6.11 Variation of Absorption and Current with Voltage

The potential was scanned from +0·2 to -1·0 V vs SCE. It can be seen from the Figure that the blank absorption follows the oxide reduction peak quite closely, whereas the absorption from the cadmium solution lags behind the current peak and appears at the potential of the peak maximum. The shape of the absorbance-voltage curve is similar to those obtained under 'static' conditions, i.e. the absorbance rises to a maximum and then levels off. In this case, however, the onset of hydrogen evolution caused the absorbance to decrease at 220 nm. In the presence of cadmium, the oxide stripping peak was apparently shifted to more cathodic potentials, due possibly to the simultaneous reduction of cadmium.

It was also found that the magnitude of the peak current was increased as the time of the anodic pretreatment was increased, but that exposure to the uv light from the source had no effect on the peak current. The photochemical decomposition of platinum surface oxide has been observed (149). A considerably larger peak was recorded when the solution was not deaerated. These results are summarized in Figure 6.12.

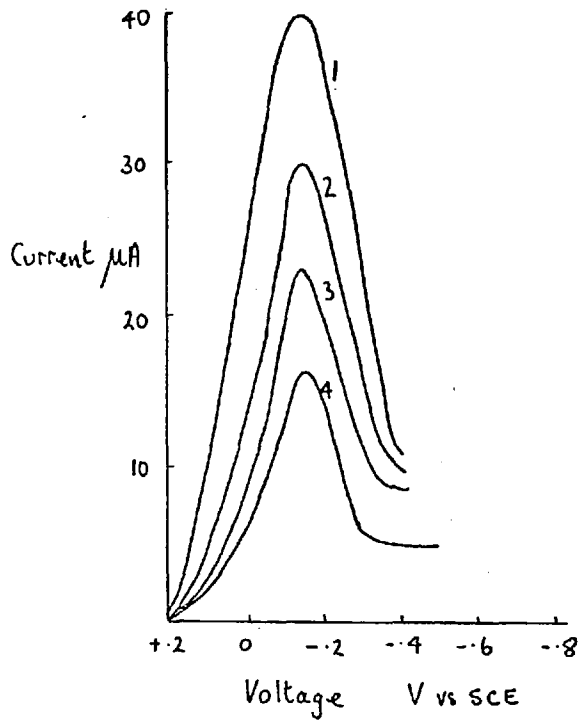

Figure 6.12 Oxide Reduction Peaks

1. solution not deaerated, 30 sec pretreatment
2. 5 min pretreatment
3. 2 min pretreatment
4. normal 30 sec pretreatment

Study of Material Deposited on the Electrode

To investigate whether any metal was deposited on the electrode surface during the reducing stage of the potential cycle, the current was monitored as the potential was scanned anodically. The relevant parts of the current-voltage curves for a number of bulk concentrations of cadmium are shown in Figure 6.13, from which it can be seen that a well defined peak is obtained which increases with increasing cadmium concentration. This peak has been interpreted as arising from the dissolution of cadmium metal from the electrode surface. From the area underneath the peak for the 10 ppm solution, the amount of cadmium stripped off the surface of the electrode was calculated to be $7{\cdot}9 \times 10^{-10}$ moles. If a metallic radius of $1{\cdot}41 \times 10^{-8}$ cm is taken for cadmium, then for monolayer coverage of 1 cm^2, 2×10^{-9} moles are required. This indicates that during the electrolysis of a 10 ppm solution, less than monolayer coverage of the electrode is obtained. The relationships between the amount of material stripped and bulk concentration and absorbance and bulk concentration are shown in Figure 6.14. The deviations from linearity in both these curves occurs at around a bulk concentration of 20 ppm. From the area under the stripping peak, the number of moles of cadmium on the surface was calculated to be $1{\cdot}43 \pm {\cdot}10 \times 10^{-9}$, which corresponds to monolayer coverage of an area of approximately $0{\cdot}6$ cm^2. From the study of the variation of current with

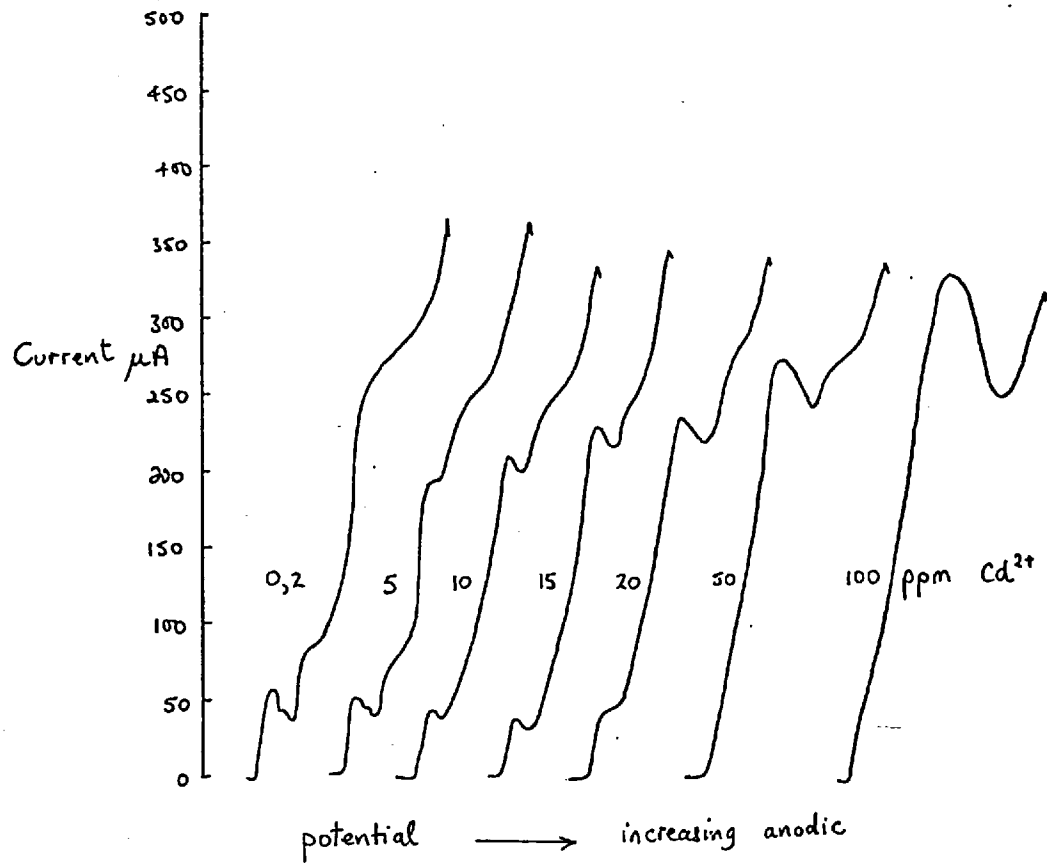

Figure 6.13 Cadmium Anodic Stripping Peaks for Different Bulk Concentrations

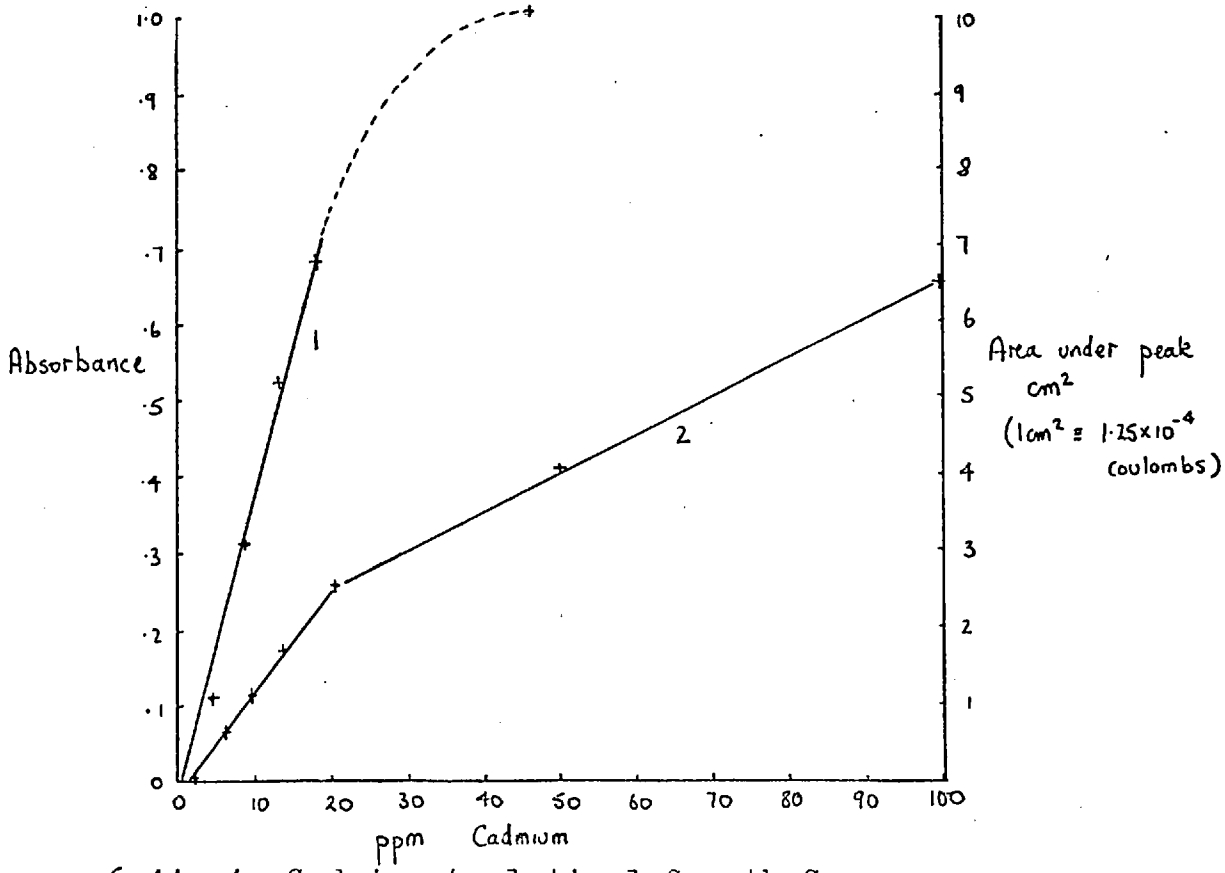

Figure 6.14 1. Cadmium Analytical Growth Curve
2. Variation of Area under Stripping Peak with Concentration

time described in Section 6.1, the electrochemical area was calculated to be 1·86 cm^2. Thus there is no strong correlation between the deviation from linearity and the attainment of monolayer coverage, though from Figure 6.14 there does seem to be a relation between the signal and the amount of material deposited on the electrode (it is assumed that the removal of a quantity of metal in the anodic scan indicates that this amount of metal was deposited during the cathodic part of the voltage scan) that suggests that, possibly, after a certain proportion of the electrode is covered, the mechanism of the reaction changes and the absorbing species is not produced to the same extent. To a certain extent this is supported by the results obtained for cobalt with an electrode surface that had already produced one absorption signal (see Figure 4.14). If the absorbance were due to an intermediate in the reduction of Cd^{2+} to Cd metal on the platinum surface, it would be expected that as the bulk concentration and consequently the coverage of the electrode increased, the underpotential effects discussed in Section 5.5 would decrease and the potential for the deposition of cadmium would shift to more cathodic values as indicated in Table 5.1. Consequently the amount of cadmium deposited would be decreased as at more cathodic potentials hydrogen evolution would occur preferentially.

6.5 Nature of the Electrode Surface

As was mentioned earlier (Section 4.14), it has long been known that a platinum electrode is not electrochemically inert. The adsorption and desorption of hydrogen in the cathodic region of the potential scan have been unambiguously resolved (148). The properties of adsorbed hydrogen on a number of electrode materials has been comprehensively reviewed by Frumkin (150). However, the situation with regard to the nature of the anodic film is still not completely resolved. Indirect evidence for the oxidation of platinum has existed in the literature for many years (66,151). The anodic film on platinum has been extensively studied by a large number of methods including chronopotentiometry (152), potential sweep methods (153), chemical dissolution of the surface layer (154), potentiostatic methods (146), X-ray methods (160), ellipsometry (155), specular reflection spectroscopy (156) and, more recently, by field ion microscopy (157) and ESCA (158). The literature has been comprehensively reviewed (159) and a particularly well presented review is given by Damjanovic (160). In a recent review (161), Appleby states "it is generally accepted that the film consists of Pt oxide phases whose stoichiometry varies with potential", though this is probably an oversimplification of the current theories of the nature of the anodic film. Nadebaum and Fahidy (162) identify four groups of postulates from the literature namely, that the anodic film is due to

1. chemisorption of oxygen species to the extent of one monolayer,
2. chemisorption of oxygen atoms to the extent of one monolayer; any excess atoms are absorbed into the underlying metal lattice (dermasorbed),
3. chemisorption of oxygen species to the extent of an O:Pt ratio of 1:1, those in excess forming phase oxide, and
4. phase oxide formation at all potentials.

These may be divided broadly into two views, namely 1) the film is a chemisorbed layer and 2) the film is an oxide. The difference between the two being that in the latter, Pt atoms are considered to have left their regular positions in the metal lattice to enter into a new arrangement of atoms, which, together with oxygen atoms, forms an arrangement similar to that in the formation of the nuclei of the respective oxides.

It has been pointed out (161) that electrochemical transient techniques only measure the amount of oxygen present and do not give any indication of its nature. The most fruitful experiments are those in which a technique for examining the surface (such as ellipsometry, specular reflection spectroscopy or X-ray crystallography) is combined with an electrochemical technique. The state of this art is well demonstrated in the report of the Fourth Symposium of the Faraday Society (6) in which the general discussion sections are particularly useful. Ellipsometric studies (155) indicate that below 1 V (vs RHE)*, the anodic

* where RHE stands for reversible hydrogen electrode

film is characterised by adsorbed species and above this potential oxides are formed. Specular refection studies appear to agree with this finding (163). Conway (164) proposes that the successive stages of oxidation are coverage of sites by hydroxide radicals then by oxygen atoms and finally phase oxide formation by place exchange amongst Pt and O species. He shows that the oxidation is progressively irreversible, and proposes that the material initially laid down is electrochemisorbed hydroxide radicals. This model is also proposed by Appleby (161), namely that in the potential range 0·8 to 1·0 V vs RHE, the chemisorbed oxygen film is reversible but becomes increasingly irreversible at higher potentials where increased film thickness gives rise to the reduction potential being constant (i.e. independent of formation potential or thickness). At the lower potentials, the O or OH radicals are merely chemisorbed with the platinum atoms remaining in their lattice positions. This is the model proposed by Conway *et al* in a series of papers (165, 166,167)which looks like providing the definitive description of the anodic film.

It would appear, then, that both views on the nature of the anodic film are true to a certain extent, depending on the formation potential. It is apparent that the conditions employed in the experiments described in Chapter 4 to clean the electrode leave the surface covered with phase oxide, and from the previous Section, that the

absorbances from the blank solutions are directly linked with the reduction of this oxide film (see Figure 6.11) and so, it is of interest to examine the reduction process. Because of the uncertainty in the nature of the anodic film, there is a corresponding uncertainty in the mechanism of oxidation or reduction. Any mechanism must account for the fact that the number of coulombs required to build up the anodic film is larger than the number required for its reduction. This is discussed by Damjanovic (160), who points out conflicting experimental evidence for most of the reasons put forward for this charge imbalance.

In many of the studies of the anodic film, it is difficult to distinguish between the reduction of the oxide film and of oxygen in solution. Most workers, apparently, are more interested in the reduction of dissolved oxygen and the products from this reaction than in the reduction of the anodic film. However, it has been established that hydrogen peroxide is not an intermediate (168). A number of mechanisms have been proposed for the reduction of the anodic film, which vary, of course, with the formulation of the oxide film, as follows. The recent literature has been reviewed by Weaver (169).

1. Kozawa (170); Nagl and Dietz (171)

$$PtO_2.nH_2O + 4H^+ + 4e^- \rightleftharpoons Pt + (n + 2)H_2O$$

2. Conway and Gilroy (172)

$$PtO + H^+ + e^- \longrightarrow PtOH$$
$$PtOH + H^+ + e^- \longrightarrow Pt + H_2O$$

3. Gilman (173)

$$PtO_2 + 2H^+ + 2e^- \longrightarrow PtO + H_2O$$
$$PtO + H^+ + e^- \longrightarrow PtOH$$
$$PtOH + H^+ + e^- \longrightarrow Pt + H_2O$$

4. Feldberg, Enke and Bricker (174)

$$Pt(O)_x + xH^+ + xe^- \longrightarrow Pt(OH)_x$$
$$Pt(OH)_x + xH^+ + xe^- \longrightarrow Pt + xH_2O$$

5. Conway (164)

$$\begin{matrix} Pt \\ Pt \end{matrix}\!\!>O + H^+ + e^- \longrightarrow PtOH + Pt$$
$$PtOH + H^+ + e^- \longrightarrow Pt + H_2O$$

6. Reddy, Genshaw and Bockris (175); Tilak, Conway and Angerstein-Kozlowska (167)

$$PtO + H^+ + e^- \longrightarrow HOPt$$
$$HOPt \xrightarrow[\text{exchange}]{\text{place}} PtOH$$
$$PtOH + H^+ + e^- \longrightarrow Pt + H_2O$$

In all cases the experimental work was done in concentrated acid solution (ca 1 F) and the final stage in the mechanisms is the reduction of a surface hydroxide species to water. In the neutral solutions used in the experiments described here, the final product of reduction might well be hydroxide ion rather than water.

Biegler and Woods (176) observed that with severe conditions of anodic polarization (>1,000 sec at 2·98 V), the oxide reduction extended into the hydrogen region. They also observed that for anodic polarizations of 10 sec, a limiting oxide coverage was obtained at 2·3 V vs RHE.

6.5.1 Reduction of Oxygen at Platinum

This reaction has also been extensively reviewed (159, 160,161) at both oxide coated and oxide free electrodes. There is also considerable controversy over the mechanism of the reaction, particularly with respect to the involvement of hydrogen peroxide. The situation is well summarized by Blurton and McMullin (177) who identify from the literature four reaction mechanisms, namely:-

1. hydrogen peroxide is an intermediate in a single reaction path (178,179)
2. hydrogen peroxide is the sole product of the reaction (170,180)
3. hydrogen peroxide is an intermediate in a reaction path parallel to a second reaction path involving the reduction of oxygen directly to hydroxide (181,182)

4. oxygen is reduced directly to hydroxide without hydrogen peroxide being formed (185).

Their own contribution is to investigate the reduction using a ring disc electrode in 7 M KOH and conclude that between 0·4 and 0·0 V vs RHE oxygen is reduced to hydroxide with hydrogen peroxide as an intermediate.

It is generally accepted that the mechanism of the reduction depends on whether the surface of the electrode is oxidised or not (183), and it appears that the reduction on a surface containing oxide is a four electron process (184). Lingane (185) in a characteristically well presented paper argued that the reduction involved four electrons from a comparison of the experimental transition times with the theoretical values for 4 and 2 electron reductions. He also found that the presence of surface oxide was essential. That peroxide is formed as an intermediate has been convincingly shown by Frumkin et al (186) using a rotating ring disc electrode (RRDE) in which hydrogen peroxide formed at the disc is swept out and detected as a current at the ring. These early experiments demonstrate the power of this type of electrode to elucidate reaction mechanisms. The RRDE has been extensively applied to the investigation of the reduction of oxygen at platinum (160). Damjanovic and coworkers (181,183) have studied the reduction in both acid and alkaline solution. They found that in acid solution no peroxide was formed even as an intermediate, but in

alkaline solution, hydrogen peroxide was produced in a second reaction path. One of the few chemical studies of the system has been made by Peters and Mitchell (187) who added Ti(IV) to the solution and detected the absorbance of a titanium peroxide complex at 410 nm at a platinum gauze electrode. They showed that hydrogen peroxide was an intermediate at active (i.e. freshly reduced) electrodes but that the surface catalyses its decomposition to water. The catalytic effect of the surface has been observed by other workers (188,189, 190),.some workers found that the surface oxide inhibited the reaction (191), while others found the overall process was accelerated in the presence of oxide (192). Others observed that the presence of surface oxide catalysed the decomposition of hydrogen peroxide (178,193,194), but inhibited the reduction of oxygen to peroxide (191).

As the product of the reduction is either hydroxide or water (depending on the pH of the solution), at electrodes which are coated with oxide, with no formation of peroxide, it would appear that the effect of applying a cathodic potential to the anodically pretreated electrodes used in the experiments described in the previous Section is to produce hydroxide near the electrode, both from the reduction of dissolved oxygen and from the reduction of the anodic film.

6.5.2 Change in pH near the Cathode

If the product of the reduction of the surface oxide or dissolved oxygen is hydroxide as suggested in the previous Section, then it should be possible to detect an increase in the pH near the cathode surface.

This change in pH was investigated using a solution of phenolphthalein (0·001%) in a manner analogous to the experiments of Peters and Mitchell (187), who detected peroxide by adding Ti(IV) and measuring the absorbance of the titanium peroxide complex. Hydroxide does not form a complex with phenolphthalein but by combining with hydrogen ions (to form water) the equilibrium between the protonated and non-protonated forms of the indicator is shifted so that more of the ionized form is produced, viz (195),

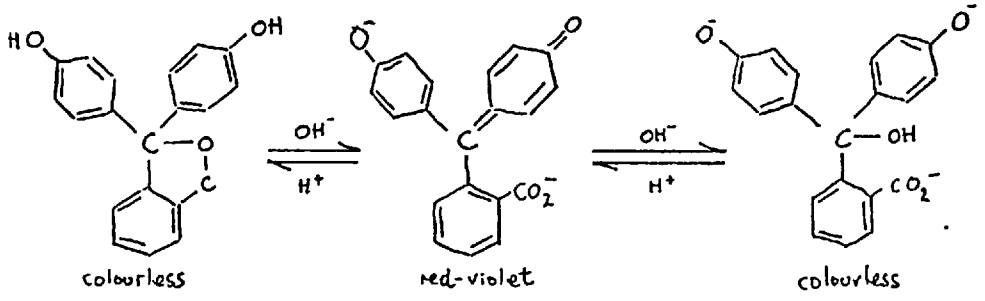

In strong alkali the indicator again becomes colourless because of the loss of the quinonoid structure.

Visual observation of the electrode surface showed that on applying a potential difference of 2 V between the electrodes with a 0·001% solution of phenolphthalein in 0·03 M potassium sulphate, the characteristic red-violet colour of the alkaline form of the indicator was produced

over the electrode surface. A visible spectrum of the indicator was recorded (Perkin Elmer model 402) from which it was found that the absorbance maximum of the alkaline form was 552 nm. The absorbance of a series of solutions of varying pH (adjusted with KOH solution and measured with an EIL Vibron 39A pH meter) was measured in 1 cm cells against the acid form of the indicator at 552 nm and a calibration curve plotted. This is shown in Figure 6.15.

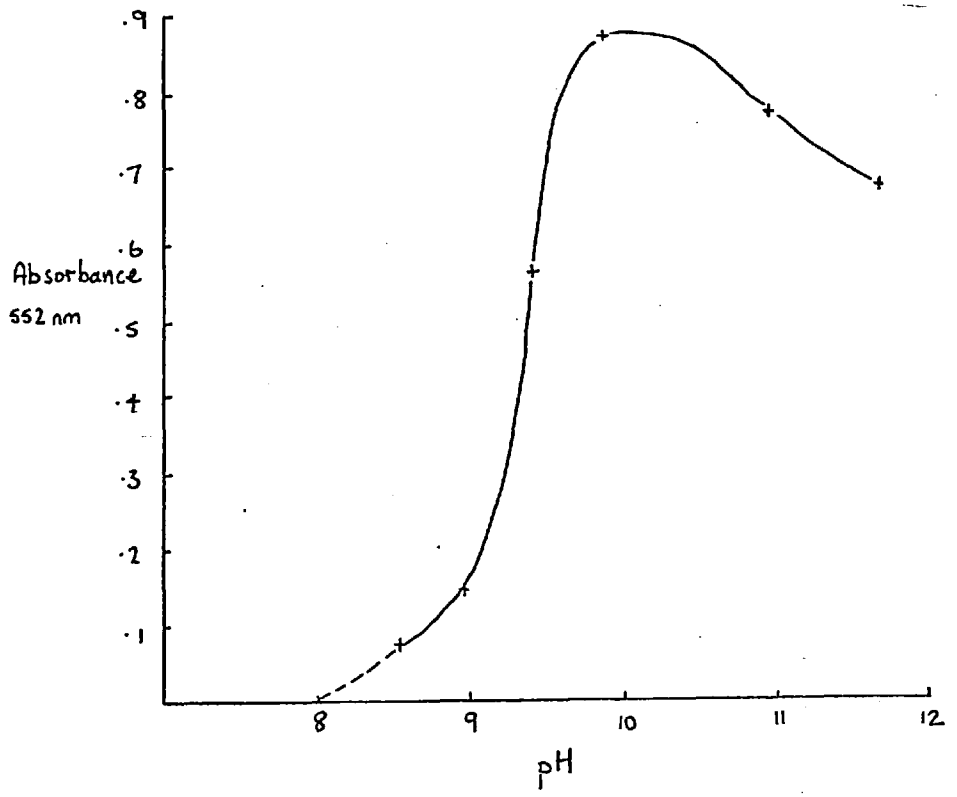

Figure 6.15 Variation of Absorbance with pH for 0·001% Phenolphthalein

The variation of absorbance with potential difference as this was changed stepwise from -2·0 to -0·4 V for a solution containing 0·001% phenolphthalein in 0·03 M potassium sulphate is shown in Figure 6.16. The electrode was anodically pretreated at 5·0 V for about 5 sec and a fresh aliquot of the indicator was taken for each potential difference. It was observed that at potential differences greater than 1·2 V, the signal maintained a maximum value until the voltage was switched off; whereas, at potential differences less than 1·2 V, the absorbance reached a maximum and then decreased.

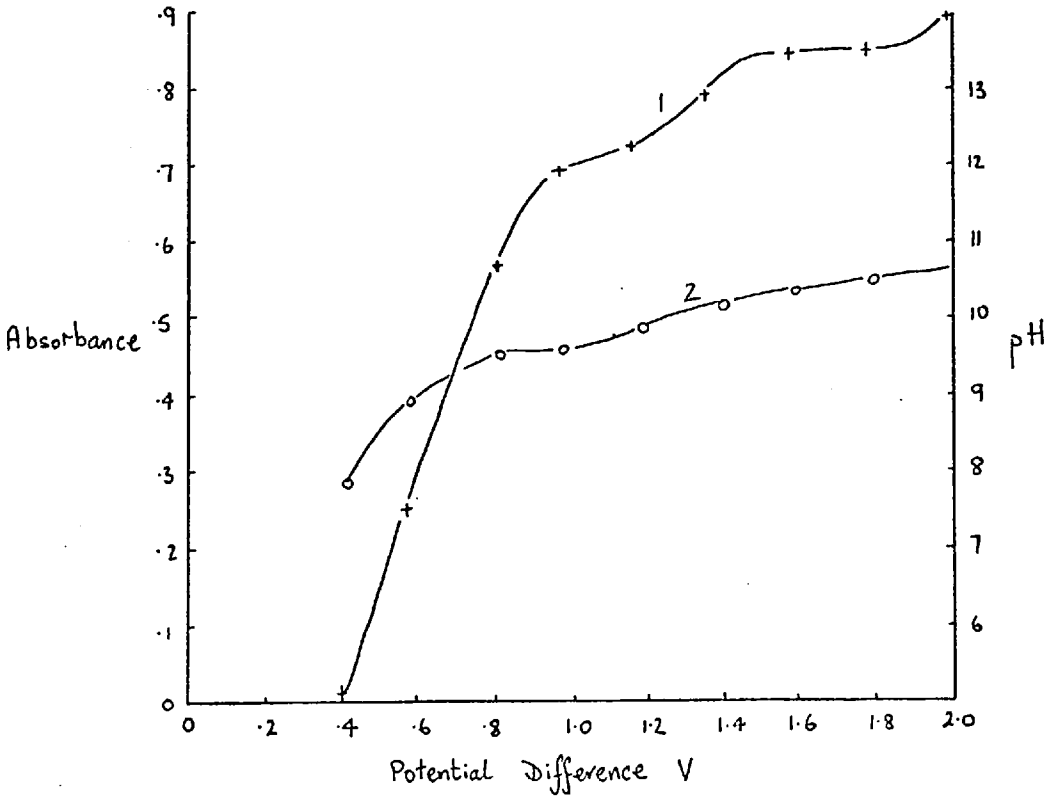

Figure 6.16 Variation of 1.Absorbance and 2.pH with Potential Difference

If the pathlength on the electrode surface were known, then the absorbance values obtained could be related to a pH value. Assuming that during the electrolysis, the maximum absorbance possible is obtained, then an absorbance of 0·85 in the electrolysis cell corresponds to an absorbance of 0·90 in a 1 cm cell. From this the pathlength is deduced to be 0·94 cm. The variation of pH with potential difference is also shown in Figure 6.16. The results show that a pH of between 10 and 11 was obtained at the cathode surface at potential differences greater than 1·0 V.

The absorption spectra of a 10^{-3} M KOH solution and of a hydrogen peroxide solution recorded in 1 cm cells vs water are shown in Figure 6.17.

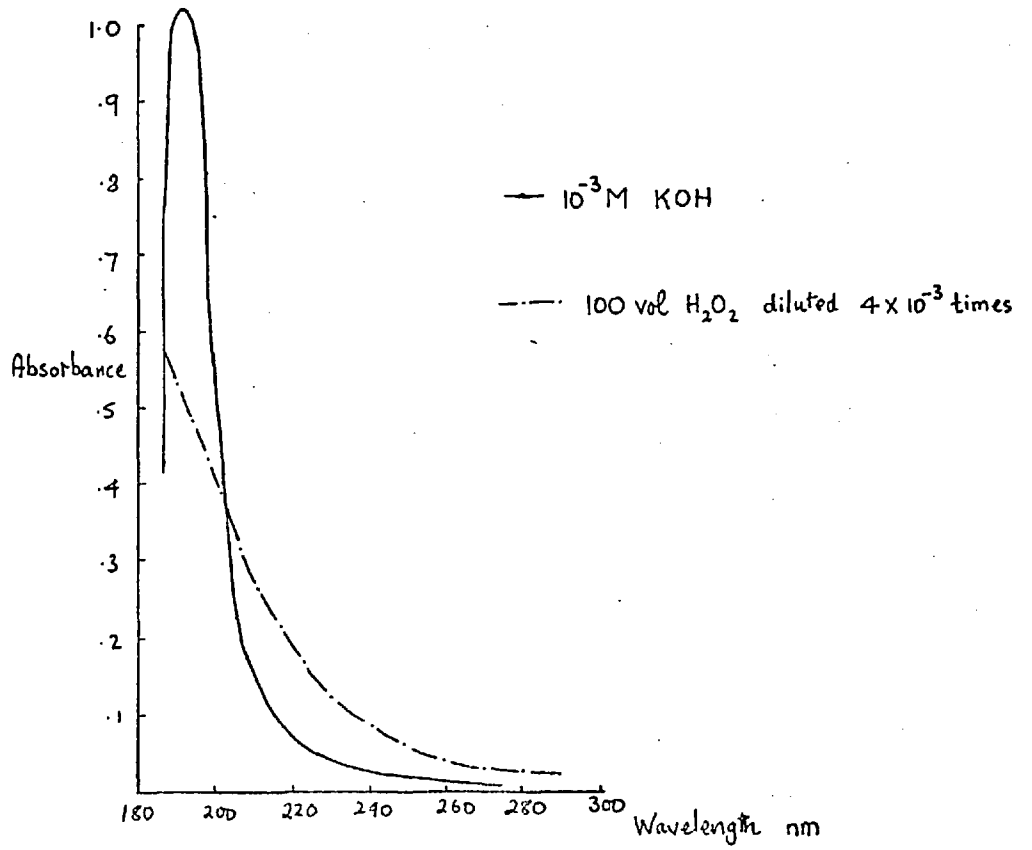

Figure 6.17 Absorption Spectra of Hydroxide and Peroxide

From a comparison with the absorption spectrum of the blank absorbance (see Figures 4.8 and 4.13), it was deduced that the absorbance from the background electrolyte solutions was due to the formation of hydroxide rather than peroxide.

6.6 Role of the Hydroxide Layer

The solubility products of the hydroxides of the metals studied are shown in Table 6.4.

Table 6.4 Solubility Products of Metal Hydroxides

Hydroxide or Oxide	Solubility Product
Ag_2O	2.0×10^{-8}
$Mg(OH)_2$	8.9×10^{-12}
$Mn(OH)_2$	2.0×10^{-13}
$Cd(OH)_2$	2.0×10^{-14}
$Fe(OH)_2$	1.8×10^{-15}
$Pb(OH)_2$	4.2×10^{-15}
$Ni(OH)_2$	1.6×10^{-16}
$Co(OH)_2$	2.0×10^{-16}
$Zn(OH)_2$	4.5×10^{-17}
$Cu(OH)_2$	1.6×10^{-19}
$Hg(OH)_2$	3.2×10^{-26}
$Sn(OH)_2$	6.3×10^{-27}
$Cr(OH)_3$	6.7×10^{-31}
$Fe(OH)_3$	6.0×10^{-38}

For equilibrium concentrations of 10^{-4} M with respect to the metal ion and 10^{-3} M with respect to hydroxide ion (pH 11), the limiting stability product for a divalent ion is 10^{-10}, and for a trivalent ion is 10^{-13}. Thus, it might be expected that the metal hydroxides would precipitate near the cathode, and that the signals from the solutions containing metal ions were due to scattering from precipitated or colloidal metal hydroxide species.

In fact, it is not easy to distinguish between true absorption and Rayleigh scattering by measuring the intensity of the transmitted light (as was done in the experiments described here). In 1871, Rayleigh deduced an equation for the intensity of the scattered radiation from a system containing particles small by comparison with the wavelength of the incident light and at high dilution. Using the same limitations, Debye (196) deduced an equation for the turbidity of the solution. He defined the turbidity, τ, as

$$\frac{I_t}{I_o} = e^{-\tau l}$$

where I_t is the transmitted intensity, I_o is the incident intensity and l is the pathlength,

and deduced that

$$\tau = \frac{32\pi^3}{3} \frac{\gamma^2 n^2}{\lambda^4} \frac{1}{N} M C$$

where γ is the refractive index increment, $\frac{\partial n}{\partial c}$, given by

$$\gamma = \frac{n_s - n}{c}$$

where n_s is the refractive index of the solution, n is the refractive index of the solvent and c is the concentration in g ml^{-1}, N is the Avogadro number and M is the molecular weight of the solute.

For sufficiently great dilution, γ may be considered constant,

$$\tau = \frac{Kc}{\lambda^4}$$

Thus

$$\frac{I_t}{I_o} = e^{-Kcl/\lambda^4}$$

$$\therefore \quad \log \frac{I_t}{I_o} = \frac{Kcl}{\lambda^4} \log e$$

and thus the function $\log(I_t/I_o)$ will be independent of the intensity of the incident light, I_o, and will also show a linear dependence on concentration whether the light is attenuated by absorption or by scatter. It has been suggested that it is possible to distinguish between true absorption and scattering by the dependence of $\log(I_t/I_o)$ on wavelength. Heller and Vassy (197) proposed that the attenuation of the light may be given by

$$k = c\,\lambda^{-n}$$

where k is an absorption coefficient, c is a constant, λ is the wavelength and n is the wavelength exponent, and that for values of n greater than 4 true absorption is occurring.

The absorption spectrum of a 10 ppm cadmium solution in 0·03 M potassium sulphate obtained at an oxidised electrode

at -0·2 V vs SCE is shown in Figure 6.18, no correction has been made for the blank absorption. From Heller and Vassy's equation,

$$\log k = \log c - n \log \lambda$$

assuming that k is directly proportional to the absorbance, A, then

$$\log A = -n \log \lambda + K$$

where K is a new constant.

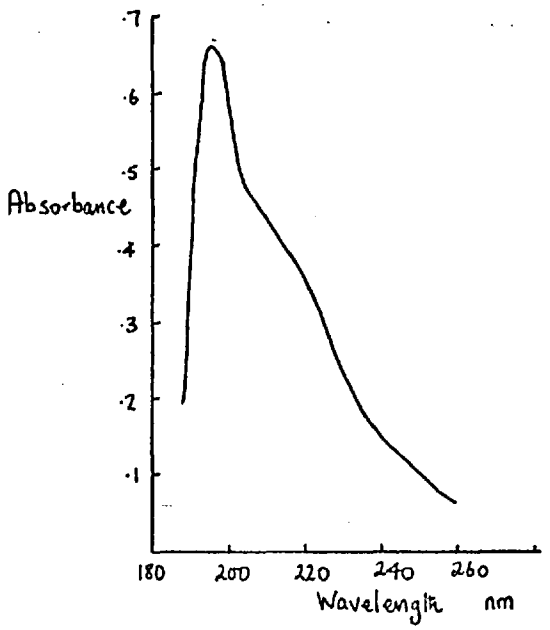

Figure 6.18 Cadmium Absorption Spectrum

A plot of log A vs log λ is shown in Figure 6.19. The slopes of the two branches of the plot are found to be 23·0 and -7·15. Any absorption peak is bound to have a negative value of n, so a negative value of the slope cannot indicate that the signal is due to scatter. The modulus of the slopes in both cases is greater than 4 and

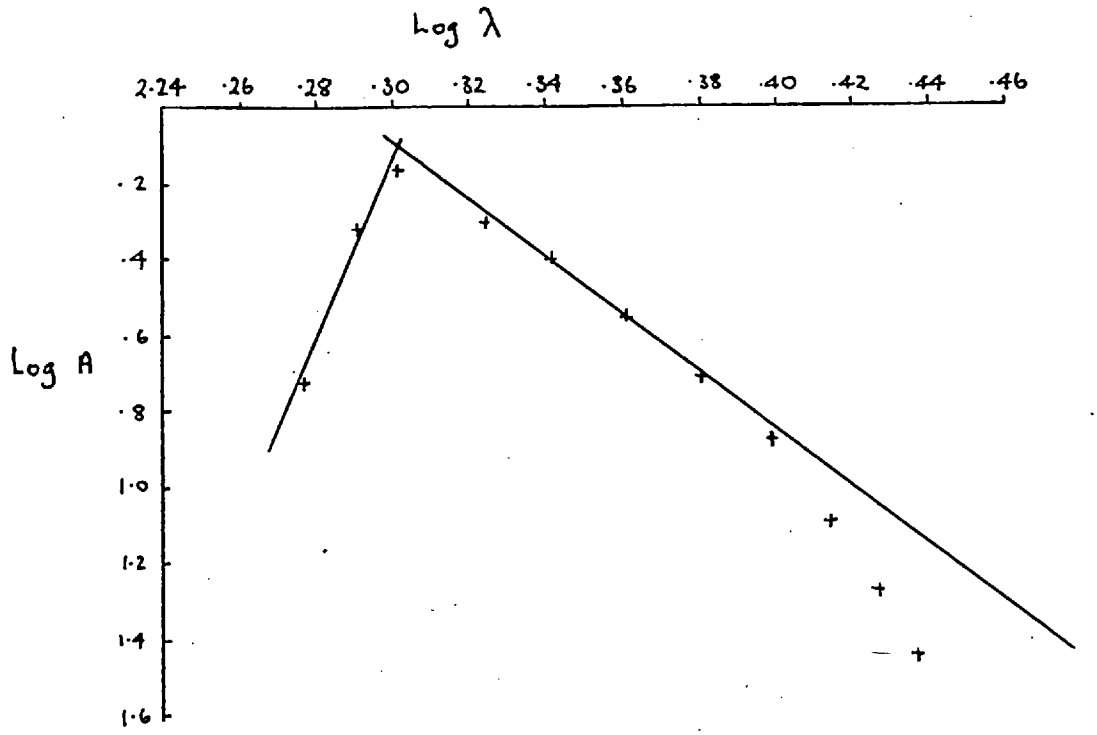

Figure 6.19 Plot of log (Absorbance) vs log (Wavelength)

so it was deduced that for cadmium, the absorbance signals were due to true absorption and not Rayleigh scattering.

The fact that true absorption was being observed does not mean, however, that the species could not be colloidal in nature, as it is known that colloidal solutions can absorb radiation in accordance with the Beer-Lambert law, $I_t = I_o\ 10^{-\epsilon kl}$, (198).

6.6.1 Variation of Absorbance with Potential

Using the linear potential sweep method described in Section 6.4, the variation of absorption with potential (vs SCE) was studied for solutions containing

1. 0·03 M potassium sulphate, at 198 nm

2. 20 ppm cadmium in 0·03 M potassium sulphate, at 220 nm
3. 0·001% phenolphthalein in 0·03 M potassium sulphate, at 552 nm

at a potential sweep rate of 50 mV sec^{-1}. At 198 nm, the blank signal has a maximum value, at 220 nm, the difference between the absorbanceof the cadmium and the blank solutions is a maximum and the blank signals are negligible, and at 552 nm, the alkaline form of the indicator has an absorbance maximum.

1. Oxidised Electrode.

The working electrode was anodically pretreated at +5·0 V for a few seconds while washing with 0·03 M potassium sulphate followed by rinsing with distilled water at 0·0 V. The electrode was polarized at +0·2 V vs SCE while deaerating with oxygen-free nitrogen for 2 minutes. The potential sweep was then applied. The results for the three solutions are shown in Figure 6.20. The results are also shown for a solution containing cadmium and phenolphthalein in 0·03 M potassium sulphate, at 220 nm.

It can be seen from the Figure that the blank and indicator signals occurred over the same potential range, starting at 0·0 V vs SCE. The cadmium signal started at -0·2 V vs SCE, just before the indicator signal reached a maximum. The solution that contained both cadmium and indicator did not show any signal until -0·76 V vs SCE.

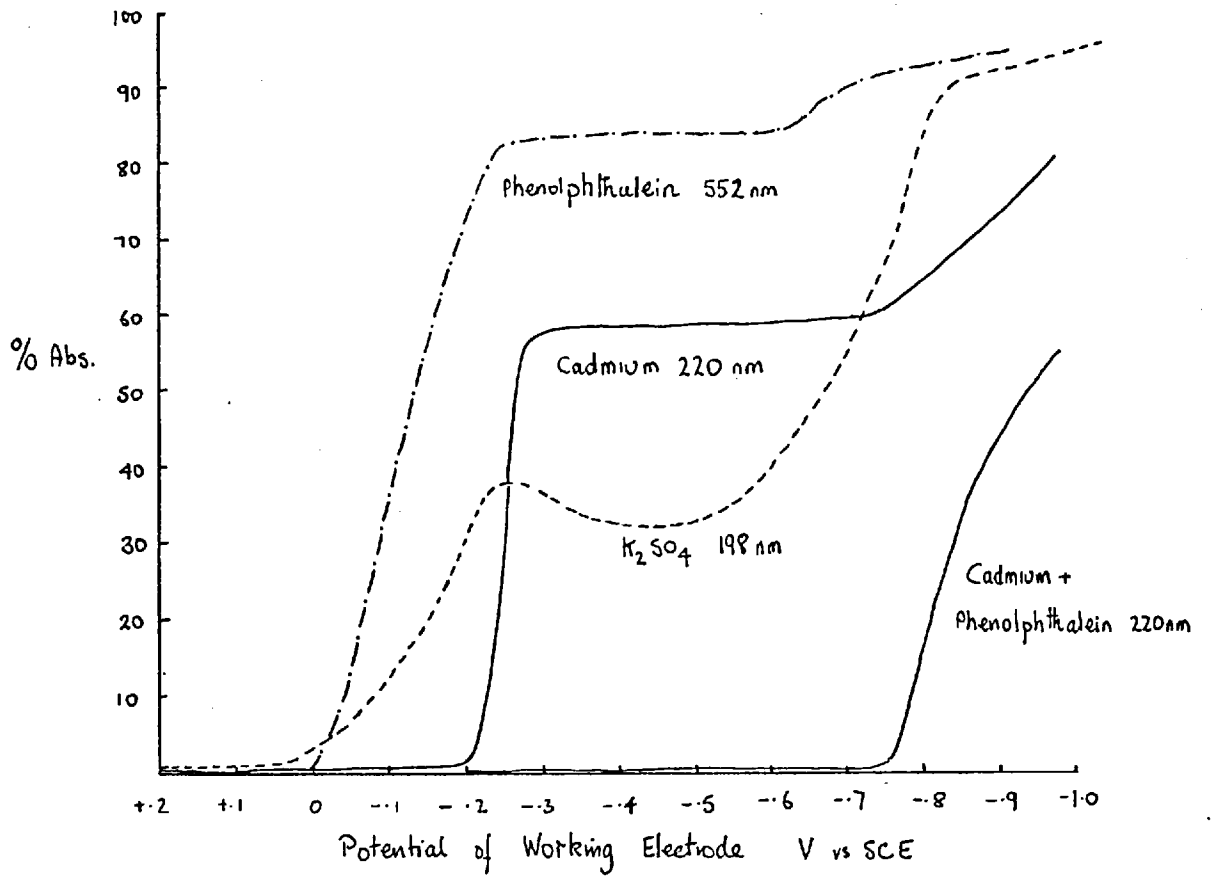

Figure 6.20 Oxidised Electrode. Variation of Absorption with Potential

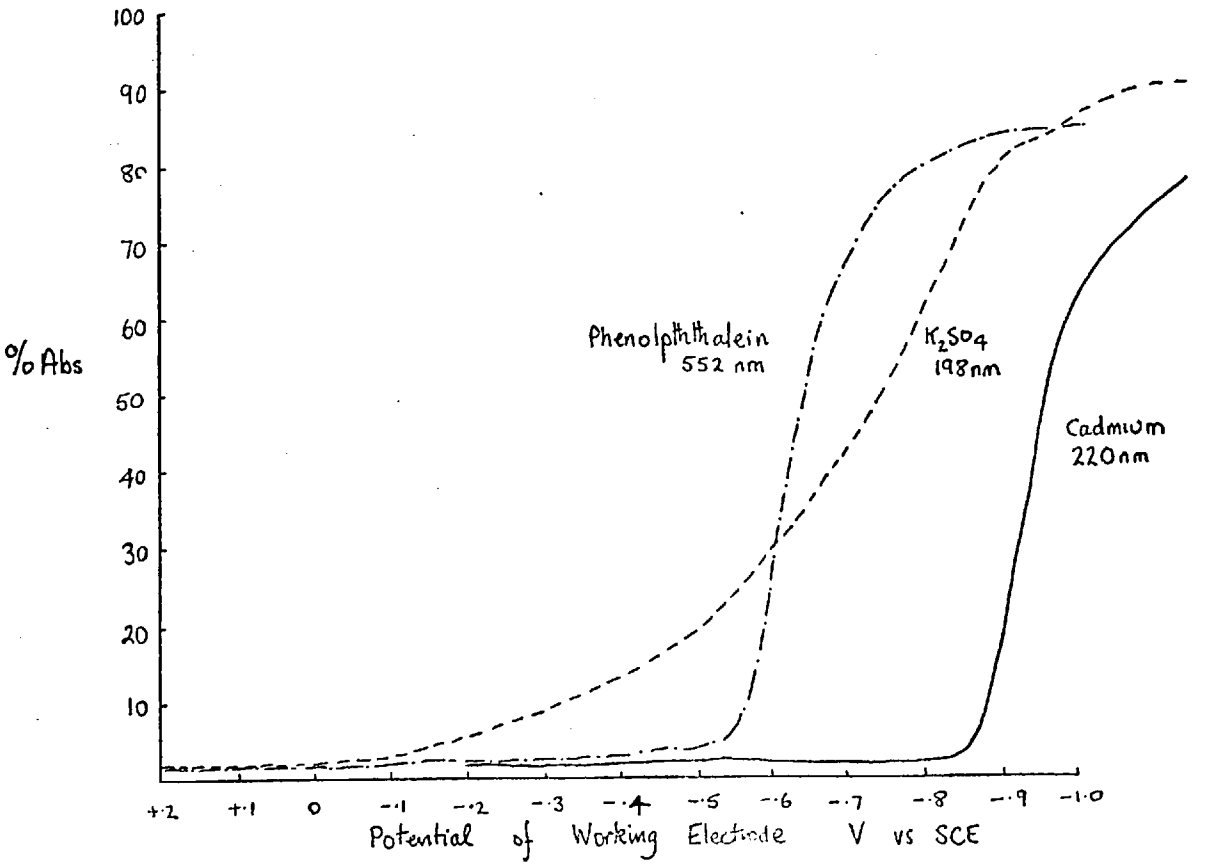

Figure 6.21 Reduced Electrode. Variation of Absorption with Potential

2. Reduced Electrode.

The surface oxide layer was reduced by applying a cathodic potential to the working electrode after the anodic stripping step. Holding the potential at +0·2 V vs SCE while deaerating removed the adsorbed hydrogen. The results obtained for the three solutions (blank, metal ion and indicator) are shown in Figure 6.21. From the Figure it was seen that, in contrast to the oxidised surface, the indicator signal did not occur until -0·54 V vs SCE with the blank signal following a similar path. There was no signal from the cadmium solution until -0·85 V vs SCE.

3. Reduced Electrode, Solutions not Deaerated.

The same pretreatment as for the previous experiment was used, but the solutions were not deaerated. The results are shown in Figure 6.22 for the blank and cadmium solutions, from which it could be seen that the presence of dissolved oxygen produced results similar to those obtained with an oxidised electrode in the absence of dissolved oxygen.

The results are presented in a different form in Figure 6.23 so that the effects of the various electrode pretreatments on the signals from each solution could be seen. From visual observation of the electrodes during the potential sweep, it was noted that there was no

observable evolution of hydrogen gas below -1·0 V vs SCE. The red-violet colour of the alkaline form of the indicator could be clearly seen.

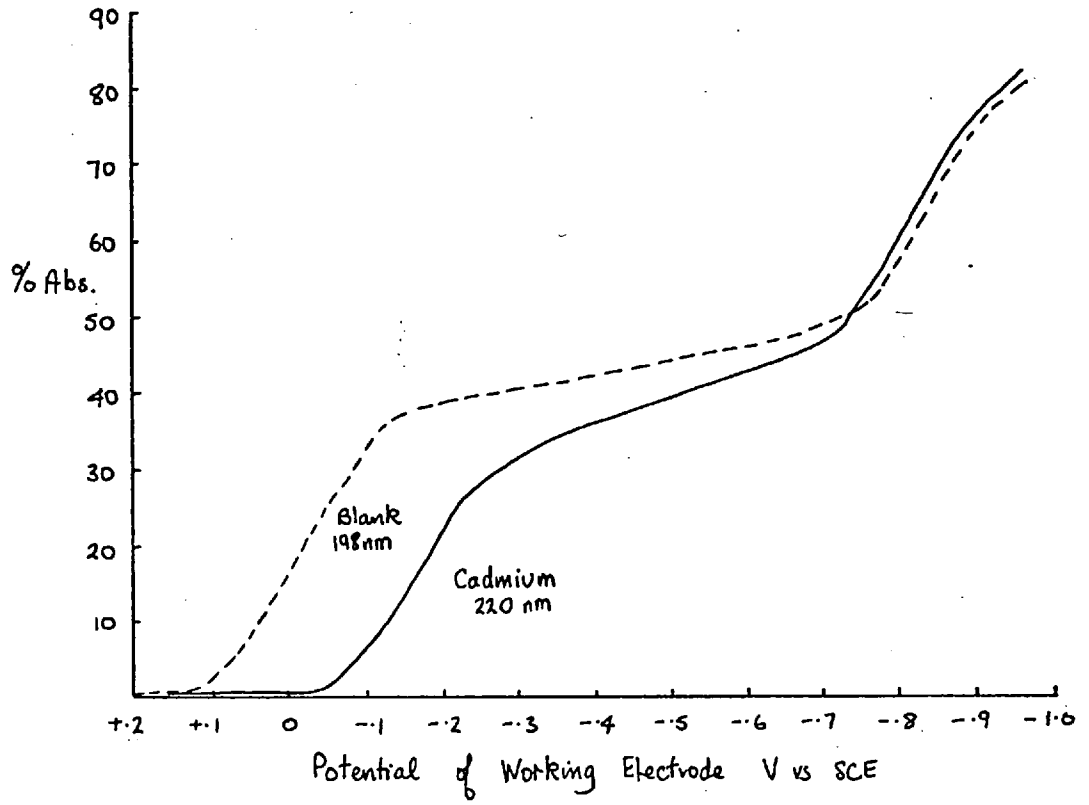

Figure 6.22 Reduced Electrode, Solutions Contain Dissolved Oxygen. Variation of Absorption with Potential

Discussion.

As the signals at 198 nm from the potassium sulphate blank solution followed the same path as those from the alkaline form of the indicator, and from the similarity of the absorption spectra of the blank and 10^{-3} M KOH solution noted in the previous Section, it was concluded

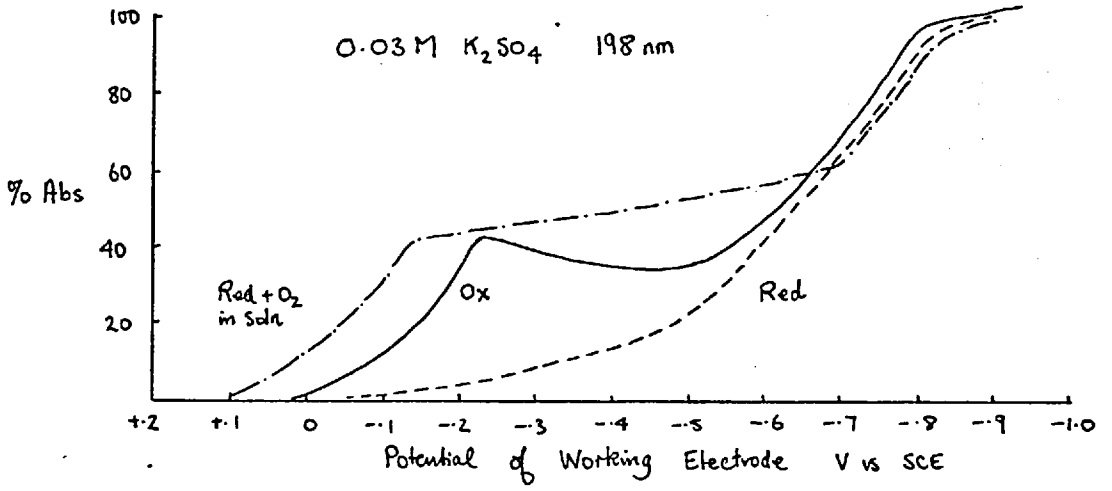

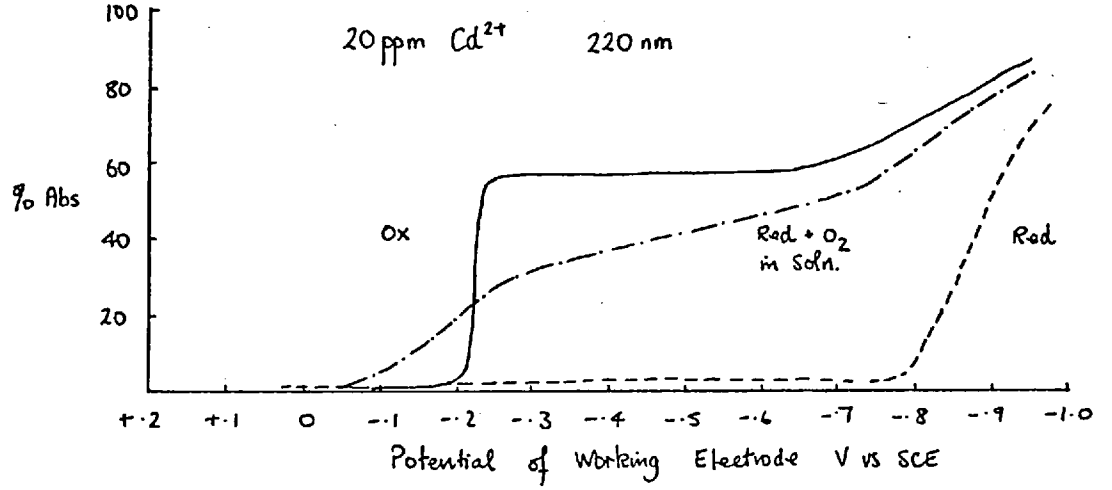

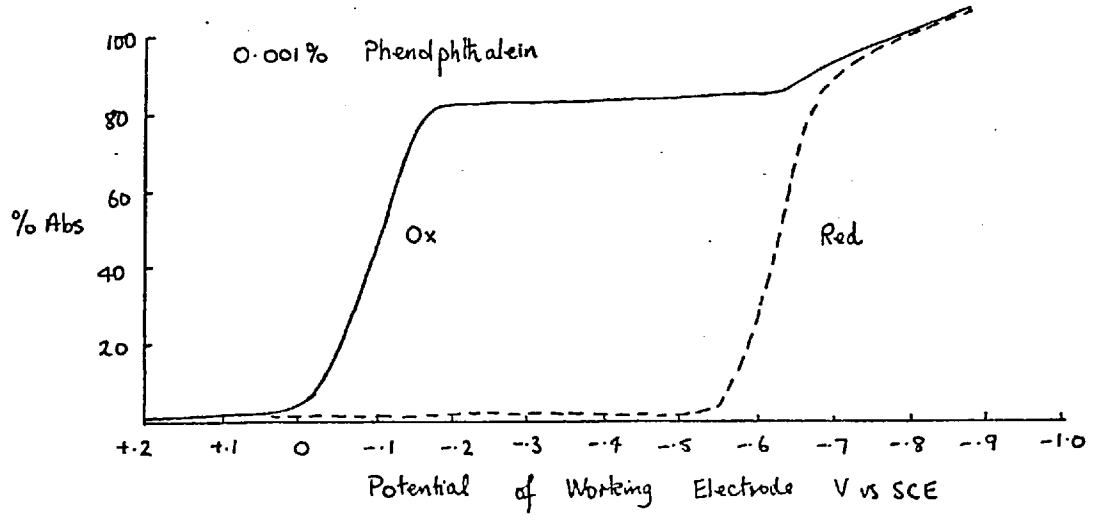

Figure 6.23 Variation of Absorption with Potential for Different Electrode Pretreatments

that hydroxide ion was formed at the cathode at a potential of 0·0 V vs SCE. From the agreement between the current-potential curve and absorption-potential curve (see Figure 6.11), it was further concluded that the hydroxide ion was produced by the reduction of the oxide layer on the electrode surface. This conclusion was further supported by the fact that when there was no oxide on the electrode (reduced pretreatment) no increase in absorption was observed for either the blank or the indicator solution at 0·0 V vs SCE. The absorbance did not increase until a potential of about -0·65 V vs SCE was reached.

It was uncertain from the experiments reported in the previous Section whether the signals from the cadmium solutions were produced at a freshly reduced electrode surface i.e. immediately after the surface oxide was removed allowing the cadmium to react at freshly exposed active sites on the electrode, or whether the product(s) from the reduction of the oxide layer reacted with the metal ions in solution to give an absorbing species. It could easily be seen, though, from Figure 6.23 that when there was no surface oxide, no signal was obtained from the cadmium solutions until a potential of -0·8 V vs SCE was reached, and it was concluded that the presence of hydroxide in the solution was necessary to cause an increase in the absorption from the cadmium solutions.

It did not seem possible to draw any conclusions concerning the nature of the metal-hydroxide species, though

from visual observation of the electrode surface and the discussion concerning colloidal solutions, it was thought that the species was soluble rather than colloidal or precipitated $Cd(OH)_2$.

The results obtained with the solutions containing dissolved oxygen suggested that the reduction product was again hydroxide, and that the reduction occurs at potentials more anodic than the reduction of the surface oxide. These results are in accordance with the conclusions reached in Section 6.5 concerning the reduction products of surface oxide and dissolved oxygen from a consideration of the results of other workers.

As there was no visible evolution of hydrogen and as the absorption in the absence of surface oxide increased at different potentials depending on the species in solution (blank and indicator solutions at approximately -0·53 V vs SCE, cadmium solutions at -0·8 V vs SCE), it was thought that these increases in absorbance were not due to the evolution of hydrogen gas obscuring the light beam. It was noted that the absorption of the cadmium solutions obtained at an oxidised electrode showed a further increase at approximately -0·75 V vs SCE. By exactly the same argument that was used in the first part of this discussion, it was concluded that at these more cathodic potentials the solution became alkaline even though the electrode had a reduced surface and there was no (or very little) dissolved oxygen present. The signal from the cadmium solution

lagged behind those from the blank and indicator solutions in exactly the same way as was observed at the more anodic potentials, and it was thought that an exactly similar process was occurring at these more cathodic potentials as was deduced for the reaction at the more anodic potentials.

The absence of a signal at 220 nm for a solution containing both cadmium and phenolphthalein at -0·2 V vs SCE even though the electrode was anodically pretreated is explained by competition between the phenolphthalein and the cadmium for the hydroxide and a signal for the cadmium hydroxo species was not observed until sufficient hydroxide had been produced to exceed the equilibrium requirements of the phenolphthalein.

6.6.2 Absorption Spectra for Different Regions of the Potential Sweep

From the preceding discussion it was thought that the absorbing species produced at potentials around -0·2 V and -0·7 V vs SCE were the same. This conclusion was also arrived at in the consideration of the effect of electrode pretreatment on the signals from solutions containing zinc (see Section 4.14). The absorption spectra of the cadmium and the blank solutions were obtained at +0·2, -0·2 V vs SCE with an oxidised electrode and at +0·2, -0·7 V vs SCE with a reduced electrode. In both cases a potential step was applied and a fresh aliquot was taken at each wavelength. The results are shown in Figure 6.24, from

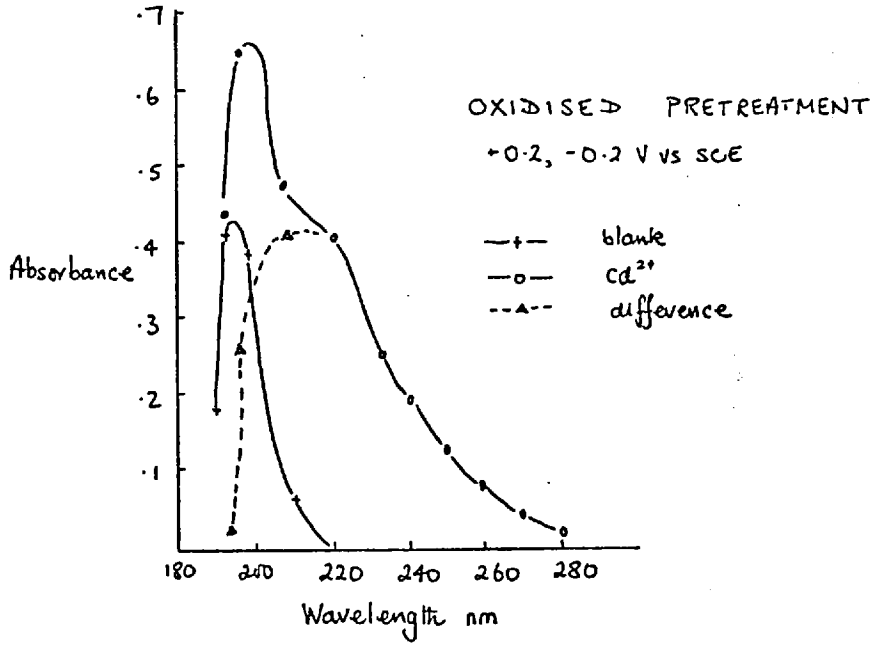

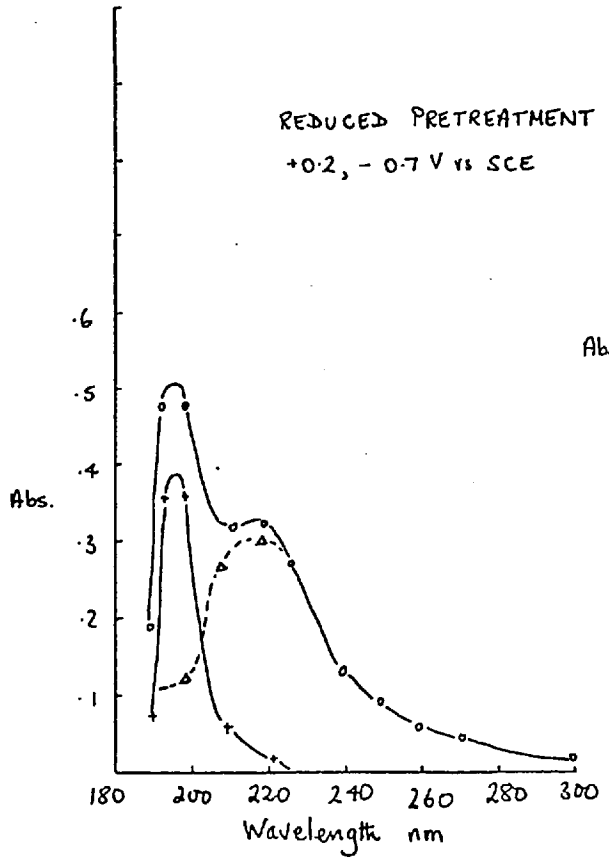

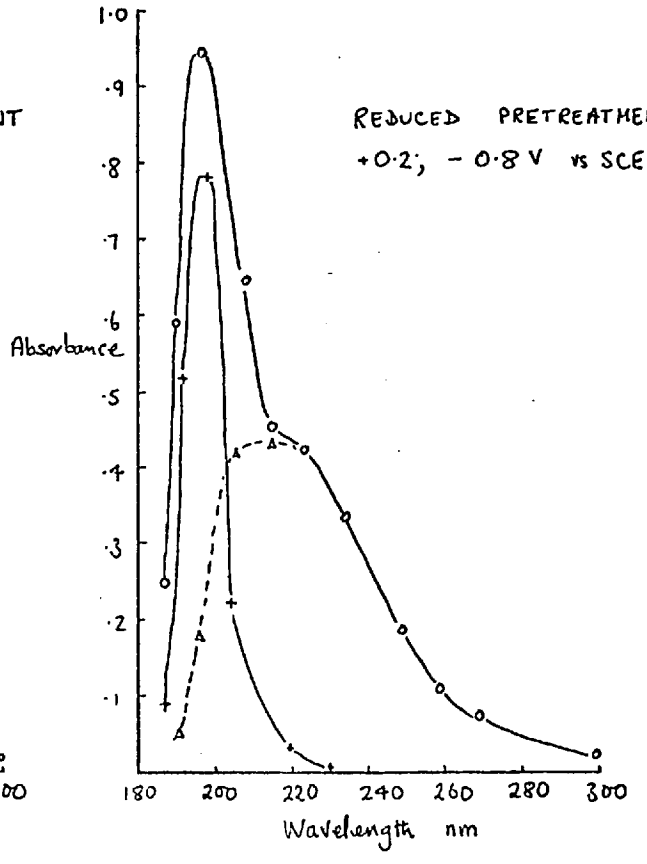

Figure 6.24 Absorption Spectra for Various Potentials and Pretreatments

which it could be seen that the spectra were, indeed, very similar, adding weight to the conclusion that the same species was produced in each case, namely hydroxide ion and a cadmium hydroxo complex. At a slightly more cathodic potential, -0·8 V vs SCE, a very slight evolution of hydrogen was observed by using a magnifying glass. The absorption signals obtained at this potential were considerably greater (see Figure 6.24) and it was noted that the absorption reached a maximum value and maintained this value until the potential was made more anodic, in contrast to the absorptions at -0·2 and -0·7 V vs SCE where the absorption passed through a maximum and then decreased.

It is known that during electrolysis at inert electrodes, the solution near the cathode (catholyte) becomes alkaline when hydrogen is evolved (199). This change in pH has been used to precipitate rare earth hydroxides on the cathode as a means of separating various isotopes, eg ^{90}Y can be prepared with less than 10^{-4}% of ^{90}Sr (200). A theoretical treatment has been given by Hansen (201) whose argument and mathematics are both difficult to follow. He does, however, produce equations which he verifies in a later publication (202). More recently, Harris (203) has published a theoretical treatment of the same problem for the case of the deposition of a divalent metal ion. His approach is to consider the equilibrium between the following species:-

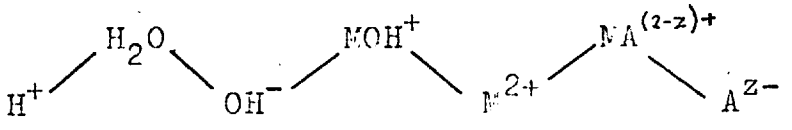

considered to be at steady state concentrations inside a 'Nernst type' diffusion layer. The various equations are solved by numerical integration using a computer. He arrives at the conclusions, firstly, that alkalization of the catholyte is due to the decomposition of water i.e.

$$H_2O + e^- \longrightarrow \tfrac{1}{2}H_2 + OH^-$$

and not due to the dissociation of water in response to the depletion of the solution of protons by reduction at the cathode, in other words, alkalization occurs because the hydrogen evolution current exceeds the Nernst limiting current i.e. the maximum current that could be carried by hydrogen ions diffusing all the way across the diffusion layer. Secondly, that this alkalization can be prevented if the hydroxide formed can immediately react to form a soluble species such as MOH^+ or H_2O (rather than an insoluble metal precipitate) as follows. If the stability constant of MOH^+ is large enough, the hydroxyl ion concentration is greatly exceeded by the concentration of MOH^+, thus effectively removing OH^- from the reaction scheme. The resulting high concentration of hydroxo complex produces a concentration gradient that causes the diffusion of this species away from the cathode against the electric field and eventually they recombine with hydrogen ions

$$MOH^+ + H^+ \longrightarrow M^{2+} + H_2O$$

However, as MOH^+ can exist at relatively high concentrations compared with OH^- even in somewhat acid solutions, the recombination process takes place over a fairly wide

transition zone in which the hydrogen evolution current is shared by H^+ and MOH^+ moving in opposite directions. The result of this is that the diffusion layer thickness can be greater than the thickness which would allow the current to be solely carried by H^+, and despite this thicker layer no precipitation of hydroxide will occur. Harris 'uses' solutions 1 M with respect to M^{2+} at pH 4·0 at 70 °C so his discussion may be of little relevance to solutions 10^{-4} M with respect to M^{2+} at 25 °C. However, although no visible evolution of hydrogen was observed, it could be seen from the current-potential scans (Figure 6.10) that at a potential of -0·7 V vs SCE there may well have been discharge of hydrogen (that the hydrogen was not visible was due to the large capacity of platinum to absorb the gas evolved) producing OH^- and possibly MOH^+ near the cathode. The spectroscopic evidence reported here certainly supports this conclusion.

As has been already mentioned, at the higher potential of -0·8 V vs SCE (at which hydrogen evolution is just visible), considerably larger and more permanent signals were recorded. This suggested that the process proposed by Harris was occurring at this potential giving rise to considerable alkalization, whereas at -0·7 V vs SCE, the alkalization occurred because of the discharge of protons as adsorbed hydrogen leaving an excess of hydroxyl ions in the solution.

6.6.3 Variation of Absorbance with pH

The variation of the thickness of the hydroxyl layer with pH of the bulk solution has been discussed by Hansen (201) who shows that the layer diminishes and then vanishes as the pH is decreased. If the hydroxide formed is reacting with the metal ions to give an absorbing species, then it would be expected that the signal would decrease if the competition for the hydroxyl ions were increased by increasing the concentration of hydrogen ions. The effect of decreasing the pH by the addition of sulphuric acid on the absorbances from solutions of 0·03 M potassium sulphate and from solutions containing 10 ppm cadmium was investigated. An anodic pretreatment was used and the solutions were deoxygenated with oxygen-free nitrogen. The potential was held at +0·2 V vs SCE and then stepped to -0·2 V vs SCE. In the more concentrated acid solutions it was found that the oxide layer was reduced at +0·2 V vs SCE and so the potential was held initially at +0·6 V vs SCE. Evolution of hydrogen obscured the light path with acid concentrations greater than 0·01 M. The absorbance from the cadmium solutions was followed at 220 nm, that from the blank solutions at 195 nm. The results are shown in Table 6.5, from which it could easily be seen that, as predicted, the signals from both the blank and the cadmium solutions decreased with increasing acid concentration. Below pH 3 (calculated from the acid concentration) no signal was observed from either solution.

Table 6.5 Variation of Absorbance with pH

Acid Conc^{n}. M	Potential V vs SCE	Absorbance Cd 220 nm	Absorbance Bl. 195 nm
none added	± 0·2	0·40	0·46
10^{-5}	± 0·2	0·00	0·36
10^{-4}	± 0·2	0·00	0·00
10^{-3}	± 0·2	0·00	0·00
10^{-2}	± 0·2	0·00	0·00
10^{-5}	+0·6,-0·2	0·41	0·47
10^{-4}	+0·6,-0·2	0·22	0·34
5×10^{-4}	+0·6,-0·2	0·04	0·05
10^{-3}	+0·6,-0·2	0·00	0·00

6.7 Absorption Spectra of Metal Ion Solutions

The spectra of the 10 ppm metal ion solutions in 0·03 M potassium sulphate were run against 0·03 M potassium sulphate as a reference in 2 cm cells on a double-beam recording instrument (Perkin Elmer model 402). The results are shown in Figure 6.25. The spectra obtained immediately after making the solution 10^{-3} M with respect to KOH are shown in Figure 6.26. The spectra were recorded against the metal ion solutions as references in 2 cm path length cells. The solutions containing Cd^{2+},Cu^{2+},Ni^{2+},Co^{2+},Zn^{2+}, Mn^{2+} and Hg^{2+} did not visibly appear to give a precipitate or colloidal suspension, whereas the solutions containing Sn^{2+},Ag^{+},Cr^{3+},Fe^{3+} and Pb^{2+} gave a visible opalescence or precipitate on making the solution alkaline. The spectra of the species obtained at the electrode surface during

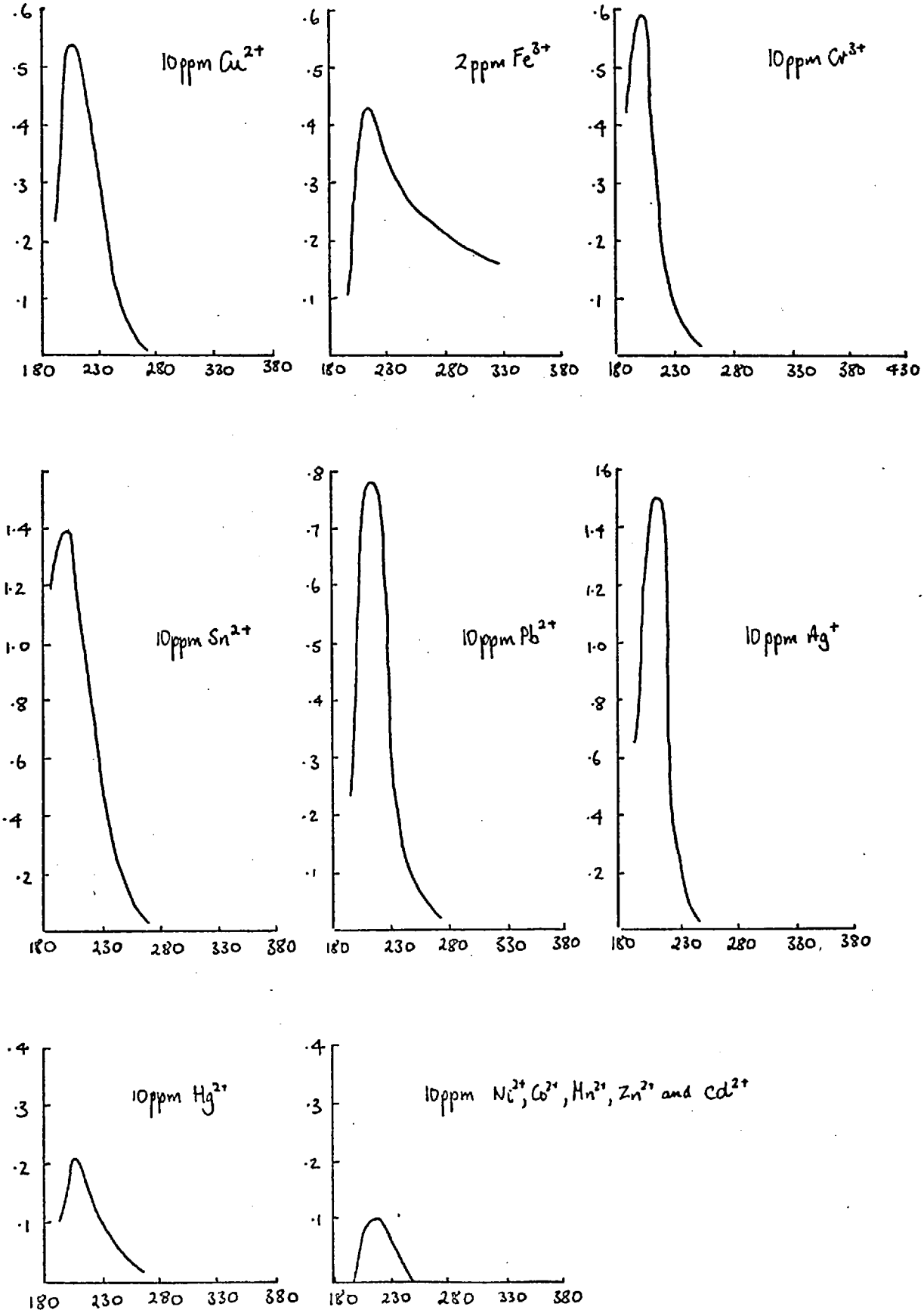

Figure 6.25 Absorption Spectra of Aquo Ions

Plots of Absorbance vs Wavelength nm

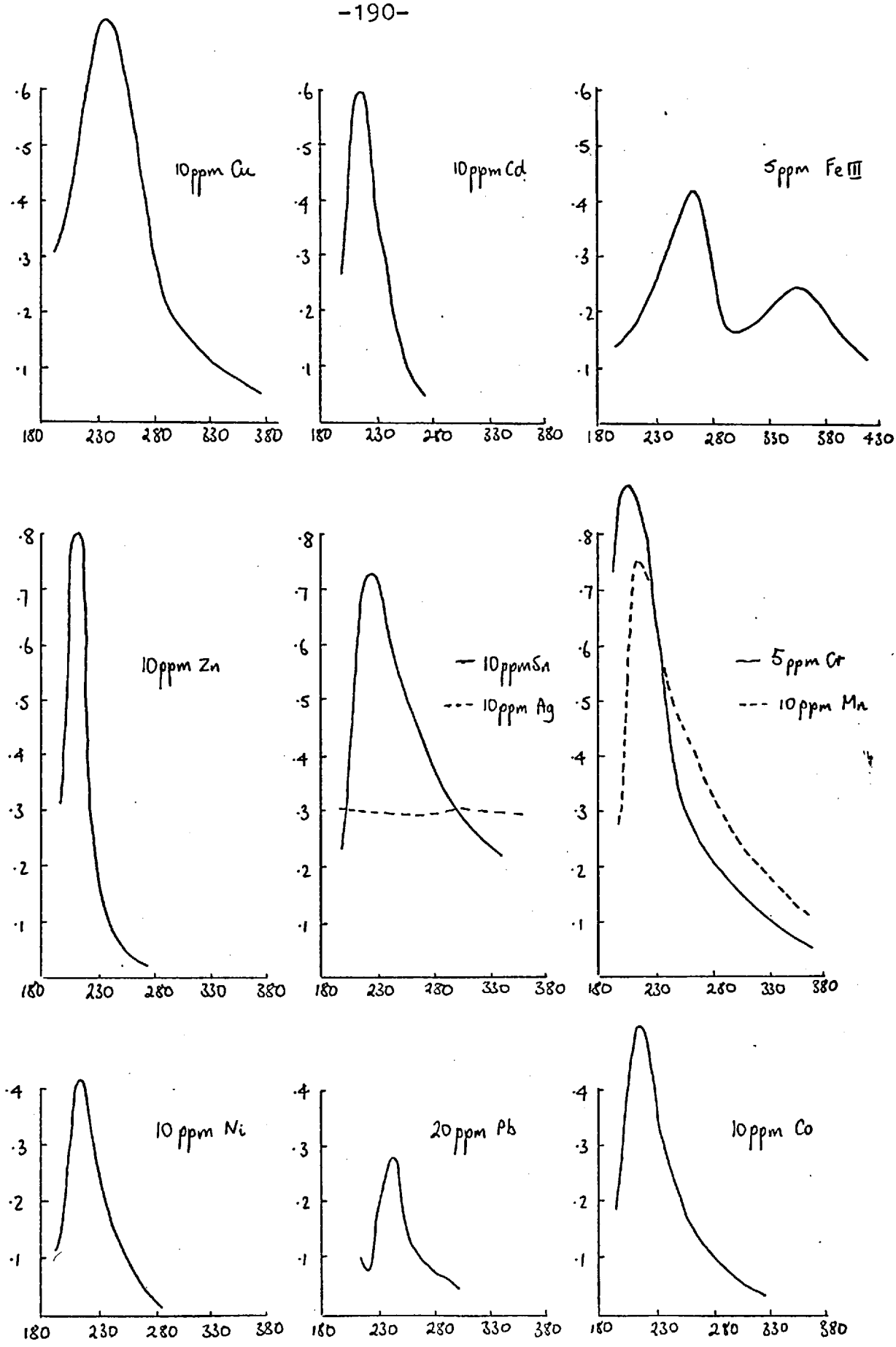

Figure 6.26 Absorption Spectra of Metal Ions in 10^{-3} M KOH

Plots of Absorbance vs Wavelength nm

electrolysis are shown at the end of Chapter 4 (see Figure 4.16) and the absorbance maxima of the two sets of spectra are compared in Table 6.6.

Table 6.6 Comparison of Absorption Maxima

Metal Ion	Catholyte Species nm	Metal Ion in 10^{-3} M KOH nm
Cu^{2+}	235	237
Cd^{2+}	215	215
Fe^{3+}	270,364	260,360
Zn^{2+}	207	207
Pb^{2+}	270	234
Cr^{3+}	215	205
Ni^{2+}	208	210
Mn^{2+}	210	215
Co^{2+}	210	212

It can be seen that, with the exception of Pb^{2+} and Cr^{3+}, there is good agreement between the two sets of values. No signal was obtained with mercury in 10^{-3} M potassium sulphate which explains the absence of any signal on electrolysis of mercury solutions. The scatter signal can be seen for silver in Figure 6.26 but it would appear that an absorption signal should have been obtained on electrolysis for tin.

The similarity between the two sets of spectra indicated that the species produced near the cathode during electrolysis is the same as that produced by adding alkali to the

neutral metal ion solutions.

6.8 Process Occurring at the Electrode Surface

The following aspects of the electrode process have been studied;

1. variation of current with time (chronoamperometry)
2. variation of absorbance with time
3. variation of current with potential (linear sweep voltammetry)
4. variation of absorbance with potential
5. pH changes near the cathode
6. pretreatment of the electrode

A mathematical model based on semi-infinite linear diffusion to plane electrodes has been used to derive an equation relating the absorbance to time, height of the light beam, etc (see Equation 6.12). The agreement (or not) of the results with this equation indicates that diffusion predominates initially, but that there are also contributions from other processes. At longer times this model breaks down as the absorbance passes through a maximum and then decreases. It has been shown that the reduction product of the surface oxide layer is hydroxide ion and that this surface oxide layer is essential for the production of absorption signals at -0·2 V vs SCE.

The process at this potential with an anodically pretreated electrode in the absence of dissolved oxygen is envisaged as:-

1. Reduction of surface oxide to give OH^- in solution near the cathode (see Section 6.5.2).
2. OH^- diffuses out into the solution under the concentration gradient.
3. Cadmium ions in the solution react rapidly to form a hydroxo complex which gives rise to the absorbance (see Sections 6.6.3 and 6.7)
4. All the surface oxide is removed so the production of OH^- decreases and then ceases.
5. Correspondingly, the absorbance decreases as the species dissociates, diffuses out of the light path, etc.

If the reaction between the hydroxide and the cadmium ions is rapid and the absorbance is due to a cadmium hydroxo complex, then the absorbance should follow the diffusion controlled arrival of hydroxide. There may be other processes contributing to the removal of the hydroxo complex such as deposition of the metal on the electrode or precipitation as insoluble hydroxide.

At higher potentials it was deduced that hydroxide was also produced in the solution at a reduced electrode. The formation of hydroxide was found to be a function of potential, electrode pretreatment and the amount of dissolved oxygen. Four mechanisms of hydroxide formation are proposed.

1. Reduction of dissolved oxygen at a platinum oxide surface.
2. Reduction of the oxide layer itself.
3. Discharge of protons as adsorbed hydrogen leaving an

excess of hydroxide in the solution.

4. Reduction of water when the proton diffusion current is exceeded, to give hydrogen gas and hydroxyl ion.

Of these, only method 4 will produce hydroxide continuously (it is possible that method 1 would as well; however, most studies have been with deoxygenated solutions as better precision was obtained in the absence of dissolved oxygen), and production of hydroxide will cease when the oxide has been completely reduced (method 2) or when all the active sites have been covered with adsorbed hydrogen (method 3). The results obtained at more cathodic potentials (see Section 6.6.2) support these conclusions.

The experimental evidence for the presence of hydroxo complexes gives no indication as to the nature of the species. For cadmium, a number of species are possible including, $CdOH^+$, $Cd(OH)_2$, (both precipitated and in solution), $Cd(OH)_3^-$ and $Cd(OH)_4^{2-}$. Cadmium species in basic solution have been extensively studied (204,205) and recently reviewed (206). It would appear that at low concentrations of OH^- the predominant species in solution is $CdOH^+$ and so it may well be that this is the species that is causing the absorption. However, it is not possible to generalize from this to the other metal ions involved.

Visual observation of the solutions used in the experiment described in Section 6.7 showed that when the hydroxide ion concentration was increased to 10^{-3} M, a precipitate or colloidal suspension was observed with Cr^{3+},

Fe^{3+} and Pb^{2+} but not with Cd^{2+},Cu^{2+},Co^{2+},Ni^{2+},Zn^{2+} or Mn^{2+}. The effect of increasing the hydroxide ion concentration to 8×10^{-2} M (pH 12·9) on the absorption spectra for Cd^{2+}, Cu^{2+},Co^{2+},Ni^{2+} and Zn^{2+} is shown in Figure 6.27, from which

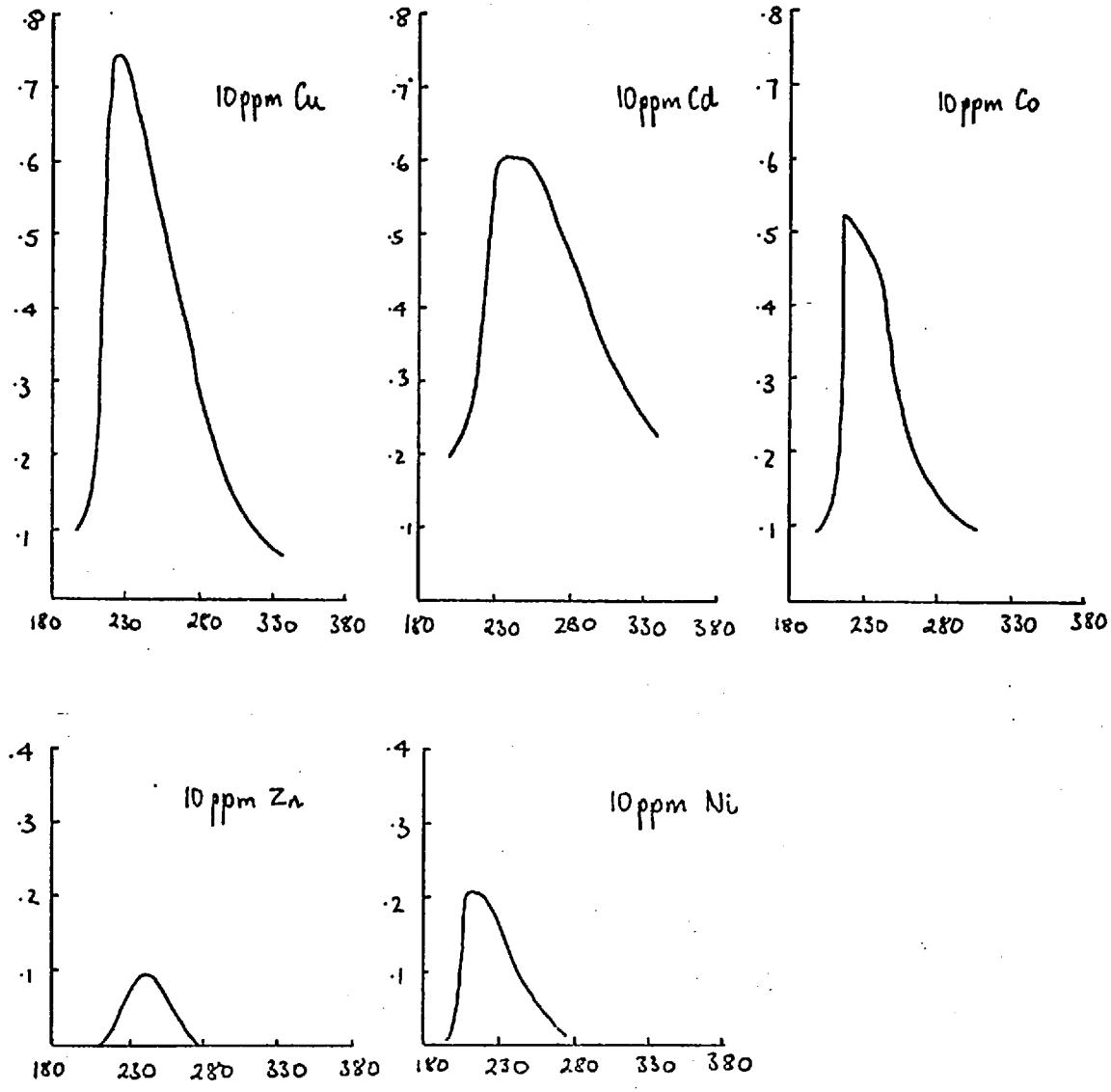

Figure 6.27 Absorption Spectra of Metal Ions in 8×10^{-2} M KOH, Plots of Absorbance vs Wavelength nm

it could be seen that in the case of Zn^{2+} and Cd^{2+} the spectra were considerably different from those in 10^{-3} M KOH suggesting that at the higher pH values, a different species was formed. The results for Co^{2+},Cu^{2+}, and Ni^{2+} suggested that the species was unaltered and was thus most likely $M(OH)_2$ either in solution or precipitated as a colloid.

The precipitation of hydroxides at the cathode during electrolysis has already been mentioned in conjunction with rare earth metals (200) and has been observed at a dropping mercury electrode for cadmium and lanthanum (207). The presence of hydroxyl ion near the cathode was demonstrated by running the polarogram in a solution of 1% ethanolic phenolphthalein and observing the colour after 16 to 40-fold magnification. Powdered silica was added to the solution to improve the colour detection. The formation of hydroxyl was attributed to the reduction of dissolved oxygen. Exactly the same conclusion was reached in a different study of Pb^{2+},Cu^{2+} and Zn^{2+} (208). The decrease in limiting current during the polarography of these ions was attributed to the formation of hydroxides, the hydroxyl ion being produced by the reduction of oxygen at the cathode. The authors noted that the effect disappeared below pH 2·5.

Ultramicroscopic observation of the space near the cathode (209) has shown that with Ni^{2+} and Ag^{+} solutions, colloidal particles are formed near the cathode a few seconds after switching on the current. Current densities

high enough to discharge hydrogen at the platinum cathode were used and the authors attributed the formation of an 'optically empty space' next to the cathode as arising from the difference in mobilities between the hydrogen ions and the hydroxyl ions.

There is considerable evidence for the alkalization of the catholyte during nickel deposition mainly in the Russian literature (210). All the work reported in the literature suggests that insoluble hydroxide is precipitated and it may well be that precipitation is occurring for all the metals studied here.

If equilibrium conditions were obtained in the diffusion layer, then the concentrations of the various species in solution could be calculated from a knowledge of the appropriate stability constants. The stability constants for the MOH species are given in Table 6.7 together with the solubility product and the potential at which the absorption first reached a maximum. If thermodynamic equilibrium is achieved near the electrode surface, then the concentration of the metal hydroxo species, MOH^+, can be calculated from the following equations (neglecting complex formation with other anions).

$$K_{sp} = \left[M^{2+}\right]\left[OH^-\right]^2$$

$$K_1 = \frac{\left[MOH^+\right]}{\left[M^{2+}\right]\left[OH^-\right]}$$

where the square brackets denote the equilibrium concentrations of the appropriate species.

Table 6.7 Stability Constants

Metal Ion	log K_{sp} (211)	log K_1 (212)	Potential V
Mg^{2+}	-11·05	2·6	no signal
Mn^{2+}	-12·69	2·8	1·9
Cd^{2+}	-13·70	5·52	2·0 used
Fe^{2+}	-14·75	6·1	-
Pb^{2+}	-14·38	7·8	2·0 used
Ni^{2+}	-15·80	5·0	1·6
Co^{2+}	-15·70	4·04	1·4
Zn^{2+}	-16·35	4·4	0·9
Cu^{2+}	-18·80	6·5	1·6
Sn^{2+}	-26·20	11·93	scatter
Hg^{2+}	-25·50	11·50	no signal
Cr^{3+}	-30·77	10·2	1·4
Fe^{3+}	-37·22	11·2	1·0

Table 6.8 Effect of pH on Complex Formation

Initial pH	Equil. pH	$[MOH^+]$	$[M^+][OH^-]^2$
8·04	7·00	$9·9\times10^{-7}$	$9·91\times10^{-19}$
9·00	7·98	$9·05\times10^{-6}$	$8·20\times10^{-17}$
9·05	8·00	$9·1\times10^{-6}$	$9·09\times10^{-17}$
9·78	9·00	10^{-6}	10^{-16}
		$(5·0\times10^{-5})$	
10·30	10·00	10^{-7}	10^{-16}
		$(9·1\times10^{-5})$	
11·04	11·00	10^{-8}	10^{-16}
		$(9·9\times10^{-5})$	

Table 6.8 shows the effect of increasing the hydroxide ion concentration for a metal with $K_{sp} = 10^{-16}$ and $K_1 = 10^5$. The initial metal ion concentration was taken as 10^{-4} M. The figures in brackets in the Table give the concentration if no precipitation occurred. It can be seen from the Table that the formation of the MOH^+ species has a slight buffering effect and that the maximum concentration of the MOH^+ species is approximately 10^{-5} M and that precipitation occurs above pH 9. If precipitation did not occur, then the concentration could rise to almost 10^{-4} M (i.e. all the metal complexed as MOH^+). The maximum concentration of MOH^+ is governed by the values of K_{sp} and K_1 and will, of course, be different for each metal. It can be seen from Table 6.7 that, to a certain extent, there is a correlation between the potential required to produce an absorption signal and the insolubility of the hydroxide, there being little correlation between this potential and the stability of the MOH^+ species, suggesting that precipitation of hydroxide causes the absorption. However, considerations from this point of view may be of little value as the conditions observed in the light path were obviously not equilibrium.

A solution to the problem of multiple equilibria in the diffusion layer has been given by Harris (203) which has already been discussed (see Section 6.6.2), in which he proposes the prevention of alkalization, and thus precipitation, by the formation of MOH^+ which diffuses away from the

cathode. There will, of course, also be a pH gradient in the diffusion layer.

Kuwana and Winograd (4) considered the absorbance-time variation (for internal reflection spectroscopy) for a reaction scheme where a first order irreversible reaction follows a rate limiting charge transfer step. The absorbance rises to a maximum and then decreases as the reaction evolves with time. This situation is, to a certain extent, analogous to the scheme proposed here where the rate limiting step is not charge transfer, but the diffusion controlled movement of OH^- into the light beam. It is thus thought possible that a complete mathematical model could be constructed in an analogous fashion, but it is likely that the equation would be very cumbersome.

The shape of the absorbance-potential curves obtained with a linear potential sweep and an oxidised electrode surface (see Figure 6.20) is explained by the fact that with a linearly increasing potential, methods 2 and 3 of hydroxide formation merge into one another and a continuous supply of hydroxide is available giving a fairly constant absorbance from the cadmium solutions. When the region in which method 4 is operative is entered the absorption increased due to a rapid increase in the hydroxide concentration. With the constant potential measurements (i.e. potential step), the absorbance is governed by the amount of cadmium present, there being an excess of hydroxide, until the potential is reached at which hydrogen

is evolved obstructing the light path.

It appears that, although the applied potential may well be cathodic enough to reduce the metal ions in solution, particularly if they are being reduced at underpotential (see Table 5.1), the reduction process does not play any significant part in the production of the absorbance signals.

7. STUDY OF DYESTUFFS

Although it has been shown that the absorption observed near the cathode surface in the presence of reducible metal ions is not, in fact, due to the reduction of the metal, it was thought that suitable organic compounds might show a behaviour characteristic of their redox properties rather than their pH properties. A number of dyestuffs having well defined colour changes in the visible region of the spectrum on oxidation or reduction (redox indicators) were chosen for study.

7.1 Variamine Blue

Variamine blue is 4-amino-4'-methoxy diphenylamine. The reduced form is a colourless cation which can be oxidised through a two electron step to a violet-red iminoquinone.

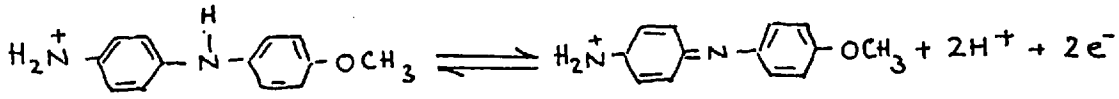

The iminoquinone combines reversibly with another molecule of the reduced species to form an intensely blue coloured quinhydrone. This partially dissociates to a blue-violet semiquinone radical (213).

The variamine blue was purified before use by re-crystallising from a saturated sodium chloride solution, and an approximately 10^{-4} M solution was made up in 0·03 M potassium sulphate as background electrolyte. The absorption

obtained on electrolysing at +2·0 V (i.e. oxidising at the electrode in the light path) using the function gererator in the two-electrode mode with a reduced electrode pretreatment was followed as a function of wavelength between 250 and 690 nm. The spectrum obtained is shown in Figure 7.1

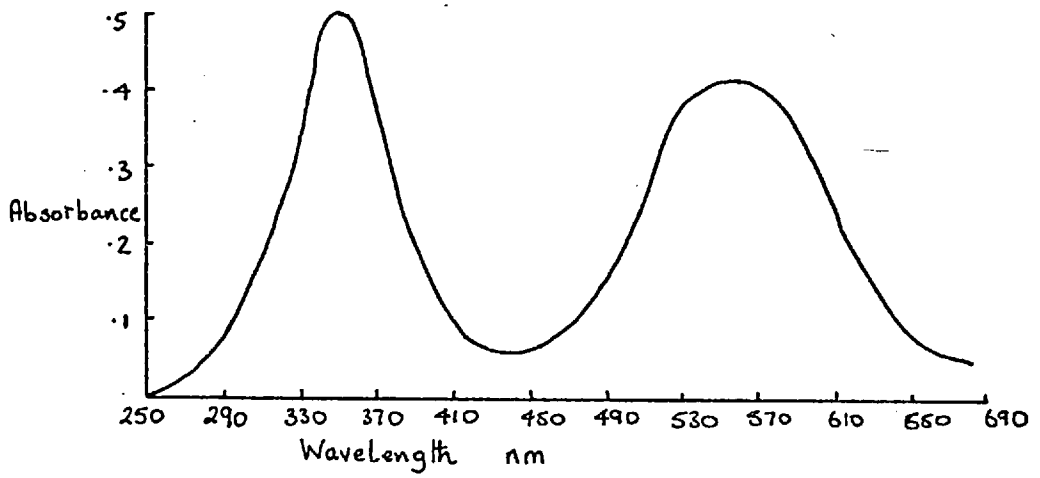

Figure 7.1 Absorption Spectrum Obtained on Oxidising Variamine Blue

In order to compare this spectrum with that of the oxidised form of variamine blue, reference must be made to Equation 6.12 viz.

$$A = \frac{2D_R^{\frac{1}{2}} l t^{\frac{1}{2}} C_R^b (\epsilon_o - \epsilon_R)}{h\pi^{\frac{1}{2}}}$$

for a reaction

$$Red \longrightarrow Ox + ne^-$$

From which it can be seen that, provided the absorbance is taken at the same time after the start of the electrolysis,

the absorbance as a function of wavelength depends on the term $\epsilon_o - \epsilon_R$ i.e. the difference between the molar absorptivities of the oxidised and reduced forms respectively, this being the only term on the right hand side of the equation that is wavelength dependent. Thus it can be seen that the spectrum obtained on the surface of the electrode is the difference between the spectrum of the oxidised form and of the reduced form. Figure 7.2 shows the spectra of the reduced and oxidised forms of variamine blue and also the difference spectrum obtained by placing the cell containing the reduced form in the reference beam of the spectrophotometer.

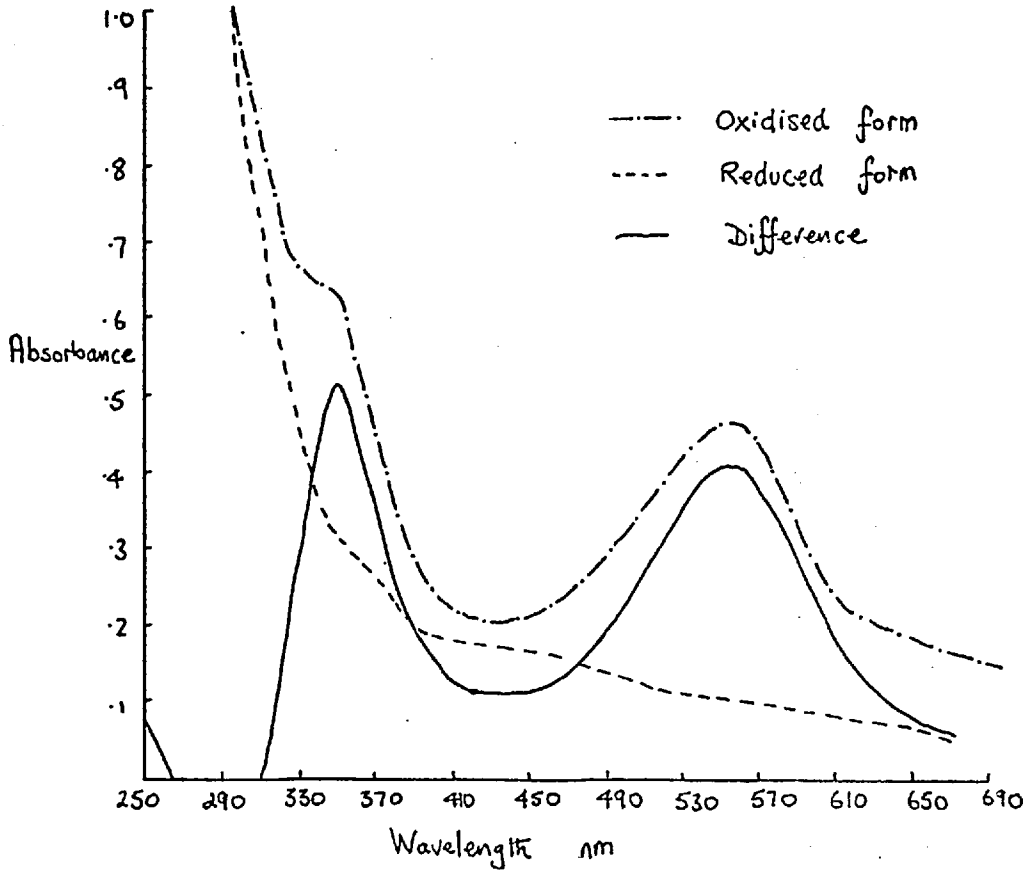

Figure 7.2 Variamine Blue Spectra

The spectra were recorded in 1 cm cells using a Perkin Elmer model 402 spectrophotometer. A comparison between the recorded difference spectrum and that obtained at the electrode surface showed that the absorption signal was due to the redox behaviour of the indicator. The variation of absorbance with concentration at the absorbance maxima is shown in Figure 7.3. The same experimental conditions were employed namely, reduced electrode surface, deoxygenated solutions and a potential of +2·0 V in the two-electrode mode.

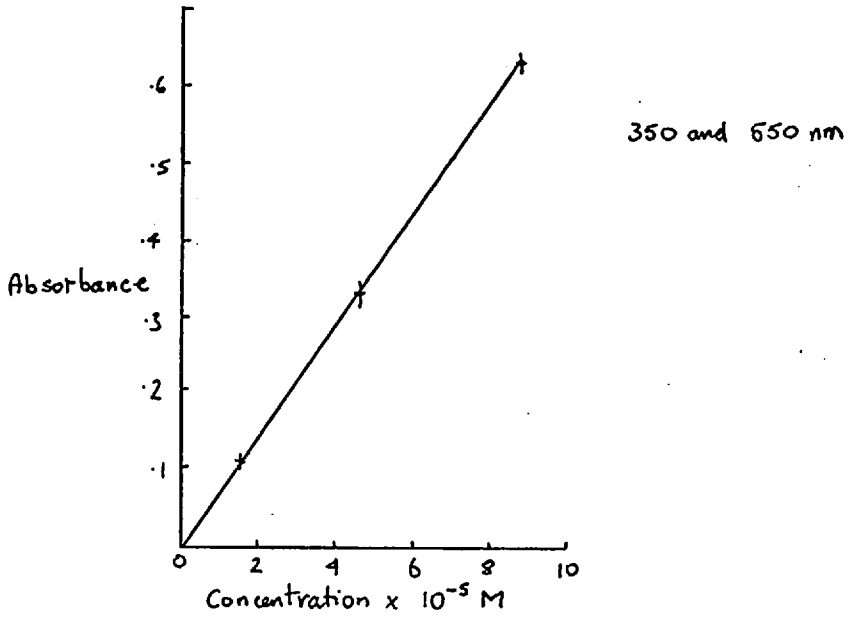

Figure 7.3 Analytical Growth Curve for Variamine Blue

The sensitivity (concentration for 1% absorption) was calculated to be $6{\cdot}5 \times 10^{-7}$ M (approximately 0·15 ppm). It was noted from the recorded difference spectrum that between 260 and 300 nm the reduced form was more strongly

absorbing than the oxidised form. The spectrum obtained by reducing the oxidised form at the electrode surface (-2·0 V, reduced pretreatment) is shown in Figure 7.4, together with the analytical growth curve at the absorbance maximum.

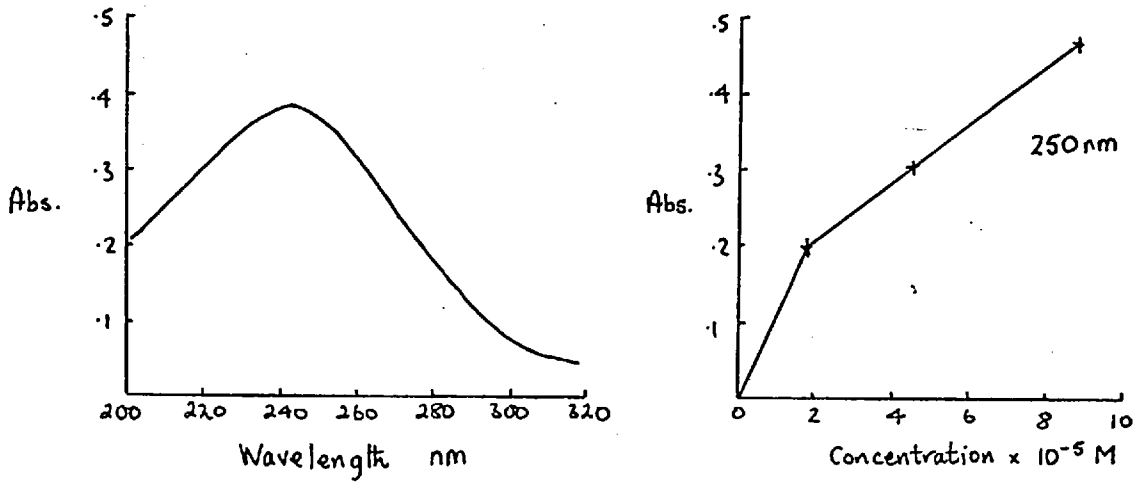

Figure 7.4 Variation of Absorbance with Wavelength and Concentration for Reduction of Variamine Blue

7.2 Tris (5-nitro-1,10-phenanthroline) Iron (II/III)

The reduced form of this compound,

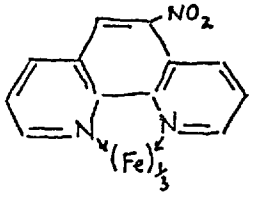

is red whereas the oxidised form is almost colourless. The effect of pH on the redox behaviour is shown in Table 7.1 The absorption spectra of the reduced and oxidised forms

Table 7.1 Effect of pH on Redox Behaviour

pH	Redox State	Colour
acid	reduced	red
neutral	reduced	red
alkaline	reduced	red
acid	oxidised	colourless
neutral	oxidised	pale yellow
alkaline	oxidised	colourless

between 400 and 600 nm are shown in Figure 7.5, from which it can be seen that the reduced form has a maximum at 505 nm.

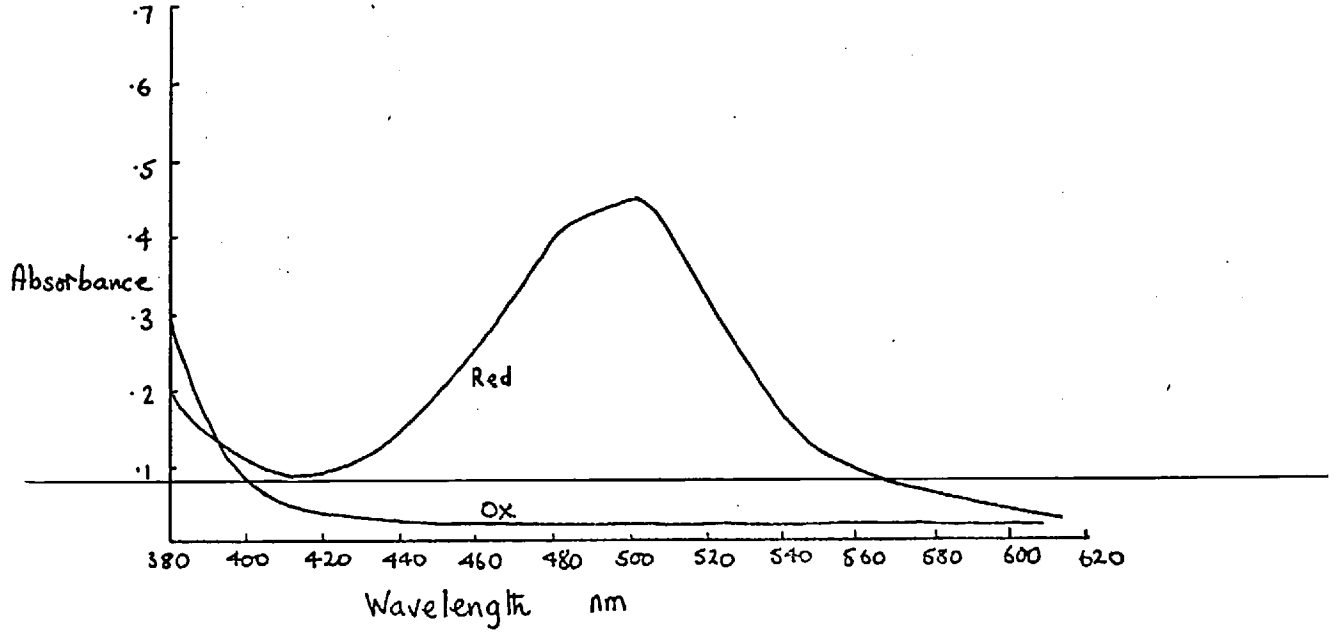

Figure 7.5 Absorption Spectra of Reduced and Oxidised Forms of Nitro-ferroin

Oxidising the reduced form at the electrode surface

at a potential of +2·0 V (two-electrode mode with reduced electrode pretreatment) was found to produce a decrease in the original signal. The variation of ΔAbs. (initial absorbance minus final absorbance) with pH and concentration is shown in Figure 7.6. The sensitivity was calculated to be $5 \cdot 0 \times 10^{-8}$ M

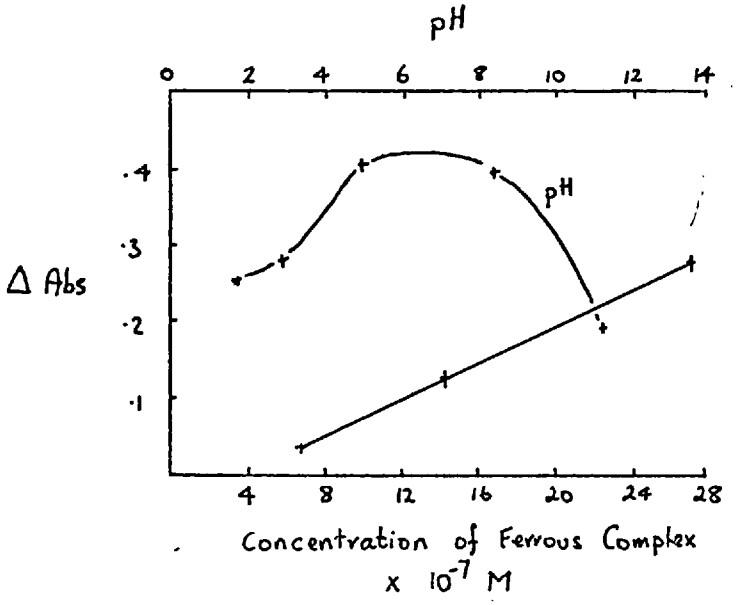

Figure 7.6 Variation of Absorbance with pH and Concentration for Oxidation of Nitro-ferroin

To study the reduction of the oxidised form at the electrode, the reduced form was titrated with ceric solution (7×10^{-3}M) until the red colour of the indicator had just disappeared. This avoided having an excess of oxidising agent in the solution, which, it was found, interfered with the reduction process at the electrode surface. The spectrum obtained by reducing the oxidised form at -0·2 V vs SCE is shown in Figure 7.7. A comparison with Figure 7.5 showed

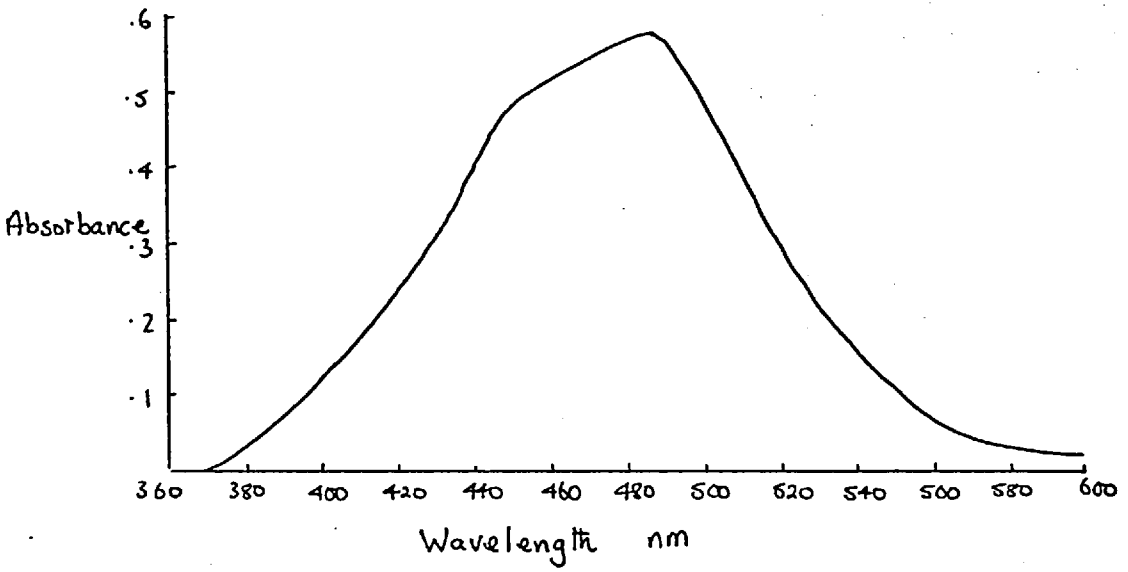

Figure 7.7 Spectrum Obtained on Reducing the Oxidised Form of Nitro-ferroin at the Electrode Surface

that the absorption was due to the formation of the reduced form at the electrode surface. As the electrolysis proceeded, visual observation of the electrode showed that the surface became coated with a red layer which diffused out into the solution.

7.3 Determination of the Pathlength on the Electrode Surface.

The fact that the molar absorptivity of one of the redox forms is zero over a particular wavelength range can be used to measure the pathlength on the electrode surface.

Suppose that the electrode reaction is

$$\text{Red} \longrightarrow \text{Ox} + ne^-$$

where the reduced form of the compound absorbs at the wavelength chosen i.e. $\epsilon_R > 0$ and the oxidised form does not, i.e. $\epsilon_o = 0$. The situation in the cell before and

and during electrolysis is shown schematically below.

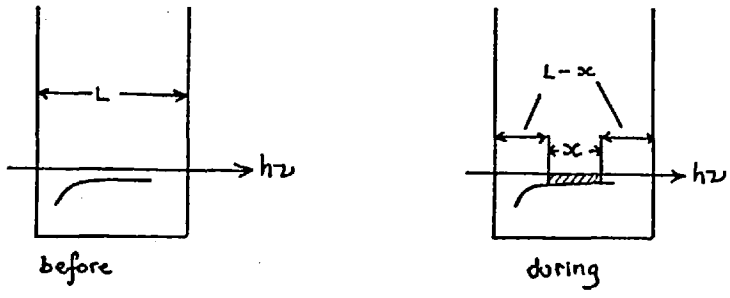

Before electrolysis, the absorbance is given by

$$A_1 = \epsilon_R C_R^b L$$

where C_R^b is the bulk concentration of the reduced species.

During electrolysis, the absorbance is given by

$$\begin{aligned} A_2 &= \epsilon_R C_R^b (L - x) + \epsilon_o C_o x + \epsilon_R C_R x \\ &= \epsilon_R C_R^b L - \epsilon_R C_R^b x + \epsilon_o C_o x + \epsilon_R C_R x \\ &= A_1 - \frac{A_1 x}{L} + 0 + \epsilon_R C_R x \end{aligned}$$

If it is assumed that at the maximum change in absorbance all the reduced species in the light path has been oxidised, then

$$C_R = 0$$

and

$$A_2 = A_1 - \frac{A_1 x}{L}$$

from which

$$x = \frac{L(A_1 - A_2)}{A_1} \qquad 7.1$$

and thus the pathlength can be calculated from a knowledge

of only the total pathlength of the cell (2 cm) and the initial and final absorbances.

The oxidation of tris (5-nitro-1,10-phenanthroline) iron II gave a value for x of 0·67±0·01 cm.

If the simplification of $C_R = 0$ is not made, then at the time the absorbance is measured

$$C_R = kC_R^b$$

where k is the fraction of the bulk concentration unreacted when the absorbance is measured.

Thus

$$A_2 = A_1 - \frac{A_1 x}{L} + \epsilon_R k C_R^b x$$

$$= A_1 - \frac{A_1 x}{L} + \frac{A_1 k x}{L}$$

$$\therefore \quad x(1 - k) = \frac{L(A_1 - A_2)}{A_1}$$

$$= 0{\cdot}67 \pm 0{\cdot}01 \text{ cm}$$

Now 1 - k is the fraction of the bulk concentration converted to the oxidised form

$$\therefore \quad 0 < 1 - k \leq 1$$

and thus the value of 0·67 cm is a lower limit for the value of x. Because of the curvature of the electrode surface, the upper limit for x is approximately 1·5 cm.

Values for the pathlength were obtained using another dyestuff, setopaline. Setopaline is a triphenylmethane dyestuff whose formula, however, is not given in the Colour Index (214). A comparison of the ir spectrum with that of patent blue V showed that the compounds are very similar.

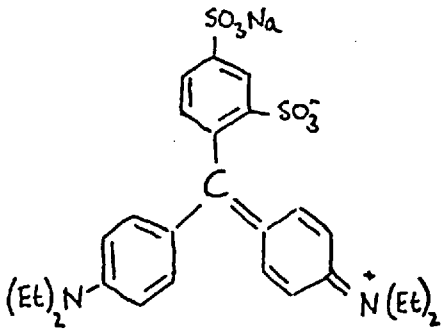

Patent Blue V

The effect of pH on the redox behaviour of setopaline is shown in Table 7.2.

Table 7.2 Effect of pH on Redox Behaviour

pH	Colour of Solution		
	reduced	as dissolved	oxidised
acid	colourless	green	colourless
neutral	colourless	blue	colourless
alkaline	pale green	blue	colourless

In neutral solution setopaline has an absorbance maximum at 630 nm. The absorbance at this wavelegth disappeared completely on reduction. The change in absorbance when the coloured form was reduced at the electrode surface (-2·0 V with reduced pretreatment) was followed at 630 nm. On the basis of Equation 7.1 the pathlength was calculated to be 0·70 ± 0·04 cm.

The values calculated using Equation 7.1 are somewhat lower than that calculated in the studies with phenolphthalein (Section 6.5.2) indicating that possibly the simple form of the Equation is not valid and that the value of k is probably not zero.

7.4 Determination of the Height of the Light Beam

Considering Equation 6.12 namely

$$A = \frac{2D_o^{\frac{1}{2}} t^{\frac{1}{2}}}{h\pi^{\frac{1}{2}}} (\epsilon_R - \epsilon_o)\ 1\ C_o^b$$

it is seen that a plot of A vs $t^{\frac{1}{2}}$ would be a straight line of slope given by

$$m = \frac{2D_o^{\frac{1}{2}}}{h\pi^{\frac{1}{2}}} (\epsilon_R - \epsilon_o)\ 1\ C_o^b \qquad 7.2$$

If a compound were chosen for which D , ϵ_R , ϵ_o were known and if a solution of known concentration were used, then the value of h, the height of the light beam, could be found from the slope of the A vs $t^{\frac{1}{2}}$ plot. The value of 1, of course, has already been determined from the experiments described in the previous Section.

The variation of A with $t^{\frac{1}{2}}$ is shown in Figure 7.8 for the reduction of tris (5-nitro-1,10-phenanthroline) iron III at a reduced electrode surface at -0·2 V vs SCE.

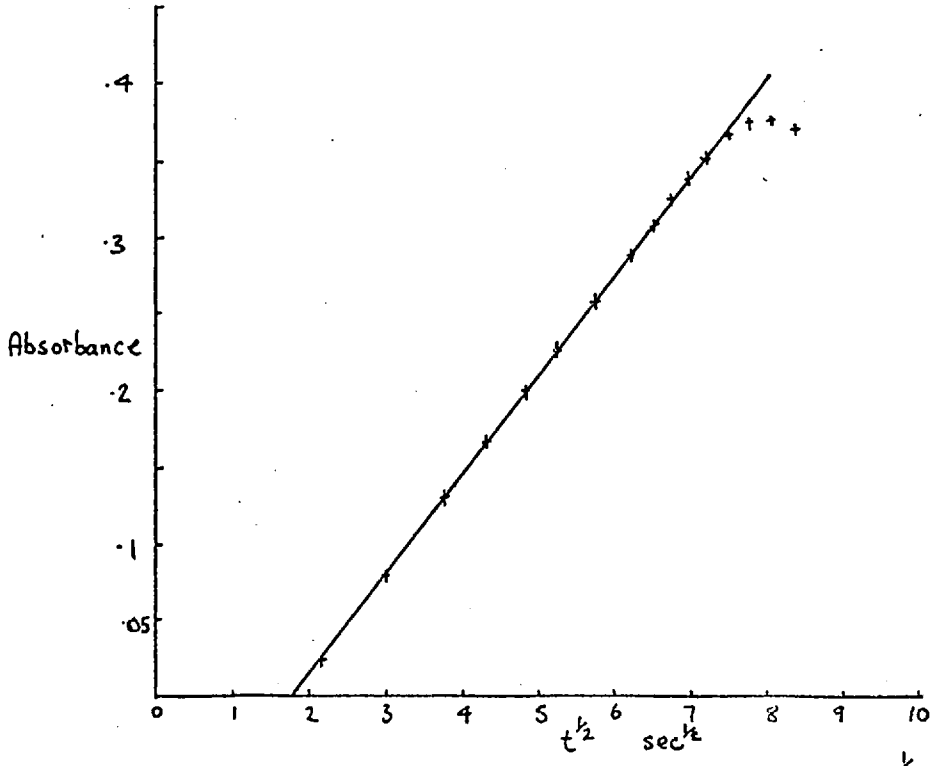

Figure 7.8 Variation of Absorbance with time$^{\frac{1}{2}}$

The concentration of the bulk solution was $9{\cdot}56\times10^{-5}$ M and tha absorbance was recorded until a maximum value was reached i.e. about 70 sec. The plot suggests that an induction period of 3·6 sec elapsed before the absorbance started to increase. In fact, the chart recording showed no increase in absorption until 3·8 sec had elapsed. The slope of the line was 0·0667 $sec^{-\frac{1}{2}}$ and using a value of 5×10^{-6} cm^2 sec^{-1} for the diffusion coefficient and taking ϵ_R = 11,500 and ϵ_o = 0 l $mole^{-1}$ cm^{-1}, the value of h was calculated to be $2{\cdot}91\times10^{-2}$ cm.

7.5 Determination of the Molar Absorptivities of the Metal Hydroxo Species

If it is assumed that the formation of the metal hydroxo complex is analogous to a diffusion controlled electrode reaction, then the value of $(\epsilon_R - \epsilon_o)$ may be obtained from the slope of the A vs $t^{\frac{1}{2}}$ plots using Equation 7.2 provided that D_o, l, h, and C_o^b are known. The values of l and h have already been determined and on the basis of the model presented in Section 6.8, the diffusion coefficient to be used is that for hydroxyl ion (as the appearance of the hydroxo species is assumed to be governed by the arrival of OH^- from the electrode surface), namely $5{\cdot}23\times10^{-5}$ cm^2 sec^{-1}.

A plot of A vs $t^{\frac{1}{2}}$ for a 10 ppm cadmium solution in 0·03 M potassium sulphate for reduction at -0·2 V vs SCE at an oxidised electrode is shown in Figure 7.9. It can be seen that the fit with the linear relation predicted is quite

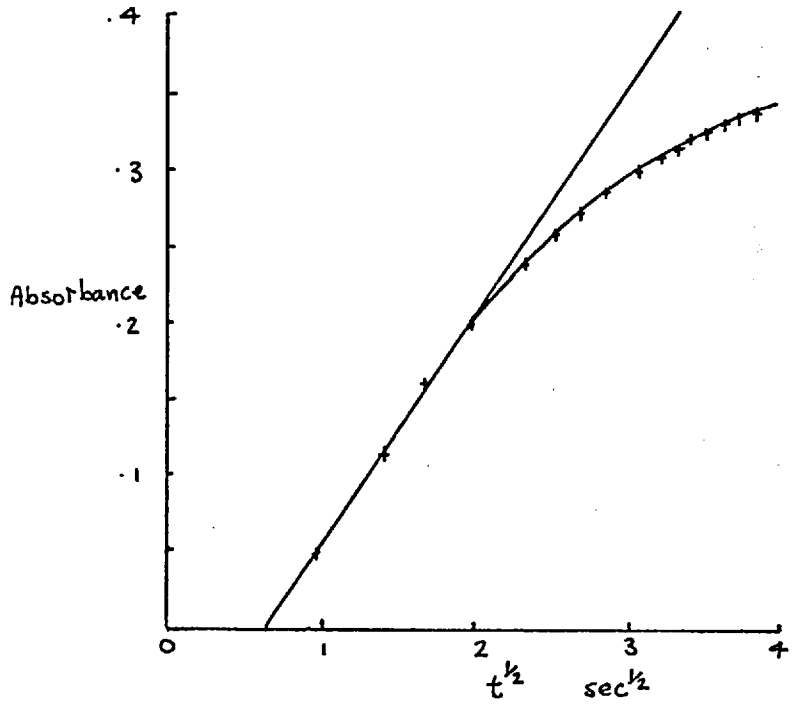

Figure 7.9 Cadmium. Plot of A vs $t^{\frac{1}{2}}$

poor after the first 5 sec. There also appeared to be an induction time of 0·5 sec. The deviation from the linear variation is in marked contrast to the behaviour of the redox indicator which maintained the straight line relation for nearly 70 sec. This shows that with the cadmium solutions, other processes were operating, preventing the concentration of the absorbing species reaching the 'diffusion only' value. The slope over the first 5 sec was 0·146 $sec^{-\frac{1}{2}}$. Using the value of h calculated in the previous Section, a value of 8,240 l $mole^{-1}$ cm^{-1} was calculated for the molar absorptivity difference, $\epsilon_R - \epsilon_o$. In fact, the separate determination of the pathlength is not necessary for this calculation, as the value of the ratio h/l may be calculated from the slope of the plot in Figure 7.8, and this value, $4{\cdot}17\times10^{-2}$, can

be used in the calculation for the other solutions.

The A-$t^{\frac{1}{2}}$ variation for the background electrolyte only is shown in Figure 7.10 for the application of -0·2 V vs SCE to an oxidised electrode surface at 198 nm. The molar absorptivity for hydroxide at this wavelength is calculated from Figure 6.17 to be 960 l $mole^{-1}$ cm^{-1}. From the value

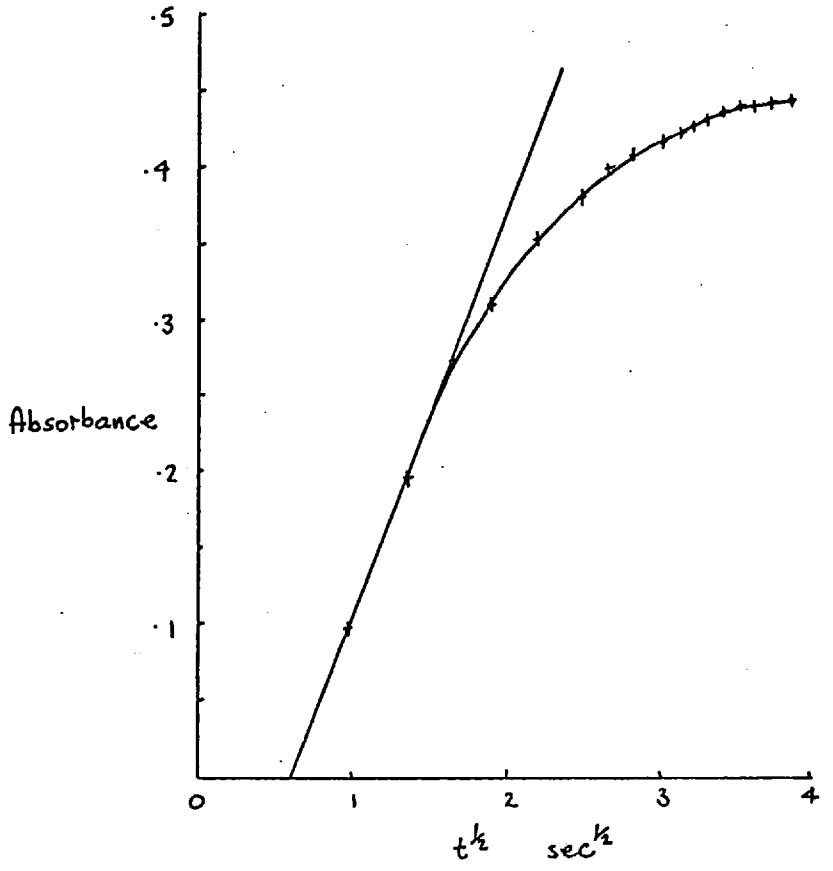

Figure 7.10 Potassium Sulphate. Variation of A with $t^{\frac{1}{2}}$

of the initial slope the value of C is calculated to be 4·31 10^{-3} M. This, in fact, is the surface concentration of hydroxide and corresponds to a pH of 11·6. The pH value calculated from the absorbance maximum in Figure 6.24 is 10·8 (assuming a path length of 0·70 cm). Using the

value of h/l calculated here, a value of 2,630 l mole^{-1} cm^{-1} is calculated for the molar absorptivity difference for the nickel solutions. The results shown in Table 6.2 were plotted in Figure 7.11.

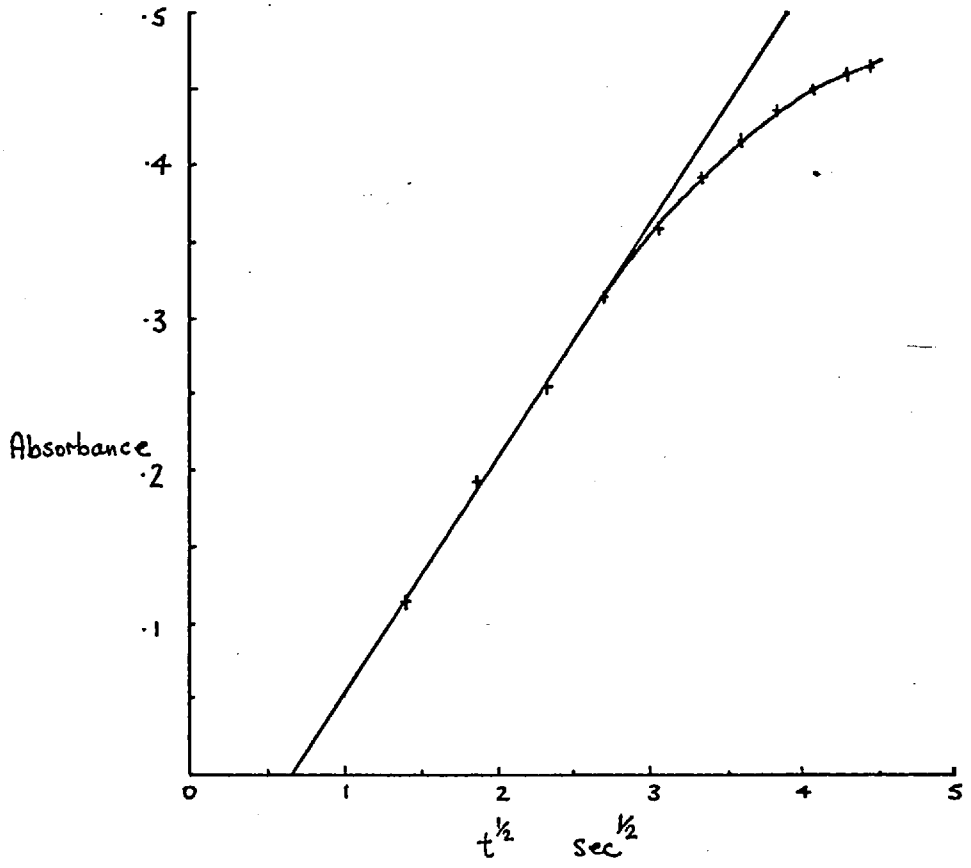

Figure 7.11 Nickel. Variation of Absorbance with Time$^{\frac{1}{2}}$

A similar calculation for the results obtained with a 10 ppm cobalt solution in 0·1 M potassium chloride at -1·6 V (two-electrode mode) with an oxidised electrode gives a value for the molar absorptivity difference of 8,330 l mole^{-1} cm^{-1}. The relevant plot is given in Figure 7.12.

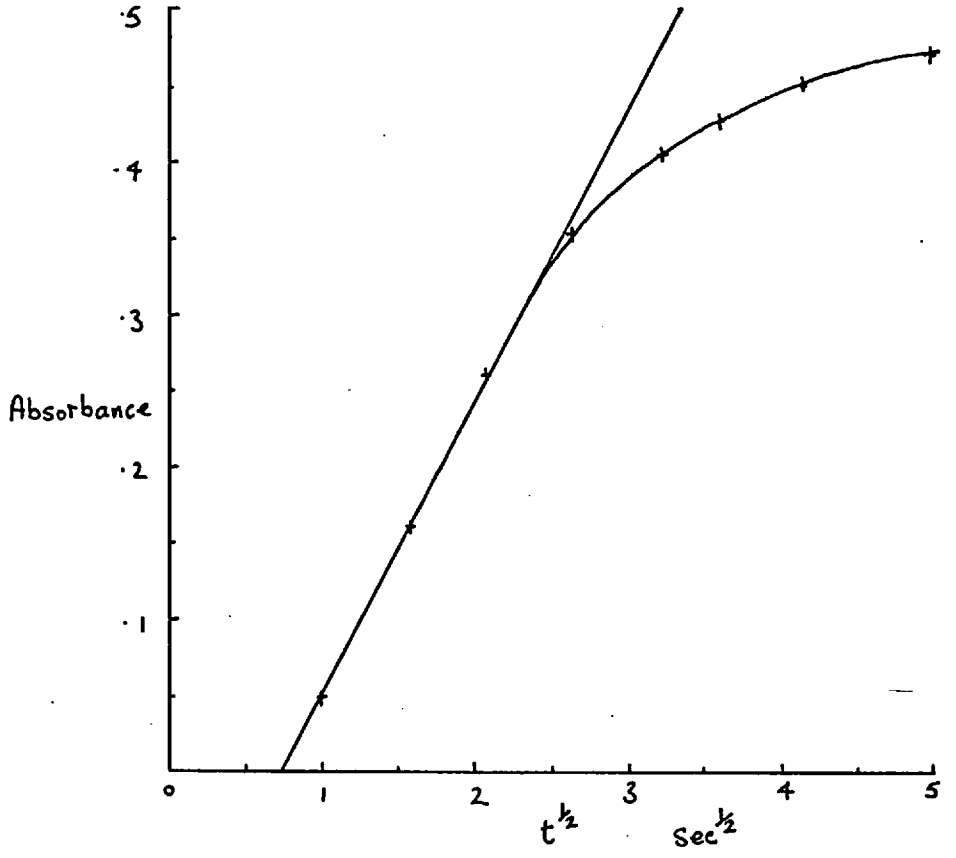

Figure 7.12 Cobalt. Variation of Absorbance with Time$^{\frac{1}{2}}$

The molar absorptivities of the aquo ions at the absorbance maximum of the hydroxo complexes are given in Table 7.3, together with the values for the hydroxo complexes calculated 1) assuming a pathlength of 0·70 cm and that the concentration of hydroxo complex is equal to the bulk concentration of the metal ion, 2) from the absorption spectra recorded in 2 cm pathlength cells (Section 6.7) again assuming the concentration is the same as the bulk value. The final values are calculated by addition. The values for cadmium, cobalt and nickel are based on the values calculated from the initial slopes of the A vs $t^{\frac{1}{2}}$ plots. The difference between the values is attributed

to the greater absorption obtained under the conditions prevailing in the diffusion layer.

Table 7.3 Molar Absorptivities (l $mole^{-1}$ cm^{-1})

Metal	Calcd. from Max Abs.	Calcd. from Secn. 6.7	Aquo Ions	Final Values
Cu	4,000	2,351	413	4,410
Cd	7,870	3,372	393	8,630
Fe II	2,300	-	-	2,300
Fe III	3,900	2,234	3,072	6,970
Zn	5,100	2,779	294	5,390
Pb	3,700	1,450	0	3,700
Cr	6,500	4,570	702	7,200
Ni	2,300	1,230	264	2,860
Mn	4,300	2,060	329	4,630
Co	3,400	1,620	265	3,570

8. CONCLUSION

8.1 Assessment of Results

Looking back to the aim of the studies, it is concluded that it is not possible to extend the technique of atomic absorption spectroscopy to the detection of atoms produced in solution by reduction at an inert electrode surface.

The results of the preliminary experiments showed that certain metal ions gave rise, on apparent reduction, to well defined absorption signals. The absorptions were found to be functions of wavelength, potential difference and concentration. The variation with wavelength suggested that the absorbances could just possibly be a broadened atomic line (an extreme case of pressure broadening) and the variation with potential difference suggested that the species was produced during the reduction of the metal ion, and the variation with concentration suggested possible analytical applications. Further studies showed that a number of other metal ion solutions gave rise to absorption signals which were also wavelength, potential and concentration dependent.

In the subsequent study of the phenomena, it was shown beyond any doubt that the solution near the cathode becomes alkaline during electrolysis, due initially to the reduction of a surface oxide layer on the platinum electrode. Furthermore, it has been shown that the presence of this

oxide coating is a prerequisite for the observation of the absorbance signals, showing that the signals are due to the formation of hydroxo complexes rather than to the formation of reduced species intermediate in the metal deposition reaction. A consideration of the theory of metal deposition indicates that intermediate species of lower oxidation states are undoubtedly produced, but the experimental evidence obtained in these studies indicates that they do not play any significant role in the production of the absorption signals. A comparison of the species observed during electrolysis with those obtained by adding hydroxide to neutral metal ion solutions provides conclusive evidence that the absorption is due to hydroxo complex formation.

It is suggested that the species is either soluble MOH^+ for metals with a high stability constant for this species, or colloidal $M(OH)_2$ for metals with a high insolubility product. It is difficult to determine the nature of the hydroxo complex as the experiments are inconclusive in this respect. It is possible, though, that several species are involved as the pH in the diffusion layer is changing continuously throughout the measurement.

Despite the uncertainty in the nature of the absorbing species, the variation of absorbance with a number of experimental parameters is amenable to analysis on the basis of semi-infinite linear diffusion to plane electrodes, for short times at least. An appropriate equation has been

derived. The validity of this equation has been demonstrated in the preliminary studies of redox indicators, where the change in absorbance observed at the electrode (either anode or cathode) has been shown to be due to the redox properties of the indicator and not to any pH changes in the vicinity of the electrode.

What emerges, then, from these studies is that two possible techniques are available. Firstly, the detection of trace metals by forming absorbing hydroxo complexes and secondly, the detection of organic compounds by observing changes in chromophores caused by oxidation or reduction. Neither of these techniques resembles atomic absorption; the techniques being solution spectrophotometric methods with the localised generation of reagent, hydroxide in one case and electrons in the other, at the electrode surface. In effect the small portion of the solution in the light path above the electrode surface is isolated as a reaction cell and an excess of reagent 'added', the resultant increase in absorbance being recorded as a function of time until a maximum is reached.

The alkalization of the catholyte during electrolysis in aqueous solutions does not appear to be a particularly extensively studied phenomenon. That interference from electrolytically generated hydroxide is not reported in the literature more often is attributed to the fact that most electrochemical studies are carried out under conditions where alkalization would not be expected to occur such as

in non-aqueous media or in strongly acidic media. In strongly basic solutions the phenomenon would probably occur but would obviously not give rise to any unexpected results as the solution is already strongly alkaline.

8.2 Analytical Applications

The combination of optical and electrochemical techniques does not yet appear to have found application in analytical chemistry in terms of the quantitative evaluation of the components of real samples.

The analytical possibilities of internal reflection spectroscopy at optically transparent electrodes (OTE's) was mentioned briefly by Kuwana et al (22) in conjunction with their studies of o-tolidine using a potential step method. The sensitivity of their method is low (5×10^{-4} M for 1% absorption) because, by the nature of the process by which the light beam samples the solution, only very small changes in absorbance are recorded. The use of OTE's with the absorbance measured through the electrode, i.e. by conventional transmission spectroscopy, would possibly circumvent this difficulty. However, in an extended study of this system, Kuwana and Strojek (12) make no mention of the variation of the absorbance with concentration; the whole study being devoted to the evaluation of electrochemical parameters such as diffusion coefficients, rate constants etc. The present situation with regard to spectro-electrochemistry at OTE's has been comprehensively reviewed

by Kuwana and Winograd (4), in which a large number of electrode types and both transmission and internal reflection methods are discussed, but there is no reference to any quantitative analysis having been performed. The methods have been confined entirely to the elucidation of reaction mechanisms and other electrochemical parameters.

Other techniques such as specular reflection spectroscopy and ellipsometry are obviously less suited for analytical applications as they are both techniques designed specifically to study the nature of the eletrode surface and to elucidate the nature of adsorbed species, thickness of films, optical properties etc. Specular reflection spectroscopy has been used to identify reaction intermediates and to study the kinetics of their decay reactions (7).

That the experimental techniques reported here as well as spectroscopy at OTE's can form the basis of an analytical method is apparent from Equation 6.12,

$$A = \frac{2D_o^{\frac{1}{2}} t^{\frac{1}{2}}}{h\pi^{\frac{1}{2}}} (\epsilon_R - \epsilon_o)\ 1\ C_o^b$$

and the analogous equations for the other techniques, from which it can be seen that for a given system the absorbance is directly proportional to the bulk concentration. That this is true, has been amply demonstrated in Chapter 4 where analytical growth curves are reported for 9 metal ions and in Chapter 7 where the results for a number of organic compounds have been discussed. In the case of the metal ion solutions, it has been shown that the absorbance

arises not from the reduction process involving the metal ion but from the interaction of hydroxide generated at the electrode, by a number of methods, with the metal ions in solution.

In effect, then, the method under discussion here is a solution spectrophotometric method using electrogenerated OH^- as reagent. In conventional solution spectrophotometry, a number of general reagents have been used, i.e. reagents which form complexes with a large number of metals. The molar absorptivities ($\times 10^{-3}$ l mole^{-1} cm^{-1}) of the metal complexes of 8-hydroxyquinoline, dithizone, diethyldithiocarbamate and 1,10-phenanthroline are shown in Table 8.1 (215). The values of the molar absorptivities of the hydroxo complexes calculated from the maximum absorbance on the basis of bulk concentration and a pathlength of 0·70 cm are also shown in the Table. The values for cobalt, cadmium and nickel were calculated from the initial slopes of the A vs $t^{\frac{1}{2}}$ plots as described in Section 7.4, and it is likely that the values for the other metals would be higher than those shown in the Table if determined by this method. It can be seen from the Table that for the group of metals studied, hydroxide forms complexes with a range of metals comparable to that of any of the other reagents and that the intensity of the absorption is comparable to that of the complexes with 8-hydroxyquinoline and diethyldithiocarbamate.

Recently, the uv monitoring of the chloride complexes

Table 8.1 Comparison of Molar Absorptivities of Metal Complexes ($\times 10^{-3}$ l mole^{-1} cm^{-1})

Metal	Hydroxyl Ion	Oxine	1,10-phen.	D.D.C.	Dithizone
Ag	-	-	-	5·4	30·0
Cd	8·6	-	35·0	0·21	88·0
Co	8·6	6·0	36·0	0·5	59·2
Cr	7·2	7·7	-	-	-
Cu	4·4	5·0	34·0	13·0	14·0
Fe II	2·3	-	11·0	2·7	-
Fe III	6·9	-	3·0	2·7	-
Hg	-	-	-	-	71·0
Mg	-	5·6	-	-	-
Mn	4·6	-	0·1	-	-
Ni	2·9	4·9	36·0	6·1	-
Pb	3·7	-	-	-	70·0
Sn	-	-	-	-	-
Zn	5·4	-	30·0	-	-

of metal ions has been suggested as a detection method for chromatography (216). The wavelength of the absorbance maximum and the molar absorptivities of the chloride and hydroxide complexes are compared in Table 8.2. The wavelength (nm) is given followed by the molar absorptivity ($\times 10^{-3}$ l mole^{-1} cm^{-1}). It can be seen that the hydroxide complexes compare favourably with the chloride complexes, and it would seem possible that with a suitably designed cell, electrogenerated hydroxide could be used in exactly the same way as a chromatographic detector with the advantage

Table 8.2 Comparison of Absorbance Maxima (nm) and Molar Absorptivities ($\times 10^{-3}$ l mole^{-1} cm^{-1}) for Chloride and Hydroxide Complexes

Metal	Chloride	Hydroxide
Ag	215*, 15	- -
Cd	215*, 0·11	200, 8·2
Co	215*, 0·22	210, 8·3
Cr	215*, 0·71	215, 6·5
Cu	275, 3·4	235, 4·0
Fe II	- -	270, 2·3
Fe III	225, 7·0	270, 3·9
	320, 2·9	364, 3·9
	360, 3·1	
Hg	229, 27	- -
Mn	215*, 1·4	210, 4·3
Ni	215*, 0·15	208, 2·6
Pb	271, 11	270, 2·7
Sn	216, 12	- -
Zn	- -	207, 5·1

* indicates that no maximum was observed, 215 nm being the lower limit of the spectrometer used.

that the addition of high concentrations of reagent (6M HCl was used) is avoided.

Hydroxyl ion has the disadvantages as a reagent in conventional solution spectrophotometry that the absorption is in the uv and thus requires the use of appropriate light sources and 'glass-ware', and that if thermodynamic equilibrium

is attained then a large number of metals would precipitate as insoluble hydroxides. The first consideration is probably of little importance nowadays, when most commercial spectrophotometers have facilities for uv monitoring. It would appear that electrogenerated hydroxide and the conditions within the diffusion layer either do not cause the precipitation of insoluble metal hydroxide or the precipitation is in a controlled reproducible fashion. Hydroxide is unselective in its complexing action, as are a number of other common reagents, and use of electrogenerated hydroxide as a spectrophotometric method would require the application of separation or masking techniques so that only the required element is available for complexing as hydroxo complexes. Separation from metals which do not form absorbing hydroxo complexes would obviously not be necessary. Some selectivity could be obtained by controlling the potential applied to the cathode as this in turn controls the pH of the catholyte. The technique should be applicable to any metal which forms an absorbing hydroxo complex of some sort and is thus not restricted to those metals with reduction potentials within the range accessible in aqueous solution.

Any analytical method for trace metals must inevitably be compared with atomic absorption spectroscopy, which, in theory at least, offers the ultimate in selectivity by virtue of the development of narrow line-width sources (hollow cathode lamps or electrodeless discharge tubes).

The sensitivities (ppm for 1% absorption) are compared in Table 8.3, from which it can be seen that the sensitivities

Table 8.3 Comparison of Analytical Sensitivities (ppm for 1% Absorption)

Metal	Electrogenerated Hydroxide	Air-Acetylene Flame (1)
Ag	-	0·10
Cd	0·09	0·03
Co	0·11	0·20
Cr	0·05	0·15
Cu	0·10	0·10
Fe	0·09	0·10
Hg	-	10·0
Mn	0·08	0·05
Ni	0·16	0·20
Pb	0·35	0·50
Sn	-	5·0
Zn	0·08	0·03

are about the same for both techniques.

Comparison with non-flame methods of atomic absorption is slightly more difficult as sensitivities are usually reported in absolute terms, i.e. the weight in g that causes 1% absorption. Resistively heated graphite furnaces or filaments have the advantage that only very small amounts of sample solution are required, typically 5 to 25 μl, and so in absolute terms very small amounts of material can be measured. However, these methods suffer a loss in

precision because of the difficulty in reproducing transfer of small volumes to the cell. The sensitivities reported for a L'vov furnace (217) recalculated for a sample volume of 5 μl are of the order of 10^{-3} ppm (absolute sensitivity of 5×10^{-12} g).

The preliminary experiments with the dyestuffs show that the technique is also applicable to organic compounds. The results show that the absorbance arises from the redox behaviour of the compound, and thus the method is potentially applicable to a wide range of compounds, as any compound which changed its absorption characteristics on oxidation or reduction could possibly be determined. As it is the electrochemical behaviour of the compound that is being observed, the technique is directly comparable with internal reflection spectroscopy or transmission spectroscopy using OTE's. In Table 8.4 the technique of 1) measuring the absorbance parallel to the electrode surface is compared with the possible analytical use of 2) internal reflection spectroscopy, 3) transmission spectroscopy at an OTE under conditions of semi-infinite linear diffusion and 4) transmission spectroscopy using an OTE in a thin layer cell. The comparison is made for the determination of o-tolidine, which has a diffusion coefficient of $3{\cdot}8\times10^{-6}$ cm^2 sec^{-1} and a molar absorptivity of $6{\cdot}18\times10^4$ l $mole^{-1}$ cm^{-1} at 438 nm. Only the oxidised form absorbs at this wavelength.

It can be seen from the Table that the most sensitive technique is method 3, but that under conditions of semi-

Table 8.4 Comparison of Spectroelectrochemical Techniques

Method	Equation	Time to Reach Abs Max	Sens M 1% Abs.
1.	$A = \epsilon l C^b \frac{2D^{\frac{1}{2}} t^{\frac{1}{2}}}{\pi^{\frac{1}{2}} h}$ $A_{max} = \epsilon l C^b$	$\frac{2D^{\frac{1}{2}} t^{\frac{1}{2}}}{\pi^{\frac{1}{2}} h} = 1$ $\therefore t = \frac{\pi h^2}{4D}$ $\therefore t = 1.76 \times 10^2$ sec	1.02×10^{-7}
2.	$A = \epsilon b_{eff} C^b \left[1 - e^{a^2 t} \operatorname{erfc}(a^2 t)\right]$ (4) where $a = D^{\frac{1}{2}}/\delta$; $b_{eff} = \delta . N_{eff}$ δ is penetration depth N_{eff} is sens. factor for particular electrode type $A_{max} = \epsilon b_{eff} C^b$	$1 - e^{a^2 t} \operatorname{erfc}(a^2 t) = 1$ $\therefore t = 10^{-3}$ sec	5.0×10^{-4} (22)
3.	$A = \epsilon C^b \frac{2D^{\frac{1}{2}} t^{\frac{1}{2}}}{\pi^{\frac{1}{2}}}$ (12) $A_{max} = \epsilon C^b$	$\frac{2D^{\frac{1}{2}} t^{\frac{1}{2}}}{\pi^{\frac{1}{2}}} = 1$ $\therefore t = \frac{\pi}{4D}$ $\therefore t = 2.06 \times 10^5$ sec	7.13×10^{-8}
4.	$A_{max} = 2\epsilon\delta C^b$ where δ is cell thickness	for $\delta = 10^{-3}$ cm $t = 0.2$ sec (43)	3.57×10^{-5}

infinite linear diffusion, it takes about 58 hours for the signal to reach a maximum, by which time of course, convectional and mechanical disturbances would cause the absorption to

deviate from the diffusion controlled value. Methods 2 and 4 give rapid signals but the sensitivity is low due to the very short pathlength in the solution that the light beam samples. With method 1, the time to reach the maximum absorbance could be shortened by decreasing the thickness of the light beam, h. By reducing h to 10^{-3} cm, the time would be reduced to approximately 2 sec. Alternatively, the delay in waiting for the absorbance to reach a maximum could be avoided by using analytical growth curves obtained by plotting the slope of the $A\text{-}t^{\frac{1}{2}}$ plot against bulk concentration (see Equation 7.2). This slope could be found after only a few seconds electrolysis, and is given by

$$\text{slope} = \frac{2\epsilon l D^{\frac{1}{2}} C^{b}}{h \pi^{\frac{1}{2}}}$$

for method 1 and by

$$\text{slope} = \frac{2\epsilon D^{\frac{1}{2}} C^{b}}{\pi^{\frac{1}{2}}}$$

for method 3 and thus for a given range of values for C^{b} the slope of the analytical growth curve would be greater for method 1 by a factor of 1/h (approximately 25).

Thus, although from an electrochemical point of view absorbance measured parallel to the electrode surface is less sensitive as a probe into the double layer region, the method offers the best possibilities from the analytical point of view.

Selectivity could be obtained by a suitable choice of working potential and wavelength. The potential range accessible could be extended by using an electrode material

which has a higher overpotential for the evolution of gaseous hydrogen and oxygen than platinum (eg glassy carbon) as, of course, the special role of the platinum oxide surface layer in providing hydroxide ions is not required. The range could also be extended by using non-aqueous solvents suitably selected to give an optical window at the required wavelength. Detection limits could probably be improved by using a modulated light source and lock-in amplifier detection and readout system to measure small changes in absorbance. An a.c. system would have the advantage that no d.c. component such as might arise from stray light or electroluminescence phenomena would be detected.

It is in this application to organic compounds, where both the electrochemical and optical properties of the system can be used to the full that further work would prove most fruitful. The simultaneous monitoring of the absorbance during chronoamperometric, chronopotentiometric or linear sweep voltammetric studies provides a powerful technique, not only in terms of quantitative analysis, but also in the determination of electrochemical parameters and reaction mechanisms.

REFERENCES

1. H.H. Willard, L.L. Merritt Jr. and J.A. Dean, Instrumental Methods of Analysis, Van Nostrand Reinhold, New York, 1970, p.346

2. G.F.Kirkbright, Analyst, 1971, 96, 609.

3. Adv. Electrochem. Electrochem. Engineering, Vol 9, Ed. R.H. Muller, John Wiley and Sons, New York, 1974.

4. T. Kuwana and N. Winograd in Electroanal. Chem. Vol 7, Ed. A.J. Bard, Marcel Dekker, New York, 1974.

5. Ber. Bunsenges. phys. Chem., 1973, 77.

6. Symposia of the Faraday Soc., No 4, London, 1970.

7. Faraday Discussions of the Chemical Society, No 56, London, 1970.

8. R. Memming and F. Mollers, Ber. Bunsenges. phys. Chem., 1972, 76, 470.

9. H.A. Laitinen, C.A. Vincent and T.M. Bednarski, J. Electrochem. Soc., 1968, 115, 1024.

10. O. Elliot, D.L. Zellmer and H.A. Laitinen, J. Electrochem. Soc., 1970, 117, 1343.

11. T. Kuwana, R.K. Darlington and D.W. Leedy, Anal. Chem., 1964, 36, 2023.

12. J.W. Strojek and T. Kuwana, J. Electroanal. Chem., 1968, 16, 471.

13. See Ref. 5, p.858.

14. A. Yildiz, P.T. Kissinger and C.N. Reilley, Anal. Chem., 1968, 40, 1018.

15. W.R. Heineman and T. Kuwana, Anal. Chem., 1971, 43, 1075.

16. idem, ibid., 1972, 44, 1972.

17. M. Petek, T.E. Neal and R.W. Murray, Anal. Chem., 1971, 43, 1069.

18. N.J. Harrick, J. Phys. Chem., 1960, 64, 1110.

19. W.N. Hansen, Spectrochim. Acta, 1965, 21, 819.

20. W.N. Hansen in Ref. 3.

21. W.N. Hansen, R.A. Osteryoung and T. Kuwana, J. Amer. Chem. Soc., 1966, 38, 1062.

22. idem, Anal. Chem., 1966, 38, 1810.

23. N. Winograd and T. Kuwana, J. Amer. Chem. Soc., 1970, 92(1), 224.

24. G.C. Grant and T. Kuwana, J. Electroanal, Chem., 1970, 24, 11.

25. N. Winograd, H. Blount and T. Kuwana, J. Phys. Chem., 1969, 73, 3456.

26. idem, ibid., 1970, 74, 3231.

27. J.W. Strojek, T. Kuwana and S.W. Feldberg, J. Amer. Chem. Soc., 1968, 90, 1353.

28. D. Laser and M. Ariel, J. Electroanal. Chem., 1972, 35, 415.

29. H.B. Mark and B.S. Pons, Anal. Chem., 1966, 38, 119.

30. W.N. Hansen and J.A. Horten, Anal. Chem., 1964, 36, 783.

31. D.E. Tallant and D.H. Evans, ibid., 1969, 41, 835.

32. D.F.A. Koch, Nature, 1964, 202, 387.

33. D.F.A. Koch and D.E. Scaife, J. Electrochem. Soc., 1966, 113, 302.

34. H.B. Mark and E.N. Randall in Ref. 6, p.157.

35. D. Laser and M. Ariel, J. Electroanal. Chem., 1972, 35, 405.

36. See discussion sections in Ref. 6.

37. D.C. Walker, Can. J. Chem., 1967, 45, 807.

38. R.H. Muller in Ref. 3.

39. J. Kruger in Ref. 3.

40. A.K.N. Reddy, M.A. Devanathon and J.O'M. Bockris, J. Electroanal. Chem., 1963, 5, 61.

41. E. Schmidt and H.R. Gygax, Chimia, 1962, 16, 165.

42. A.T. Hubbard and F.C. Anson in Electroanal. Chem. Vol 4, Ed. A.J. Bard, Marcel Dekker, New York, 1970.

43. C.N. Reilley, Rev. Pure and Appl. Chem., 1968, 18, 137.

44. P.T. Kissinger and C.N. Reilley, Anal. Chem., 1970, 42, 12.

45. R.W. Murray, W.R. Heineman and G.W. O'Dom, Anal. Chem., 1967, 39, 1666.

46. J.C. Saidington and G.R. Hoey, J. Electrochem. Soc., 1973, 120, 1475.

47. S.P. Perone and J.R. Birk, Anal. Chem., 1966, 38, 1589.

48. S.P. Perone, ibid., 1972, 44, 443.

49. H.V. Malmstadt and C.B. Roberts, ibid., 1956, 28, 1408.

50. N.H. Furman and A.J. Fenton, ibid., 1956, 28, 515.

51. E.N. Wise, P.W. Gilles and C.A. Reynolds Jr., ibid., 1953, 25, 1344

52. See Ref. 1, p. 618.

53. S.Glasstone and D. Lewis, Elements of Physical Chemistry, 2nd Ed., Macmillan, London, 1965, p. 501.

54. G.D. Parfitt, Principles of the Colloidal State, R.I.C. London, 1967, p. 19.

55. G.A. Kenney and D.C. Walker in Electroanal. Chem., Vol 5, Ed, A.J. Bard, Marcel Dekker, New York, 1971, p. 15.

56. F.A. Cotton and G. Wilkinson, Advanced Inorganic Chemistry, 2nd Ed., Interscience, London, 1966, p. 568.

57. S. Gilman in Electroanal. Chem. Vol 2, Ed. A.J. Bard, Marcel Dekker, New York, 1967, p. 111.

58. M. Breiter, Electrochim. Acta, 1963, 8, 925.

59. J.O'M. Bockris and A. Damjanovic in Modern Aspects of Electrochemistry, Vol 3, Ed, J.O'M. Bockris and B.E. Conway, Butterworths, London, 1964.

60. B.E. Conway and J.O'M. Bockris, Proc. Roy. Soc. (London), 1958, 248, 394.

61. idem, Electrochim. Acta, 1960, 3, 340.

62. H. Gerisher, Anal. Chem., 1959, 31, 33.

63. E. Mattson and J.O'M. Bockris, Trans. Faraday Soc., 1959, 55, 1586.

64. D.B. Matthews and J.O'M. Bockris in Modern Aspects of Electrochemistry, Vol 6, Ed, J.O'M. Bockris and B.E. Conway, Butterworths, London, 1971.

65. R.W. Gurney, Proc. Roy. Soc. (London), 1931, A134, 137.

66. F.P. Bowden, ibid., 1929, A125, 446.

67. H. Gerisher, Z. Physik. Chem. (Frankfurt), 1960, 26, 223.

68. J.O'M. Bockris and D.B. Matthews, Proc. Roy. Soc. (London), 1966, A292, 479.

69. J.O'M. Bockris and A.K.N. Reddy, Modern Electrochemistry, Vol 2, MacDonald, London, 1970.

70. J.O'M. Bockris and H. Kita, J. Electrochem. Soc., 1962, 109, 928.

71. J.O'M. Bockris and M. Enyo, Trans. Faraday Soc., 1962, 58, 1187.

72. J.O'M. Bockris and A.R. Despic in Physical Chemistry, an Advanced Treatise, Ed, H. Eyring, D. Henderson and W. Jost, Vol IXB, Academic Press, London, 1970.

73. R.A. Marcus, J. Chem. Phys., 1963, 39, 1734.

74. J. Weiss, Proc. Roy. Soc. (London), 1954, A222, 128.

75. W.F. Libby, J. Phys. Chem., 1952, 56, 863.

76. J.H. Baxendale and G. Hughes, Z. Physik. Chem. (Frankfurt), 1958, 14, 322.

77. M. Anbar, Quart. Reviews, 1968, 22, 578.

78. F.S. Dainton, Fast Reactions and Primary Processes in Chemical Kinetics, Ed, S. Claesson, Interscience, New York, 1967.

79. J.H. Baxendale, Current Topics in Radiation Research, Ed, H. Ebert and A. Howard, Vol VII, Wiley, London, 1967.

80. J.K. Thomas, Radiation Res. Rev., 1968, 1, 183.

81. S.R. Logan, J. Chem. Educ., 1967, 44, 345.

82. H.A. Swarz, Ann. Rev. Phys. Chem., 1965, 16, 347.

83. D.C. Walker, Quart. Reviews, 1967, 21, 79.

84. B.E. Conway in Modern Aspects of Electrochemistry, Vol 7, Ed, J.O'M. Bockris and B.E. Conway, Butterworths, London, 1972, p. 83.

85. T. Pyle and C. Roberts, J. Electrochem. Soc., 1968, 115, 247

86. G.J. Hills and D.R. Kinnibrugh, J. Electrochem. Soc., 1966, 113, 111.

87. A.N. Frumkin, J. Electroanal. Chem., 1965, 9, 173.

88. B.E. Conway and D.J. MacKinnon, J. Phys. Chem., 1970, 74, 3663.

89. J. Baxendale, Rad. Research Suppl., 1964, 4, 139.

90. R.A. Marcus, J.Electrochem. Soc., 1966, 113, 1199.

91. idem, Adv. Chem., 1965, 50, 138.

92. idem, J. Chem. Phys., 1965, 43, 3477.

93. U. Schindewolf, R. Vogelgesang and K.W. Boddeker, Angew. Chem., 1967, 6, 1076.

94. B.E. Conway, J. Electrochem. Soc., 1966, 113, 1120.

95. L.I. Kristalik, ibid., 1966, 113, 1117.

96. D.C. Walker, Can. J. Chem., 1966, 44, 2226.

97. A. Bewick, B.E. Conway and A.M. Tuxford, J. Electroanal. Chem., 1973, 42, 11.

98. J.D.E. McIntyre in Ref. 3, p. 128.

99. D. Postl and U. Schindewolf, Ber. Bunsenges. phys. Chem., 1971, 75, 662.

100. D.C. Walker, J. Electroanal. Chem., 1973, 42, 17.

101. V.A. Yurkov in Soviet Electrochemistry Symposium, 1959, Vol II, p. 85. Consultants Bureau, New York, 1961.

102. H.H. Uhlig and R.C. Krutenat, J. Electrochem. Soc., 1964, 111, 1303.

103. F. Will and C.A. Knorr, Z. Electrochem., 1960, 64, 258.

104. D. Gilroy and B.E. Conway, Can. J. Chem., 1968, 46, 875.

105. M.W. Brieter, Ann. N.Y. Acad. Sci., 1963, 101, 709.

106. F.P. Bowden, Trans. Faraday Soc., 1931, 28, 505.

107. M. Heýrovsky, Proc. Roy. Soc. (London), 1967, A301, 411.

108. G.C. Barker, A.W. Gardner and D.C. Sammon, J. Electrochem. Soc., 1966, 113, 1183.

109. idem, Trans. Faraday Soc., 1970, 66, 1498, 1509.

110. G.C. Barker, Electrochim. Acta, 1968, 13, 1221.

111. P. Delahay and V.S. Srinivasan, J. Phys. Chem., 1966, 20, 420.

112. J.O'M. Bockris in Modern Aspects of Electrochemistry, Vol 1, Ed, J.O'M. Bockris and B.E. Conway, Butterworths, London, 1954.

113. D.C. Walker, Anal. Chem., 1967, 39, 896.

114. J.H. Baxendale, E.M. Fielden and J.P. Keene, Proc. Roy. Soc. (London), 1965, A286, 320.

115. N. Kobosev and N. Nekrasov, Z. Electrochem., 1930, 36, 529.

116. V. Bagotsky and S. Jofa, Compt. Rend. (Doklady) Acad. Sci. (URSS), 1946, 53, 439.

117. H.H. Uhlig and R.C. Krutenat, Electrochim. Acta, 1966, 11, 469.

118. R. Petty, A. Davidson and J. Kleinberg, J. Amer. Chem. Soc., 1954, 76, 363.

119. L.B. Rogers and A.F. Stehny, J. Electrochem. Soc., 1949, 95, 25.

120. J.T. Byrne and L.B. Rogers, J. Electrochem. Soc., 1951, 98, 457.

121. M.M. Nicholson, J. Amer. Chem. Soc., 1957, 79, 7.

122. E. Schmidt, P. Moser and W. Reisen, Helv. Chim. Acta, 1963, 46, 2285.

123. E. Schmidt and H.R. Gygax, ibid., 1965, 48, 1584.

124. idem, ibid., 1966, 49, 733, 1105.

125. G.W. Tindall and S. Bruckenstein, Anal. Chem., 1968, 40, 1051, 1637.

126. idem, Electrochim. Acta, 1971, 16, 245.

127. B.J. Bowles, ibid., 1965, 10, 717, 731.

128. idem, ibid., 1970, 15, 589, 737.

129. M.W. Brieter, J. Electrochem. Soc., 1967, 114, 1125.

130. T. Takamura, K. Takamura, W. Nippe and E. Yeager, J. Electrochem. Soc., 1970, 117, 626.

131. J.D.E. McIntyre and D.M. Kolb in Ref. 6, p.99.

132. D.M. Kolb in Ref.7, p. 138.

133. R. Adzic, E. Yeager and B.D. Cahan, J. Electrochem. Soc., 1974, 121, 475.

134. D.M. Kolb in Ref. 5, p. 891.

135. W.J. Lorenz. H.D. Hermann, N. Wuthrich and F. Hilbert, J. Electrochem. Soc., 1974, 121, 1167.

136. Kh.Z. Brainina, Talanta, 1971, 18, 513.

137. H.S. Carshaw and J.C. Yeager, Conduction of Heat in Solids, 2nd Ed, Clarendon, Oxford, 1959.

138. R.V. Churchill, Operational Mathematics, McGraw-Hill, New York, 1958.

139. P. Delahay, New Instrumental Methods of Electrochemistry, Interscience, New York, 1954, p. 58.

140. G. Herzberg, Atomic Spetra and Atomic Structure, Dover, New York, 1944.

141. C. Candler, Atomic Spectra, 2nd Ed, Hilger and Watts, London, 1964.

142. K.M. Mackay and R.A. Mackay, Introduction to Modern Inorganic Chemistry, Intertext, London, 1968, p. 142.

143. T.M. Dunn in Modern Co-ordination Chemistry, Ed, J. Lewis and R.G. Wilkins, Interscience, New Yory, 1964.

144. Handbook of Electrochemical Constants, Compiled by R. Parsons, Butterworths, London, 1959, p. 79.

145. W. Nernst, Z. Physik. Chem., 1904, 47, 52.

146. M.A. Genshaw, A.K.N. Reddy and J.O'M. Bockris, J. Electroanal. Chem., 1964, 8, 406.

147. M.W. Brieter, Electrochim. Acta, 1963, 8, 925.

148. I.M. Koltoff and N. Tanaka, Anal. Chem., 1954, 26, 632.

149. T. Kuwana in Electroanal. Chem. Vol 1, Ed, A.J. Bard, Marcel Dekker, New York, 1966.

150. A.N. Frumkin in Advances in Electrochem. Electrochem. Engineering, Vol 3, Ed, P. Delahay, Interscience, New York, 1963, p. 287.

151. A. Hickling, Trans. Faraday Soc., 1945, 41, 333.

152. H.A. Laitinen and C.G. Enke, J. Electrochem. Soc., 1966, 107, 733.

153. K. Sasaki and Y. Nishigakiuchi, Electrochim. Acta, 1971, 16, 1099.

154. F.C. Anson and J.J. Lingane, J. Amer. Chem. Soc., 1957, 79, 4901.

155. J.O'M. Bockris, M.A.V. Devanathon and A.K.N. Reddy, Proc. Roy. Soc. (London), 1964, 279, 327.

156. See Ref. 6, pp. 72, 99, 114.

157. C.C. Schubert, C.L. Page and B. Ralph, Electrochim. Acta, 1973, 18, 33.

158. K.S. Kim, N. Winograd and R.E. Davis, J. Amer. Chem. Soc., 1971, 93, 6296.

159. J.P. Hoare in Advances in Electrochem. Electrochem. Engineering, Vol 6, Ed, P. Delahay, Interscience, New York, 1967, p. 201.

160. A. Damjanovic in Modern Aspects of Electrochemistry, Vol 5, Eds, J.O'M. Bockris and B.E. Conway, Plenum Press, New York, 1969, p. 369.

161. A.J. Appleby, ibid., Vol 9, 1974, p. 369.

162. P.R. Nadebaum and T.Z. Fahidy, Electrochim. Acta, 1972, 17, 1659.

163. M.A. Barret and R. Parsons, in Ref. 6, p. 72.

164. B.E. Conway in Ref. 6, p. 96.

165. H. Angerstein-Kozlowska, B.E. Conway and W.B.A. Sharp, J. Electroanal. Chem., 1973, 43, 9.

166. B.E. Conway and S. Gottesfeld, J. Chem. Soc. Farad. Trans., 1973, 69, 1090.

167. B.V. Tilak, B.E. Conway and H. Angerstein-Kozlowska, J. Electroanal. Chem., 1973, 48, 1.

168. A.N. Frumkin, E.I. Kruscheva, M.R. Tarasevich and N.A. Shumilova, Electrokhim, 1965, 1, 17.

169. M.J. Weaver, J. Electroanal. Chem., 1974, 51, 231.

170. A. Kozawa, ibid., 1964, 8, 20.

171. K. Nagl and H. Dietz, Electrochim. Acta, 1961, 4, 161.

172. B.E. Conway and S. Gilroy, Can. J. Chem., 1968, 46, 875.

173. S. Gilman, Electrochim. Acta, 1964, 9, 1025.

174. S.W. Feldberg, C.G. Enke and C.E. Bricker, J. Electrochem. Soc., 1963, 110, 826.

175. See Ref. 160, p. 400.

176. T. Biegler and R. Woods, J. Electroanal. Chem., 1969, 20, 73.

177. K.F. Blurton and E. McMullin, J. Electrochem. Soc., 1969, 116, 1476.

178. L. Muller and L.N. Nekrassov, Electrochim. Acta, 1964, 9, 1015.

179. idem, J. Electroanal. Chem., 1965, 9, 282.

180. R.J. Bowen and H.B. Urbach, J. Chem. Phys., 1968, 49, 1206.

181. A. Damjanovic, M.A. Genshaw and J.O'M. Bockris, J. Electrochem. Soc., 1967, 114, 1107.

182. idem, J. Phys. Chem., 1966, 70, 3761.

183. A. Damjanovic and J.O'M. Bockris, Electrochim. Acta, 1966, 11, 791.

184. J.P. Hoare, Electrochim. Acta, 1966, 11, 203.

185. J.J. Lingane, J. Electroanal. Chem., 1961, 2, 203.

186. A.N. Frumkin, L.N. Nekrassov, B. Levich and Ju. Ivanov, ibid., 1959, 1, 84.

187. D.G. Peters and R.A. Mitchell, ibid., 1965, 10, 306.

188. G.Bianchi, F. Mazza and T. Mussini, Electrochim. Acta, 1962, 7, 457.

189. idem, ibid., 1965, 10, 445.

190. J.P. Hoare, J. Electrochem. Soc., 1965, 112, 608.

191. N.W. Brieter, Electrochim. Acta, 1964, 9, 441.

192. D.T. Sawyer and L.V. Interrante, J. Electroanal. Chem., 1961, 2, 310.

193. J.P. Hoare, J. Electrochem. Soc., 1965, 112, 1129.

194. L. Muller and N. Nekrassov, J. Electroanal. Chem., 1965, 9, 282.

195. I.L. Finar, Organic Chemistry, Vol 1, The Fundamental Principles, Longmans, London, 1961, p. 791.

196. P. Debye, J. Phys. Coll. Chem., 1947, 51, 18.

197. W. Heller and E. Vassy, J. Phys. Chem., 1946, 14, 565.

198. B. Jirgensons and M.E. Strausmanis, A Short Textbook of Colloid Chemistry, Pergamon, London, 1962, p. 119.

199. C.V. King, J. Electrochem. Soc., 1955, 102, 195.

200. G. Lange, G. Herrmann and F. Strassman, J..Inorg. Nucl. Chem., 1957, 4, 146.

201. P.G. Hansen, J. Inorg. Nucl. Chem., 1959, 12, 30.

202. idem, ibid., 1961, 17, 232.

203. L.B. Harris, J. Electrochem. Soc., 1973, 120, 1034.

204. K.H. Gayer and L. Wootner, J. Phys. Chem. 1957, 61, 364.

205. D.E. Ryan, J.R. Dean and R.M. Cassidy, Can. J. Chem., 1965, 43, 999.

206. R.D. Armstrong, K. Edmondson and G.D. West in Electrochemistry Vol 4, Chem. Soc. Specialist Periodical Report, Chem. Soc., London, 1974.

207. W. Kemula and Z.R. Grabowski, Coll. Czech. Chem. Commun., 1950, 15, 1085.

208. V.A. Khadeev and Ya.I. Okalova, Trudy Sredneaziat. Gosudarst. Univ. im. V.I. Lenina, Khim., 1958, 84 No 10, 23 from Chem. Abs., 1959, 53, 16810i.

209. O.V. Belyi, O.M. Dolgaya and A.V. Pamfilov, Ukr. Khim. Zh., 1967, 33, 577.

210. See Ref. 203 and references therein.

211. T. Moeller and R. O'Connor, Ions in Aqueous Systems, McGraw-Hill, New York, 1972.

212. Stability Constants of Metal Ion Complexes, 2nd Ed. Compiled by L. Sillen et al, Chem. Soc. Special Publ. No 17, 1964.

213. E. Bishop, Indicators, Pergamon, Bramsdweig, 1972, p. 509.

214. Colour Index, 2nd Ed, The Society of Dyers and Colourists, Bradford, 1956.

215. I.U.P.A.C. Spectrophotometric Data for Colorimetric Analysis, Butterworths, London, 1963.

216. L. Goodkin, M.D. Seymour and J.S. Fritz, Talanta, 1975, 22, 245.

217. B.V. L'Vov, Spectrochim. Acta, 1968, 23B, 215.